Hamish D. Meikle

WILEY-VCH

A New Twist to Fourier Transforms

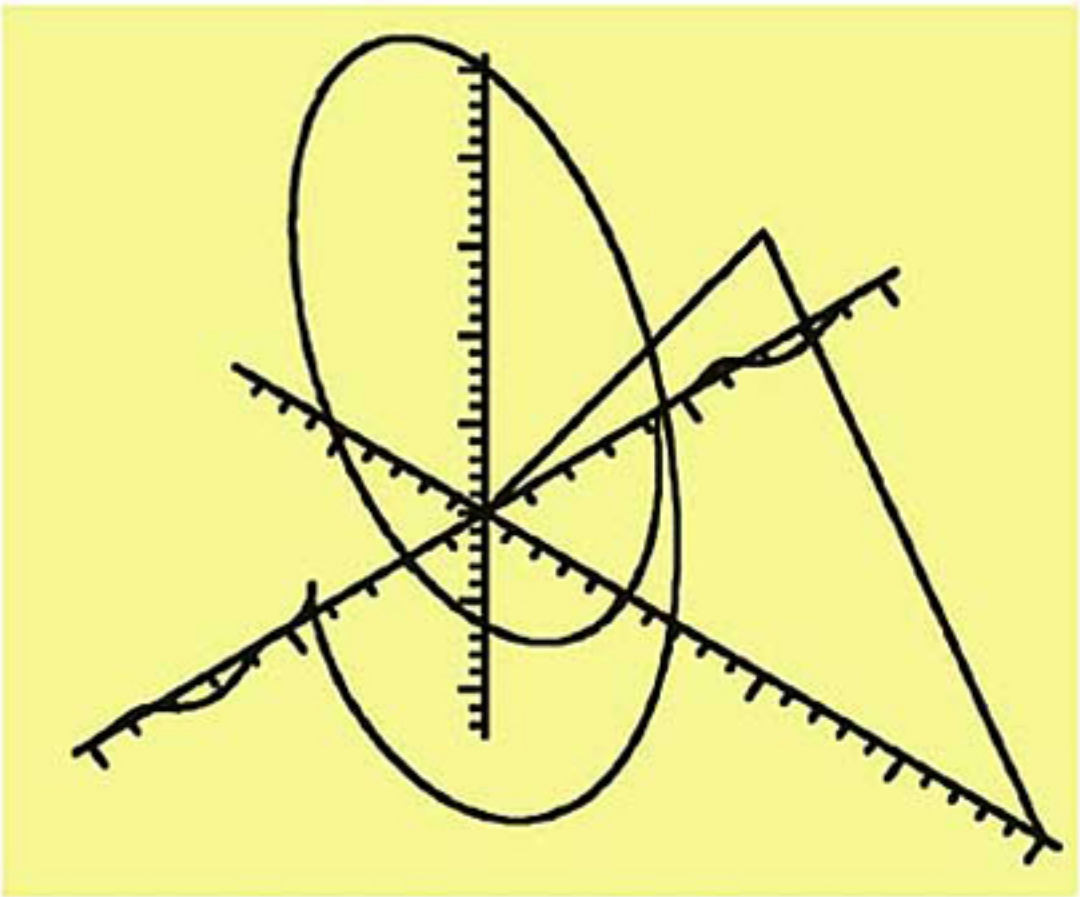

Hamish D. Meikle

A New Twist to Fourier Transforms

A New Twist to Fourier Transforms. Hamish D. Meikle

ISBN: 3-527-40441-4

Hamish D. Meikle

A New Twist to Fourier Transforms

WILEY-VCH Verlag GmbH & Co. KGaA

Author

Hamish D. Meikle
Systems Consultant
e-mail: meiklehd@t-online.de

Library of Congress Card No.
applied for

British Library Cataloguing-in-Publication Data
A catalogue record for this book is available from the British Library.

Bibliographic information published by Die Deutsche Bibliothek
Die Deutsche Bibliothek lists this publication in the Deutsche Nationalbibliografie; detailed bibliographic data is available in the Internet at <http://dnb.ddb.de>.

Printed in the Federal Republic of Germany

Printed on acid-free paper.

Composition Kühn & Weyh, Freiburg
Printing betz-druck GmbH, Darmstadt
Bookbinding Großbuchbinderei J. Schäffer GmbH & Co. KG, Grünstadt

ISBN 3-527-40441-4

Cover Picture The cover shows a triangular pulse centred on 1.0 and its complex spectrum.

To my wife, Monika

Table of Contents

A New Twist to Fourier Transforms. Hamish D. Meikle

ISBN: 3-527-40441-4

Introduction

As a student, and later, I have always needed a physical explanation for the mathematics that I have had to learn. In [1] the author used a new approach to illustrate Fourier transforms in their normally complex form that occur in everyday life in radar systems. This book is completely general, though often dealing with time and frequency relationships as an example, and extends the treatment to characteristic functions in statistics. Note that two conventions are used: one with $j = \sqrt{-1}$ and the frequency convention for engineering uses, and $i = \sqrt{-1}$ and the ω convention for statistics to be consistent with the existing literature.

Power engineering was part of the syllabus with its three phases and a rotating voltage vector that can be made to describe a helix with time. The division of electrical engineering into power engineering and light-current engineering has limited the helical forms to 50 Hz, 60 Hz, and for high frequencies up to 400 Hz. The concepts of power engineering are very useful to describe the amplitude and phase modulation of carrier waves and signals that suffer a frequency shift such as radar echoes. The formula for the Fourier transform contains the expressions $\exp(-j\,2\pi f t)$, or $\exp(i\,\xi\,x)$ for statistics, that are themselves helical functions so it is only reasonable to feature them as such.

Charles Dodson, who taught mathematics at Oxford at the time when operational mathematics was being developed, wrote *Through the Looking-Glass* using his pen-name Lewis Carrol. Students, like Alice, learn to step through the looking-glass separating, say, the time and spectral worlds and lose sight of the world that they have left. Diagrams capable of showing functions and their Fourier transforms together have been developed to allow Alice to sit in her looking-glass and see both worlds together.

Drawing spirals in three dimensions and placing them onto a flat page is extremely difficult to accomplish convincingly and luckily mathematics programs are available for this: Maple V has been used for practically all the diagrams used in this book.

Reference

1 Meikle, H.D., *Modern Radar Systems,* Norwood, Massachusetts: Artech House, 2001.

A New Twist to Fourier Transforms. Hamish D. Meikle

ISBN: 3-527-40441-4

Conventions

The conventions of Maple and a number of programming languages have been used in the text. Generally round brackets are used to

Group expressions $a\,(b + c)$;

Captions for equations (30).

Square brackets are used for indices, ordered lists, and for references

Indices $A[i, j]$, as an alternative to the algebraic form A_{ij} ;

Lists A_list := [red, blue, green] A_list[2] is blue;

References [10].

Curly brackets are reserved for sets

A_set := {red, blue, green} brown in A_set is false.

Two dots are used to indicate a range

$A..B$ is the range from A to B.

The function $\exp(x)$ is used instead of e^x to avoid small print.

The letters i and j are used for $\sqrt{-1}$ in chapters where the omega, ω, and –*f* conventions are used. In most chapters the Fourier transform and inverse are given by

$$\mathrm{F}(f) = \int_{-\infty}^{+\infty} \mathrm{f}(t)\,\exp(-j2\pi ft)\,\mathrm{d}t \qquad \mathrm{f}(t) = \int_{-\infty}^{+\infty} \mathrm{F}(f)\,\exp(+j2\pi ft)\,\mathrm{d}f$$

To be consistent with the literature for mathematical statistics, the ω convention is used for Fourier transforms in Chapter 6 and is labelled by the use of *i*.

$$C(\xi) = \int_{-\infty}^{+\infty} \mathrm{p}(x)\,\exp(+ix\xi)\,\mathrm{d}x \qquad \mathrm{p}(x) = \frac{1}{2\pi}\int_{-\infty}^{+\infty} \mathrm{C}(\xi)\,\exp(-ix\xi)\,\mathrm{d}\xi$$

The European term Gaussian distribution is used for the term "normal distribution", which is common in English texts.

Where Dirac's δ functions are shown in diagrams, their amplitude represents the area under the Dirac δ function.

A New Twist to Fourier Transforms. Hamish D. Meikle

ISBN: 3-527-40441-4

Symbols

The symbols are sorted in the alphabetical orders of the Greek, Roman, and Russian (Cyrillic) alphabets.

Symbol	Meaning	Section
a	A variable or constant	
a	A constant used with Chebyshev tapering	Ch. 5 (21)
β	A variable or constant	
β_1	Pearson skewness	Tbl. 6.1
β_2	Pearson kurtosis	Ch. 6 (15)
γ_1	Fisher skewness	Tbl. 6.1
γ_2	Fisher excess kurtosis	Sec. 6.1.1
$\delta(t)$	Dirac function	
δ_{mn}	Kronecker delta function $\delta_{mn} = 1$ when $m = n$ $\delta_{mn} = 0$ when $m \neq n$	
θ	Angle, radians	
λ	Wavelength (for antennae).	Ch. 5
μ	Population mean	
μ_1	First moment of area of the population	
μ_1'	First moment of area of the population about the origin, μ_1	
μ_2	Second moment of area of the population about the mean, the variance	
μ_2'	Second moment of area of the population about the origin	
μ_3	Third moment of area of the population about the mean	Tbl. 6.1
μ_3'	Third moment of area of the population about the origin.	
μ_4	Fourth moment of area of the population about the mean	Ch. 6 (15)

A New Twist to Fourier Transforms. Hamish D. Meikle

ISBN: 3-527-40441-4

Symbol	Meaning	Section
μ_4'	Fourth moment of area of the population about the origin.	
μ_r'	*r* the moment about the origin	Ch. 6 (17)
ξ	Variable in a characteristic function	Ch. 6 (19)
π	3.14159...	
σ	Population standard deviation	
τ	Spacing of samples, seconds	Fig. 4.10
τ	Time of centre of pulse, seconds	Ch 3. (40)
${}_1F_1$	Confluent hypergeometric or Kummer's function [1, Eq. 13.1.2, p. 504]	Sec. 6.3.5
${}_2F_1$	Hypergeometric function	Sec. 6.4.2
A_t	Constant defining a Taylor tapering characteristic.	Ch. 5
a	Constant	
a_0	The constant part of a Fourier series	
a_m	The *m*th cosine coefficient in a Fourier series	Ch. 3 (2)
b	Constant	
b_m	The *m*th sine coefficient in a Fourier series	
B	Bandwidth, Hz	Ch. 7
$C(\xi)$	Characteristic function	Ch. 6 (19)
c_m	The *m*th combined coefficient in a Fourier series	
$D(\xi)$	Characteristic function (alternative form)	Sec. 6.2
E_+	Positive phase sequence component	Ch. 2 (13)
E_0	Zero phase sequence component	Ch. 2 (13)
E_-	Negative phase sequence component	Ch. 2 (13)
f	Frequency, Hz	Ch. 2 (14)
$F(f)$	Fourier transform with *f*, Hz, as the frequency variable	Ch. 3 (1)
$F(k)$	Discrete Fourier transform with counter *n*	Ch. 4 (3)
$f(t)$	Time waveform with *t*, seconds as the variable	Ch. 3 (1)
$f(x)$	Function of *x*	
$G(f)$	Fourier transform with variable *f*	Sec. 3.4
$g(x)$	Function of *x*	
$H(f)$	Fourier transform	Ch. 5 (51)
$h(t)$	A time function	
i	$\sqrt{-1}$ with $+\omega$ convention	
I	Moment of inertia	Ch. 3 (96)
$Im(z)$	Imaginary part of *z*	
j	$\sqrt{-1}$ with $-f$ convention	
J_n	Bessel function of the first kind order *n*.	
k	A counting variable	
k	Bolzmann's constant 1.38×10^{-23} J/K	Ch. 7
L_{quant}	Quantisation noise	Ch. 4 (25)
m	Sample mean	Ch. 6 (1)

Symbol	Meaning	Section
$M(t)$	Moment generating function	Ch. 6 (16)
m_1	First moment of area of the sample	Ch. 6 (4)
m_1'	First moment of area of the sample about the origin= m_1.	
m_2	Second moment of area of the sample about the mean.	
m_2'	Second moment of area of the sample about the origin	
m_3	Third moment of area of the sample about the mean.	
m_3'	Third moment of area of the sample about the origin	
m_4	Fourth moment of area of the sample about the mean.	
m_4'	Fourth moment of area of the sample about the origin	
M_n'	nth moment	Ch. 3 (80)
M_n	nth moment about the centre of gravity	Ch. 3 (81)
m_r	rth moment about the mean	Ch. 6 (11)
n	Number of columns	Ch. 6 (2)
N	Number of samples	Ch. 6 (1)
N	Number of samples	Ch. 4 (3)
N	A number	
$\overline{NF}$	Noise figure	Ch. 7 (4)
$\bar{n}$	Control constant for Taylor tapering	Ch. 5 (25)
P	The period of integration in a Fourier series	
$P_\gamma(a, x)$	The cumulative gamma distribution (or incomplete gamma) function [1, Eq. 6.5.1, p. 260].	

$$P(a,x) = \frac{1}{\Gamma(a)} \int_0^x \exp(-t) t^{a-1} \, dt$$

$p(x)$	Probability distribution function of x.	
$P(x)$	Cumulative distribution function of x	
$q(x)$	Probability distribution function (alternative) of x.	
r	Radius	
R, S, T	Phases in a three-phase circuit	Sec. 2.2
R	Resistance, O.	Ch. 7
R	Sidelobe voltage ratio	Ch. 5 (19)
$\mathrm{Re}(z)$	Real part of z	
SLL	Sidelobe level, dB	Ch. 5 (19)
s	Sample standard deviation	Ch. 6 (6)
t	Parameter	
t	Time, seconds	
T	Pulse width, seconds	Ch. 3 (28)
T	Temperature, K	Ch. 7 (1)
$T_n(x)$	Chebyshev polynomial of the first kind order n.	Ch. 5 (17)
$v[k]$	kth time sample	Ch. 4 (3)
$W[k]$	The kth weight in a Chebyshev tapering function.	Ch. 5 (21)

Symbol	Meaning	Section
w	Width of an antenna.	Ch. 5
x	x coordinate;	
$X(k)$	variable in a probability distribution function	Ch. 3 (12)
x_k	Sample value	Ch. 6 (1)
y	y coordinate	
y_k	Number in a column	Ch. 6 (2)
z	z coordinate	
$\text{Ш}(t)$	Repetition function	Ch. 3 (99)

Acknowledgments

The author would like to thank Waterloo Maple Inc, the makers of Maple V, who made this book possible and the producers of WordPerfect 6.1 that was used for the text and equations.

Reference

1 Abramowitz, M. and I.A. Stegun, *Handbook of Mathematical Functions*, Dover, New York, 1964.

1
The Fourier Transform and the Helix

The Fourier transform is a common tool in physics, engineering, and statistics. Examples of Fourier transformations are

- A voltage or current that varies with time into its frequency spectrum;
- The illumination function of an antenna into its pattern in sine space;
- The probability density function in statistics into the characteristic function.

The use of the Fourier transform has been introduced into a number of disciplines independently and unfortunately each uses its own convention. Other than finding spectra, antenna patterns, and so on, the Fourier transforms of functions are added or multiplied and then undergo an inverse Fourier transform to produce the required results as in other forms of operational mathematics.

1.1
Fourier Transform Conventions

The conventions in physics, electrical engineering, and statistics are often different and vary from country to country [1].

1.1.1
Fourier Transforms in Physics

As the fundamental unit of angle is the radian and of frequency radians/second, the Fourier transform used in physics and given in mathematics programs (such as Maple) uses the minus omega convention, –ω, given by

$$F(\omega) = \int_{-\infty}^{+\infty} f(t)\, \exp(-i\omega t)\, dt \tag{1}$$

A New Twist to Fourier Transforms. Hamish D. Meikle

ISBN: 3-527-40441-4

Where $F(\omega)$ is the Fourier transform with variable ω;
$f(t)$ is a time function with variable t;
and i is $\sqrt{-1}$.
The inverse transform used here is given by

$$f(t) = \frac{1}{2\pi} \int_{-\infty}^{+\infty} F(\omega) \exp(+i\omega t) \, d\omega \tag{2}$$

This convention will not be used further in this book.

1.1.2 Fourier Transform in Electrical Engineering

Electrical engineers measure frequency in cycles or rotations per second (Hz) so that ω is replaced by $2\pi f$ to give Fourier transforms using the $-f$ convention. The Fourier transform which connects, among others, waveforms and their spectra can be given by [1, p. 381, 4, p. 27]

$$F(f) = \int_{-\infty}^{+\infty} f(t) \exp(-j2\pi ft) \, dt \tag{3}$$

where $F(f)$ is the Fourier transform with variable f;
$f(t)$ is a time function with variable t;
and j is $\sqrt{-1}$.
The inverse transform used here is given by

$$f(t) = \int_{-\infty}^{+\infty} F(f) \exp(+j2\pi ft) \, df \tag{4}$$

Notice that this convention that is used in all chapters, except for Chapter 6, has the convenient property the Fourier transform of the Fourier transform returns the original function. The $1/2\pi$ in (2) is the result of the fact that $df = d\omega/2\pi$.

1.1.3 Fourier Transform in Statistics

In statistics the following form for the Fourier transform to obtain the characteristic function is used to be consistent with other statistics texts in Chapter 6. This convention is called the +omega convention in this book.

$$C(\xi) = \int_{-\infty}^{+\infty} p(x)\ \exp(+i\xi x)\ dx \tag{5}$$

where $C(\xi)$ is the characteristic function with variable ξ;
$p(x)$ is a probability density function with variable x;
and i is $\sqrt{-1}$.

The inverse transform used here is given by

$$p(x) = \frac{1}{2\pi} \int_{-\infty}^{+\infty} C(\xi)\ \exp(-i\xi x)\ d\xi \tag{6}$$

1.2
The Fourier Transform and the Helical Functions

The Fourier transform used by electrical engineers contains the helical function $\exp(-j\ 2\pi ft)$ that interacts with the $f(t)$ function. The function $\exp(+j\ 2\pi ft)$ is shown in Figure 1.1.

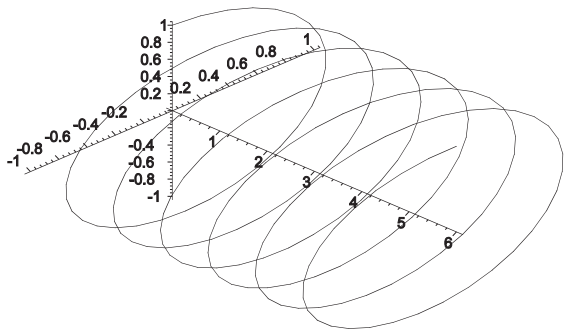

Figure 1.1 The helix $1\exp(j\ 2\pi ft)$.

The coordinates in Figure 1.1 have been chosen to give positive upwards and to the right when looking from the side (in this case a cosine wave) or from the top (in this case a sine wave). Notice that this waveform is balanced, the vector traces a circle, and rotates in the direction called in electrical engineering *positive phase sequence*. The helix in the Fourier transform in (3) has a *negative phase sequence*.

The function $f(t)$ can be also a spatial spiral, so that the Fourier transform in mathematics, engineering, and statistics becomes much easier to understand. The Fourier transform is described in engineering form in Chapter 3, and later chapters, and its use in statistics in Chapter 6.

The helix of radius A can be given by $A\ \exp(j\ 2\pi ft)$, in polar coordinates as $A\angle 2\pi ft$, or may be expressed in Cartesian coordinates as

$$x = A\sin 2\pi ft$$
$$y = A\cos 2\pi ft \quad (7)$$

where A is the amplitude (voltage or current);
x is the horizontal component;
y is the vertical component;
f is the frequency, Hz;
t is time in seconds;
and j is $\sqrt{-1}$.

Pure helices occur in spiral springs and the position of a point on a rotating shaft when plotted in three dimensions against time. This form of illustration may be extended to other phenomena that occur in the distribution of electrical power or signals where the cross-section is not purely circular, examples are

- The most common occurrence of a helical waveform is in the three-phase power distribution used to distribute electricity throughout the world. The voltages and currents in balanced three-phase electrical power circuits at a fixed frequency, typically 50, 60, or 400 Hz may be represented by a single rotating vector and is also true for any electrical system with more than two phases. The phase angle, ϕ, between the voltage and current vectors allows the load factor, $\cos\phi$ to be calculated. The load factor is the ratio of the real power used to the product of voltage and current. When the voltages and currents are not equal the rotating vector no longer traces a circle and symmetrical component theory is used (see Section 2.2). This is also true for radar and sonar echo signals (Section 1.3).
- The modulation of (notional) carrier waves by two-phase quadrature amplitude modulation (QAM) waveforms in communications and echo signals received by radar and sonar from moving objects (Sections 1.3 to 1.5). The vector representation of the waveform does not have a constant radius the form is called in this book a *spatial spiral*.
- Circularly polarised waves (Section 1.7)
- Noise, discussed in Section 1.8, has the form of a *random spatial spiral*.

These waveforms are not able to be displayed on a normal oscilloscope, though those from the individual phases may be. The use of helices to represent these and alternating waveforms gives a physical explanation to the helical function in the Fourier transform and allows their explanation to technicians.

The spatial spiral forms, their appearance in the physical world, calculation methods, and the relationships to alternating functions are described in Chapter 2.

1.3 Radar and Sonar Echo Signals

The waves from radio-frequency transmitters are scattered or reflected by objects they meet. The phase of the waves entering a receiver contain fine distance informa-

tion for the length of the path between transmitter and receiver. In a radar, a coherent oscillator (COHO) is used as a common phase reference for both transmitter and receiver so that differences in phase may be measured. If the scatterer moves towards the radar, the phase angle will decrease with time so that vector detection will give rise to a vector rotating at the Doppler frequency. For a receding scatterer the phase of the vector rotates in the opposite sense, the negative phase sequence. The filtering of such signals is the basis of the rejection of ground echoes that clutter up the radar displays and would overload the equipment that extracts aircraft echoes, for example. Radar (and sonar) echo signals contain a combination of background echo signals and echo signals from approaching and receding objects, that is a direct voltage component and components with both phase sequences. The method of symmetrical components is discussed in Chapter 2.

1.4 Colour Television Signals

The NTSC and PAL colour television systems use quadrature or Cartesian modulation to modulate the two colour difference signals (R–Y and B–Y) onto a common subcarrier. The reference phase is given by the colour burst signal that occurs after the end of each line synchronisation pulse and this is used to keep the subcarrier oscillator at the correct phase. The quadrature outputs of this oscillator are used in the two synchronous detectors to recover the two colour difference signals.

1.5 Modulation and Demodulation

Signal vectors must be represented as two separate signals (normally considered to be voltages) representing the two coordinate systems: Cartesian or polar (each branch of electrical engineering uses different terminology that has changed with time, hence the use of basic English here [2]). Both vector modulation and demodulation may be carried out in terms of these coordinates and are shown in Figures 1.2 and 1.3 [3].

The two phase and amplitude modulation stages in Figure 1.2 may take place in any order since the two processes are linear without any suppression of signals.

1.6 Communications

Digital communications over normal telephone lines is limited to approximately 1200 signal changes per second. To increase the amount of information transferred in each element, a number of types of element must be used that carry more than one bit. Examples are

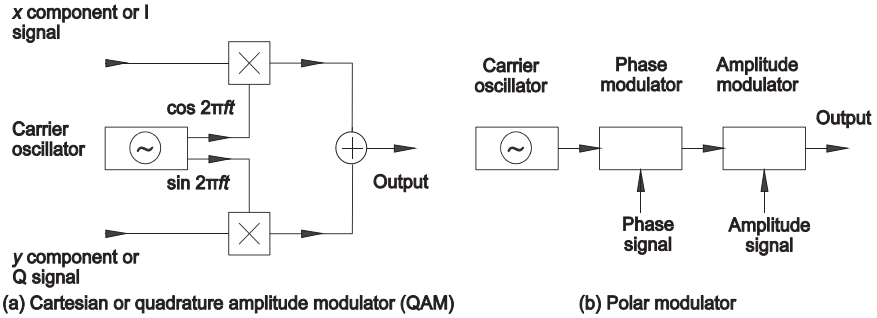

(a) Cartesian or quadrature amplitude modulator (QAM) (b) Polar modulator

Figure 1.2 Vector modulators.

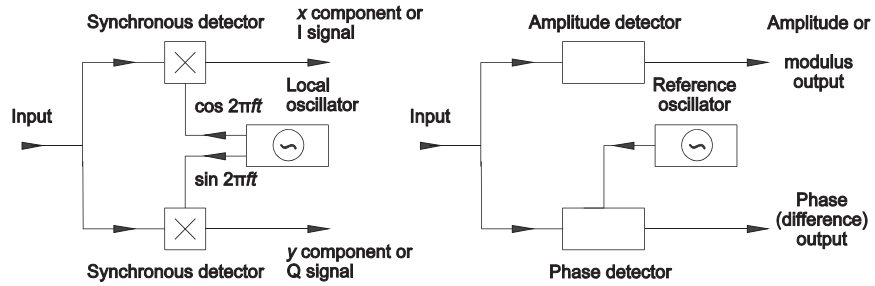

(a) Cartesian or two phase (I and Q) demodulator (b) Polar demodulator

Figure 1.3 Vector demodulators or detectors.

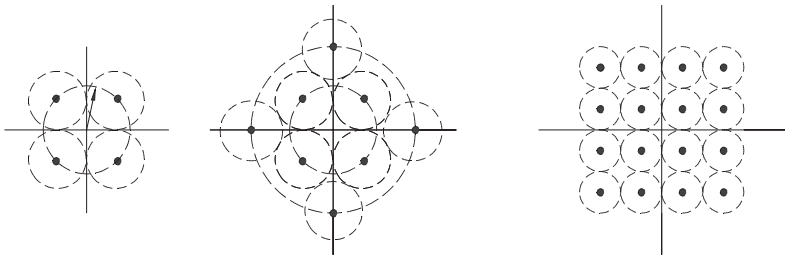

(a) Four state (b) Eight state (c) Sixteen state

Figure 1.4 Signal space or constellation diagrams.

- Phase modulation with more than two states
- Quadrature amplitude modulation (QAM).

In Figure 1.4(a), the four states may be obtained by phase modulation alone. Amplitude and phase modulation are needed in parts (b) and (c) in Figure 1.4. The dots in the state diagram represent the states and the circles around them represent the combined tolerances in the modulation, transmission, and demodulation processes.

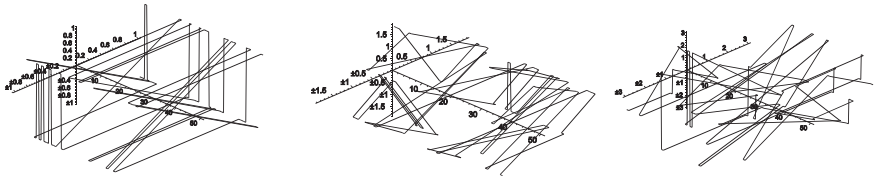

Figure 1.5 The complex waveforms for the four, eight, and sixteen states in Figure 1.4.

The complex waveforms for modulating signals using these states are shown in Figure 1.5. The four-state modulation uses simple phase modulation and the shape of the complex waveform is a box. With more states the complex modulation and when random characters are transmitted, the waveform becomes more like equally distributed noise.

1.7 Circularly Polarised Waves

Circularly polarised electromagnetic waves are generated when either the electric or magnetic component has its phase delayed by 90 degrees. These waves are used in microwave communications to avoid polarisation alignment and radar to reduce rain echoes.

1.8 Noise

The transformation from a recognisable modulation to a complex waveform similar to noise can be heard when logging onto an Internet provider as the protocol tries

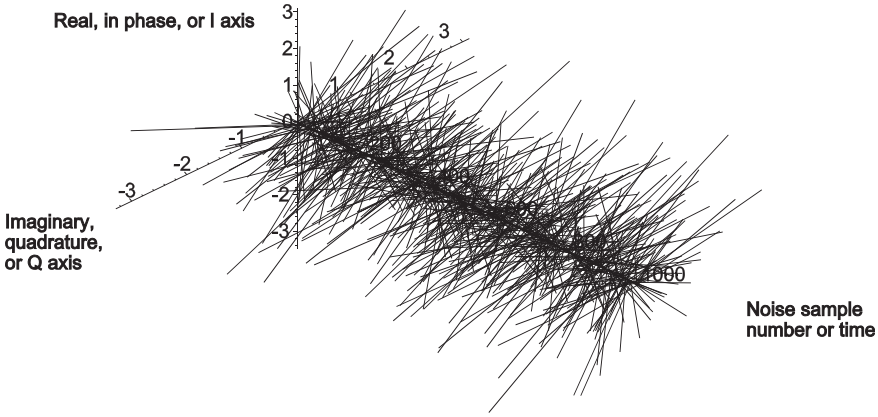

Figure 1.6 Gaussian noise samples demodulated from a (notional) carrier. [Source: Meikle, H.D., *Modern Radar Systems*, Artech House, Norwood, Massachusetts, 2001]

higher and higher transmission speeds. In contrast to communication systems where each state is equally likely, Gaussian noise is normally (Gaussian) distributed in the two Cartesian coordinates and looks like the shaggy bottlebrush in Figure 1.6. Complex noise waveforms are discussed in Chapter 7.

1.9 Other Forms of the Fourier Transform

The Fourier transform in $-f$ notation, discussed in Chapter 3, is the continuous Fourier transform with the limits of integration being from the beginning to the end of time. In real life time is limited and the finite transform is introduced in Chapter 4 together with the discrete Fourier transform for sampled waveforms that lend themselves to manipulation by digital logic and computers.

Erdélyi [4] and others describe the Fourier sine and cosine transforms that, being flat functions, are not treated further. The transforms are

$$\text{Fourier sine transform} = \frac{1}{\sqrt{2\pi}} \int_0^\infty f(x)\, \sin(xy)\, dx$$
$$\text{Fourier cosine transform} = \frac{1}{\sqrt{2\pi}} \int_0^\infty f(x)\, \cos(xy)\, dx \tag{8}$$

Notice that both these transforms are one-sided, the limits for integration are from zero to infinity, in contrast to the exponential transforms elsewhere in this book.

The sampling of signals over finite times, shorter than the length of the signal, puts an unwanted modulation on the transform giving repetition and extra sidelobes and these effects are described in Chapter 4. Chapter 5 shows ways of reducing the sidelobes. Chapter 6 shows the Fourier transforms of probability distribution functions used in statistics in three dimensions. Statistical signals and noise are treated in Chapter 7.

References

1 Press, W.H., B.P. Flannery, S.A. Teukolsky, and W.T. Vetterling, *Numerical Recipes*, Cambridge University Press, Cambridge, England, 1986.

2 Meikle, H.D., *Modern Radar Systems*, Artech House, Norwood, Massachusetts, 2001.

3 Mazda, F. (Ed.), *Telecommunications Engineer's Reference Book*, Butterworth-Heinemann, Oxford, 1993.

4 Erdélyi, A., *Tables of Integral Transforms*, McGraw-Hill, New York, 1954.

2
Spiral and Helical Functions

There are many functions that give a spiral on paper when they are plotted, some examples are given below, though in the rest of the book only the spirals are often in three dimensions called here *spatial spirals*.

Some spirals, in two dimensions, are

- Archimedes [1, p. 68] or arithmetic spiral radius is given by $r = a\theta$.
- Circle involute [1, p. 251] was investigated by Huygens as a possible motion to replace pendulums in ships chronometers. It is given by the parametric equations
  $x = a(\cos t + t\sin t)$
  $y = a(\sin t - t\cos t)$
- Cornu spiral [1, p. 331] is used to describe the diffraction from the edge of a half-plane. It is given in complex form by

$$B(z) = C(t) + jS(t) = \int_0^t \exp(j\pi x^2/2)$$

where $C(t)$ and $S(t)$ are the Fresnel cosine and sine integrals respectively.

- Daisy [1, p. 397], phyllotaxes describe the arrangement of flower petals [1, p. 1355], that are much too numerous to illustrate here.
- Fermat's spiral [1, p. 625] radius is $r = a\theta^{\frac{1}{2}}$
- Hyperbolic spiral [1, p. 867] has a radius given by $r = a/\theta$
- Logarithmic spiral [1, p. 1097] radius is $r = a\ \exp(b\theta)$
- Polygonal spiral [1, p. 1403] is formed by tracing the sides of concentric polygons.

Examples of some of the spirals are shown in Figure 2.1.

Examples in three dimensions are:

- Conical spirals may be used to model sea shells [1, p. 307]. One form of the parametric equations is
  $x = 2[1 - \exp(u/6\pi)]\ \cos u\ \cos^2(v/2)$
  $y = 2[-1 + \exp(u/6\pi)]\ \cos^2(v/2)\ \sin u$
  $z = 1 - \exp(u/3\pi)\ -\ \sin v\ +\ \exp(u/6\pi)$

A New Twist to Fourier Transforms. Hamish D. Meikle

ISBN: 3-527-40441-4

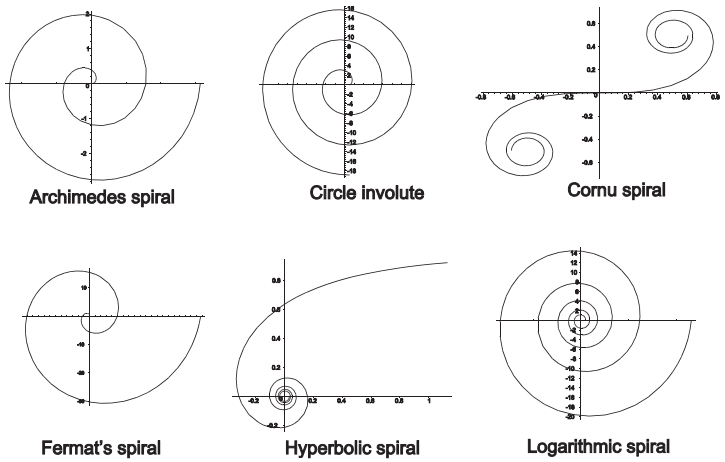

Figure 2.1 Some typical spirals in two dimensions.

- Spherical spirals [1, p. 1698] may describe the course of a ship from north to south poles if it sails at a constant angle to the meridians. The parametric equations are
  $x = \cos t \cos c$
  $y = \sin t \cos c$
  $z = -\sin c$
  $c = \arctan(at)$

These are shown in Figure 2.2.

For the rest of this book only forms of the helix introduced in [3] and the often irregular spatial spirals introduced in [2] are considered.

- Spiral spring or helix [1, p. 811] has the parametric equations
  $x = r \cos t$
  $y = r \sin t$
  $z = c\ t$

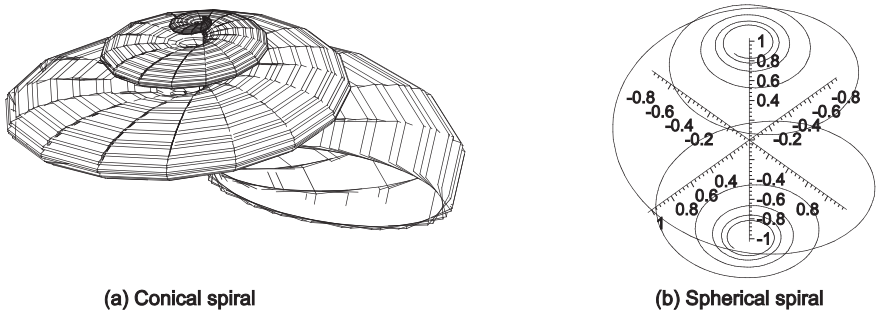

Figure 2.2 Conical and spherical spirals.

The curve is a helix going up and around the z axis that badly represents a polyphase voltage rotating in time [3, Figure 1]. The usual representation of alternating or other waveforms has a horizontal time axis and the sequence of voltages is plotted using the scale given by the vertical y axis. In order to give the same impression on paper when a rotating or other complex function is plotted, the following parametric equations are used

$$x = t$$
$$y = \text{Im } f(t)$$
$$z = \text{Re } f(t)$$

where f(t) is the complex function that varies with time, t.

In order to conform to the left is minus convention the conventional axes are modified[1)] as shown in Figure 2.3(b). This allows the imaginary axis to be used for the orthogonal plotting of frequency for spectra in the next chapter.

If the rotating voltage is constant, the result is a helix. This represents the constant voltage vector present in a balanced polyphase power system.

In the general case, for example signals, the voltage may change in amplitude and vary in phase over a range of 360 degrees (2π radians). The bandwidth of the circuit limits the rate of change and thus the smallest pulse width. When the neighbouring pulses occur at random we have noise (see Chapter 7). Such vector signals may be modulated onto a (notional) carrier or may be carried by three or more conductors at baseband. The signals on the conductors are either x and y Cartesian components (also called I and Q phases) or r (amplitude) and θ (phase) polar components and both may use a common earth return.

Figure 2.3(b) is a powerful way of illustrating both cases and is independent of the vector representation used and whether the processing is analogue or digital. A normal oscillograph can only display the separate signals with time and does not show the vector relationships in amplitude and phase.

A helix with unit amplitude is shown in Figure 2.3(b). If we look from – to + along the imaginary axis, we see the projection of the spiral as a cosine wave and,

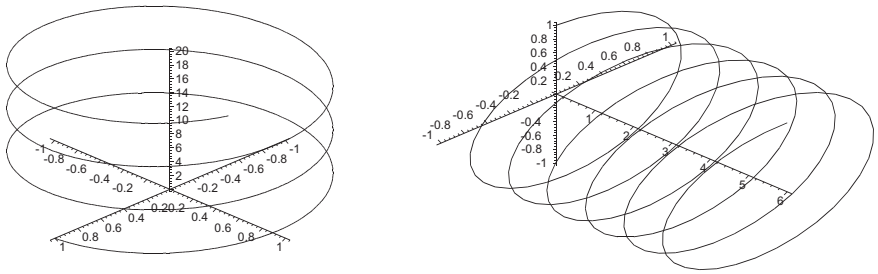

(a) Traditional helix and coordinates

(b) Basic helix in the new coordinates (Section 1.2)

Figure 2.3 The coordinate system used in this book for helices.

1) When the program Maple V is used, the change of coordinates may be accomodated by plots [spacecurve]([t, Im(f(t)), Re(f(t))], t=start..end, *orientation=[–45, 45]*), where t is time.

similarly, along the real (vertical) axis we see a sine wave. Thus the complex representation of the helix is

$$\begin{aligned} f(t) &= r(\cos 2\pi ft + j\sin 2\pi ft) && \text{Cartesian form} \\ &= r\exp(j\,2\pi ft) && \text{Exponential form} \\ &= r\angle 2\pi ft && \text{Polar form} \end{aligned} \tag{1}$$

Notice that the helix may be made to rotate to the right or to the left.

An example of polyphase equipment is the synchronous motor shown diagrammatically in Figure 2.4. The synchronous motor has a rotor winding fed with direct current through slip-rings to give fixed north and south poles. The stator is fed with polyphase current that creates a rotating magnetic field vector and the rotor follows this vector. Three or more stator windings are needed to provide this rotating magnetic field that will rotate, depending on the mains supply frequency, at 50 or 60 times a second (3000 or 3600 revolutions per minute). The speed of the motor may be reduced to a fraction of these speeds by doubling, quadrupling, and so on, the number of poles. The current passing through the stator windings depends on the load. With load the rotor lags the rotating magnetic field and if the motor is used for braking, the rotor leads the rotating field and current is generated. This behaviour may be observed by using a stroboscope illuminating a mark on a disk (this is a case of sampling).

The vectors are subject to the rules of normal complex arithmetic: addition and subtraction are defined in Cartesian coordinates and multiplication and division are defined in polar coordinates.

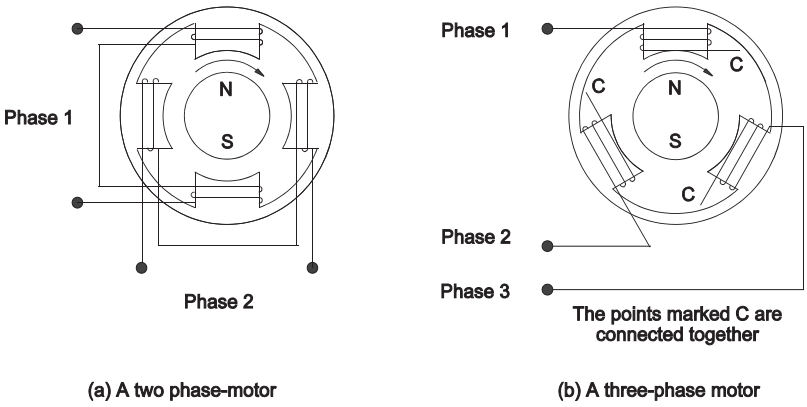

Figure 2.4 Examples of two- and three-phase synchronous motors.

2.1
Complex Arithmetic

A problem with complex arithmetic is that some functions are defined in Cartesian coordinates and others in polar coordinates so that coordinate conversion during calculations is a necessary evil.

2.1.1
Unary Operations

A unary operation is an operation on one number or symbol, in normal arithmetic negation is the changing of the sign or multiplying by –1. Complex arithmetic has the additional operation, the complex conjugate where the imaginary part only is negated or the sign of the phase angle is changed (Table 2.1).

Table 2.1 Unary operations.

Operation	Original function		Operated function	
	Cartesian	Polar	Cartesian	Polar
Negation	$a + jb$	$r \angle \theta$	$-a - jb$	$r \angle (\theta + \pi)$
Complex conjugate	$a + jb$	$r \angle \theta$	$a - jb$	$r \angle -\theta$

These processes are shown graphically in Figure 2.5.

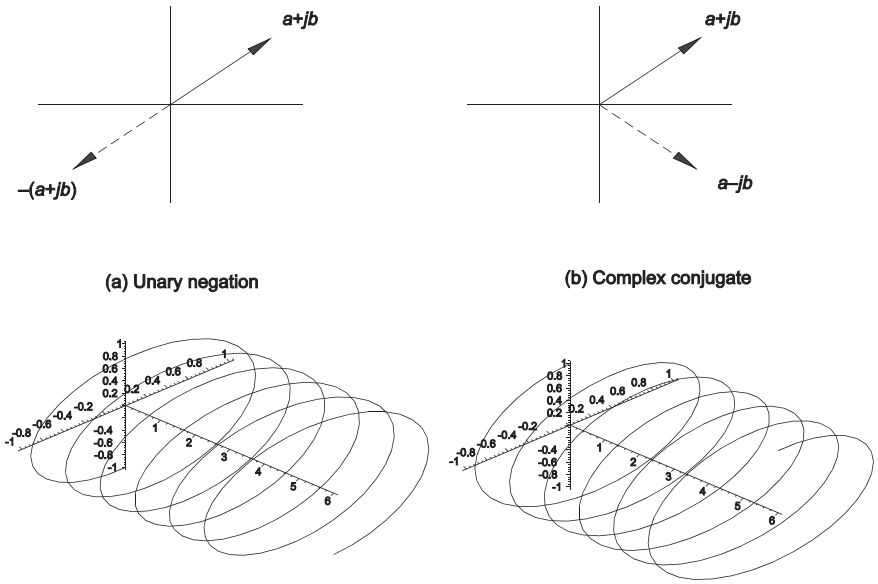

Figure 2.5 Unary negation and the complex conjugate in complex arithmetic.

In the calculation of polyphase electrical power, the voltage vector is multiplied by the current vector with its sense of rotation reversed. The sense of rotation may be reversed either by using a "negative" time or using the complex conjugate, namely

$$V_{\text{right rotation}} = exp(j2\pi ft) = \cos 2\pi ft + j\sin 2\pi ft \tag{2}$$

The complex conjugate is obtained by changing the sign of the imaginary term only

$$\cos 2\pi ft - j\sin 2\pi ft = \exp(\, j2\pi f(-t)\,) = V_{\text{left rotation}} \tag{3}$$

The factor $-t$ in (3) leads to the expression "negative time".

2.1.2 Vector Addition and Subtraction

Addition and subtraction are defined in Cartesian coordinates, namely

$$\begin{array}{ll} \text{Addition} & (a + jb) + (c + jd) = a + c + j(b + d) \\ \text{Subtraction} & (a + jb) - (c + jd) = a - c + j(b - d) \end{array} \tag{4}$$

Addition and subraction are shown graphically in Figure 2.6.

The addition and subtraction of vectors occurs generally in physics. In electrical engineering radar echoes, which exhibit a Doppler frequency shift, have a spatial spiral form and the echo signals from a number of objects in a single range cell are summed (Figure 2.7).

Figure 2.6 Vector addition and subtraction.

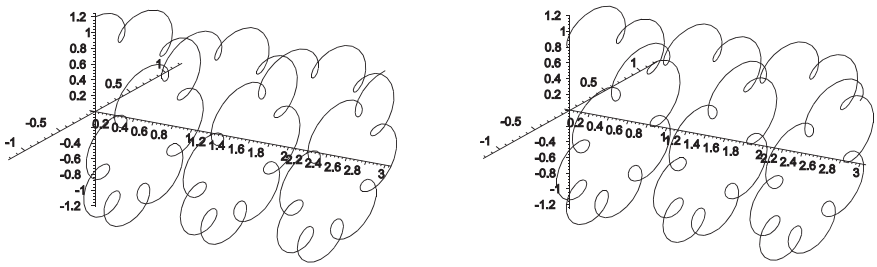

Figure 2.7 The addition and subtraction of spatial spiral waveforms.

2.1.3 Vector Multiplication

Multiplication and division are defined in polar coordinates as in Figure 2.8, namely

$$\begin{aligned}\text{Product} &= A \angle \alpha \times B \angle \beta \\ &= AB \angle \alpha + \beta\end{aligned} \tag{5}$$

which may be expressed in Cartesian coordinates as

$$(a + jb) \times (c + jd) = ac - bd + j(ad + bc) \tag{6}$$

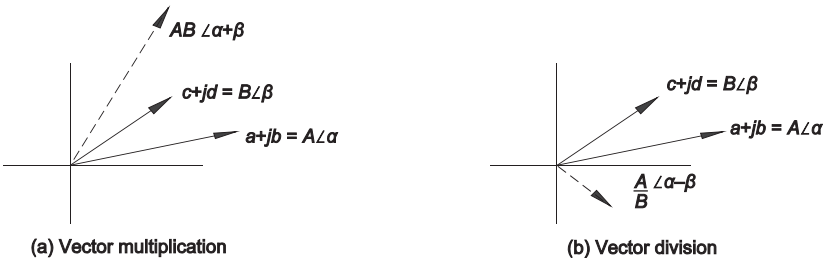

Figure 2.8 Vector multiplication and division.

In direct current theory the power dissipated in a load is the product of the voltage and the current. With alternating current, power is calculated as the product of the voltage and the complex product of the current. For a root mean square voltage V volts at a phase angle α to some reference and a root mean square current I with a phase angle β to the same reference

$$\begin{aligned}\text{Electrical power} &= V \angle \alpha \times I \angle -\beta \quad \text{W} \\ &= VI \cos(\alpha - \beta)\end{aligned} \tag{7}$$

In Cartesian coordinates for a voltage of *a+jb* and current of *c+jd* the electrical power is

$$\text{Electrical power} = (a + jb) \times (c - jd) = ac + bd + j(bc - ad) \text{ W} \tag{8}$$

Figure 2.9 shows the process to calculate the power dissipated in a load, $V \times V^*/R$, where V^* is the complex conjugate of V. Note that both helical components multiply to give a line representing the direct power.

Multiplication is used to calculate power or demodulate when the two waveforms are of the same frequency and for modulation or frequency changing when the waveforms are of different frequencies.

2.1.3.1 Power

For polyphase waveforms the power is calculated by multiplying the voltage by the complex conjugate of the current as shown in Figure 2.10. In the example shown 2V

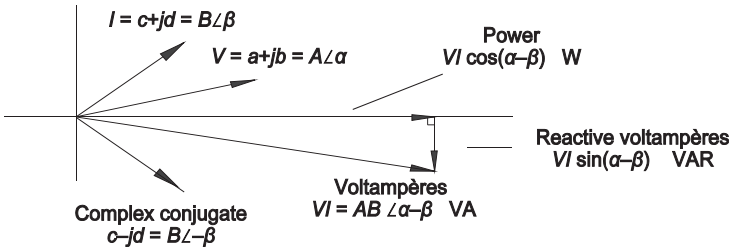

Figure 2.9 The calculation of power with root mean square quantities.

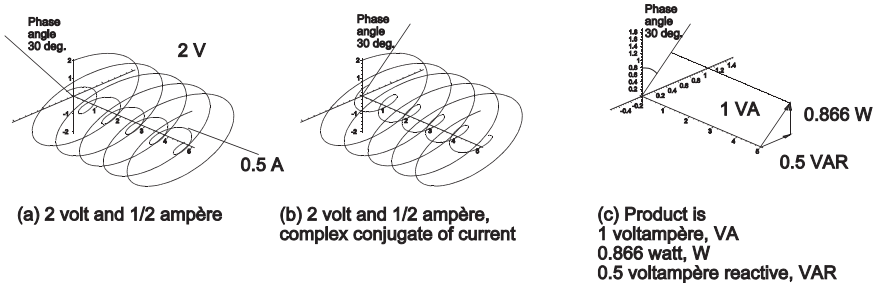

Figure 2.10 Power in a balanced polyphase circuit.

is multiplied by $^1/_2$ A with a phase angle of 30 degrees. The product is 1 VA, and the power is 0.866 W. Notice that the power is constant and not pulsating as in alternating current circuits.

Commonly in signal processing theory a voltage is multiplied by its complex conjugate to give the power that would be dissipated in one ohm. Figure 2.11 shows the power from a 2 V signal. Note that the power factor is always unity with the complex conjugate.

2.1.3.2 **Demodulation**

Figure 2.10 and Figure 2.11 show the effect of synchronous demodulation when a polyphase waveform is "stopped" by its complex conjugate.

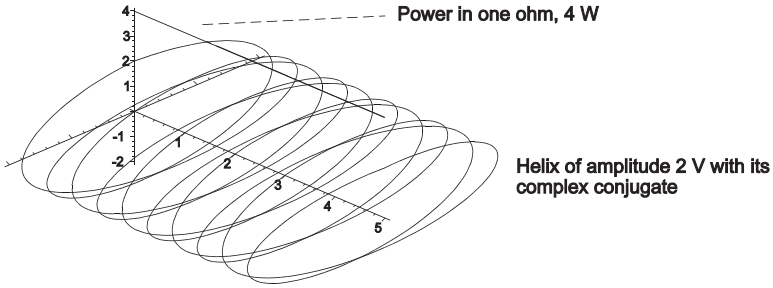

Figure 2.11 The power developed in 1 ohm by 2 V.

2.1.3.3 **Single-sideband modulation**

A number of transmission systems use amplitude modulation with a suppressed carrier wave. Examples are frequency division multiplex telephone transmission where thousands of conversations pass over the same coaxial cable or microwave radio link and short wave radio channels in the same waveband. Both systems use electrical power to transmit the information only and have to replace the carrier wave to demodulate or recover the information. Commonly filters are used but two-phase modulation is used when narrow band filters are not appropriate, as shown in Figure 2.12.

The path ①④⑥⑦ in Figure 2.12 may be described by the sine component in the equation (1) and the path ①③⑤⑦ by the cosine component in (1). When the signals are added the difference frequency is available at the output. If the adding stage is replaced by a subtractor the output is at the sum frequency. The process may be described more simply using polyphase ideas as shown in Figure 2.13.

In some polyphase rotating machinery currents at frequencies that are the difference of the rotation frequency and power-supply frequency are generated, as in the Schrage motor. The effect corresponds to the multiplication of helices and the result is unambiguous and depends on the phase sequence of the spirals.

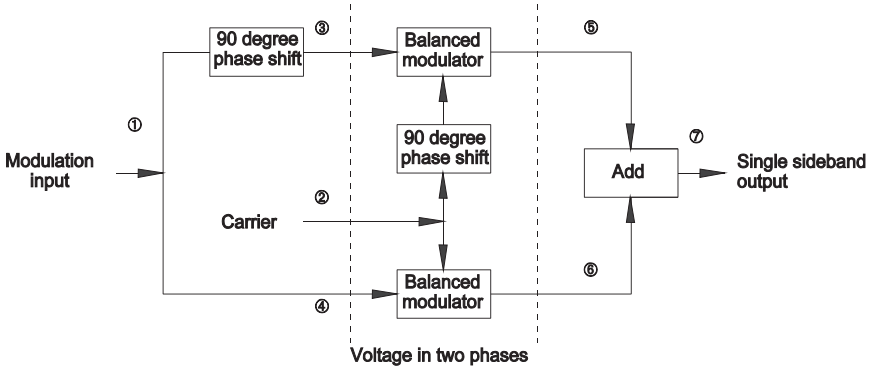

Figure 2.12 The phasing method of single sideband modulation.

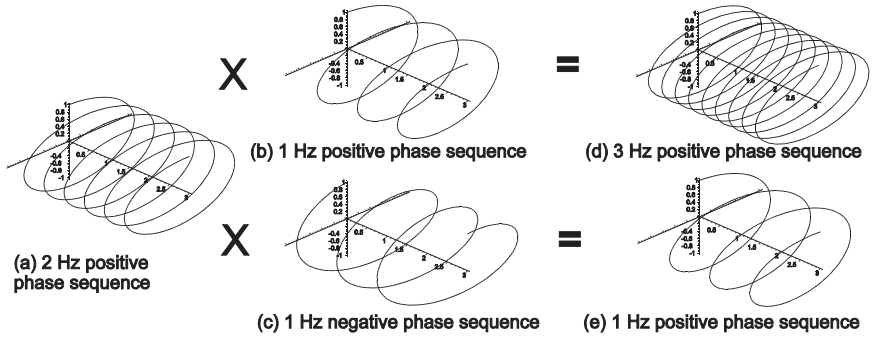

Figure 2.13 The effects of single-sideband modulation.

2.2.1.4 Double sideband modulation

When two sine waveforms of different frequencies are passed through a multiplier, the output consists of two signals at the sum and difference frequencies, namely

$$A\sin 2\pi f_1 t \times B\sin 2\pi f_2 t = \frac{AB}{2}\left(-\cos(f_1 + f_2) + \cos(f_1 - f_2)\right) \tag{9}$$

For two cosine waves

$$A\cos 2\pi f_1 t \times B\cos 2\pi f_2 t = \frac{AB}{2}\left(\cos(f_1 + f_2) + \cos(f_1 - f_2)\right) \tag{10}$$

The output from the perfect multiplier is two signals at the sum and difference frequencies and the desired frequency is selected by filtering. Most modulation processes are not so pure and remnants of both frequencies, harmonics, and cross-modulation signal components are present at the output. Note that the sidebands in amplitude modulation are complex conjugates of each other.

2.1.4 Division

Division is defined in polar coordinates as

$$\text{Quotient} = \frac{A \angle \alpha}{B \angle \beta} = \frac{A}{B} \angle (\alpha - \beta) \tag{11}$$

There are no electrical components that perform pure division.

2.1.5 Powers of Vectors

The calculation of powers of a complex variable is an extension of multiplication, namely

$$\begin{aligned} n^{th}\ \text{power} = (A \angle \alpha)^n &= A^n \angle n\alpha \\ &= A^n(\cos n\alpha + j\sin n\alpha) \quad \text{de Moivre} \end{aligned} \tag{12}$$

Many semiconductor components are nonlinear and produce currents at the harmonics or multiples of the frequency of the applied voltages and are the basis of analogue frequency multipliers.

2.2 Unbalanced Polyphase Voltages and Currents

In polyphase power circuits there is not always the same voltage in each phase nor is the load current the same in each phase. The vector representing voltage or current no longer traces a circular path as in Figure 2.14.

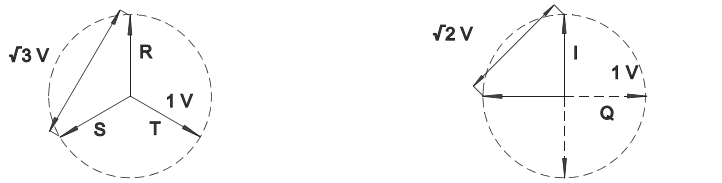

(a) The voltages of the R, S, and T phases (b) The voltages in a two- or four-phase circuit

Figure 2.14 The voltage relationships in two-, three-, and four-phase circuits.

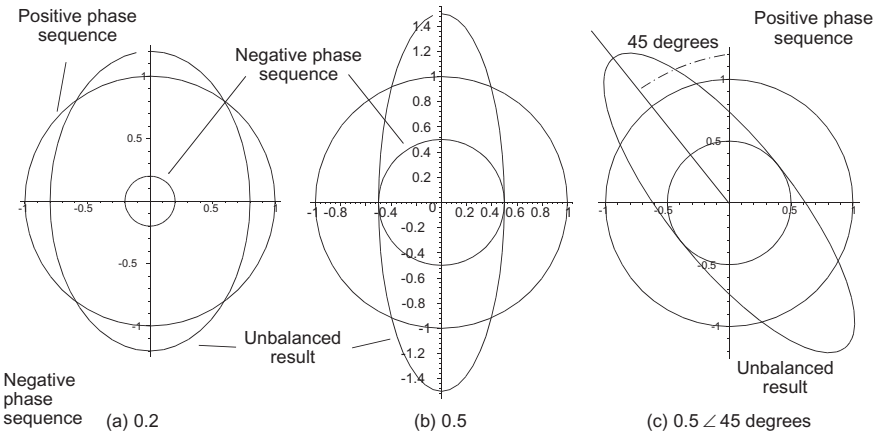

Figure 2.15 The effect of the amplitude and phase of the negative phase sequence component.

Electrical power engineers resolve unbalanced polyphase quantities into symmetrical components [4, 5]. The desired phase rotation is called the postive phase sequence. If the vector traces an elliptical path, the deviation from the ideal circle may be accommodated by a helical component with the opposite phase rotation, called the negative phase sequence component (see Figure 2.15(a) and (b)). The phase angle between the two components determines the direction of the ellipse as shown in Figure 2.15(c).

Figure 2.15(c) also shows the form of the electric or magnetic field inside some types of circular polariser during the process of circular polarisation or back. Figure 2.16 shows the effect of a direct voltage offset or the zero phase sequence component.

The symmetrical components for N phases are calculated from the vector sums [4, p.112]

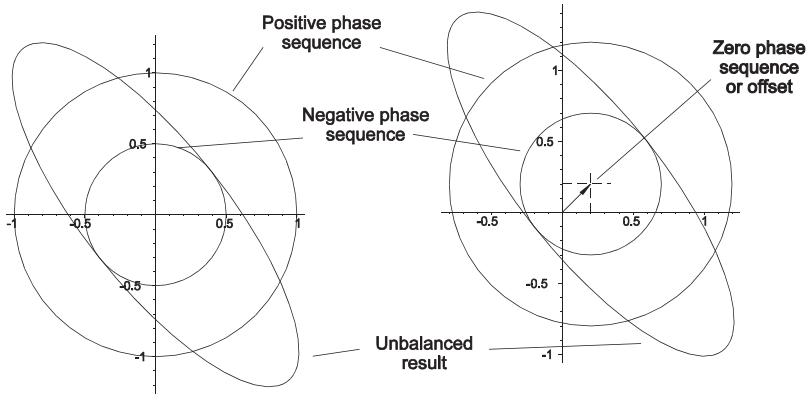

Figure 2.16 The effect of the zero phase sequence component or offset.

$$E_0 = \frac{\sum_{1}^{N} E_n}{N}$$

$$E_+ = \frac{E_1 + \sum_{2}^{N} \lambda^{n-1} E_n}{N} \tag{2.13}$$

$$E_- = \frac{E_1 + \sum_{2}^{N} \lambda^{N-n-1} E_n}{N}$$

where λ is the unit vector representing the phase angle between two adjacent phases, that is

$$\lambda = \exp\left(\frac{j2\pi}{N}\right) = \sqrt[N]{-1}$$

Figure 2.17 shows the addition of an increasing negative phase sequence component to give an alternating waveform when both are equal. Mathematically

$$\cos 2\pi ft = \frac{\exp(j\ 2\pi ft) + \exp(-j\ 2\pi ft)}{2} \tag{14}$$

Conversely an alternating function may be resolved into two contrarotating helices for consideration inside the expression for the Fourier transform.

Analogue-to-digital converters are used to convert signals from receivers, for example in Figure 1.3(a), into a form where they may be handled by digital signal processing systems. Imbalance in the I and Q channels changes the possible circle

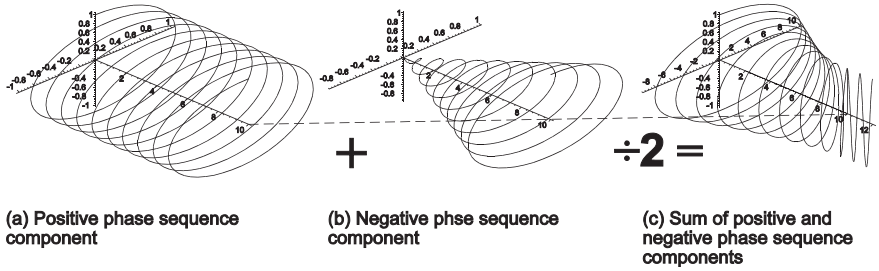

Figure 2.17 The effect of increasing the negative phase sequence component until an alternating waveform occurs.

described by the signal vector into an ellipse, negative phase sequence or image frequency components are generated. The offset represents the residual direct voltage error that must be compensated.

In a polyphase system the phases of the currents in each phase, lead or lag, may be different and this case is also covered by symmetrical components.

References

1 Weisstein, E.W., *CRC Concise Encyclopedia of Mathematics*, Chapman and Hall/CRC, Boca Raton, Florida, 1999.

2 Meikle, H.D., *Modern Radar Systems*, Artech House, Norwood, Massachusetts, 2001.

3 Campbell, G.A. and R.M. Foster, *Fourier Integrals for Practical Applications*, D. van Nostrand Company, Princeton, New Jersey, 1948. This book replaces the paper The Practical Application of the Fourier Integral, *Bell System Technical Journal*, October 1928, pp. 639–707.

4 Say, M.G., *Electrotechnology*, George Newnes, 2nd edn, London, 1955.

5 M.G. Say [4] gives two vague references: Stokvis, L.G. Comptes Rendus, 1914 Fortescue, C.L., The Method of Symmetrical Components Applied to the Solution of Polyphase Networks, AIEE, 1918.

3
Fourier Transforms

The Fourier transform is best known as the link between a waveform, f(t), and its spectrum, F(f). This chapter derives the Fourier transform from the Fourier series and discusses what happens when complex arithmetic or algebra is applied to Fourier transforms. This approach is unusual and Table 3.1 contains a short cross-reference.

Table 3.1 Cross-reference with common terms

Common name	Section in this chapter
Linearity	3.4.1
Scaling	3.4.1
Complex conjugate	3.4.1
Time or frequency shift	3.4.2.1
Modulation	3.4.2.1
Convolution	3.4.2.2
Cross-correlation	3.4.2.3
Autocorrelation	3.4.2.4
Differentiation	3.4.4
Parseval's theorem	3.4.2.6

The Fourier transform is the form used by Woodward [1, p. 27] and is one of three conventions namely,

$$\begin{aligned} \mathrm{F}(f) &= \int_{-\infty}^{+\infty} \mathrm{f}(t)\ \exp(-j\ 2\pi\ f\ t)\ \mathrm{d}t \qquad \text{Transform} \\ \mathrm{f}(t) &= \int_{-\infty}^{+\infty} \mathrm{F}(f)\ \exp(+j\ 2\pi\ f\ t)\ \mathrm{d}f \qquad \text{Inverse transform} \end{aligned} \tag{1}$$

where f(t) is a time waveform with t in seconds;
F(f) is the spectrum with the variable f Hz;
j is $\sqrt{-1}$.

A New Twist to Fourier Transforms. Hamish D. Meikle

ISBN: 3-527-40441-4

The exponential function is recognisable as a helical function from Chapter 2 and the train of ideas leading from the Fourier series to the Fourier transform is described in the next section and the properties of Fourier transforms in the sections that follow.

3.1 From Fourier Series to Fourier Transform

The Fourier series is used to describe non-sinusoidal periodic forms as a series of sinusoidal waves [2, p. 6]. In Figure 3.1 the continuous waveform with period, P seconds, is approximated by a number of sinusoidal waves, a Fourier series, with frequencies $1/P$, $2/P$, etc., Hz.

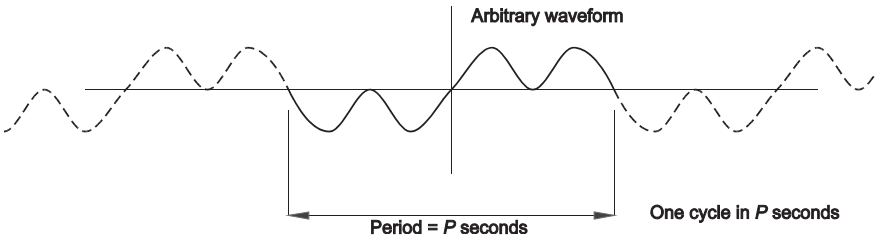

Figure 3.1 An arbitrary waveform of period P seconds.

Further calculations may be made using the components of the Fourier series.

3.1.1 Fourier Series

If f(t) is a repeating time function where the magnitude is integrable over its period. Then the Fourier series is given by

$$f(t) = \frac{a_0}{2} + \sum_{m=1}^{\infty}\left(a_m \cos\frac{2\pi mt}{P} + b_m \sin\frac{2\pi mt}{P}\right) \tag{2}$$

where a_0 is the steady component of the Fourier series coefficients;
a_m are the cosine coefficients;
b_m are the sine coefficients;
m is an integer number of cycles in P seconds.

The values of the coefficients are found by multiplying both sides of (3.2) by $\cos(2\pi kt/P)$ and integrating symmetrically over one period from $-P/2$ to $+P/2$, namely

$$\int_{-P/2}^{+P/2} f(t)\,\cos\frac{2\pi kt}{P}\,dt = \int_{-P/2}^{+P/2} \frac{a_0}{2}\cos\frac{2\pi kt}{P}\,dt$$

$$+\sum_{m=1}^{\infty} a_m \int_{-P/2}^{+P/2} \cos\frac{2\pi mt}{P}\,\cos\frac{2\pi kt}{P}\,dt \qquad (3)$$

$$+\sum_{m=1}^{\infty} b_m \int_{-P/2}^{+P/2} \cos\frac{2\pi mt}{P}\,\cos\frac{2\pi kt}{P}\,dt$$

Using the orthogonality relations of sines and cosines during the period

$$\frac{2}{P}\int_{-P/2}^{+P/2} \sin\frac{2\pi mt}{P}\,\cos\frac{2\pi kt}{P}\,dt = 0 \qquad \text{(a)}$$

$$\frac{2}{P}\int_{-P/2}^{+P/2} \sin\frac{2\pi mt}{P}\,\sin\frac{2\pi kt}{P}\,dt = \delta_{km} \qquad \text{(b)} \qquad (4)$$

$$\frac{2}{P}\int_{-P/2}^{+P/2} \cos\frac{2\pi mt}{P}\,\cos\frac{2\pi kt}{P}\,dt = \delta_{km} \qquad \text{(c)}$$

where δ_{km} is the Kronecker delta function, namely

$$\delta_{km} = 1 \quad \text{when } k = m$$
$$\text{or } 0 \quad \text{otherwise} \qquad (5)$$

Inserting Equations (3.4a) and (3.4b) into (3.3) gives

$$a_k = \frac{2}{P}\int_{-P/2}^{+P/2} f(t)\,\cos\frac{2\pi kt}{P}\,dt, \qquad k = 0, 1, 2, \ldots \qquad (6)$$

The sine coefficients b_k are found by multiplying both sides of Equation (2) by $\sin(2\pi kt/P)$, integrating over one period, and using Equations (4a) and (4c)

$$b_k = \frac{2}{P} \int_{-P/2}^{+P/2} \mathrm{f}(t)\ \sin\frac{2\pi kt}{P}\ \mathrm{d}t, \qquad k = 0, 1, 2, \ldots \tag{7}$$

The Fourier series may be expressed in terms of exponential functions, as

$$\exp(j\theta) = \cos\theta + j\sin\theta \tag{8}$$

Rearranging we have

$$\cos\theta = \frac{\exp(j\theta)\ +\ \exp(-j\theta)}{2} \quad \text{and} \quad \sin\theta = \frac{\exp(j\theta)\ -\ \exp(-j\theta)}{2j} \tag{9}$$

If $\theta = 2\pi kt/P$, and replacing the trigonometric functions in Equation (2) using (3.9), then

$$\begin{aligned}
\mathrm{f}(t) &= \frac{a_0}{2} + \frac{1}{2}\sum_{k=1}^{\infty}\left(a_k(\exp(j\theta)\ +\ \exp(-j\theta)) + \frac{1}{j}b_k(\exp(j\theta)\ -\ \exp(-j\theta))\right) \\
&= \frac{a_0}{2} + \frac{1}{2}\sum_{k=1}^{\infty}\left((a_k - jb_k)\exp(j\theta)\ +\ (a_k + jb_k)\exp(-j\theta)\right) \\
&= \sum_{k=-\infty}^{\infty}\frac{1}{2}(a_k - j\,\mathrm{sign}(k)b_{|k|})\exp(j\theta)
\end{aligned} \tag{10}$$

where the sign function is

$$\begin{aligned}
\mathrm{sign}(k)\ &=\ +1,\ \text{when } k \geq 0 \\
&=\ -1,\ k < 0
\end{aligned} \tag{11}$$

If we define

$$\mathrm{X}(k)\ =\ \frac{1}{2}\ \left(\ a_{|k|}\ -\ j\ \mathrm{sign}\ b_{|k|}\ \right) \tag{12}$$

then Equation (12) reduces to

$$\mathrm{f}(t) = \sum_{k=-\infty}^{+\infty} \mathrm{X}(k)\ \exp(j2\pi kt/P) \qquad k = \ldots, -2, -1, 0, +1, +2, \ldots \tag{13}$$

The orthogonality conditions of Equations (4 a–c) apply to exponential functions, namely

$$\frac{1}{P}\int_{-P/2}^{+P/2} \exp(-j2\pi kt/P)\ \exp(-j2\pi mt/P)\ \mathrm{d}t = \delta_{km} \tag{14}$$

Changing the summation index in Equation (13) from k to m and multiplying both sides by $\exp(-j2\pi kt/P)$ and integrating over the period from $-P/2$ to $+P/2$ and putting these into Equation (14), we have

$$X(k) = \frac{1}{P} \int_{-P/2}^{+P/2} f(t)\ \exp(-j2\pi kt/P)\ dt \tag{15}$$

where $X(k)$ is a discrete series of complex quantities and plots of $X(k)$ must be shown in three dimensions.

3.1.2
Period of Integration for a Fourier Series

The integrals are taken over one period of the composite curve or waveform [2, p. 10]. If, for example, the curve is the sum of a 3 Hz and a 5 Hz sine wave then the sum passes through a fixed chosen value each second (compare with Figure 3.1).

3.1.3
Fourier Transform

The Fourier series with complex coefficients in Equations (13) are given by the integral in (3.15) [2, p. 10]. Multiply both sides of Equation (15) by P to give

$$PX(k) = \int_{-P/2}^{+P/2} f(t)\ \exp(-j2\pi kt/P)\ dt \tag{16}$$

Note that the frequency of the sinusoids with argument $2\pi kt/P$ is k/P. As P becomes arbitrarily large, the spacing between the frequencies k/P and $(k + 1)/P$ becomes arbitrarily small, and the frequency becomes a continuous variable.

Thus the frequency may be defined as

$$f \quad = \quad \text{limit}_{P\to\infty}\ \frac{k}{P} \tag{17}$$

It is assumed that the left-hand side of Equation (16) is meaningful for all P and we define

$$X(f) = \ \text{limit}_{P\to\infty}\ PX(k) \tag{18}$$

Combining Equations (16) and (18) we have

$$X(f) = \int_{-\infty}^{+\infty} f(t) \quad \exp(-j2\pi ft)\ dt \tag{19}$$

3.1.4
Inverse Transform

The signal f(t) may be recovered from its spectrum X(f) using the inverse Fourier transform. The numerator and denominator of the Fourier series with complex coefficients in Equation (13) are multiplied by P to give

$$\mathrm{f}(t) = \sum_{k=-\infty}^{+\infty} P\ \mathrm{X}(k)\ \exp(j2\pi kt/P)\ /P \tag{20}$$

As P tends to infinity, let the difference of frequencies k/P and $(k+1)/P$ be defined as df, that is

$$\mathrm{d}f = \mathrm{limit}_{P\to\infty}\ \frac{k+1}{P} - \frac{k}{P} = \mathrm{limit}_{P\to\infty}\ \frac{1}{P} \tag{21}$$

The summation in Equation (20) becomes an integration as the spectral line separation df becomes arbitrarily small. Thus with Equations (17) and (21)

$$\mathrm{f}(t) = \int_{-\infty}^{+\infty} \mathrm{X}(f)\ \exp(j2\pi ft)\ \mathrm{d}f \tag{22}$$

3.2
Three of the Conventions for Fourier Transforms

The helical function is multiplied by the time function and integrated over all time for each value of frequency, f, to give a plot of the spectrum. The inverse transform "undoes" the helix in the Fourier transform to give the original time waveform. The variable f gives the name f convention that is used with the symbol j for $\sqrt{-1}$ and is used in the greater part of this book.

There is another form which has [3, p. 381].

$$\begin{aligned} \mathrm{F}(f) &= \int_{-\infty}^{+\infty} \mathrm{f}(t)\ \exp(+\,j\ 2\pi\ f\ t)\ \mathrm{d}t \qquad \text{Transform} \\ \mathrm{f}(t) &= \int_{-\infty}^{+\infty} \mathrm{F}(f)\ \exp(-\,j\ 2\pi\ f\ t)\ \mathrm{d}f \qquad \text{Inverse transform} \end{aligned} \tag{23}$$

Physicists, mathematicians, and statisticians use the ω convention given by

$$\mathrm{F}(\omega) = \int_{-\infty}^{+\infty} \mathrm{f}(t)\, \exp(+\, i\, \omega\, t)\, \mathrm{d}t \qquad \text{Transform}$$

$$\mathrm{f}(t) = \frac{1}{2\pi} \int_{-\infty}^{+\infty} \mathrm{F}(\omega)\, \exp(-\, i\, \omega\, t)\, \mathrm{d}\omega \qquad \text{Inverse transform} \tag{24}$$

where $\mathrm{f}(t)$ is a time waveform with t in seconds;
$\mathrm{F}(\omega)$ is the spectrum with the variable ω radians/second;
$\mathrm{d}\omega = 2\pi\, \mathrm{d}f$
i is $\sqrt{-1}$.

This convention is used in Chapter 6 for the characteristic functions, $\mathrm{C}(\xi)$, that are the equivalent of spectra of the probability distributions, $\mathrm{p}(x)$, in statistics. The symbol i is used for $\sqrt{-1}$ in this book where the $+\omega$ convention is used. The term $1/2\pi$ in the inverse transform comes from the fact that $\mathrm{d}f = \mathrm{d}\omega/2\pi$.

There is also an omega form with the signs of the exponential functions reversed.

In eastern Europe there is still another form used for Fourier transforms where the scaling constant is divided between the transform and its inverse, namely [4, p. 591 and 5, p. 1148]

$$\mathrm{F}(\omega) = \sqrt{\frac{2}{\pi}} \int_{-\infty}^{+\infty} \mathrm{f}(t)\, \exp\,(+j\, \omega\, t)\, \mathrm{d}t \qquad \text{Transform}$$

$$\mathrm{f}(t) = \sqrt{\frac{2}{\pi}} \int_{-\infty}^{+\infty} \mathrm{F}(\omega)\, \exp\,(-j\, \omega\, t)\, \mathrm{d}\omega \qquad \text{Inverse transform} \tag{25}$$

Waveforms and their spectra, antenna illumination functions and their antenna patterns, and so on, are linked by Fourier transforms. Students breathe a sigh of relief when they have completed a transform, whereas in everyday life, both sides have to be held in view together and are mostly complex (in two dimensions). If the time and frequency domains are plotted orthogonally in three dimensions, both are

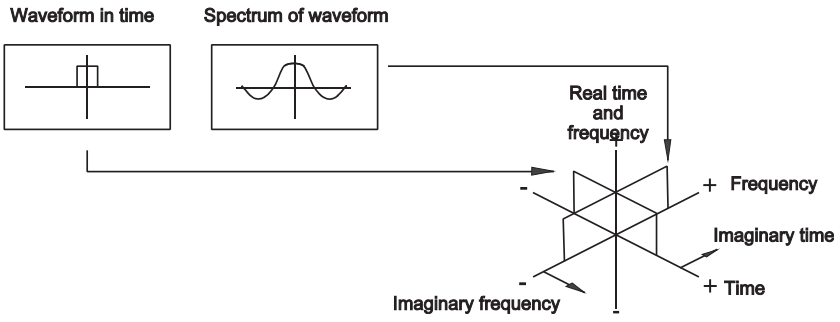

Figure 3.2 The convention used to illustrate Fourier transform pairs.

in view and may remembered at the same time also if the time waveform is complex and not able to be displayed on an oscilloscope. The convention for this is shown in Figure 3.2 and maintains mostly the same view as the separate plots with the capability of the illustration of complex waveforms and spectra.

Note that the direction and use of the axes has been changed from the conventional form and that this form of projection has a quirk: for the conventional view of the imaginary frequency plane, the plane must be viewed from underneath.

3.3 Fourier Transforms and Spatial Spirals

Equation (3.19) gave the mathematical definition of the Fourier transform commonly used in antenna theory and signal processing: Figure 3.3 describes what happens physically with a cosine wave $f(t) = 2\cos 2\pi ft$ with $f = 3$ Hz (Figure 3.3(a)).

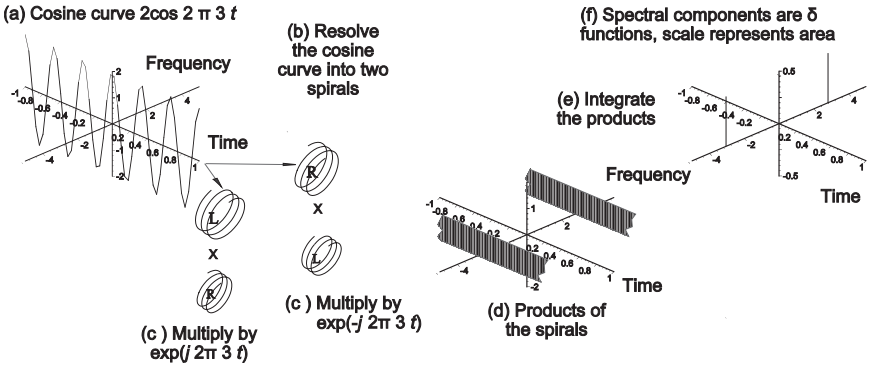

Figure 3.3 Stages in the calculation of the Fourier transform of cos 2π 3 t.

The cosine function is plotted along the time axis (Figure 3.3(a)) and it is resolved into two contrarotating helices in Figure 3.3(b), namely.

$$2\cos 2\pi ft \quad = \quad \exp(+j2\pi ft) \; + \; \exp(-j2\pi ft) \tag{26}$$

Using the rules in Section 2.1.3, the time functions are multiplied by a helix at each frequency on the frequency axis (Figure 3.3(c)) and integrated. The sum of the x and y components of the points around a complete circle is zero, as is the sum of the points around a whole number of turns of a helix around its axis. The spatial spirals when multiplied by a helix will only give a stationary result when the frequency is the same and the rotation is opposite (see Section 2.1.3). This is represented by the shaded surfaces drawn through +3 and –3 on the frequency axis in Figure 3.3(d). When these surfaces are integrated from $-\infty$ to $+\infty$ in time (Figure 3.3(e)) a function of infinite height, width approaching zero, and area unity occurs, the Dirac function. The exponential function in the Fourier transform may be made to match

the cosine function resolved into helices at two frequencies, here +3 Hz and "–3 Hz". Note that there are no negative frequencies, only that one of the helices has a negative phase sequence and that the Fourier transform convention used shows a positive phase sequence as having a "positive" frequency. Conventional mathematics speaks of othogonal functions where

$$\int_a^b \mathrm{f}(x)\ \mathrm{g}(x) = 0 \tag{27}$$

where f(x) and g(x) are said to be orthogonal between the limits a and b. This is the case with sine and cosine functions with the ambiguity that cos(x) = cos(–x) and sin(x) = –sin(–x). In contrast, with spatial spirals there is no such ambiguity.

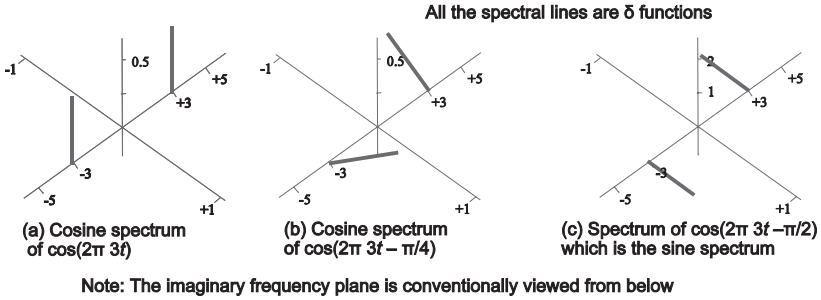

Figure 3.4 The effect of phase shift on cosine spectra to give the sine spectrum.

The cosine waveform is at a maximum at zero time. If the waveform passes through zero time at a point given by a phase angle ϕ, multiplication by the helix gives a vector in the frequency domain. Figure 3.4 shows phase shifts of 45 degrees ($\pi/4$ radians) and 90 degrees ($\pi/2$ radians), the Fourier transform of the sine curve. The coordinate system used has a quirk: though the appearance of the real time and frequency planes as is the imaginary time plane are normal looking from the front, the imaginary frequency plane looks correct only when looking from underneath. Readers will remember that the Fourier transform of a sine curve is a negative delta function for positive phase sequences and a positive delta function for negative phase sequences.

As an example of an event that happens once, a rectangular pulse may be examined of width unity, amplitude unity, and occurring around zero time shown in Figure 3.5.

The pulse is given by

$$\begin{aligned} \mathrm{f}(t) &= 1 \text{ if } t^2 < \frac{T^2}{4} \\ &= 0 \text{ otherwise} \end{aligned} \tag{28}$$

where T is the width of the pulse. Its Fourier transform is

$$\mathrm{F}(f) = \int_{-\infty}^{+\infty} \mathrm{f}(t)\exp(-j2\pi ft)\,\mathrm{d}t = \int_{-T/2}^{+T/2} 1\,\exp(-j2\pi ft)\,\mathrm{d}t$$

$$= \frac{\sin\pi fT}{\pi f} \tag{29}$$

A number of authors name the function rect(t) when T=1. The function sin (πx)/(πx) is so common that it is given the name sinc$x$,

$$\mathrm{sinc}x = \frac{\sin\pi x}{\pi x} \quad \text{when } x = 0,\ \mathrm{sinc}x = 1 \tag{30}$$

and is shown in Figure 3.5.

The sinc function has a number of oddities, for example

- The integral to infinity outside $x = 0.6132$ is zero;
- As x appears in the denominator, the integrals for moments do not converge.

It has been mentioned previously that the integrals of spatial spirals with an integral number of turns are zero. In the case of the rectangular pulse for helices with a frequency of less than 1 Hz the spatial spiral is an arc with equal positive and negative imaginary parts. Integrating over the width of the pulse (in Figure 3.6(a) the pulse width is unity) thus gives a purely real result. At $\pm f$ (here 1 Hz) the turn of the spatial spiral is complete and the integral is zero. Between frequencies of n f Hz, where n is an integer, the turns are not complete and positive and negative values for the integral are possible, which can be seen in Figure 3.6(c).

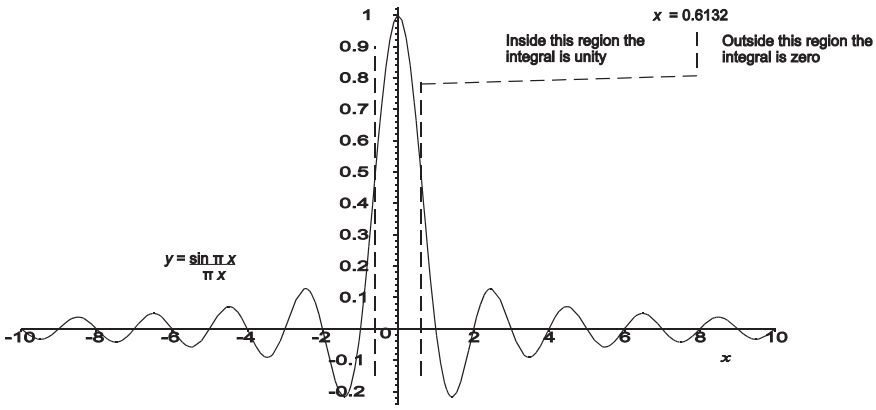

Figure 3.5 The sinc function [After: Meikle, H.D., *Modern Radar Systems*, Artech House, Norwood, Massachusetts, 2001].

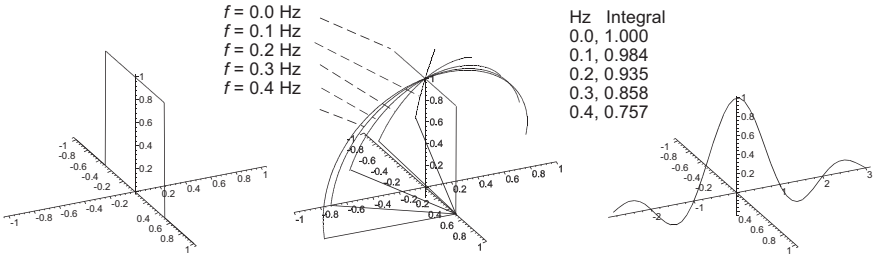

(a) Rectangular pulse (b) Multiply by spirals at *f* Hz (c) Integrate to give spectrum

Figure 3.6 A rectangular pulse and intermediate steps to its Fourier transform.

The spectrum extends to plus and minus infinity in frequency, ever decreasing in amplitude with higher frequency.

When the pulse does not occur at zero time, the Fourier transform may be obtained by changing the limits of integration.

$$\mathrm{F}(f) = \int_{\tau - T/2}^{\tau + T/2} 1 \exp(-j2\pi f t)\, \mathrm{d}t$$

$$= \frac{\sin \pi f T}{\pi f} \exp(-j\, 2\pi f \tau) \tag{31}$$

The result is the original spectrum multiplied by a helical term of pitch $1/\tau$ and this is shown in Figure 3.7 (a) to (c).

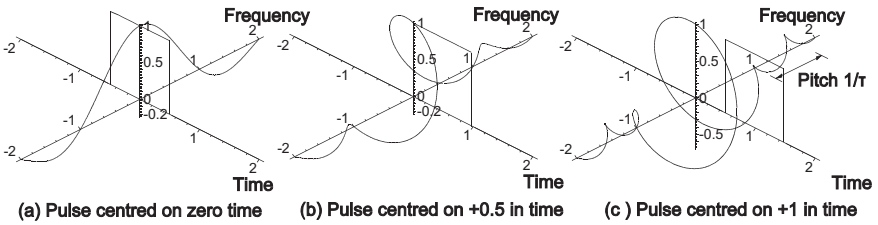

(a) Pulse centred on zero time (b) Pulse centred on +0.5 in time (c) Pulse centred on +1 in time

Figure 3.7 Spectrum of a rectangular as it moves from zero.
[Source: Meikle, H.D., *Modern Radar Systems*, Artech House, Norwood, Massachusetts, 2001]

Illustrations in the form of Figures 3.2 and 3.7 are capable of showing phase angle. Figure 3.8 represents the demodulated vector signal on a carrier where the phase difference is ϕ as the waveform cuts zero time. The vectorial representation of the Fourier transform shows a phase angle of ϕ at zero frequency.

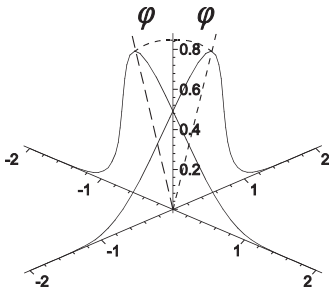

Figure 3.8 The effect of phase shift on the complex spectrum.

3.4 Properties of Fourier Transforms

Relatively few Fourier transforms are available directly and the properties of Fourier transforms are used to build up Fourier transforms from simpler components. These properties may be described in terms of how complex arithmetic or algebra may be used to manipulate the spatial spiral functions in the Fourier transform.

The multiplication of the Fourier transforms of functions is used for convolution, correlation, and the calculation of energies and are discussed generically under multiplication.

The following notation is used: time functions f(t), g(t), and so on, and Fourier transforms F(f), G(f), and so on.

3.4.1 Addition, Subtraction, and Scaling – Linearity

The transform of the sum of two functions is the sum of the Fourier transforms [6, p. 104]

$$f(t) + g(t) \text{ has the Fourier transform } F(f) + G(f) \tag{32}$$

Similarly if the amplitude of a time waveform is multiplied by a factor a, then its Fourier transform is multiplied by the same factor, namely

$$a\, f(t) \text{ transforms to } aF(f) \tag{33}$$

If Fourier transform of f(t) is F(f) then f(at) has the Fourier transform [6, p. 101]

$$f(at) \text{ has the Fourier transform } \frac{1}{|a|}\, F\left(\frac{f}{a}\right) \tag{34}$$

Consequently changing the sign of the time function (see Section 2.1.1) alters the sign of the frequency in the spectrum if a is negative in Equation (34) above.

The Fourier transform of the complex conjugate of a time waveform is given by

$$\begin{aligned} &\text{when } \mathrm{f}(t) \text{ transforms to } F(f) \\ &\text{then } f^*(t) \text{ transforms to } F^*(-f) \end{aligned} \tag{35}$$

The time waveform rotates in the opposite sense giving negative phase sequence spectral components.

3.4.2 Multiplication of Transforms

The multiplication of Fourier transforms may be divided into

- Multiplication by the spectrum of a Dirac delta function or time shift;
- Multiplication of two transforms or convolution;
- Multiplication of a transform by the complex conjugate of another or correlation;
- Multiplication of a transform by its own complex conjugate or autocorrelation.

3.4.2.1 Multiplication by the Spectrum of a Dirac Delta Function – Modulation

The transform of a spatial spiral time waveform is a Dirac delta function at its frequency and conversely a spatial spiral spectrum with pitch $a = 1/T$ is a delta function at time T [6, p. 104].

$$\begin{aligned} &\mathrm{f}(t \pm T) \text{ has the Fourier transform} && \mathrm{F}(f)\ \exp(\pm j2\pi fT) \\ &\mathrm{F}(f \mp a) \text{ has the (inverse) Fourier transform} && \mathrm{f}(t)\ \exp\ (\pm j2\pi ta) \end{aligned} \tag{36}$$

The second function in Equation (36) is also known as single-sideband modulation (see Section 2.1.3).

3.4.2.2 Multiplication of Two Transforms or Convolution

The product of the Fourier transforms of two functions, $\mathrm{F}(f)$ and $\mathrm{G}(f)$, is called convolution. The convolution integral is given by [6, p. 108 and 7, p. 327]

$$\mathrm{H}(f) = \int_{-\infty}^{+\infty} \mathrm{f}(u)\ \mathrm{g}(t-u)\ \mathrm{d}u \tag{37}$$

If $\mathrm{F}(f)\ \mathrm{G}(f) = \mathrm{H}(f)$ then taking the Fourier transform

$$\begin{aligned} \mathrm{H}(f) &= \int_{-\infty}^{+\infty} \mathrm{h}(t)\ \exp(-j2\pi ft)\ \mathrm{d}t \\ &= \int_{-\infty}^{+\infty} \left(\int_{-\infty}^{+\infty} \mathrm{f}(u)\ \mathrm{g}(t-u)\ \mathrm{d}u \right) \exp(-j2\pi ft)\ \mathrm{d}t \\ &= \int_{-\infty}^{+\infty} \left(\int_{-\infty}^{+\infty} \mathrm{f}(u)\ \mathrm{g}(t-u)\ \exp(-j2\pi f(t-u))\ \exp(-j2\pi fu)\ \mathrm{d}u \right) \mathrm{d}t \end{aligned} \tag{38}$$

Changing the order of integration H(f) becomes

$$\begin{aligned} \mathrm{H}(f) &= \int_{-\infty}^{+\infty} \mathrm{f}(u)\, \exp(-j2\pi f u) \left(\int_{-\infty}^{+\infty} \mathrm{g}(t-u)\, \exp(-j2\pi f(t-u))\, \mathrm{d}t \right) \mathrm{d}u \\ &= \mathrm{F}(f)\mathrm{G}(f) \end{aligned} \tag{39}$$

This example uses Gaussian pulses for simplicity, given by (see Figure 3.9(a))

$$\mathrm{f}(t) \;=\; \exp\left(-\pi\left(\frac{-\tau}{T}\right)^2\right) \tag{40}$$

where t represents time in seconds;
τ is the time of the centre of the pulse;
T is the pulse width in seconds.
Such Gaussian pulses centred on 3 and 6 time units are shown in Figure 3.9(a).

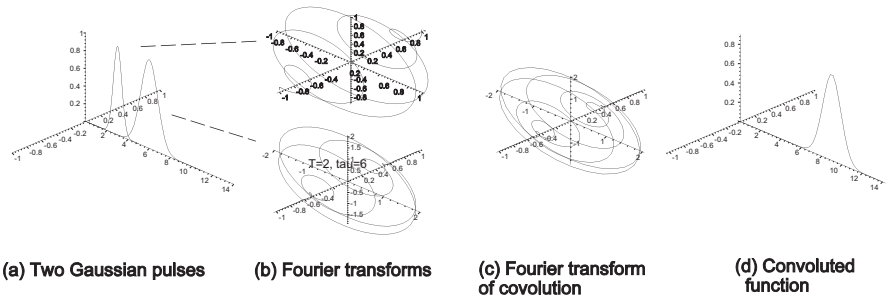

Figure 3.9 The convolution of two Gaussian pulses, after [8].

The Fourier transforms of the Gaussian pulses are given by [10, p. A-12]

$$\begin{aligned} \mathrm{F}(f) &= \int_{-\infty}^{+\infty} \mathrm{f}(t)\, \exp(-j2\pi f t)\, \mathrm{d}t \\ &= T\, \exp(-j2\pi f \tau)\, \exp(-\pi (fT)^2) \end{aligned} \tag{41}$$

Convolution is performed by multiplying the transforms, that is multiplying the moduli and adding the angles to give

$$T_1 T_2\, \exp(\, -j2\pi f(\tau_1 \;+\; \tau_2)\,)\, \exp\Big(\, -\pi f^2 (T_1^2 \;+\; T_2^2)\,\Big) \tag{42}$$

Notice that the process of vector multiplication increases the number of turns per Hz or slope at f=0. The slope is the sum of the slopes of the multiplicands.
The time function is the inverse Fourier transform

$$\mathrm{h}(t) \;=\; \frac{T_1\; T_2}{\sqrt{T_1^2 + T_2^2}}\, \exp\left(-\pi\; \frac{(t - \tau_1 + \tau_2)^2}{T_1^2 + T_2^2}\right) \tag{43}$$

Looking at the exponential function, the width of the Gaussian expression is the root mean square sum of the original Gaussian pulse widths positioned at the sum of the times in Figure 3.9 (a) (see also the sums of centroids and variances at the end of this section).

Traditionally [2] and [6] the example for convolution in most textbooks uses two negative exponential curves and the convolution curve may be obtained analytically. The curves are given by

$$\mathrm{f}(t) \;=\; a\,\exp(-\alpha t) \tag{44}$$

In Figure 3.10(a) the two curves are exp(–t) (a=1, α=1) and 0.5 exp(–2t) (b=0.5, β=2).

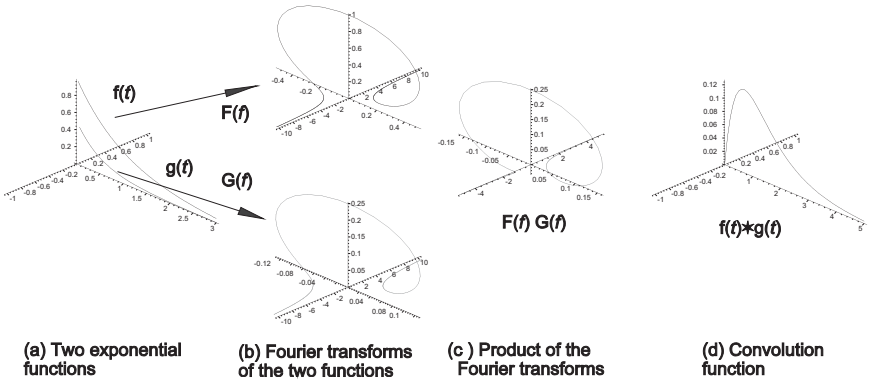

Figure 3.10 The convolution of two exponential functions.

The exponential functions have Fourier transforms of the form

$$\mathrm{F}(f) = \frac{a}{\alpha \;-\; j2\pi f} \tag{45}$$

The product is

$$\frac{a}{\alpha \;-\; j2\pi f}\;\frac{b}{\beta \;-\; j2\pi f} \;=\; \frac{ab}{\alpha\beta+4\pi^2 f^2-j2\pi f\,(\alpha-\beta)} \tag{46}$$

The form of the convolution curve (the inverse Fourier transform) is available using Campbell's and Foster's pair 448 [11]

$$\text{Convolution function} = ab\,\frac{\exp(-\alpha t)-\exp(-\beta t)}{\beta-\alpha} \tag{47}$$

or directly using Equation (37)

$$\mathrm{h}\ (t) = \int_{-\infty}^{+\infty} \mathrm{f}\ (t)\ \mathrm{g}\ (t-u)\ \mathrm{d}u = \int_{-\infty}^{+\infty} \mathrm{f}\ (t-u)\ \mathrm{g}\ (t)\ \mathrm{d}u \tag{48}$$

if f(t) is a negative exponential function, nex, of the form

$$\begin{aligned} \mathrm{nex}(t) &= a\exp(-\alpha t) \quad t > 0 \\ &= 0 \qquad\qquad \text{otherwise} \end{aligned} \tag{49}$$

Performing the convolution "on paper" using Equation (48)

$$a\ \mathrm{nex}(\alpha t) * b\ \mathrm{nex}(-\beta t) = ab \int_{-\infty}^{+\infty} \mathrm{nex}(\alpha u)\ \mathrm{nex}(\beta t - \beta u)\ \mathrm{d}u \quad \text{(a)}$$

$$= ab\ \mathrm{nex}(\beta t) \int_{0}^{t} \exp(\alpha u - \beta u)\ \mathrm{d}u \quad \text{(b)} \tag{50}$$

$$= ab\ \mathrm{nex}(\beta t)\ \frac{\mathrm{nex}(\alpha t - \beta t) - 1}{\beta - \alpha} \quad \text{(c)}$$

$$= ab\ \frac{\mathrm{nex}(-\alpha t) - \mathrm{nex}(-\beta t)}{\beta - \alpha} \quad \text{(d)}$$

The form of the result of convolution of a exp(–αx) and b exp(–βx) is shown in Figure 3.11.

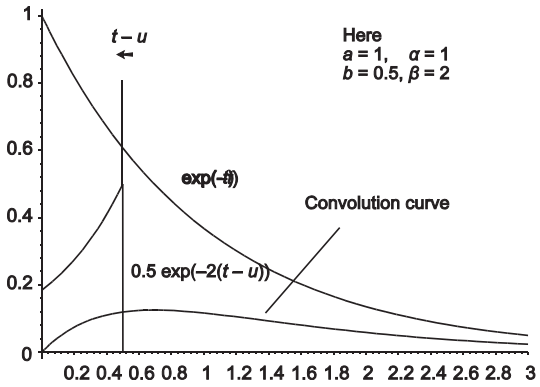

Figure 3.11 The convolution of two negative exponential curves in the example above.

Notice that the smaller of the functions is folded about a vertical line, hence the German term *Faltung* or folding. The convolution curve is a smeared or smoothed version of the individual curves.

The convolution theorem has a number of properties [6, p .110 and 7, p. 328]

- The Fourier transform of a convolution is the product of the Fourier transforms of the individual functions,
  $\mathrm{H}\,(\mathrm{f}(t) * \mathrm{g}(t)) = \mathrm{F}(f)\,\mathrm{G}(f)$
- The transform of a product is the convolution of the Fourier transforms
  $\mathrm{H}\,(\mathrm{f}(t)\,\mathrm{g}(t)) = \mathrm{F}(f) * \mathrm{G}(f)$
- The convolution of two functions is the Fourier transform of the product of their Fourier transforms
  $\mathrm{f}(t) * \mathrm{g}(t) = \mathrm{H}(\mathrm{F}(f)\,\mathrm{G}(f))$
- The product of two functions is the transform of the convolution of their transforms.
  $\mathrm{f}(t)\,\mathrm{g}(t) = \mathrm{H}(\mathrm{F}(f) * \mathrm{G}(f))$
- Convolution follows the rules of multiplication [see 6, pp. 111 – 112]

$$\begin{aligned} f * g &= g * f && - \text{commutive} \\ f * (g * h) &= (f * \mathrm{g}) * h && - \text{associative} \\ f * (g + h) &= f * \mathrm{g} + \mathrm{g} * h && - \text{distributive} \end{aligned} \tag{51}$$

- The moments of the transforms may be used for checking the form of the convolution curve. The "zeroth" moment or area (see Section 3.4.5) is the product of the areas under the individual curves [7, p. 327], namely

$$\begin{aligned} \int_{-\infty}^{+\infty} \mathrm{f}(t) * \mathrm{g}(t)\,\mathrm{d}t &= \int_{-\infty}^{+\infty} (\,\mathrm{f}(u)\,\mathrm{g}(t-u)\,du)\,\mathrm{d}t \\ &= \int_{-\infty}^{+\infty} \mathrm{f}(u) \left(\int_{-\infty}^{+\infty} \mathrm{g}(t-u)\,\mathrm{d}t \right) \mathrm{d}u \\ &= \int_{-\infty}^{+\infty} \mathrm{f}(u)\,\mathrm{d}u \int_{-\infty}^{+\infty} \mathrm{g}(t)\,\mathrm{d}t \end{aligned} \tag{52}$$

The abcissas of the centres of gravities or centroids add [7, p. 327]. If $\langle x \rangle$ is the expected value of x in statistics

$$\int_{-\infty}^{+\infty} \langle\, x\,(\,\mathrm{f}(t) * \mathrm{g}(t))\,\rangle\,\mathrm{d}t = \langle\, x\mathrm{f}(t)\,\rangle + \langle\, x\mathrm{g}(t)\,\rangle \tag{53}$$

where $\langle\, x^n\,\mathrm{f}(t)\,\rangle = \dfrac{\int_{-\infty}^{+\infty} x^n\,\mathrm{f}(t)\,\mathrm{d}t}{\int_{-\infty}^{+\infty} \mathrm{f}(t)\,\mathrm{d}t}$

The variances add also [7, p. 327], as

$$\int_{-\infty}^{+\infty} < x^2 \; (\; f(t) * g(t) \;) \; > \; dt = < \; x^2 \; f(t) \; > \; + \; < \; x^2 \; g(t) \; > \tag{54}$$

Convolution involves a loss of detail and examples of convolution are

- Smoothing of data to remove spikiness;
- Misalignment of the angle between a light slit for the tone tracks on films or the heads on tape recorders.

3.4.2.3 Multiplication of a Transform by the Complex Conjugate of Another or Correlation

If one of the functions in the convolution integral has its sense reversed and replaced by its complex conjugate, the correlation integral is obtained, namely

$$\begin{aligned} h(t) = f(t) \; \star \; g(t) &= \int_{-\infty}^{+\infty} f^*(u-t) \; g(u) \; du \\ &= \int_{-\infty}^{+\infty} f(u-t) \; g^*(u) \; du \end{aligned} \tag{55}$$

The five-pointed star is used to denote correlation in contrast to the asterisk for convolution or complex conjugate. The complex conjugate of a spatial spiral function is also obtained by changing the sign of the time function (see Section 2.1.1), giving

$$\begin{aligned} &\text{Convolution} && h(t) = f(t) \; * \; g(t) = \int_{-\infty}^{+\infty} f(t-u) \; g(u) \; du \\ &\text{Cross-correlation} && h(t) = f(t) \; \star \; g(t) = \int_{-\infty}^{+\infty} f(t-u) \; g^*(u) \; du \\ & && \quad = \int_{-\infty}^{+\infty} f(u+t) \; g(u) \; du \end{aligned} \tag{56}$$

In terms of Fourier transforms [6, p. 46 and 7, p. 352]

$$h(t) \; = \; f(t) \; \star \; g(t) \; = \; F^*(f) \; G(f) = F(-f) \; G(f) \tag{57}$$

Correlation is the inverse of convolution in Section 3.3.2.2 instead of letting one function spread another, correlation finds the measure of commonality between two functions. Correlation may be cross-correlation, the commonality between two functions, or auto-correlation, often used to find the energy in an undefined waveform. Cross-correlation is related to convolution by

$$f(t) \star g(t) = f^*(t) * g(t) \tag{58}$$

Repeating the Gaussian pulse example in Section 3.4.2.2, Figure 3.12 shows what happens when the two pulses are correlated.

In contrast to the Fourier transform for convolution, that for correlation is

$$T_1\ T_2\ \exp(-j2\pi f(\tau_1 - \tau_2))\ \exp\left(-\pi f^2 (T_1^2 + T_2^2)\right) \tag{59}$$

Note that the resultant Gaussian curve is centred on the difference of the timing of the two original curves and the time difference or lag is directly available, and this process is not reversible as is convolution. The time difference is given by the fact that the slopes of the Fourier transforms of the multiplicands subtract.

Repeating the example in Section 3.4.2.2 with correlation, the process and results for two functions of the form f(*t*) = a exp(–α*t*) are shown in Figure 3.13.

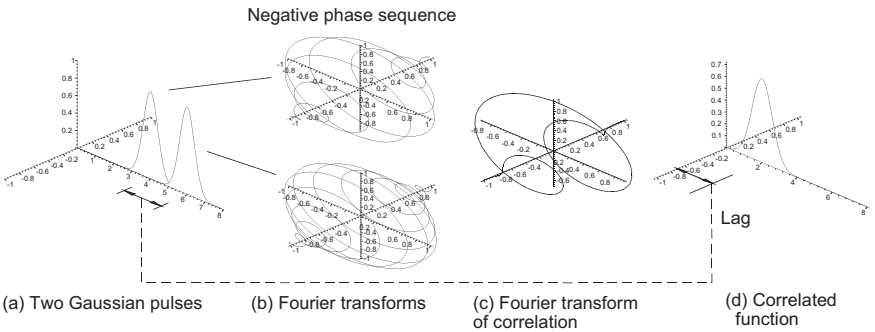

Figure 3.12 The cross-correlation of two Gaussian pulses.

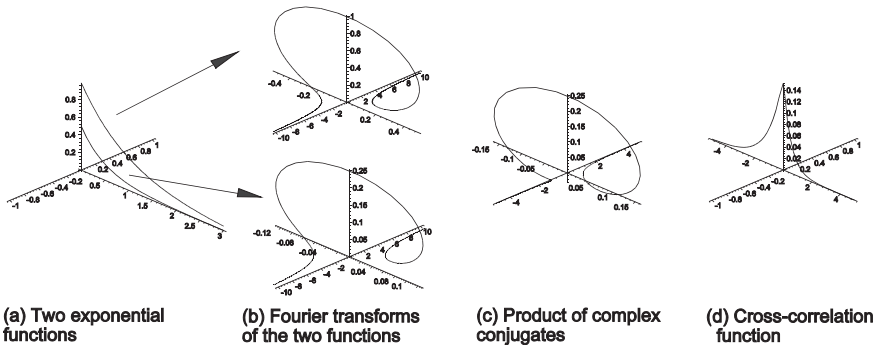

Figure 3.13 The cross-correlation process with negative exponential curves.

They have Fourier transforms of the form

$$\mathrm{F}(f) = \frac{a}{\alpha - j2\pi f} \quad \text{and } \mathrm{F}^*(f) = \frac{a}{\alpha + j2\pi f} \tag{60}$$

and the product is

$$\frac{a}{\alpha - j2\pi f}\ \frac{b}{\beta + j2\pi f} = \frac{ab}{\alpha\beta + 4\pi^2 f^2 + j2\pi f(\alpha - \beta)} \tag{61}$$

The form of the correlation curve (the inverse Fourier transform) is available using Campbell's and Foster's pair 448.8

$$\text{Correlation function} = a\frac{b}{\alpha+\beta}\exp(-\alpha t)\ t > 0$$

$$\text{or } a\frac{b}{\alpha+\beta}\exp(\beta t)\ t < 0 \tag{62}$$

The correlation function in time is available directly as in Section 3.4.2.2 and shown also in Figure 3.14 [6, p. 29].

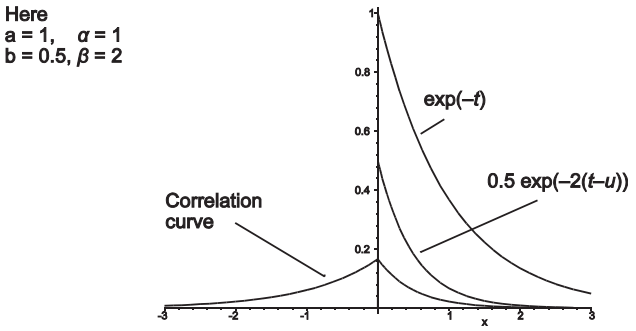

Figure 3.14 The cross-correlation curve for the example in Equation (62).

Using the nex function from Equation (49) in Section 3.4.2.2

$$a\ \mathrm{nex}(-\alpha t)\ \star\ b\ \mathrm{nex}(\beta t) = ab\int_{-\infty}^{+\infty} \mathrm{nex}(-\alpha(u-t))\ \mathrm{nex}(\beta u))\ \mathrm{d}u \tag{a}$$

$$= ab\ \exp(\alpha t)\int_{t}^{+\infty} \exp(-(\alpha u - \beta u))\ \mathrm{d}u\ t > 0 \tag{b 1}$$

$$= ab\ \exp(\alpha t)\int_{0}^{+\infty} \exp(-(\alpha u - \beta u))\ \mathrm{d}u\ t < 0 \tag{b 2}$$

$$= ab\ \frac{\mathrm{nex}(-\alpha t) + \mathrm{nex}(\beta t)}{\beta + \alpha} \tag{c}$$

(63)

The nex function has the value zero when its parameter is less than zero, that is, in contrast to the convolution function in Figure 3.3, the correlation function in Figure 3.6 has a peak at the centre and decays with the constant α to the left and β to the right [6, p. 29].

Cross-correlation over longer time periods is used in selective voltmeters and, over times corresponding to the inverse of the bandwidth, in synchronous detectors.

3.4.2.4 Multiplication of a Transform by its own Complex Conjugate or Autocorrelation

The autocorrelation function is used to find the energy in time waveforms or their spectra and the width of the function is used where the moments of a function are unruly.

Repeating the example in Section 3.4.2.2 for the Gaussian pulse in Equation (3.40) has the Fourier transform

$$\mathrm{F}(f) \;=\; T\,\exp\left(-j\pi f\left(2\tau - jfT^2\right)\right) \tag{64}$$

The product with its complex conjugate is

$$\mathrm{F}(f)\;\mathrm{F}^{*}(f) \;=\; \exp(-2\pi f^2 T^2) \tag{65}$$

The product has no imaginary part so that the autocorrelation function is symmetrical and centred on zero frequency, giving

$$\text{Autocorrelation function} = \frac{\exp\left(-\dfrac{\pi t^2}{2T^2}\right)}{\sqrt{2}T} \tag{66}$$

This process is shown in Figure 3.15.

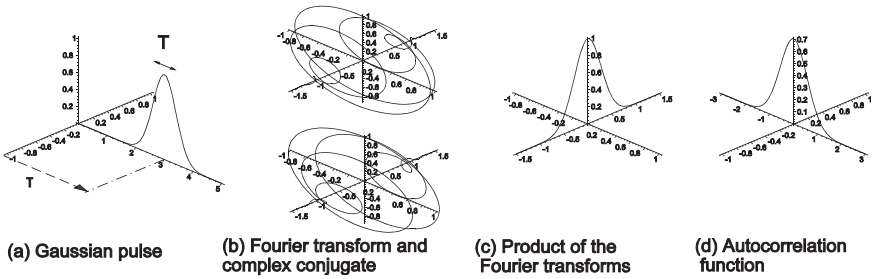

Figure 3.15 The autocorrelation of a Gaussian pulse.

Repeating the example with an exponential waveform, f(*t*)=*a* exp(–α*t*), in Section 3.4.2.2, the product of the Fourier transform with its own complex conjugate is

$$\text{product is } \frac{a}{\alpha - j2\pi f}\;\frac{a}{\alpha + j2\pi f} \;= \frac{a^2}{\alpha^2 + 4\pi^2 f^2} \tag{67}$$

As with the Gaussian function the product is real and symmetrical giving a correlation curve peaked at the centre as in Figure 3.16.

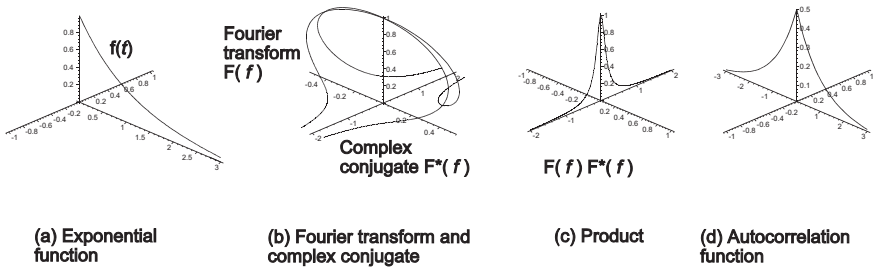

Figure 3.16 The autocorrelation of a negative exponential waveform.

The autocorellation function may be obtained using Campbell and Foster pair 444 and is shown in Figure 3.17.

$$\text{Autocorrelation function} = \frac{a^2}{2\alpha}\exp(-\alpha|t|) \tag{67}$$

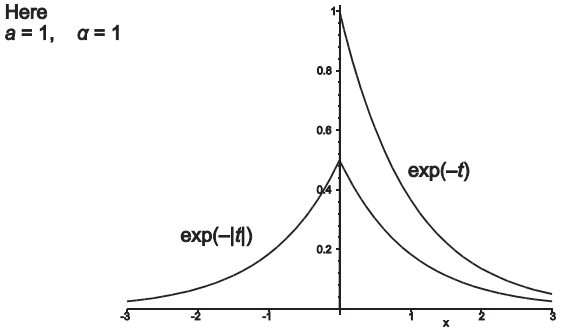

Figure 3.17 An exponential function and its autocorrelation function.

In signal processing the autocorrelation function of a voltage waveform represents the energy dissipated in a resistive load of one ohm.

3.4.2.5 Widths of Functions

It is often useful to give a number representing the width of a function that is not rectangular, for example it is difficult to measure the width of the curve in Figure 3.18 with dividers. Two measures are commonly employed

- The width of a rectangle with the same area and height;
- The root mean square width or second moment of area of the one that is the equivalent of the standard deviation in statistics of a curve of unit height.

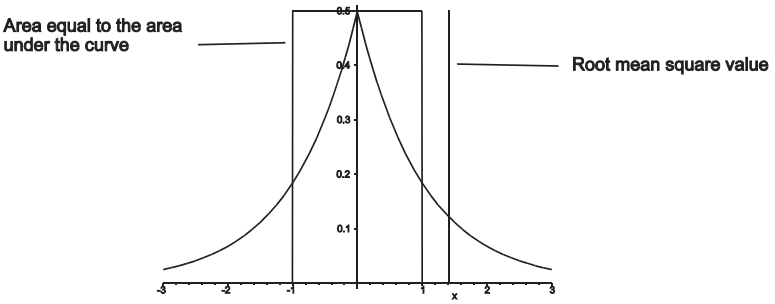

Figure 3.18 The widths of the autocorrelation function in Figure 3.17.

The width of the rectangle with the same area is given by

$$\frac{\text{Area}}{\text{Height}} = \frac{\int_{-\infty}^{+\infty} \mathrm{f}(x)\ \mathrm{d}x}{\mathrm{f}(0)} \tag{69}$$

In the case on Figure 3.18, the area under the curve is unity so the rectangle stretches from –1 to +1.

The root mean square width, σ, is derived from the square root of second moment of area divided by the height, namely

$$\frac{\text{Second moment of area}}{\text{Height}} = \frac{\int_{-\infty}^{+\infty} x^2\ \mathrm{f}(x)\ \mathrm{d}x}{\mathrm{f}(0)} = \sigma^2 \tag{70}$$

It must be noted that the integral for the second moment of area for some shapes does not converge, examples are the $\sin x/x$ function and the Cauchy distribution $1/(1+x^2)$.

3.4.2.6 Energy and Power

Parseval established that the energy in one cycle may be represented by the sum of the energies represented by its Fourier series [7, p. 1317] and this was extended by Rayleigh [6, p. 112] to phenomena represented by Fourier transforms. Later, Plancherel established the conditions under which the theorem is true. The name Parseval is mostly used but all three names are to be found in the literature.

If the voltage or current waveform or spectrum is multiplied by its complex conjugate (see Sections 2.1.3 and 3.4.2.6), the energy dissipated in one ohm is obtained. The same is true if the absolute values are squared, called the Wiener-Khinchin theorem [7, p. 1942]. If the energy is calculated each second then the power is obtained.

The relationship may be expressed mathematically,

$$\int_{-\infty}^{+\infty} \mathrm{f}(t)\ \mathrm{f}^*(t)\ \mathrm{d}t = \int_{-\infty}^{+\infty} |\mathrm{f}(t)|^2\ \mathrm{d}t = \int_{-\infty}^{+\infty} |\mathrm{F}(f)|^2\ \mathrm{d}f = \int_{-\infty}^{+\infty} \mathrm{F}(f)\ \mathrm{F}^*(f)\ \mathrm{d}f \tag{71}$$

3.4.3 Division

Though the division of one spectrum by another is possible, as far as the author is aware, there is no known use.

3.4.4 Differentiation

The Fourier transforms of the derivatives of functions have the following properties:

- The smoother the function, the greater the number of number of continuous derivatives of its Fourier transform;
- The first derivative of a Fourier transform gives the mean of the original function and the second moment with the standard deviation may be found from the second derivative

The classical derivation of the Fourier transform of the differential of the time function, $f'(t)$, as the increment δt tends to zero, is given by

$$\int_{-\infty}^{+\infty} f'(t)\ \exp(-j2\pi ft)\ dt = \int_{-\infty}^{+\infty} \text{limit}_{\delta t\to 0}\ \frac{f(t+\delta t)-f(t)}{\delta t}\ \exp(-j2\pi ft)\ dt$$

$$= \text{limit}_{\delta t\to 0} \int_{-\infty}^{+\infty} \frac{f(t+\delta t)}{\delta t}\ \exp(-j2\pi ft)\ dt \tag{72}$$

$$- \text{limit}_{\delta t\to 0} \int_{-\infty}^{+\infty} \frac{f(t)}{\delta t}\ \exp(-j2\pi ft)\ dt$$

$$= \text{limit}_{\delta t\to 0}\ \frac{\exp(j2\pi f\delta t)\ F(f)\ -\ F(f)}{\delta t}$$

$$= j2\pi f\ F(f)$$

Remembering that $\text{limit}_{\delta t\to 0}\ \frac{\exp(j2\pi f\ \delta t)-1}{\delta t}\ =\ j2\pi f$

If the differentiation is repeated n times, we have for the Fourier transform of $f^n(t)$

$$\int_{-\infty}^{+\infty} f^n(t)\ \exp(-j2\pi ft)dt\ =\ (j2\pi f)^n\ F(f) \tag{73}$$

As an example, a rectangular pulse is shown in Figure 3.19(a). The rectangular pulse may be given in terms of Heaviside steps by

$$\mathrm{f}(t) \;=\; \mathrm{Heaviside}(t-0.5) \;-\; \mathrm{Heaviside}(t-1.5) \tag{74}$$

The Heaviside step has the value zero when $t < 0$ and unity when $t > 0$.

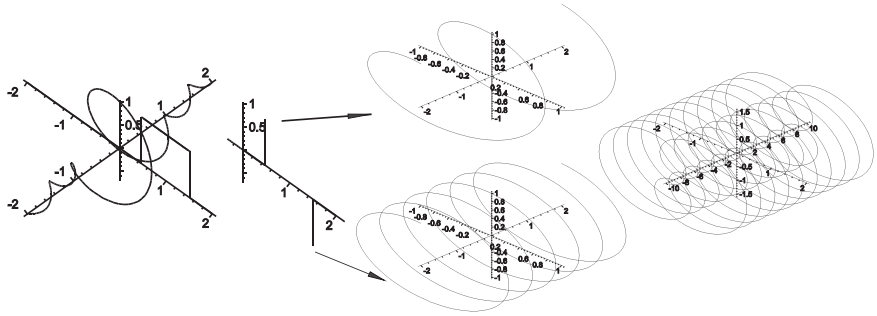

Figure 3.19 Spectrum of the differential of a rectangular pulse.

The spectrum of the rectangular pulse, time function is

$$\mathrm{F}(\mathrm{f}) \;=\; \int_{+1/2}^{+3/2} 1.\exp(-j2\pi ft)\;\mathrm{d}t = \frac{\sin(\pi f)}{\pi f}\;\exp(-j2\pi f) \tag{75}$$

The differential of the rectangular pulse is composed of two Dirac functions

$$\frac{\mathrm{d}}{\mathrm{d}t}\;\mathrm{f}(t) \;=\; \delta(t-\;0.5) \;-\; \delta(t-\;1.5) \tag{76}$$

The spectra of the two Dirac functions are given by $+\exp(-j\pi f) \;-\; \exp(-j3\pi f)$, extend to $\pm\infty$, and are shown separately in Figure 3.19(c) and their sum in Figure 3.19(d). Using the differentiation theorem, the spectrum is

$$j2\pi f \;.\; \frac{\sin(\pi f)}{\pi f}\;\exp(-j2\pi f) \;\;=\;\; \exp(-j\pi f) \;-\; \exp(-j3\pi f) \tag{77}$$

The Fourier transform of the derivative of the convolution $\mathrm{f}(t) * \mathrm{g}(t)$ is [6, p. 119]

$$\mathrm{F}\left(\frac{\mathrm{d}}{\mathrm{d}t}\;(\;\mathrm{f}(t) * \mathrm{g}(t)\;)\right) \;=\; j2\pi f\;\;(\mathrm{F}(f).\mathrm{G}(f)) \tag{78}$$

alternatively the right hand side of Equation (78) may be parsed as

$$\begin{aligned} j2\pi f\mathrm{F}(f)\;.\;\mathrm{G}(f) \;&=\; F\Big(\mathrm{f}'(t) * \mathrm{g}(t)\;\Big) \\ \mathrm{F}(f)\;.\;j2\pi f\;\mathrm{G}(f) \;&=\; F\Big(\mathrm{f}(t)\;* \mathrm{g}'(t)\Big) \end{aligned} \tag{79}$$

Thus the derivative of a convolution is the convolution of either of the functions with the derivative of the other.

3.4.5 Moments

The idea of moments is used generally in physics and the nth moment, μ'_n about the origin is defined as (the letter μ is used to be the same symbol as is used in statistics)

$$\mu_n = \int_{-\infty}^{+\infty} x^n \, f(x) \, dx \tag{80}$$

A number of examples in mechanics and statistics are shown in Table 3.2. In electricity a direct voltage is represented by the statistical mean and the power in an alternating voltage by the variance. Higher-order moments are used in parametric statistics to describe the shapes of probability distributions, often as a test to see how near a distribution in practice is to the theoretical Gaussian or normal distribution. Many measures, such as variance, are the moments about the centre of gravity or mean that are defined as

$$\mu_n = \int_{-\infty}^{+\infty} (x - \bar{x})^n \, f(x) \, dx \tag{81}$$

where μ_n is the nth moment about the centre of gravity;
$\bar{x}$ is the mean value of x, or the first moment divided by the area.

The zeroth moment or the integral of the time waveform is given as the value of the Fourier transform at zero frequency, namely

$$\int_{-\infty}^{+\infty} f(t) \, dt = \int_{-\infty}^{+\infty} f(t) \exp(-j2\pi ft) \, dt\Big|_{f=0} = F(0) \tag{82}$$

A number of examples are shown in Figure 3.20 that have zero phase shift at the origin. Examples of phase shift are shown in Section 3.3.

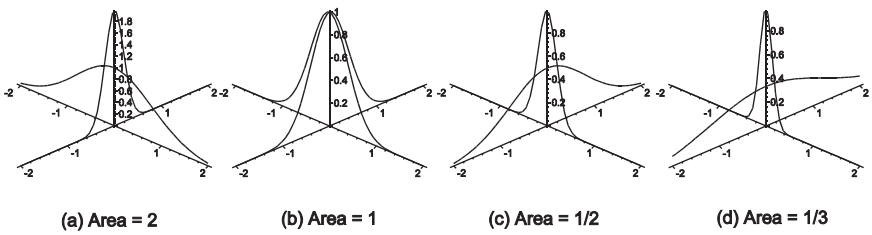

Figure 3.20 The area under the time curve is the ordinate of the spectrum at f=0.

Table 3.2 The use of moments

Moment	Mathematics	Examples Mechanics	 Statistics
0	Integral, μ_0	Area	Area
1	μ'_1	Centroid = μ_1 / μ_0	Mean = μ_1 / μ_0
2	μ'_2	Moment of inertia	Variance, $\mu_2 = \mu'_2 - \mu'^2_1$
3	μ'_3		$\mu_3 = \mu'_3 - 3\mu'_2\mu'_1 + 2(\mu'_1)^3$ Skewness [7, p. 10] = μ'_3 / μ'^3_2
4	μ'_4		$\mu_4 = \mu'_4 - 4\mu'_3\ \mu'_1 + 6\mu'_2\ \mu'^2_1 - 3\mu'^4_1$ Kurtosis (peakedness [7, p. 15]) = μ_4 / μ_2^2

The areas under a number of selected functions are given in Table 3.3.

Table 3.3 Areas of selected functions

Integral from $-\infty$ to $+\infty$		Integral from 0 to $+\infty$	
f(t)	**F(0)**	**f(t)**	**F(0)**
sinc(at)	$1/a$	J_0 (at)	$1/a$
sinc^2(at)	$1/a$	J_1 (at)/t	$1/a$
$\exp\left(-\pi(at)^2\right)$	$1/a$		
$\delta(at)$	$1/\lvert a\rvert$		
$\exp(j\ t)$			

where J_n (x) is a Bessel function of the first kind, order n [9, p. 360, Eq. 9.1.10].

Translation or shifting leaves the value at $f = 0$ unchanged, namely

$$\text{The Fourier transfor m of } f(t-a)\big|_{f=0} \text{ is } \exp(-j2\pi fa)\ F(f)\big|_{f=0} = F(0) \tag{83}$$

The first moment. [6, p. 138] The first moment, as mentioned in Table 3.2 is used in mechanical engineering and statistics and is given by.

$$\mu_1 = \int_{-\infty}^{+\infty} t\, f(t)\, dt \tag{84}$$

Taking the pulse of unit width displaced at +1 from Figure 3.21 as an example, the position of the mean of the time waveform may be calculated from the Fourier transform.

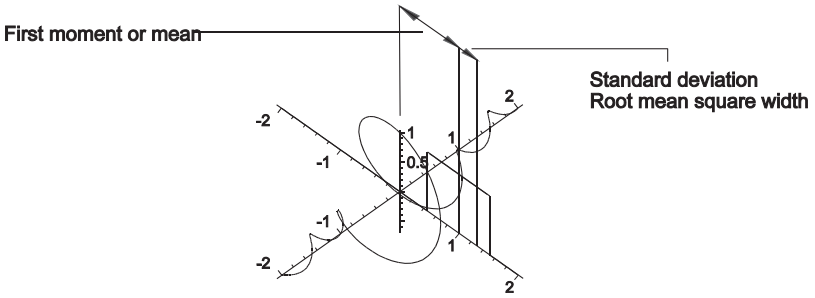

Figure 3.21 A rectangular pulse showing its mean and standard deviation.

The Fourier transform is, by definition

$$\mathrm{F}(f) = \int_{-\infty}^{+\infty} \mathrm{f}(t)\, \exp(-j2\pi ft)\, \mathrm{d}t \tag{85}$$

Differentiating with respect to f

$$\begin{aligned} \mathrm{F}'(f) &= \frac{\mathrm{d}}{\mathrm{d}f} \int_{-\infty}^{+\infty} \mathrm{f}(t)\, \exp(-j2\pi ft)\, \mathrm{d}t \\ &= \int_{-\infty}^{+\infty} -j2\pi t\, \mathrm{f}(t)\, \exp(-j2\pi ft)\, \mathrm{d}t \\ &= -j2\pi \int_{-\infty}^{+\infty} t\, \mathrm{f}(t)\, \exp(-j2\pi ft)\, \mathrm{d}t \end{aligned} \tag{86}$$

Setting $f = 0$ the equation becomes

$$\mathrm{F}'(0) = -j2\pi \int_{-\infty}^{+\infty} t\, \mathrm{f}(t)\, \mathrm{d}t \tag{87}$$

and the first moment μ_1 is

$$\mu_1' = \frac{\mathrm{F}'(0)}{-j2\pi} \tag{88}$$

Extending Equation (88) to the nth moment about the origin, we have, generally

$$\mu_n' = \int_{-\infty}^{+\infty} t^n \, f(t) \, dt = \frac{F^n(0)}{(-j2\pi)^n} \tag{89}$$

where $F^n(x)$ is the nth differential of $F(x)$.

For the example in Figure 3.21, the Fourier transform is

$$\begin{aligned} F(f) &= \int_{1/2}^{3/2} 1 \exp(-j2\pi ft) \, dt \\ &= \frac{\sin(\pi f)}{\pi f} \exp(-j2\pi f) \end{aligned} \tag{90}$$

The Fourier transform is composed of two parts: the $\sin(\pi x)/(\pi x)$ form and the helix $\exp(-j2\pi f)$ that represents the displacement or position of the mean. The first derivative is

$$F'(f) = \left(\frac{\cos(\pi f)}{f} - \frac{\sin(\pi f)}{\pi^2 f^2} - j2\frac{\sin(\pi f)}{f} \right) \exp(-j2\pi f) \tag{91}$$

Taking the limit as f approaches zero, $F'(0)$ tends to $-j\,2\pi$. When this is divided by $-j\,2\pi$ the first moment is unity as shown in Figure 3.22 and Figure 3.23. The $-j$ shows that this is the angle between the curve and the plane through the imaginary axis at $f = 0$.

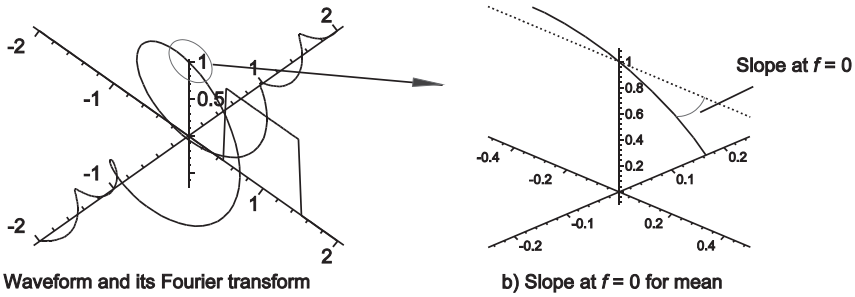

Figure 3.22 Time waveform, its spectrum, and pitch at $f = 0$.

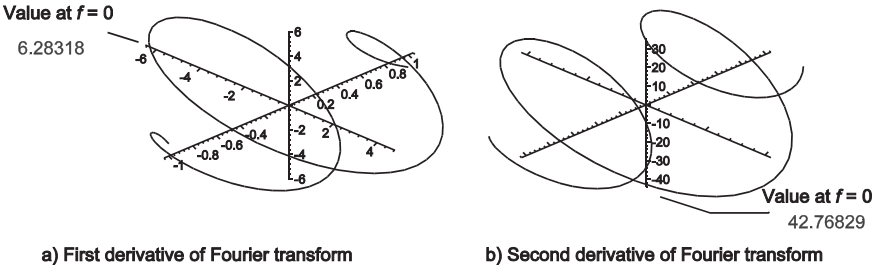

Figure 3.23 Examples of the first and second derivatives.

The centroid, the position of the centre of gravity, or the mean in statistics, is given by the first moment divided by the area, that is

$$\text{Centroid} = \frac{\mu_1'}{\mu_0'} = -\frac{F'(0)}{j2\pi\ F(0)} \tag{92}$$

The first moment at $f = 0$ represents the pitch of the curve as it passes through zero frequency.

Second moment. The second moment is given by

$$\mu_2' = \int_{-\infty}^{+\infty} t^2\ f(t)\ dt \tag{93}$$

Using the second differential of the Fourier transform

$$\begin{aligned} F''(f) = \frac{d}{df}\ F'(f) &= \frac{d}{df} \int_{-\infty}^{+\infty} f(t)\ \exp(-j2\pi ft)\ dt \\ &= \int_{-\infty}^{+\infty} (-j2\pi)^2\ t^2\ f(t)\ \exp(-j2\pi ft)\ dt \\ &= -4\pi^2 \int_{-\infty}^{+\infty} t^2\ f(t)\ \exp(-j2\pi ft)\ dt \end{aligned} \tag{94}$$

Again setting $f = 0$, the second moment about the origin is

$$\mu_2' = -\frac{F''(0)}{4\pi^2} \tag{95}$$

In mechanics, the second moment about the origin is the sum of the square of the first moment plus the moment of inertia, I, squared,

$$\mu_2' = \mu_1^2 + I^2 \tag{96}$$

Dividing by the areas, the second moment about the mean is

$$\mu_2 = \frac{\mu_2'}{\mu_0'} - \left(\frac{\mu_1'}{\mu_0'}\right)^2 \tag{97}$$

In statistics μ_2 is the variance that is the square of the standard deviation s and in signal processing and antenna theory the value s represents the root mean square bandwidth or beamwidth. Note that this is a one-sided value and the normal 3dB widths are double-sided. In the example of the rectangular pulse the value of the ordinate for $f = 0$ in Figure 3.23 is 42.768 giving a second moment μ'_2 of $42.768/4\pi^2 = 1.0866$. Taking out the first moment gives a variance of 1/12 giving a root

mean square bandwidth, beamwidth, or standard deviation of $1/\sqrt{12}$ or 0.2887. Another example is the spatial spiral spectrum generated by the waveform $\delta(t–a)$ namely $\exp(2\pi fa)$. The nth moment of the spectrum is a^n thus the first moment is a and the second is $a^2 - a^2 = 0$, the variance of Dirac's delta function. All higher moments about the mean are also zero.

A further example is the function $\exp(-\pi((t-\mu_1)/s)^2)$. The area is s and the first moment is $\mu_1 s$ giving a mean of μ_1. The second moment is $s^3/2\pi + s\mu_1^2$, and dividing by the area s gives the variance as $s^2/2\pi$.

A summary is given in Table 3.4.

Table 3.4 Summary of centroids and root mean square values

f(t)	Mean or centroid	Variance (root mean square)^2	F″(0)	f″(0)	$(\Delta t)^2$
sinc t	0	Oscillating	0	$-\frac{\pi^2}{3}$	$\frac{1}{12}$
$\text{sinc}^2\, t$	0	∞	∞	$-\frac{2\pi^2}{3}$	∞
$\exp(-\lvert t\rvert)$	0	4	$-16\pi^2$	∞	1
$\frac{1}{1+x^2}$	0	∞	∞	–2	
$\exp(-\pi x^2 a^2)$	0	$\frac{1}{2\pi a^2}$	$\frac{2\pi}{a^3}$	$-2\pi a^2$	$\frac{1}{4\pi a^2}$ 0

The variances of both the sinc$t$ and sinc^2t functions may be calculated over limited values of t on each side. The moments become indeterminate as when $\text{sin}t/t$ is multiplied by t^n to form the moments the expression diverges.

3.5 Special Functions used for Fourier Transforms

A number of extra functions have been proposed as shorthand to describe special shapes and the repeating nature of some waveforms and spectra, for example the rect(t) and the sinc(f) functions in Section 3.2. One of the first, Woodward [1, p. 28], having invented the sinc function (Section 3.3), introduced the repetition function in time shown in Figure 3.24, namely

$$\text{rep}_P\ \text{f}(t) \;=\; \sum_{n=-\infty}^{+\infty} \text{f}(t - nP) \tag{98}$$

where t is the time variable;
P is the period of time for repetition;
n is an integer counter

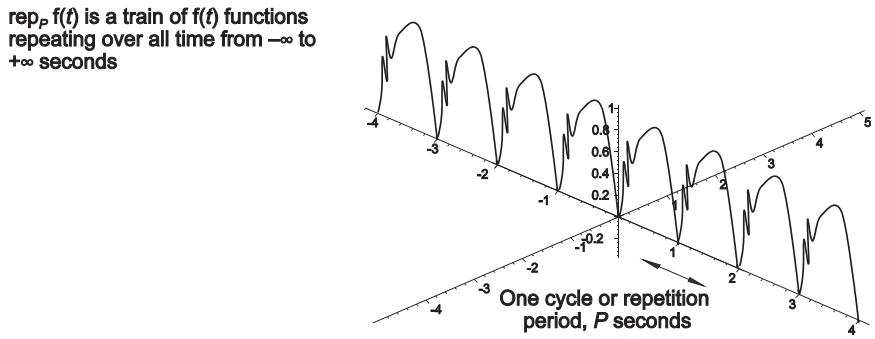

Figure 3.24 The rep or repetition function.

A number of waveforms are defined for one cycle or repetition period only and the rep function extends the definition over all time.

If $\delta(t)$ is a Dirac delta function, then the repetition function becomes a comb function as shown in Figure 3.25. A number of authors use different forms, namely for integer values of n

$$\text{comb}_P = \sum_{n=-\infty}^{+\infty} \delta(t - nP) \quad [10 \text{ p. A} - 83]$$

$$\text{Ш}(t) = \sum_{n=-\infty}^{+\infty} \delta(t - n) \quad [6, \text{ p. } 78] \tag{99}$$

$$\text{comb}_B \ \text{H}(f) = \sum_{n=-\infty}^{+\infty} \text{H}(nB)\ \delta(f - nB)\ [7, \text{p. } 28]$$

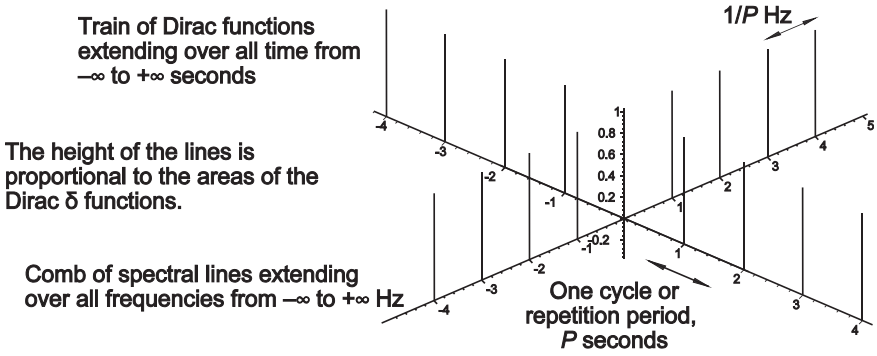

Figure 3.25 The comb or Ш function and its Fourier transform.

Bracewell [6, p. 78] used the Cyrillic letter ШШ (shah) to represent the comb of delta functions with unit period. For other periods the scaling property is used

$$Ш(at) = \frac{1}{|a|} \sum_{n=-\infty}^{+\infty} \delta\left(t - \frac{n}{a}\right) \tag{100}$$

ШШ functions are illustrated in Figure 3.25.
Bracewell expresses Woodward's comb function as

$$Ш(af) * \mathrm{F}(f) = \frac{1}{|a|} \sum_{n=-\infty}^{+\infty} \delta\left(f - \frac{n}{a}\right) * \mathrm{F}(f) \tag{101}$$

Woodward used his comb function to represent a comb of spectral components H(f) and convolution with the delta functions is used for the other forms. Other functions used by Bracewell [6] are

- Π for the rect function
- Λ the triangle function
- H Heaviside function
- sign the signum function.

3.6 Summary of Fourier Transform Properties

Table 3.5 gives a summary of Fourier transform properties [2, p. 24] [6, p. 183].

Table 3.5 Summary of Fourier transform properties

Property	In time domain, f(t)	In frequency domain, F(f)
Linearity	a f(t) + b g(t)	a F(f) + b G(f)
Scaling	f(a t)	$\frac{1}{\lvert a\rvert}$ F$\left(\frac{f}{a}\right)$
Sign change	f(–t)	F(–f)
Complex conjugation	x*(t)	F*(–f)
Time shift	f($t \pm a$)	exp(±j 2 π $f a$) F(f)
Frequency shift[1)]	exp(±j 2 π $f a$) f(t)	F($f \mp a$)
Double-sideband modulation	cos(2πat) f(t)	$^1/_2$ [F(f + a) + F(f – a)]
Differentiation in time domain	$\frac{\mathrm{d}}{\mathrm{d}t}$ f(t)	$j2\pi f$ F(f)
Differentiation in frequency domain	–$j2\pi t$ f(t)	$\frac{d}{df}$ F(f)
Integration in time domain	$\int_{-\infty}^{t}$ f(t) dt	$\frac{\mathrm{F}(f)}{j2\pi f} + \frac{\mathrm{F}(0)\delta(f)}{2}$
Integration in the frequency domain	$\frac{\mathrm{f}(t)}{-j2\pi t} + \frac{f(0)\delta(t)}{2}$	$\int_{-\infty}^{f}$ F(f) df

1) Also called single-sideband modulation

Property	In time domain, f(*t*)	In frequency domain, F(*f*)
Convolution in time domain	$f(t) * g(t)$	$F(f)\,G(f)$
Convolution in frequency domain	$f(t)\,g(t)$	$F(f) * G(f)$
Symmetry	$F(t)$	$f(-f)$
Delta function in time domain	$\delta(t - t_0)$	$\exp(-j2\pi f t_0)$
Delta function in frequency domain	$\exp(-j2\pi f_0 t)$	$\delta(f - f_0)$
Parseval's, Rayleigh's, or Plancherel's theorem	$\int_{-\infty}^{+\infty} \lvert f(t)\rvert^2\,dt$	$\int_{-\infty}^{+\infty} \lvert F(f)\rvert^2\,dt$

3.7 Examples of Fourier Transforms

The purpose of this section is to show the shapes of selected waveforms in their complex form. Accurate values may be calculated these days using commonly available computers. The scales on a number of diagrams show the area of Dirac's δ functions they contain as they have width approaching zero, height approaching infinity.

Other tables of Fourier integrals or transforms are those of Campbell and Foster [11], Erdélyi [12], Bracewell [6], and many other textbooks.

The basic waveform in this book is the polyphase voltage rotating with time extending over all time shown in Figure 3.26.

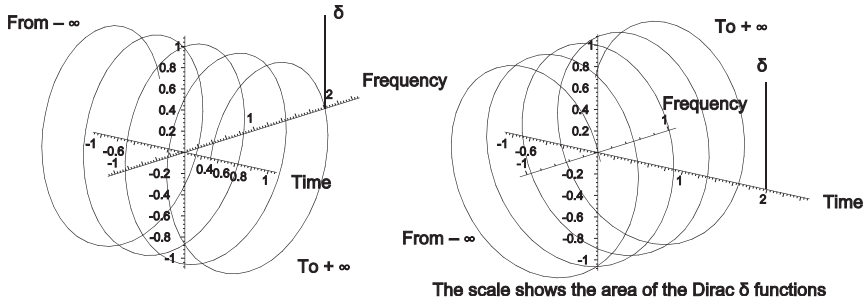

Figure 3.26 The transforms for helical waveforms and spectra.

Left-hand side of Figure 3.26	Right-hand side of Figure 3.26
$f(t) = \exp(j2\pi f_0 t) \quad t = -\infty$ to $+\infty$	$F(f) = \exp(j2\pi t_0 f) f = -\infty$ to $+\infty$
$F(f) = \delta(f - f_0)$	$f(t) = \delta(t - t_0)$

When the spatial spiral does not cut the axis at zero, the phase angle is reflected in the spectrum.

3.7.1
Cosine and Sine Waveforms

Commonly cosine and sine waveforms are used to introduce Fourier series and transforms and these are shown in Figure 3.27. Note that the choice of axes gives the conventional view of the imaginary plane from below, namely the delta function is positive for negative phase sequences; denoted by –*f*.

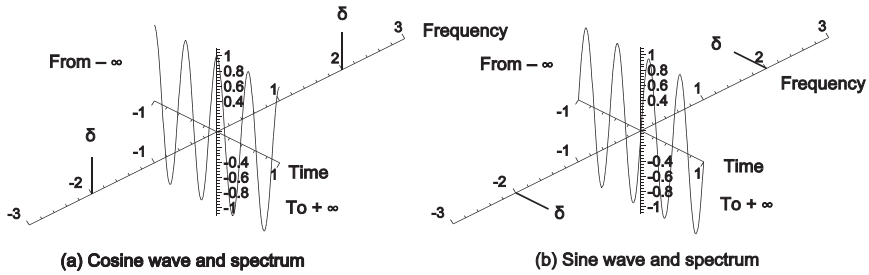

Figure 3.27 The Fourier transforms of sine and cosine waves.

Left-hand side of Figure 3.27(a)
$f(t) = \cos(2\pi_0)\ t = -\infty \,..\, +\infty$
$F(f) = \delta(f - f_0)/2 + \delta(f + f_0)/2$

Right-hand side of Figure 3.27(b)
$f(t) = sin(2\pi_0\, f)\ t = -\infty \,..\, +\infty$
$F(f) = -j\delta(f - f_0)/2 + j\delta(f + f_0)/2$

A cosine half-wave is used as a tapering function in Section 5.2.3.

3.7.2
Rectangular Pulse

The common presentation of the Fourier transform of a rectangular pulse is shown in Figure 3.28(a). The rectangular pulse of width T is given by

$$f(t) = \text{when } t^2 < \frac{T^2}{4} \text{ then } 0 \quad \text{else } 1 \tag{102}$$

Its Fourier transform may be obtained by integrating over the pulse width

$$F(f) = \int_{-\frac{T}{2}}^{+\frac{T}{2}} \exp(-j2\pi ft)\ \mathrm{d}t = \frac{\sin(\pi fT)}{\pi f} = T\ \mathrm{sinc}(fT) \tag{103}$$

The sinc notation is that of Woodward [1].

When the pulse is moved in time, τ, the spectrum assumes the spatial spiral forms of Figures 3.28(b) and 3.28(c).

$$F(f) = \frac{\sin(\pi fT)}{\pi f} \exp(-j2\pi f\tau) \tag{104}$$

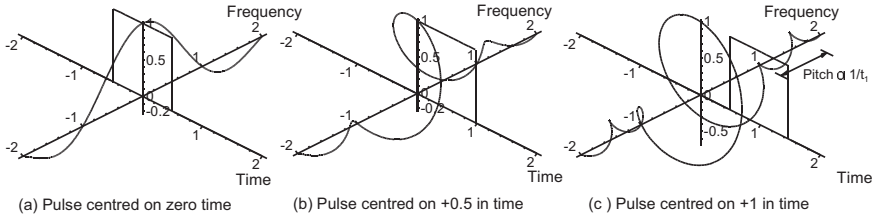

Figure 3.28 Spectrum of a rectangular pulse as it moves from zero. [Source: Meikle, H.D., *Modern Radar Systems*, Artech House, Norwood, Massachusetts, 2001.]

Representations of the rectangular function are given in Section 5.2 1.

3.7.3 Triangular Pulse

The other common function with linear sides is the triangular function that has the Fourier transform

$$\mathrm{F}(f) = \frac{\sin^2 \pi f T}{\pi^2 f^2} \tag{105}$$

The curve is illustrated in Figure 3.29(a) and movement of the peak away from zero time is shown in Figures 3.29(b) and (c). More exact diagrams for a centred triangle are to be found in Section 5.2.1.

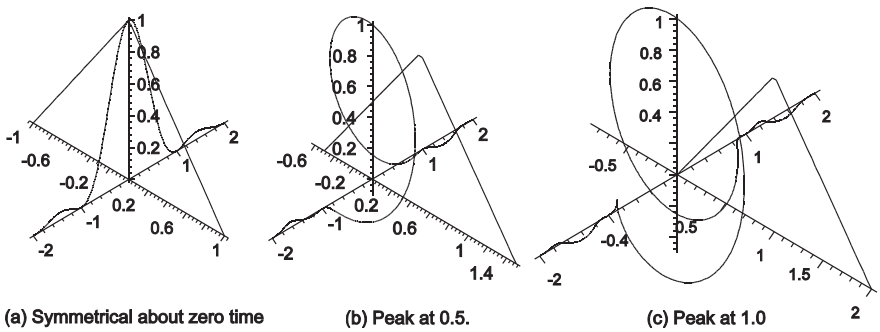

Figure 3.29 The triangle function and its Fourier transform.

3.7.4
Ramp Pulse

The linear ramp is an example of an odd function, that is f(–*t*) = –f(*t*). Very many of the Fourier transforms in everyday practice are complex and are calculated by machine whereas in the text books they are divided into even, f(–*t*) = f(*t*), and odd functions. Truly balanced odd functions have a Fourier transform that is purely imaginary. The function occurring at various times is illustrated in Figure 3.30 and a more exact treatment is to be found in [13, Appendix B].

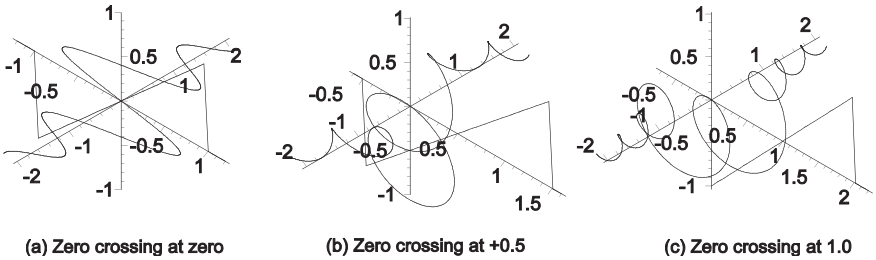

Figure 3.30 Ramp functions and their Fourier transforms.

3.7.5
Gaussian Pulse

Many theoretical discussions and practical approximations use the Gaussian form for simplicity, namely

$$\begin{aligned} f(t) &= \exp(-\pi t^2) \\ F(f) &= \exp(-\pi f^2) \end{aligned} \tag{106}$$

Notice that the Fourier transform of a Gaussian function is another Gaussian function and the functions are shown in Figure 3.31 and with greater detail in Sections 5.2.6 and 6.3.2.

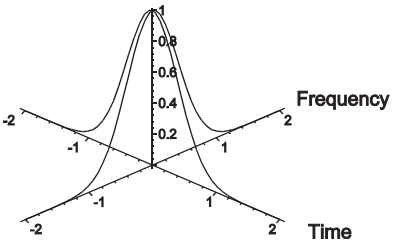

Figure 3.31 The Fourier transform of the Gaussian function.

3.7.6
Unequally Spaced Samples

Until now Fourier transforms have been taken from equally spaced samples from waveforms. An example where the samples may not be equally spaced is the moving target indicator (MTI) processor is used by radar equipment to suppress the signals coming from fixed echoes so that only echoes scattered back from moving objects are displayed [13, Chapter 11]. The vector form of illustration gives a better insight into how the characteristics are changed.

The radial component of velocity is responsible for a Doppler frequency shift in the returned echo signals given by

$$f_{\text{Doppler}} = \frac{2 \text{ Radial velocity}}{\lambda} \tag{107}$$

where f_{Doppler} is the Doppler frequency Hz;
Radial velocity is in m/s;
λ is the wavelength of the radar in metres.

The most common form of radar transmits pulses so that the echo signals are pulses at the pulse repetition frequency of the radar. A typical moving target indicator filter is shown in Figure 3.32 and the delay line has a delay equal to the time between two transmitted pulses.

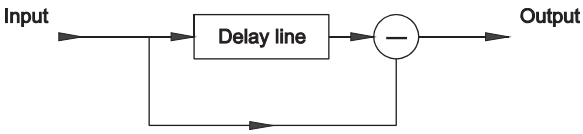

Figure 3.32 A single delay moving target indicator filter for radar.

The impulse response of the filter centred on zero time is

$$f(t) = \delta(t - \tau/2) - \delta(t + \tau/2) \tag{108}$$

where $\delta(t)$ is Dirac's delta function;
τ is the delay line delay or the time between two pulses.

Dirac's delta function is used for simplicity as in real radars the pulses have a near Gaussian shape giving a spectrum that is nearly Gaussian. From Chapter 3 the Fourier transform of a delta function is a spiral. The frequency response is the Fourier transform of Equation (108), given by

$$F(f) = \int_{-\infty}^{+\infty} (\delta(t-\tau/2) - \delta(t+\tau/2)) \exp(-j2\pi ft)\, dt \tag{109}$$

$$= \exp(j\pi f\tau) - \exp(-j\pi f\tau)$$

$$= j2\sin(\pi f\tau)$$

The impulse response and its Fourier transform are shown in Figure 3.33. Note that the convention for showing the imaginary frequency curve requires viewing from underneath. In moving target indicator processing absolute values of the signals are used and most of the later diagrams will only show absolute values.

The curve is a continuous sine characteristic with a period of $2\pi f\tau$. In a typical example of an S-band ($\lambda = 0.1$ m) radar with a range of 60 nautical miles, the pulse repetition frequency is 1000 Hz. The radial velocity for which the response is zero is called the blind speed given by

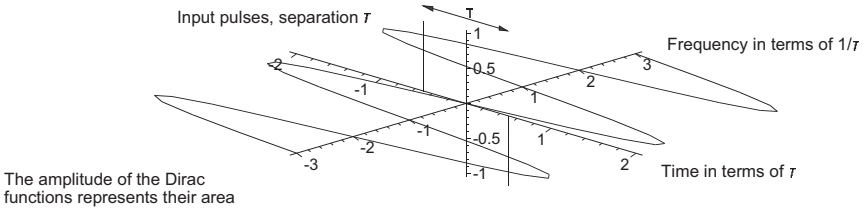

Figure 3.33 The impulse response of a single moving target indicator filter.

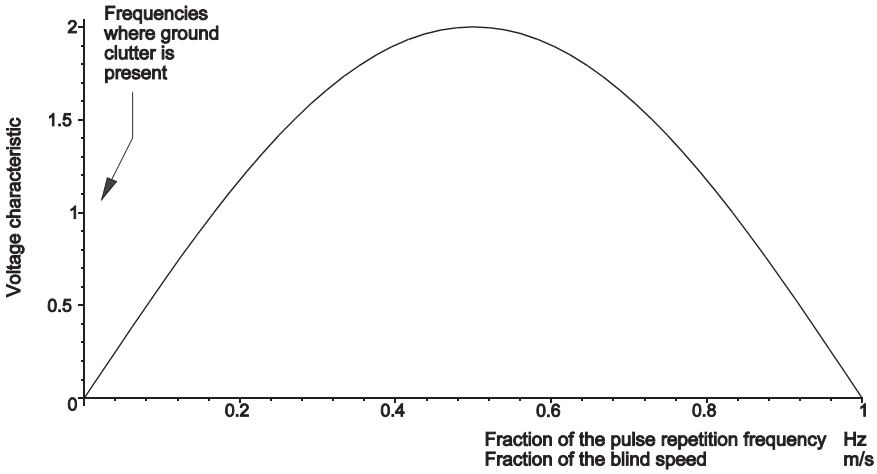

Figure 3.34 The shape of the frequency response (voltage) of a single moving target indicator canceller.

$$\text{Blind speed} = \frac{f_{\text{prf}}\,\lambda}{2}$$

$$= 1000 \times 0.1 / 2 = 50 \text{ m/s} \tag{110}$$

where f_{prf} is the pulse repetition frequency and
λ is the wavelength.

The velocity of 50 m/s is 180 km/h or 97 knots, whereas the radar expects to see aircraft with a radial component of speed between zero and, say, half the speed of sound (Mach 0.5 or 164 m/s).

In order to remove the echo signals from trees, other objects waving in the wind, and ground vehicles, two consecutive stages are used giving a sine squared characteristic with a wider notch, shown in Figure 3.35. Such moving target indicator cancellers are called double delay or three-pulse cancellers.

When the radial component of the aircraft velocity corresponds to the blind speeds, the aircraft will not be seen on the displays of the controllers who are trying to bring it in to land. Before coherent integrating filters were used, one solution was to use unequal periods between the transmitter pulses, called pulse repetition frequency staggering. If the stagger fraction is ε, then the impulse response for a dual delay or three pulse canceller is

$$h(t) = \delta(t + \tau(1 - \varepsilon)) + 2\delta(t) - \delta(t - \tau(1 + \varepsilon)) \tag{111}$$

Note when canceller stages are cascaded the effect is to give binomial weighting, namely, $-(1 - x)^2$ or $-1 + 2x - x^2$.

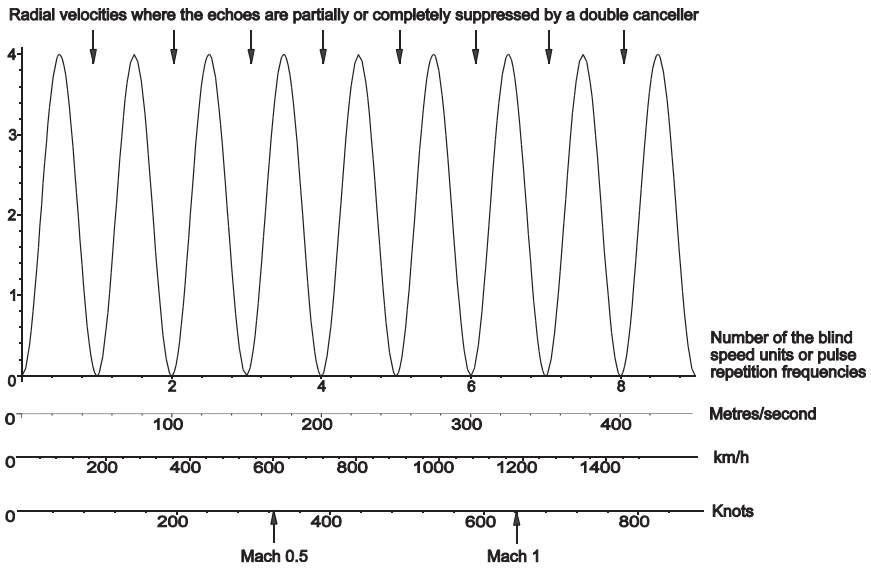

Figure 3.35 The radial velocity for the double canceller in the example.

The Fourier transform is the sum of two contrarotating helices of different frequencies shown in Figure 3.36 and given by

$$\mathrm{F}(f) = \int_{-\infty}^{+\infty} (\,\delta(t+\tau(1-\varepsilon)) + 2\delta(t) - \delta(t-\tau(1+\varepsilon)))\exp(-j2\pi ft)\,\mathrm{d}t$$

$$= -\exp(\,j2\pi f\tau(1-\varepsilon)) + 2 - \exp(-j2\pi f\tau(1+\varepsilon)) \qquad (112)$$

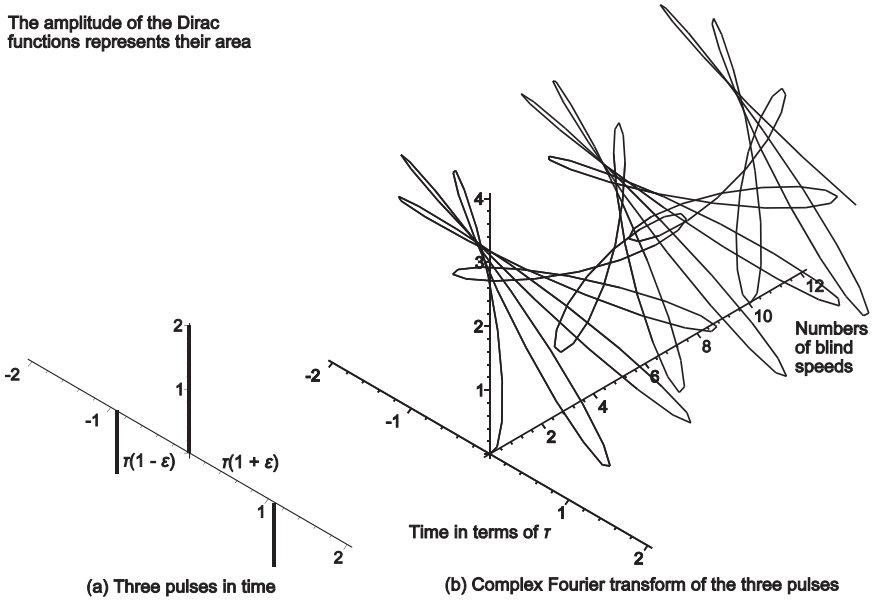

Figure 3.36 The frequency characteristic of a staggered moving target indicator filter (staggering fraction, $\varepsilon = 0.1$).

The two contrarotating spirals in (112) with different frequencies (ratio $1 + \varepsilon : 1 - \varepsilon$) give a number of fingers that rotate around the constant 2. Instead of the characteristic touching the frequency axis every blind speed in the unstaggered case, the fingers nearer the frequency axis cause the minima when the modulus is plotted in Figure 3.37. A real blind speed, in this example, first occurs at ten times the original blind speed. This allows aircraft to be seen by the radar flying at all radial velocities at least up to the speed of sound without blind notches.

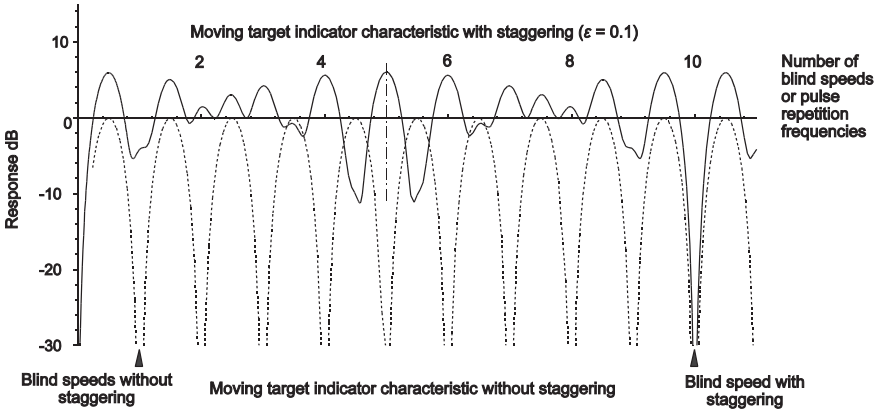

Figure 3.37 Dual canceller moving target indicator characteristics in the example radar without and with staggering (ε = 0.1).

References

1 Woodward, P.M., *Probability and Information Theory with Applications to Radar*, 2nd edn, Pergamon Press, Oxford, 1964.

2 Elliott, D.F., and K.R. Rao, *Fast Transforms*, Academic Press, Orlando, Florida, 1982.

3 Press, W.H., B.P. Flannery, S.A. Teukolsky, and W.T. Vetterling, *Numerical Recipes*, Cambridge University Press, Cambridge, 1986.

4 Bronshtein, I.N. and K.A. Semendyayev, *Handbook of Mathematics*, Verlag Harri Deutsch, 3rd edn, Thun and Frankfurt am Main, 1979.

5 Gradshtein, I.S:, and I.M. Ryzhik, *Table of Integrals, Series, and Products*, New York: Academic Press, 1980.

6 Bracewell, R.N., *The Fourier Transform and its Applications*, McGraw-Hill, New York, 1978.

7 Weisstein, E.W., *CRC Concise Encyclopedia of Mathematics*, Chapman and Hall/CRC, Boca Raton, Florida, 1999.

8 Meikle, H.D., Another way of representing echo signals, their spectra, and their statistics, *Proceedings of the German Radar Symposium GRS 2002*, Bonn, Germany: DGON, 5th to 9th of September 2002, pp. 509–513.

9 Abramowitz, M. and I.A. Stegun, *Handbook of Mathematical Functions*, Dover, New York, 1964.

10 Ludloff, A., *Handbuch Radar- und Radarsignalverarbeitung*, Vieweg Verlag, Braunschweig, 1993.

11 Campbell, G.A. and R.M. Foster, *Fourier Integrals for Practical Applications*,D. van Nostrand Company, Princeton, New Jersey, 1948. This book replaces the paper The Practical Application of the Fourier Integral, *Bell System Technical Journal*, October 1928, pp. 639–707.

12 Erdélyi, A., *Tables of Integral Transforms*, McGraw-Hill, New York, 1954.

13 Meikle, H.D., *Modern Radar Systems*, Artech House, Norwood, Massachusetts, 2001.

4
Continuous, Finite, and Discrete Fourier Transforms

Chapter 3 introduced Fourier transforms as the link between a waveform and its spectrum. Fourier transforms of continuous waves are relatively seldom in practice (Figure 4.1(a)) as observation times are limited over a finite time or antennas exist over a finite length (from –2.5 to +2.5 in Figure 4.1(b)). Digital computers require the information to be a list of points along the waveform in order to produce a number of points representing the spectrum and some antenna arrays have discrete feeding points. Discrete values existing between –2.5 and +2.5 are shown in Figure 4.1(c).

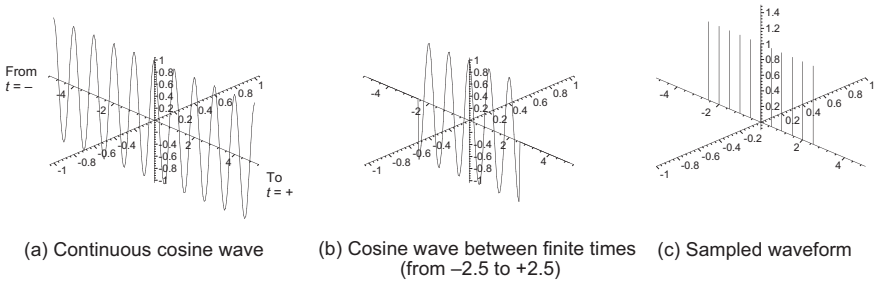

Figure 4.1 Continuous, finite, and sampled waveforms.

To recapitulate from Chapter 3, the spectrum of the helical waveform with a frequency of 0.5 Hz in Figure 4.2(a) is a delta function and is shown in Figure 4.2(b). The equivalent cosine waveform is shown in Figure 4.3 with two spectral lines as a cosine waveform may be resolved into two contrarotating helices.

A New Twist to Fourier Transforms. Hamish D. Meikle

ISBN: 3-527-40441-4

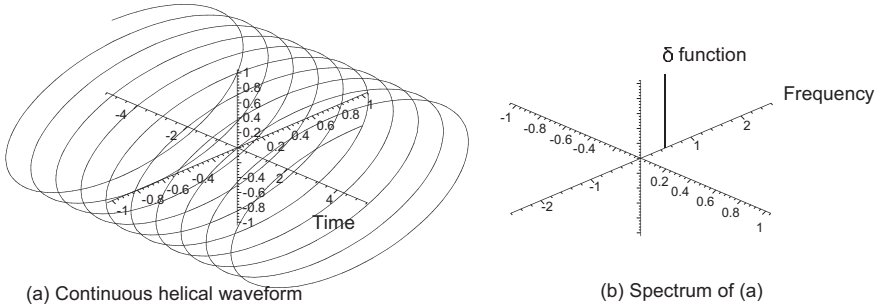

Figure 4.2 A helical waveform of frequency 0.5 Hz and its spectrum.

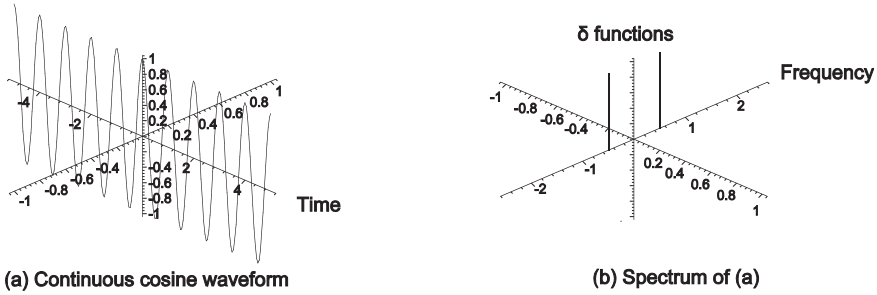

Figure 4.3 A cosine waveform of frequency 0.5 Hz and its spectrum.

4.1
Finite Fourier Transforms – Limited in Time or Space

The time of observation is always limited and arrays of sensors or antenna elements always have a limited size and this has an effect on their spectra and patterns. The effects are discussed in terms of time and frequency spectra, although it applies equally to the other fields where Fourier transforms are used.

A helix existing between –1/2 and +1/2 is shown together with its envelope in Figure 4.4(a). The envelope may be considered to modulate the continuous helix in Figure 4.2(a) and its spectrum in Figure 4.4(b) shows the effects of modulation (see Section 3.2.4). Instead of a spectral line there are a number of peaks of decreasing magnitude and opposite phase called sidebands in signal processing and sidelobes in antenna array processing. The equivalent for a cosine pulse is shown in Figure 4.5. The spurious signals may be reduced by tapering functions, described more fully in Chapter 5, at the cost of a lower signal gain or signal-to-noise ratio.

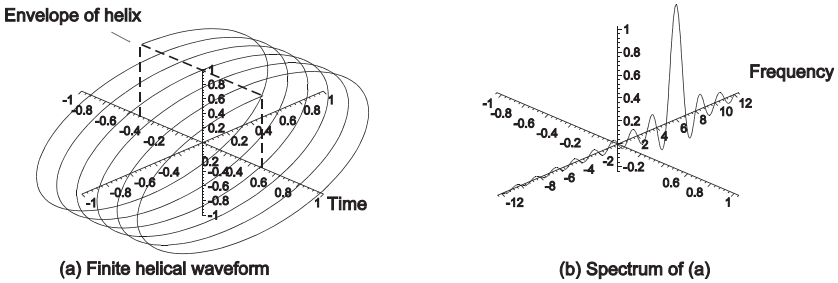

Figure 4.4 A 6 Hz finite, or time limited, helical waveform and its spectrum.

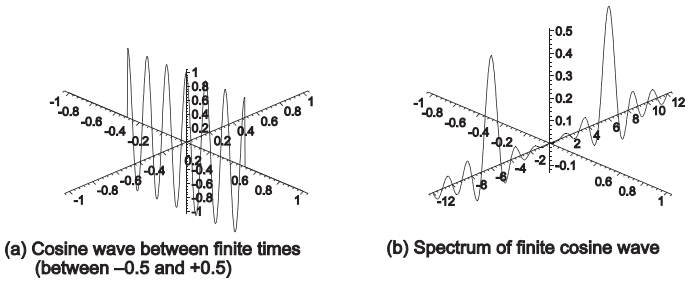

Figure 4.5 A 6 Hz finite, or time limited, cosine waveform and its spectrum.

The limits of integration of the Fourier transform are no longer from minus infinity to plus infinity but from the starting to ending times of the event, namely

$$F(f) = \int_{t=\text{start}}^{t=\text{end}} f(t)\ \exp(-j2\pi ft)\ \mathrm{d}t \tag{1}$$

The shape of the curve depends on the length of the observation time. Repeating Equation (16) of Chapter 3, for T seconds the transform is

$$F(f) = \int_{-\frac{T}{2}}^{+\frac{T}{2}} f(t)\ \exp(-j2\pi ft)\ \mathrm{d}t = \frac{\exp(j\pi fT) - \exp(-j\pi fT)}{j2\pi fT} = \frac{\sin(\pi fT)}{\pi fT} \tag{2}$$

The width of the spectral "line" or array pattern is inversely proportional to the observation time or array width and examples are shown in Figure 4.6.

The spectrum is unambiguous over all frequencies (from –∞ to +∞) and does not repeat itself as if the waveform was continuous. Figures 4.4 and 4.5 comply with the integration span for the coefficients in the Fourier series, namely over one or more complete cycles. Figure 4.7 shows what happens when the frequency is varied between 6 and 7 Hz, that is the sampling time does not contain an integral number of cycles. For the spectrum to be unambiguous, notionally the waveform must be con-

tinuous, as in Figure 4.7(a). The kinks caused by fractions of the number of cycles are shown in Figure 4.7(b) and these increase the sidelobe level in the spectrum in Figure 4.7(c) and 4.7(d). The sidelobe level for 6 Hz is the minimum line in Figure 4.7(d).

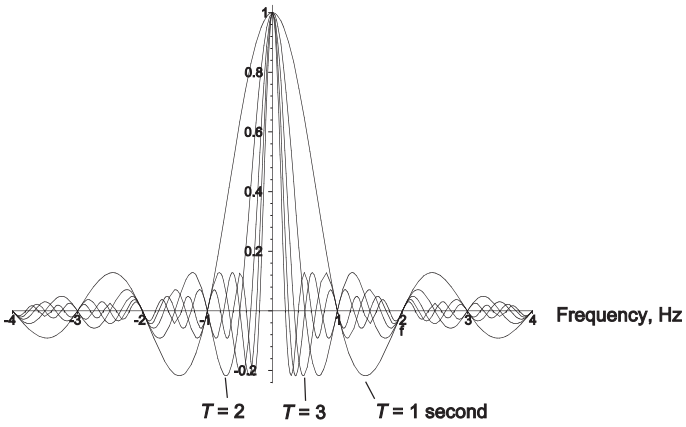

Figure 4.6 The shape of spectral lines for times of observation from one to five seconds.

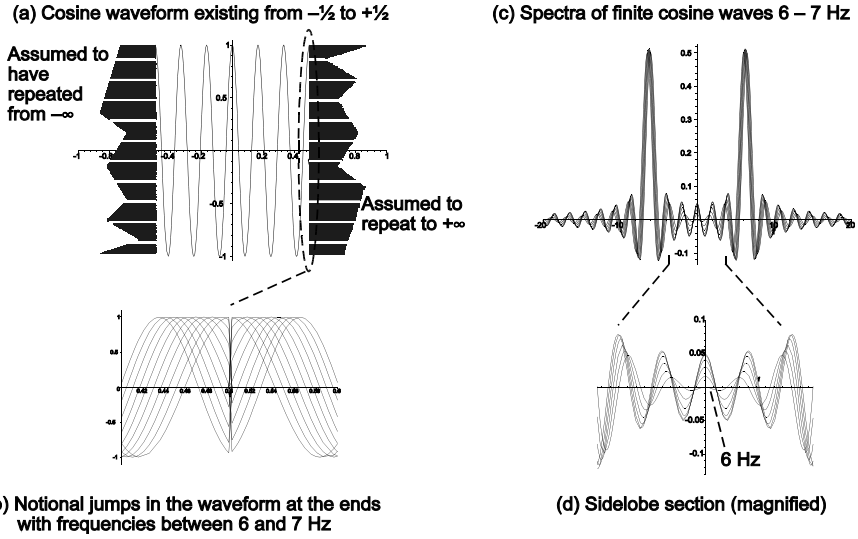

Figure 4.7 The existence of extra sidelobes in a finite Fourier transform with frequencies between 6 Hz and 7 Hz.

The increase in line width of the spectrum with the decrease of the width of the sampling time limits the accuracy of frequency measurement [1] and the sidelobes hinder the interpretation of spectra, they allow the entry of spurious interfering signals into antennae. Sidelobes may be reduced by fading the waveform at its start

and end by tapering the amplitude as in Figure 4.8(a). The sidelobes are reduced to that of the tapering waveform and those caused by the misfitting of the number of cycles are reduced also, note the higher magnification in Figure 4.8(d).

The reduction of sidelobes comes at a cost. The amount of energy integrated is reduced by tapering, the peaks in Figure 4.8(c) are lower and wider reducing sensitivity, accuracy of frequency estimation, and the resolution of two neighbouring signals. The interference of sidelobes into near by signals is called spectral leakage. Tapering is discussed more fully in Chapter 5.

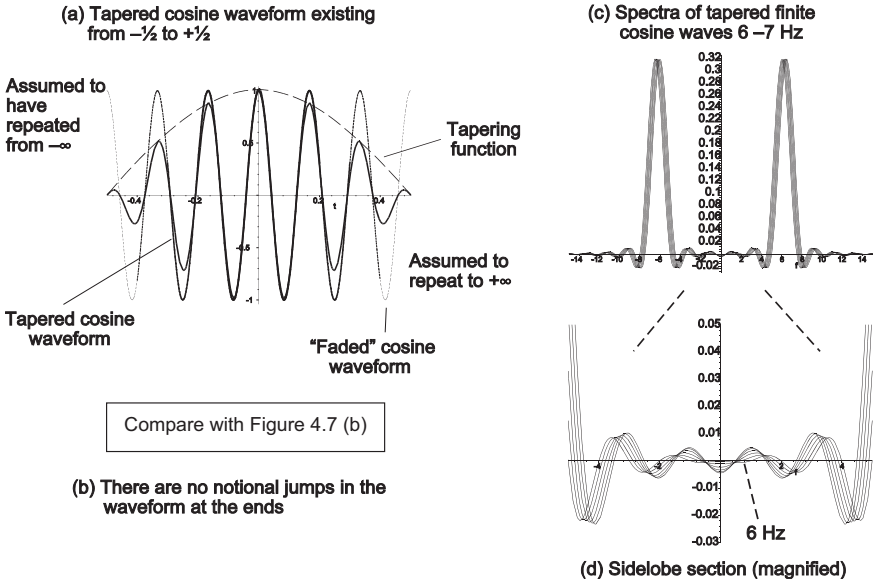

Figure 4.8 The reduction of spectrum peak and sidelobes with tapering.

4.2 Discrete Fourier Transforms

Section 3.1 described the sequence of ideas leading from the Fourier series to the Fourier transform, namely the integration interval is increased from one cycle of a repeating waveform to all time (–∞ to +∞) and increased the number of points in the Fourier series to give a continuous spectrum.

If the continuous spectrum repeats itself each B Hz, then this is the inverse of the situation with the repeating waveform in Section 4.1. Inverting the spectrum using the Fourier series formula gives a series of equally spaced time samples of amplitude representing the values of the Fourier series as in Figure 4.9.

The row of time pulses is a sampled time waveform as used in digital processors that use numbers for the amplitude taken at specific times. Signal processing takes place, often in batches, quasi-continuously and this leads to the concept of a sampling function existing over all time.

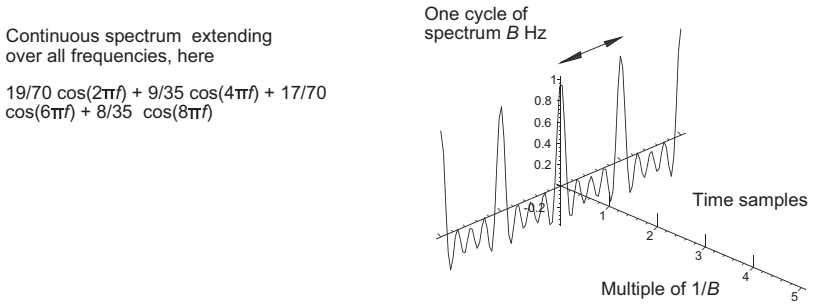

Figure 4.9 The invasion of a repeating spectrum to give a sampled times series.

The discrete Fourier transform algorithms are used on digital computers to compute the list of points representing the Fourier transform. First, the values representing the waveform with time are selected, called sampling and described in the next section, then the values are changed into digital form so that digital numerical algorithms may be used to calculate the Fourier transform.

The arrays of N equally spaced sample values in time and (complex) voltage, $t[n]$, $v[n]$, may be used in a discrete Fourier transform

$$F(k) = \frac{1}{N}\sum_{n=0}^{N-1} v[n]\ \exp\left(-j2\pi\frac{n}{N}k\right) \qquad n = 0, 1, 2, \ldots\ N-1 \tag{3}$$

An example with purely real samples, balanced about zero time, is shown in Figure 4.10 and compared with the underlying finite Fourier transform.

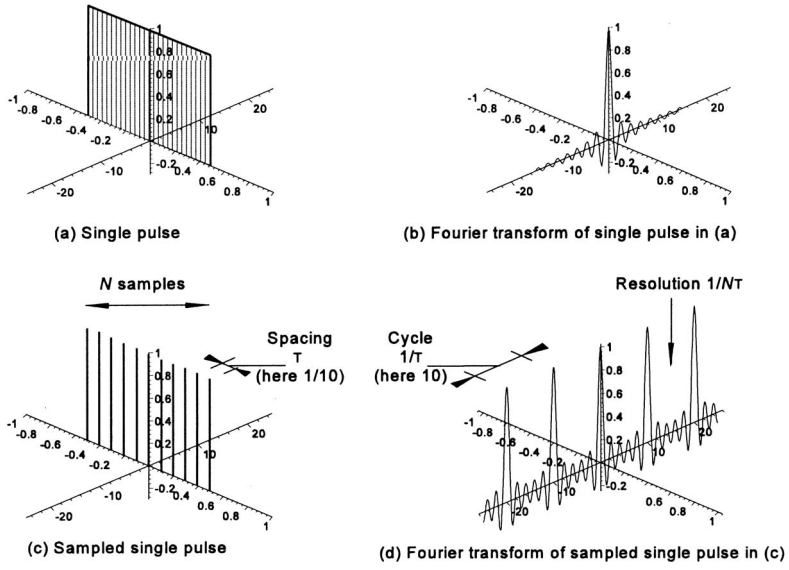

Figure 4.10 Comparison of the finite Fourier transform with an equivalent discrete Fourier transform.

In Figure 4.10(c) the pulse waveform sampled is at 1/10 second intervals and these samples are summed for the Fourier transform. In Equation (3) the exponential is cyclic between $-\infty$ and $+\infty$ with a period N representing $1/\tau$ Hz. The resolution, as with the sampled waveform, is N points.

Commonly, the samples are not equally spaced about zero but start at zero time, as in Figure 4.11, where a train of 21 pulses with unit spacing is set in a time frame length 41. The spectrum is the Fourier transform from Equation (3) and Figure 4.11(b) shows the transform when n is continuous (over a finite interval) and when n is confined to integer values (discrete). In this case the finite transform values could be said to interpolate between the discrete values. The inverse transform is given by

$$f(n) = \sum_{k=0}^{N=1} F[k] \exp\left(+j2\pi \frac{n}{N} k\right) \quad k = 0, 1, 2, \ldots N-1 \tag{4}$$

is shown in Figure 4.11(b) and 4.11(c). In contrast to the forward transform, the finite inverse transform in Figure 4.11(c) has wild excursions between the integer values of time, showing that it may take any value waveform between the sampling points represented by the dotted lines. Here, the intermediate values cannot be taken to be interpolations. The time space in Figure 4.11(c) has been extended to show the repeating feature of the inverse transform by the start of a repeated time block by the dotted bar at the end of the time axis.

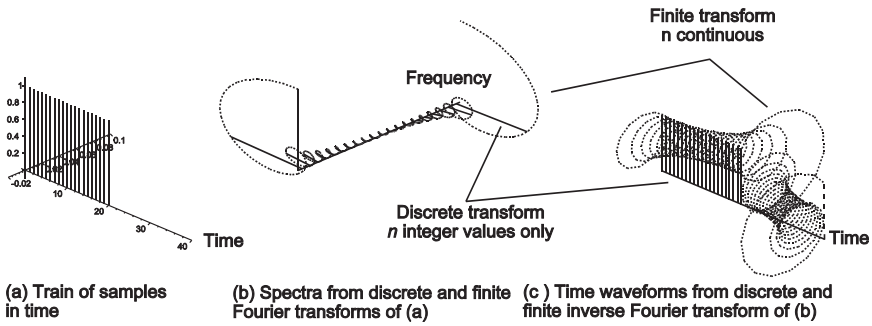

Figure 4.11 Time samples (a) with their discrete and finite Fourier transforms in the frequency domain (b) and the inverse transforms back into the time domain (c).

4.2.1 Cyclic Nature of Discrete Transforms

The main use of Fourier transforms is to change a waveform into a spectrum, perform an operation on a spectrum, and change the result back into a time waveform. Figures 4.9 to 4.11 show the cyclic nature of the transformed quantities. There must be enough empty space around the waveform ($N > 2k$) in order to avoid interference [2, p. 362]. The cyclic nature is shown in Figure 4.12.

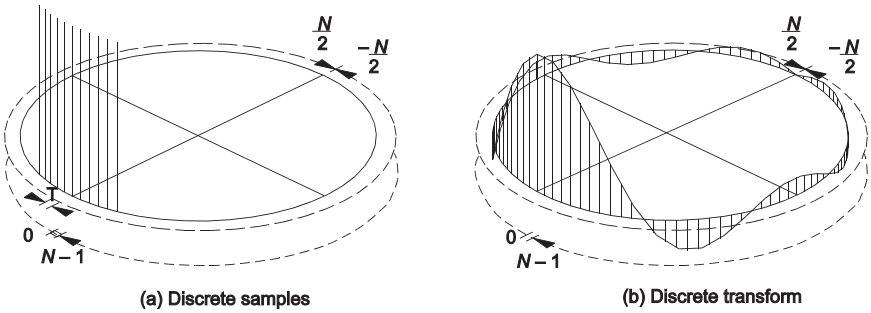

Figure 4.12 The circular nature of the discrete Fourier transform. After [2].

In both convolution and correlation, the samples representing time waveforms are moved past each other, the components are multiplied and added, and the result is plotted. Then one of the waveforms is moved to the next step and the process repeats. The same applies in the frequeny domain where multiplication of the spectra takes place. N must be chosen large enough so that the highest frequency components are small enough not to cause noticeable interference in the next cycle.

4.2.2
Other Forms of the Discrete Fourier Transform

The Fourier transform is used extensively in signal processing, for example in radar and sonar systems. Digital systems require inputs that are binary words representing numbers arranged in lists, arrays, or files and the computing power needed to change these into spectra is considerable. The matrix representation of the discrete Fourier transform leads to the development of the fast Fourier transform [3] that reduces the numbers of operations from N^2 to $N \log_2 N$ with the restriction that $N = 2^m$, where m is an integer. Other algorithms referred to as *reduced multiplication fast Fourier transforms* (RMFFT) are referred to in [4, Chapter 5].

These transforms are discrete Fourier transforms and are not discussed further here.

4.2.3
Summary of Properties

The result of summing a number of discrete values is different from that obtained from an integral. Figure 4.13 shows the finite or continuous Fourier transforms of rectangular pulses compared to their discrete Fourier transforms. As one would expect, the higher the number of pulses or points, the smaller the differences between the continuous and discrete transforms become.

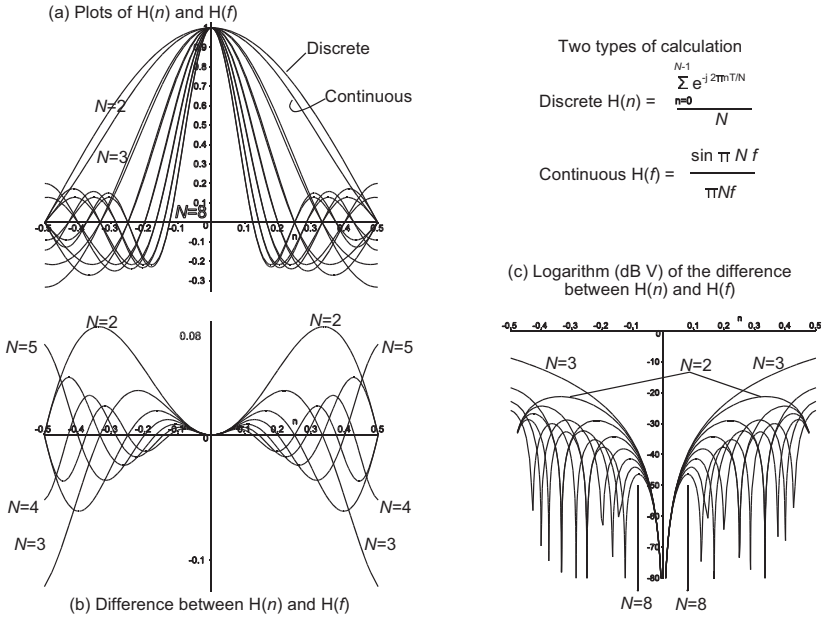

Figure 4.13 Differences between continuous and discrete rectangular Fourier transforms [Source: Meikle, H.D., *Modern Radar Systems*, Norwood, Massachusetts: Artech House, 2001].

Table 4.1 Correspondence between Fourier series and normal, finite, and discrete transforms

Type	Formula	
Series	$\int_0^P f(t)\exp(-j2\pi nft)\ dt$	For each coefficient where n is the coefficient number from 0 to N.
Transform	$\int_{-\infty}^{+\infty} f(t)\exp(-j2\pi ft)\ dt$	Integrated over all time
Finite	$\int_{t=\text{start}}^{t=\text{end}} f(t)\exp(-j2\pi ft)dt$	Integrated over limited time
Discrete	$\frac{1}{N}\sum_{n=0}^{N-1} v[n]\ \exp\left(-j2\pi\ \frac{n}{N}\ k\right)$	Discrete data points

4.3 Sampling

The sampling process is similar to observing a disk on an electric motor shaft using a flashing light or stroboscope, for example. Another example is the use of a stroboscope to look at the timing of a petrol engine. In both cases the stroboscope flashes

may be timed either by an external generator, by mains, or the engine ignition. In both cases nothing is known about the movement between the flashes and if the shaft turns more than one complete revolution between the flashes we do not know. If the motor runs at half the stroboscope speed, the markings will be seen twice so that this effect is easily recognised.

Figure 4.14(a) shows a sine wave sampled at 8 times its frequency. A line drawn through the samples allows the reconstruction of the original wave. If the sampling frequency is reduced to double the sinewave frequency there will be two samples per cycle. Only when the samples are taken at the positive and negative maxima, can the original wave be reconstructed knowing that it was a sinewave. In other cases the samples will not show the true amplitude and in an extreme case the sample may fall on the zero points, giving rise to the "blind phase" phenomenon.

Figure 4.14(b) shows sampling at 7/8ths of the sine waveform. When a line is drawn through the sampled data, a negative sinewave appears, the equivalent of the waggon wheels in old films rotating backwards. In Figure 4.15, this process is repeated at 9/8 and 15/8 the frequency and the result is the same sine waves as in Figures 4.14(a) and 4.14(b). This effect is called *aliasing*. The spectrum, drawn over a number of ambiguous cycles, is shown in Figure 4.16.

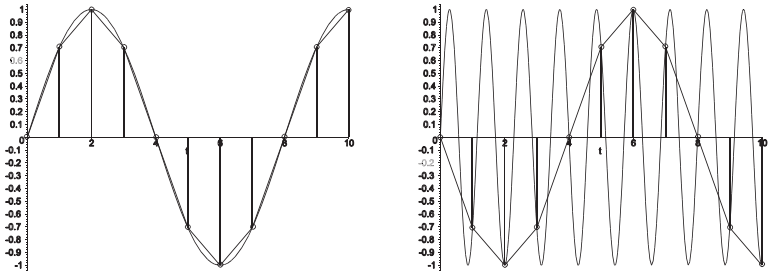

(a) Sine wave frequency=1, sampling frequency =8 (b) Sine wave frequency=7, sampling frequency =8

Figure 4.14 Sampling at 8 times and 7/8ths of the frequency of a sine wave [Source: Meikle, H.D., *Modern Radar Systems*, Norwood, Massachusetts: Artech House, 2001].

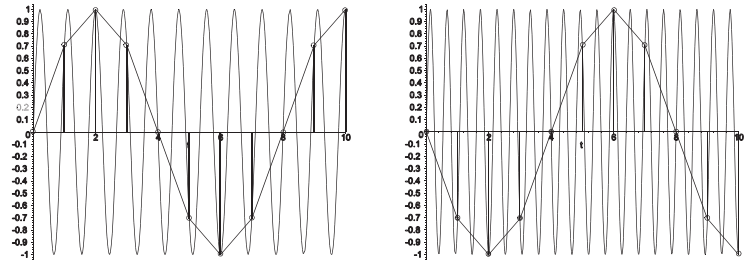

(a) Sine wave frequency=8, sampling frequency =9 (b) Sine wave frequency=8, sampling frequency =15

Figure 4.15 Sampling at 9/8 times and 15/8ths of the frequency of a sine wave [Source: Meikle, H.D., *Modern Radar Systems*, Norwood, Massachusetts: Artech House, 2001].

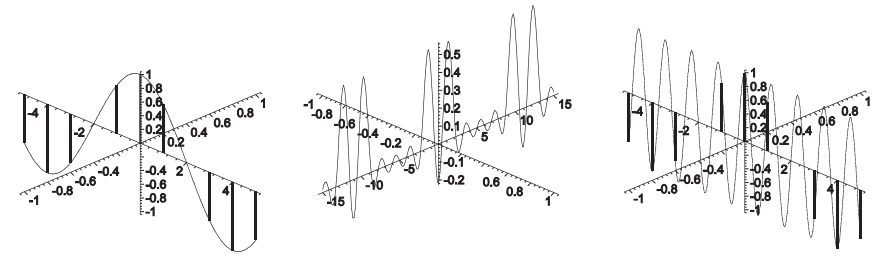

Figure 4.16 The spectrum from two aliased waveforms sampled at frequencies of 8*f* and 7/8 *f*.

The frequencies of the sampled waveforms for a sampling rate of 1000 Hz are shown in Figure 4.17. Up to a frequency of 500 Hz the frequency of the sampled wave is the same as that of the original according to Shannon's sampling theorem. Above 500 Hz the effect of Figure 4.16(c) takes hold and with increasing input frequency the frequency of the waveform represented by the samples falls. At 1000 Hz the process repeats and the effect on frequencies up to 3000 Hz is shown in Figure 4.17.

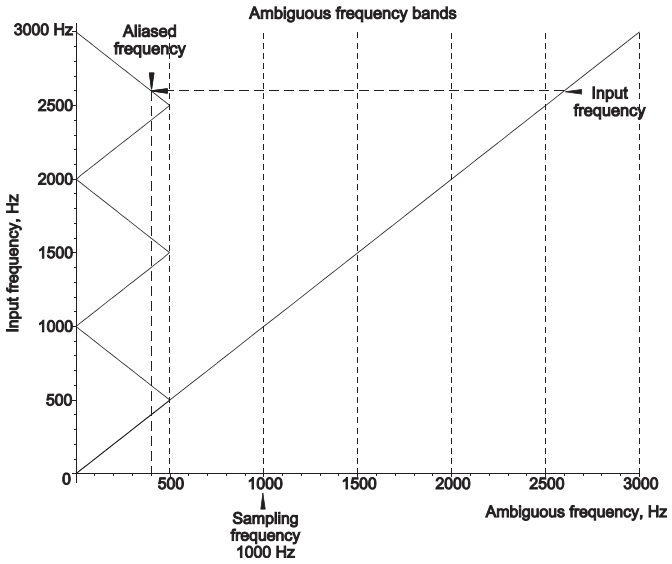

Figure 4.17 Aliasing with simple or single phase sampling [Source: Meikle, H.D., *Modern Radar Systems*, Norwood, Massachusetts: Artech House, 2001].

The sampling frequency is chosen to be at least twice the highest expected signal frequency to obey the Nyquist criterion. Other signal components above half the sampling frequency must be removed, even when they do not interfere directly, as they add to the noise in the system. Such a filter, shown in Figure 4.18, is called an *anti-aliasing* filter.

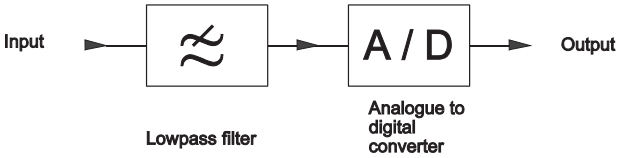

Figure 4.18 The placement of the antialiasing filter.

The arrays of sample values in time and voltage, $t[i]$, v[i], may be used in a discrete Fourier transform

$$\mathrm{F}(n) = \frac{1}{N}\sum_{k=1}^{N} v[k]\ \exp\left(-j2\pi\frac{n}{N}t[k]\right) \tag{5}$$

Commonly it is assumed that the time interval between samples is exactly the same and known, giving rise to

$$\mathrm{F}(n) = \frac{1}{N}\sum_{k=0}^{N-1} v[k]\ \exp\left(-j2\pi\frac{n}{N}k\right) \tag{6}$$

In the case of a rectangular pulse having all samples unity the spectrum is given in Figure 4.9(b).

Generally, the data taken at definite equal time steps is in the form of an array or list. And the Fourier transform for unit samples becomes

$$\begin{aligned}
\mathrm{F}_{\mathrm{rect}}(n) &= \frac{1}{N}\sum_{k=0}^{N-1} 1\ \exp\left(-j2\pi\frac{n}{N}k\right) && \text{discrete form} \\
&= \frac{1}{N}\,\frac{1-\exp(-j2\pi n)}{1-\exp\left(-j2\pi\dfrac{n}{N}\right)} && \text{sum the geometric progression} \\
&= \frac{1}{N}\,\frac{\sin(\pi n)}{\sin\left(\pi\dfrac{n}{N}\right)}\ \exp\left(-j\pi n\left(1-\frac{n}{N}\right)\right) && \text{amplitude and phase}
\end{aligned} \tag{7}$$

where n is $f\tau$ in the case of signal processing or $\dfrac{2\pi d}{\lambda}\ \sin(\theta\ +\ \alpha)$ for antennae.

Sampling hides the information between the samples and only values at the sampling points may be trusted, as in Figure 4.11.

Table 4.2 The relationships between discrete and continuous Fourier transform quantities [4 p. 52]

Discrete Fourier transform		Fourier transform	
Symbol	**Meaning**	**Symbol**	**Meaning**
$\sum_{n=0}^{N=1}()$	sum of samples	$\int_{0}^{P}()dt$	integration
N	number of samples	P	observation time, s
k	coefficient or frequency bin number	f	frequency, Hz
n	sample number	t	time, s
$x(n)$	sampled value of $x(t)$ at $t=nT$	$x(t)$	value of x(t) at time t

Table 4.3 Relationships between continuous and discrete variables [2, p. 358]

	Continuous	**Discrete**
Time	t, s	T, nT time steps
Frequency	f, Hz	n/N

4.3.1 Sampling Errors

If the calculation of the Fourier transform assumes that the samples are equally spaced in time, any error in timing gives a value with an error. The errors become significant in processes that depend on the subtraction of large numbers.

4.3.2 Sampling of Polyphase Voltages

The outputs from vector detectors may be in one of two forms: polar (r, θ) or Cartesian (x, y). Commonly components for the Cartesian form are available so two phase sampling is used when the waveform cannot be expressed as an alternating current and the phase sequence of the samples is important. The use of a second phase avoids the "blind phase" phenomenon with simple sampling. The complex values from the list of data are used to calculate the Fourier transform in Equation (4) and an example with a helical waveform is shown in Figure 4.19.

The waveform in Figure 4.19 has been redrawn about the origin in Figure 4.20(a) to avoid the (helical) effects of being off-centre. The spectrum is therefore fully real and is shown in Figure 4.20(b). There is a single peak at a frequency of +1.25 and no twin peaks at ±1.25 as in Figure 4.16(b).

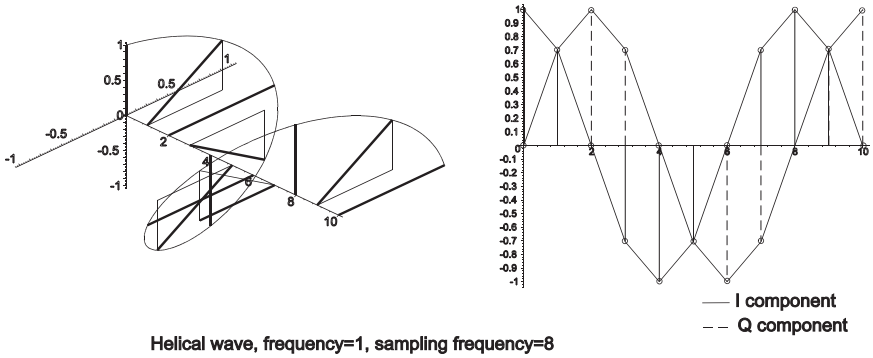

Figure 4.19 A helical waveform, its Cartesian components, and complex sampling at 8 times its frequency [Source: Meikle, H.D., *Modern Radar Systems*, Norwood, Massachusetts: Artech House, 2001].

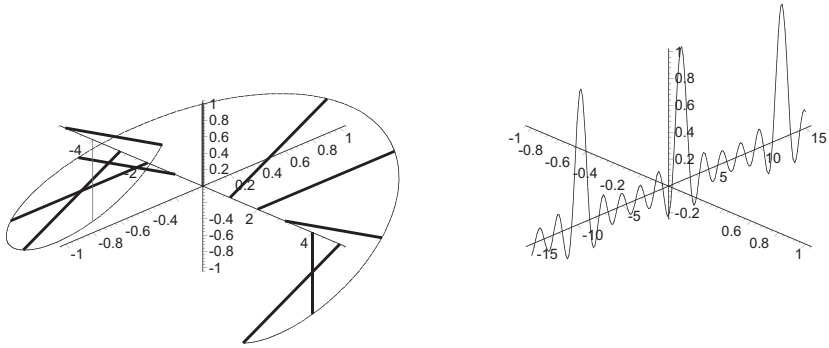

(a) Helical wave at 1/8 th of sampling frequency

(b) Spectrum of (a)

Figure 4.20 Spectrum from the helical waveform in Figure 4.19 but drawn between ±5.

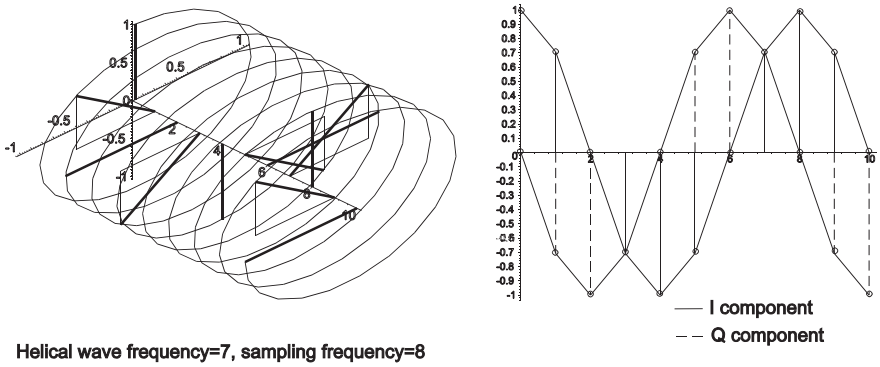

Figure 4.21 A helical waveform, its Cartesian components, and complex sampling at 7/8 times its frequency [Source: Meikle, H.D., *Modern Radar Systems*, Norwood, Massachusetts: Artech House, 2001].

When the frequency is raised to 7/8 of the sampling frequency in Figure 4.21, the Q component is the negative of the Q component in Figure 4.19.

The negative Q component represents a negative phase sequence and the spectrum in Figure 4.22 has peaks at –1.25 and 8.75, representing the true frequency.

With this type of sampling the waggon wheels in black and white films do not rotate backwards and the second phase doubles the number of samples allowing an unambiguous frequency range up to the sampling frequency. The effects are shown in Figure 4.23.

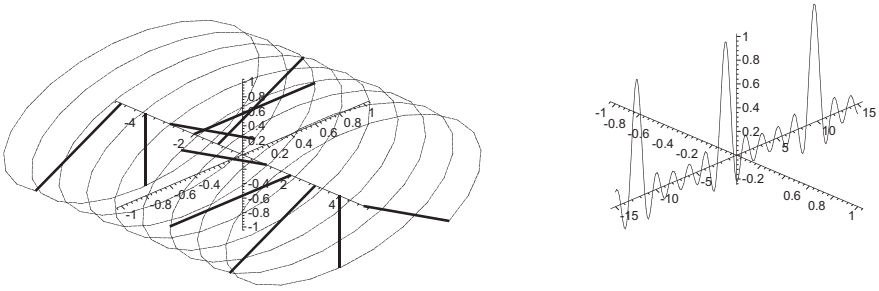

(a) Helical wave at 7/8 th of sampling frequency

(b) Spectrum of (a)

Figure 4.22 Spectrum of a helical waveform at 7/8 of the sampling frequency.

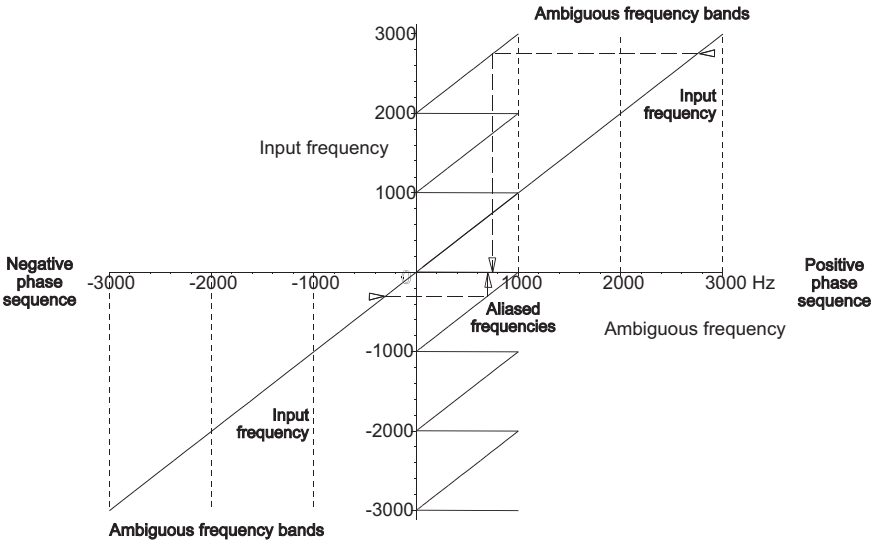

Figure 4.23 Aliasing with two phase sampling [Meikle, H.D., *Modern Radar Systems*, Norwood, Massachusetts: Artech House, 2001].

The ambiguities caused by aliasing may be resolved by taking two or more looks at the waveform with different sampling frequencies. Within the region up to the smallest sampling frequency, the results from the different sampling frequencies will be the same. In the region above, the spectrum at each sampling frequency will be different. Algorithms such as the Chinese remainder theorem [5, p. 360] [6, p. 17.22] [7, p. 242] may be used to estimate the centre frequency of the true spectrum.

4.4 Examples of Discrete Fourier Transforms

Discrete Fourier transforms, including fast Fourier transforms, are widely used and a small number of examples are given in the sections that follow, namely:

- Finite impulse response filters
- Arrays of sensors
- Sampled synthesis of patterns

4.4.1 Finite Impulse Response Filters and Antennae

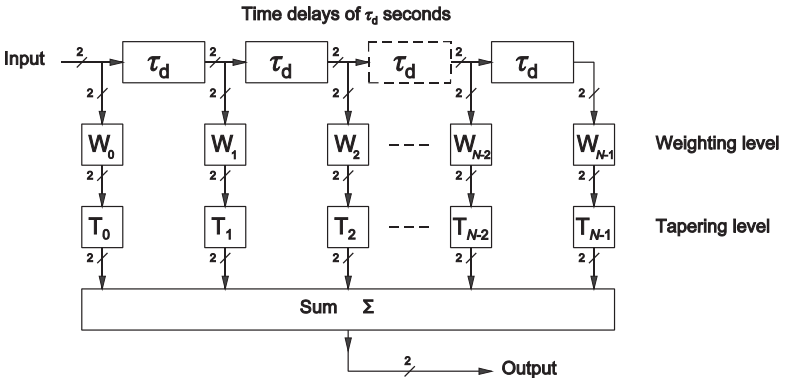

Figure 4.24 Block diagram of a vector finite impulse response (FIR) filter.

One of the most common occurrences of the fourier transform in signal processing is in finite impulse response (FIR) filters, shown in Figure 4.24.

The dash and the label 2 on each connection indicate that the connections are two- or polyphase, though single-phase versions also exist.

The incoming signals are delayed τ_d seconds by each delay stage that may be delay lines or digital storage elements. The signals in between are weighted (changed either or both in amplitude and phase), tapered (see later in this section and Chapter 5), and summed for the output. Thus the output, neglecting tapering, is

$$\text{Output} = \sum_{n=0}^{N-1} s[n]\ W[n] \tag{8}$$

where $s[n]$ is the vector or complex signal delayed by $n\tau_d$ seconds;
$W[n]$ is the complex weighting factor for the nth stage.

The complex weighting factor, $W[n]$, may be represented by

$$W[n] = |w[n]|\ \exp(j\phi[n]\ ) \tag{9}$$

Rewriting Equation (8), we have

$$\text{Output} = \sum_{n=0}^{N-1} s[n]\ |w[n]|\ \exp(j\phi[n]) \tag{10}$$

The signals in Figure 4.25 represent a sample of 11 pulses occurring one per second passing through the filter in Figure 4.24 with the weighting and tapering constants set to unity. The result is the discrete Fourier transform as in Equation (10) that repeats itself each $1/\tau_d$ Hz, or the sampling frequency f_s, as the outputs from the delay lines are samples in time.

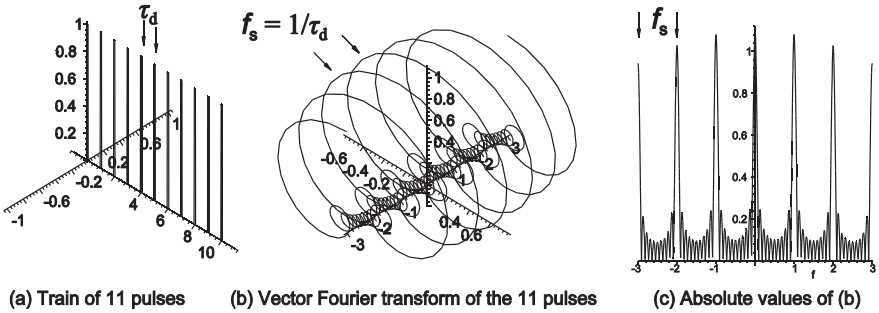

Figure 4.25 The Fourier transforms of a train of 11 pulses.

Figure 4.26 shows a sample of 11 pulses that are not a multiple of the sampling frequency, for example echo signals with a Doppler frequency shift in radar or sonar, the phase of each sample changes from sample to sample. If the vector sum of the samples equally spaced in a circle is taken, the result is zero, the sum of the pulses in Figure 4.26 is small. The spectra in Figure 4.26 show that the peak has moved away from zero giving the difference of frequency with a multiple of the sampling frequency.

When the signal $s[n]$ and the weighting function, $w[n]$ are complex conjugates in phase, correlation or filtering takes place as shown in Figure 4.27. The output of the filter is the sum of signals of the same phase and generally all phases are possible.

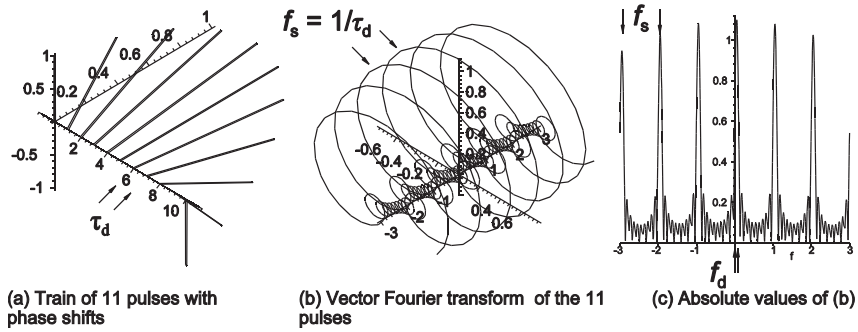

Figure 4.26 The Fourier transforms of a train of 11 pulses with phase shifts between pulses.

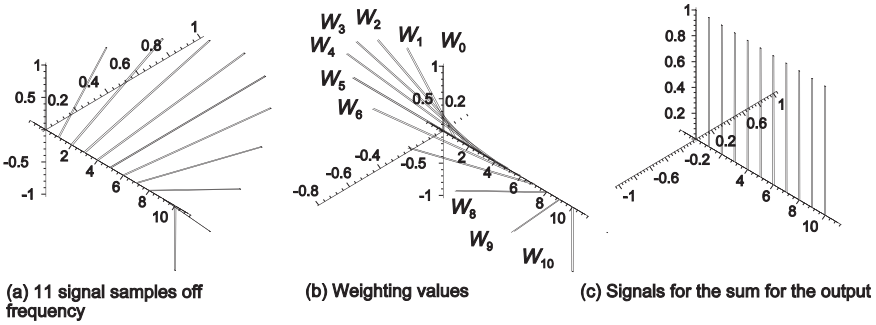

Figure 4.27 The correlation of signals and a weighting function.

This type of filtering is used to select Doppler frequences in radar, sonar, and similar signal processors either at a known single frequency or using a bank of adjoining filters as in a moving target detector processor.

Though the signal samples are at a single frequency, their limited extent in time gives a $\sin x/x$ spectrum with a high first sidelobe. As with the Fourier transform, a tapering function scaled over the list of $s[n]$ between the values of –1/2 to +1/2, provides an improvement, namely

$$\text{Output} = \sum_{n=0}^{N-1} s[n]T[n]\ |w[n]|\ \exp(j\phi[n]) \tag{11}$$

One such family of tapering functions, cosine to the power n, is shown in Figure 4.28 and other functions are discussed more fully in Chapter 5.

The best tapering function is a matter for compromise, normally the greater the reduction of sidelobes has an accompanying widening of the main lobe. What happens with cosine to the power n tapering is shown in Figure 4.29.

Both the signal and the noise are shaped by the tapering function so that the effective loss is the loss in signal-to-noise ratio, not the loss in signal alone as with antennae. The tables in Chapter 5 show the loss as *processing gain* and loss in decibels is always smaller than the *coherent gain* for antennae.

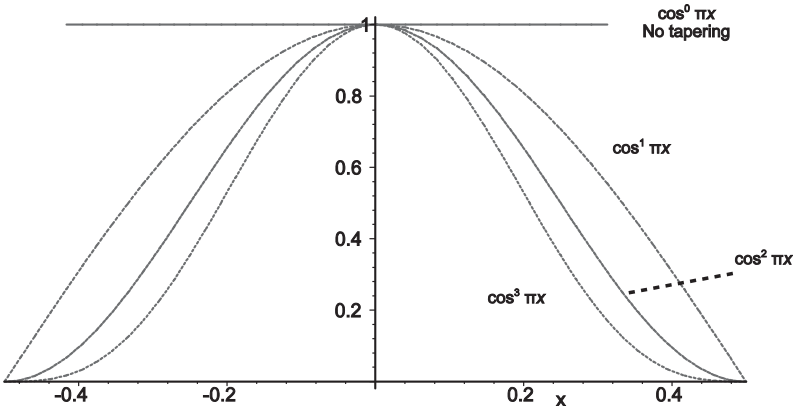

Figure 4.28 Cosine to the power *n* tapering functions.

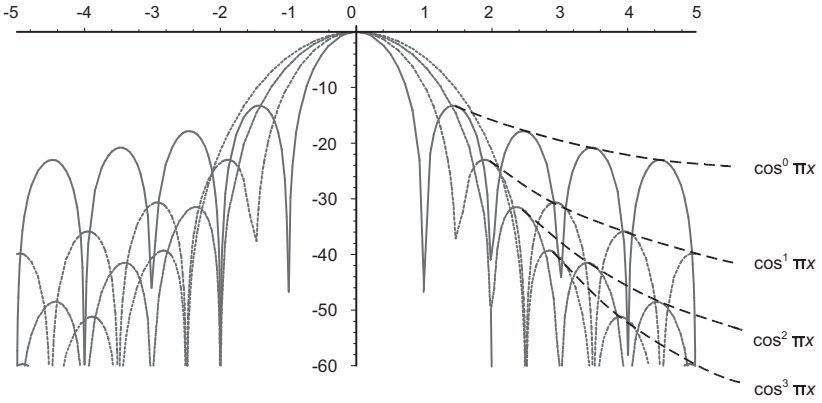

Figure 4.29 The results of tapering using cosine to the power *n* functions.

Most fast signal processing still takes place using hardware and there are no two- or polyphase semiconductor components. Commonly when the vector signal has been detected, using synchronous detectors for each phase, the two separate phases are processed in two separate channels as shown in Figure 4.30. Alternating voltage signals only need either the I or the Q channel.

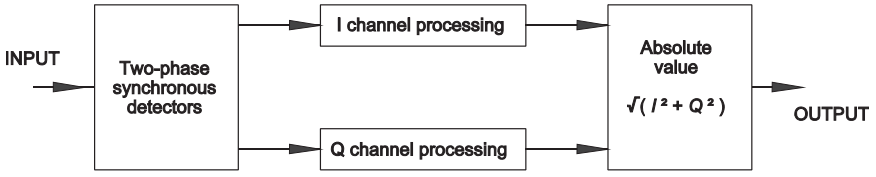

Figure 4.30 Normal arrangement for vector signal processing with two phases.

Other shapes of $w[n]$ provide other types of filtering or correlation for code matching, the sinc function for example may be used for high- and lowpass filtering as well as bandpass and bandstop.

4.4.2 The z-transform

The outputs of the delay lines with equal delays in Figure 4.24 are of the form

$$\begin{aligned} \text{Output} &= e^{j2\pi ft} + e^{j2\pi f(t+\tau_d)} + e^{j2\pi f(t+2\tau_d)} + e^{j2\pi f(t+3\tau_d)} + .. \\ &= e^{j2\pi ft}\left(e^{j2\pi f\tau_d} + e^{j2\pi f2\tau_d} + e^{j2\pi f3\tau_d} + ..\right) \end{aligned} \tag{12}$$

if $z = e^{j2\pi f\tau_d}$, then

$$\text{Output} = e^{j2\pi ft}\left(1 + z + z^2 + z^3 + ..\right) \tag{13}$$

z-transforms are principally used as shorthand to simplify the use of exponential functions into polynomials. They are described in texts such as [8] and further treatment is outside the scope of this book.

4.4.3 Inverse Fourier Transforms, a Lowpass Filter

Finite impulse response filters work in real time and the weights in the frequency selective filter described above are also calculated for real, never negative, time. The time delay depends on the delay time, τ_d , and the number of taps that define how close the discrete form approaches the finite form.

For a lowpass filter having the shape of characteristic in Figure 4.31(a), a weighting function of the shape of a sinc function[1)] is required. Since negative time is not allowed [9], the frequency curve must be given a linear phase variation to shift the sinc function into real time. The weights derived from the sinc function are samples and the limited number of samples limits the shape of the filter.

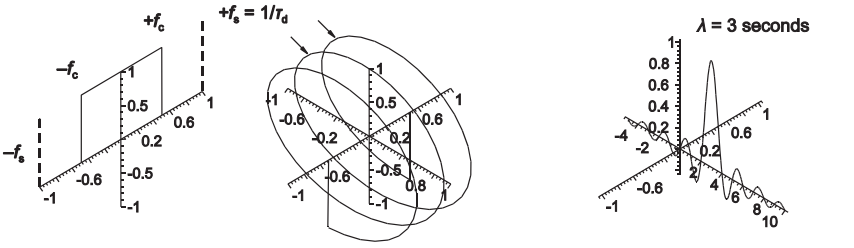

Figure 4.31 The vector frequency characteristic for a lowpass filter.

1) $\text{Sinc}(x) = \sin(x)/x$. When $x = 0$, the sinc(0) = 1.

If the time delay at the output of the filter is λ seconds, the pitch of the spatial spiral frequency characteristic is $2\pi f\lambda\tau_d$ radian/Hz and is chosen so that $n - \lambda$ gives a number of integer values about zero that is symmetric.

If the lowpass characteristic is from zero to the cutoff frequency f_c, the negative phase sequence components are necessary to create an alternating voltage from positive and negative phase sequence components, then the inverse Fourier transform is

$$\begin{aligned} h_{LP}(n) &= \int_{-f_c}^{+f_c} \exp(j2\pi f(n-\lambda)\tau_d)\, df \\ &= j\,\frac{\exp(-j2\pi f_c(n-\lambda\tau_d) - \exp(j2\pi f_c(n-\lambda)\tau_d)}{2\pi(n-\lambda)\tau_d} \\ &= \frac{\sin(2\pi f_c(n-\lambda)\tau_d)}{\pi(n-\lambda\tau_d} \end{aligned} \tag{14}$$

Substituting f_s for $1/\tau_d$ and multiplying both numerator and denominator by f_s

$$h_{LP}(n) = \sin\left(2\pi\frac{f_c}{f_s}\,(n-\lambda)\right)\,\frac{f_s}{\pi\,(n-\lambda)} \tag{15}$$

The filter with $N - 1$ delays or uses N samples has the frequency response

$$H_{LP}(f) = \sum_{n=0}^{N-1} h_{LP}(n)\exp\left(j2\pi\frac{f}{f_s}\,(n-\lambda)\right) \tag{16}$$

The constant λ is chosen so that the central point $n - \lambda = 0$, then for an odd number of points

$$\begin{aligned} H_{LP}(f) &= h_{LP}(0)e^{-j2\pi f\frac{N-1}{2}} + h_{LP}(N)e^{j2\pi f\frac{N-1}{2}} \\ &+ h_{LP}(1)e^{-j2\pi f\,\left(\frac{N-1}{2}-1\right)} + h_{LP}(N-1)e^{j2\pi f\left(\frac{N-1}{2}-1\right)} \\ &+ \ldots \\ &+ h_{LP}\left(\frac{N}{2}\right)e^{j2\pi f} \end{aligned} \tag{17}$$

The exponential terms may be expressed, for a symmetrical response, as

$$\begin{aligned} H_{LP}(f) &= h_{LP}\left(\frac{N-1}{2}\right) + 2\sum_{n=0}^{\frac{N-1}{2}} h_{LP}(n)\cos\left[\left(\frac{N-1}{2}-n\right)2\pi\frac{f}{f_s}\right] \\ &= \sum_{n=0}^{N-1} h_{LP}(n)\cos\left[\left(\frac{N-1}{2}-n\right)2\pi\frac{f}{f_s}\right] \end{aligned} \tag{18}$$

or for an unsymmetrical response

$$H_{LP}(f) = \sum_{n=0}^{N-1} h_{LP}(n) \sin\left[\left(\frac{N-1}{2} - n\right) 2\pi \frac{f}{f_s}\right] \tag{19}$$

As an example, if the cutoff frequency f_c is f_s /8 and there are 20 delays ($N = 21$ and $\lambda = 10$), then

$$h_{LP}(n) = \frac{\sin(n\ \pi/4(n-10))}{n\ \pi(n-10)} \tag{20}$$

The weighting function in the example is shown in Table 4.4 and diagrammatically in Figure 4.32.

Table 4.4 Weights for a lowpass filter, width f_s /8

N°	Weight	N°	Weight	N°	Weight
0	0.031831	7	0.075026	14	0.0
1	0.025009	8	0.159155	15	–0.045016
2	0.0	9	0.225079	16	–0.053052
3	–0.032154	10	0.25	17	–0.032154
4	–0.053052	11	0.225079	18	0.0
5	–0.045016	12	0.159155	19	0.025009
6	0.0	13	0.075026	20	0.031831

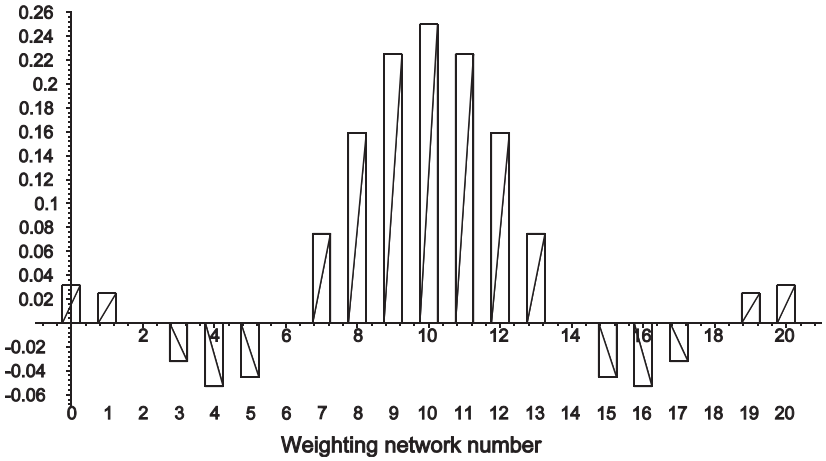

Figure 4.32 Weights for the weighting networks for the lowpass filter in the example.

The frequency response of the filter is shown in Figure 4.33(a) in linear form from zero to the sampling frequency. The response above half the the sampling frequency shows the mirror effect up to the sampling frequency. Figure 14.33(b) shows the traditional form in decibels up to half the sampling frequency.

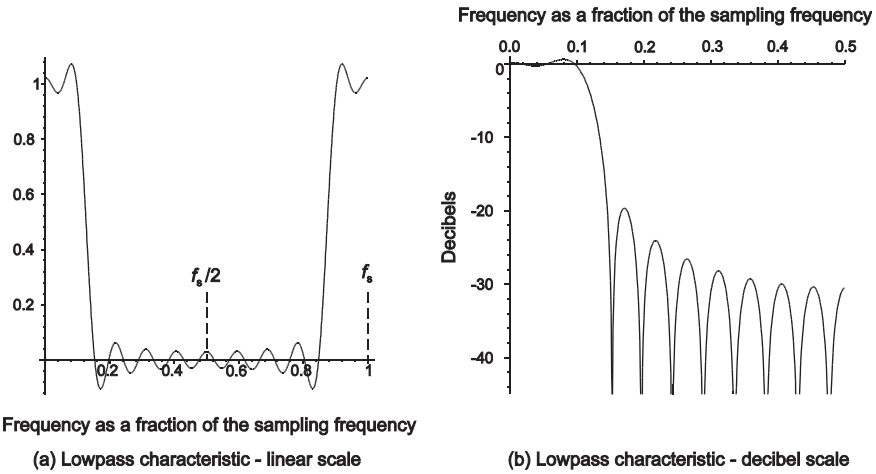

Figure 4.33 Frequency characteristic of the lowpass filter in the example.

4.4.4

Inverse Fourier Transforms, a Highpass Filter

The centre frequency f_0 is zero for a lowpass filter and $f_s/2$ for a highpass filter with a cutoff frequency f_c as illustrated in Figure 4.34 that shows the modulus of the filter characteristic, its vector form, and the Fourier transform needed for the weighting function.

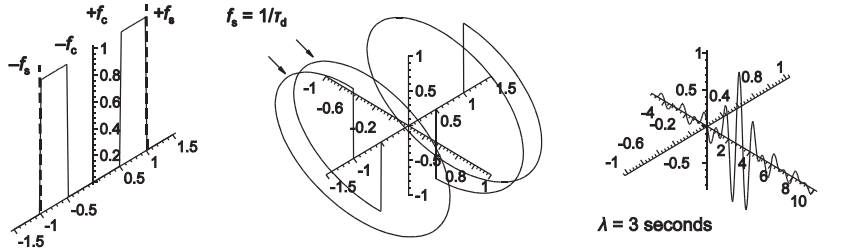

Figure 4.34 The modulus of a highpass filter characteristic, its vector form, and the weighting function in time.

It can be shown [9] that the weighting function for the highpass filter is related to that of the lowpass filter by

$$\begin{aligned} h_{HP}(n) &= h_{LP}(n)\cos\left(2\pi f_s/2\ (n-\lambda)\ \tau_d\right) \\ &= h_{LP}\cos((n-\lambda)\ \pi) \\ &= h_{LP}\ (-1)^{n-\lambda} \end{aligned} \tag{21}$$

where $n - \lambda = 0, \pm 1, \pm 2, \pm 3, ..$

The time weighting function for the highpass filter is that for the lowpass filter (Table 4.4 and Figure 4.32) with alternating signs as shown in Figure 4.34.

4.4.5
Inverse Fourier Transforms, Bandpass and Bandstop Filters

The design formulae for the bandpass h_{BP} and band stop h_{BS} filters, band centre f_0 and bandwidth $2f_c$ are

$$h_{BP}(n) = 2\cos\left(2\pi\frac{f_0}{f_s}n\right) h_{LP}(n) \tag{22}$$

and for the bandstop filter

$$\begin{aligned} h_{BS}(0) &= 1 - h_{LP}(0) \\ h_{BS}(n) &= -h_{BP}(n) \end{aligned} \tag{23}$$

4.4.6
Arrays of Sensors, Linear Antennae

Arrays of sensors may be treated in a similar form to finite impulse response (FIR) filters and a block diagram is shown as Figure 4.35. Sensor arrays are reciprocal when they do not contain switches (three-dimensional stacked beam radar antennae normally contain switches) so they may be used to receive or transmit signals. For transmitting signals the summing network becomes a power divider and the directions of the signals are reversed.

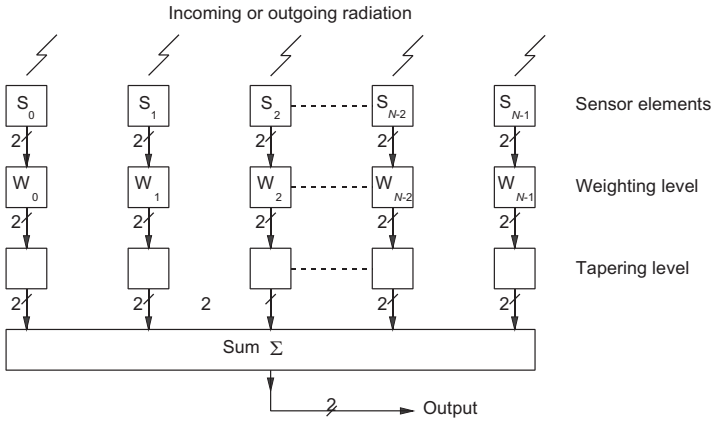

Figure 4.35 The use of weighting with a linear sensor array.

Instead of a time delay there is a defining distance, d, between the elements that send or receive radiation of wavelength, λ, both being measured in the same units. For incident plane radiation when the wavefronts are parallel to the line of elements, there is no phase difference in the signals received by the elements. Signals coming from a source not at 90 degrees to the line of elements, coming in at an angle, θ, have a phase difference of

$$\text{Phase shift} = \frac{2\pi d}{\lambda}\sin\theta \tag{24}$$

Thus the angle off normal is mapped onto phase shift as the angle θ is moved from $-\pi/2$ through zero to $+\pi/2$ (or –90 degrees through zero to +90 degrees) and the value of $\sin\theta$ moves from –1 through zero to +1.

The weighting function level may be used to provide a progressive phase shift between elements to steer the beam off the normal to the surface. The tapering function level is used to shape symmetrical beams, tapering functions are treated in Chapter 5.

4.4.7
Pattern Synthesis, the Woodward-Levinson Sampling Method

Radar antennae and filters do not always have symmetric characteristics and the Woodward-Levinson method can be used to design them. An example with the elevation angle coverage for an antenna for an air surveillance radar is shown in Figure 4.36. The antenna gain in part A is held small to reduce the echoes from the ground and part B has maximum gain to maximise the range. Shaping is used in part C to achieve an upper part of the characteristic that has a constant height.

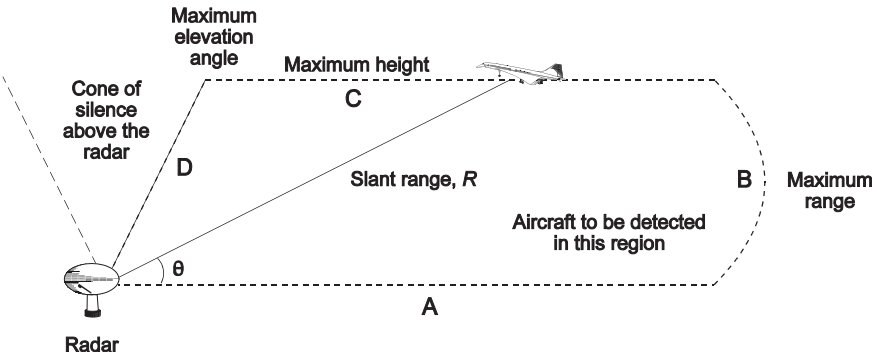

Figure 4.36 Elevation angle coverage for an air surveillance radar.

The echo signal power from an aircraft is inversely proportional to the fourth power of the range ($1/R^4$). The influence of the antenna is during transmission and reception so that antenna gain is proportional to the square of the maximum range. Part C of the characteristic has a constant height, h, so that the range at an elevation angle, θ, is $\text{cosec}\theta$ requiring an antenna gain proportional to $\text{cosec}^2\theta$, shown in Figure 4.37, plotted in decibels.

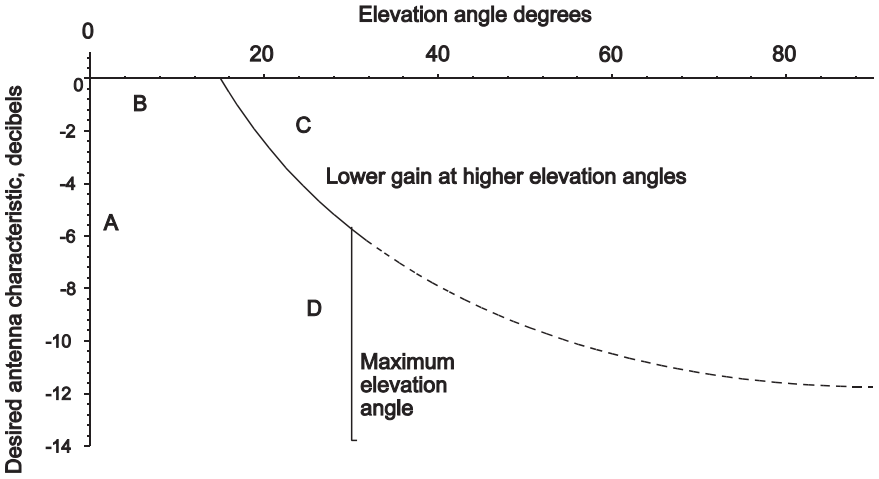

Figure 4.37 Required elevation pattern for constant height boundary.

The desired pattern is approximated by the peaks of a number of sinc curves placed next to each other, that is the number of degrees of freedom, the number of elements in an antenna or the number of taps of a finite impulse response filter, in the example, 23 shown in Figure 4.38. The width of the sinc function is the reciprocal of the number of degrees of freedom and represents the pattern without shaping.

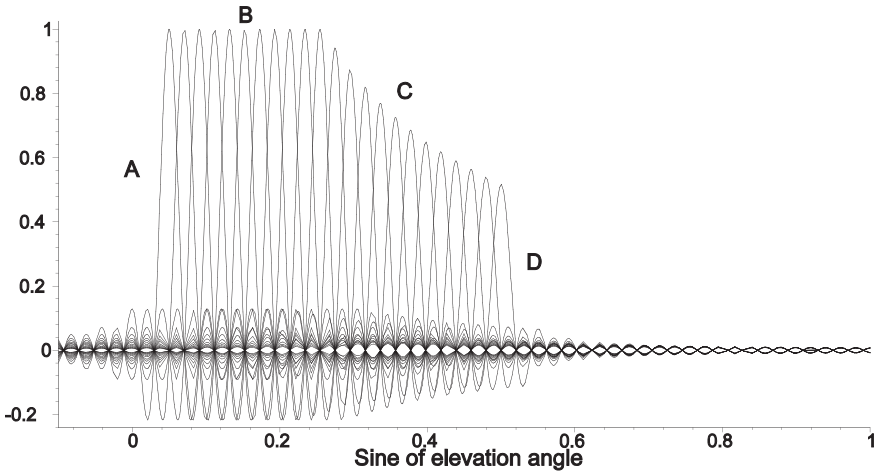

Figure 4.38 Elevation angle coverage expressed as sinc functions in sine space.

The sidelobes of the sinc function decrease at the rate of 6 dB/octave and those from the sum of adjacent sinc functions in Figure 4.39 at 12 dB/octave giving the very near approximation in Figure 4.40.

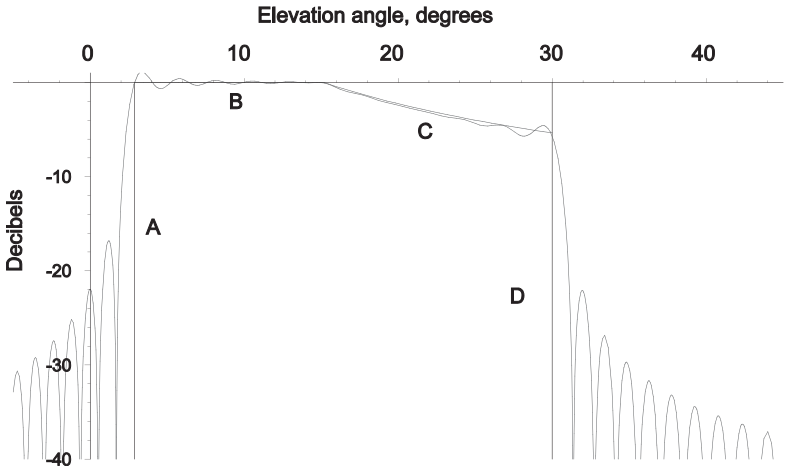

Figure 4.39 The elevation coverage expressed as the sum of sinc functions.

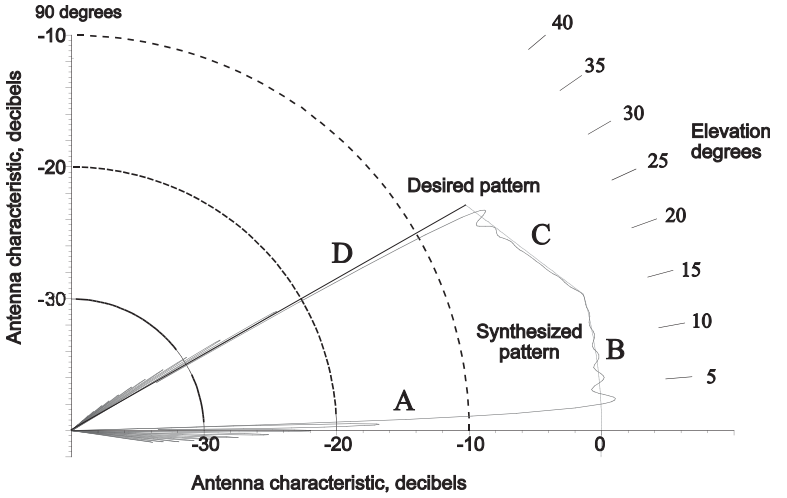

Figure 4.40 The desired and synthesized elevation patterns.

The approximated characteristic is shown in polar coordinates in Figure 4.40.

The inverse Fourier transform of each of the sinc functions is a simple helix over the length of the antenna with a pitch depending on the position of the centre of the sinc function in the characteristic. The individual inverse Fourier transforms from each of the sinc functions and their sum are shown in vector form Figure 4.41.

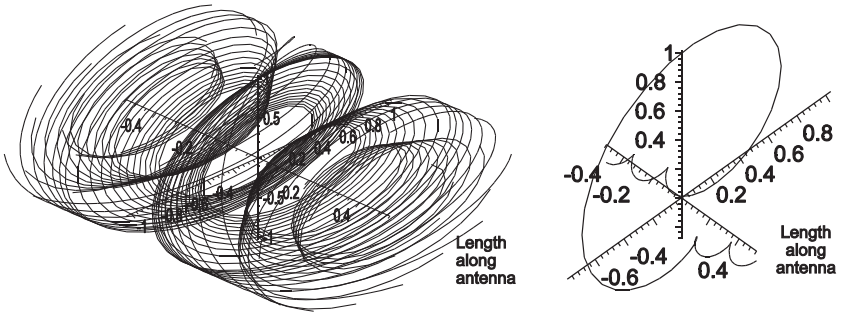

(a) Inverse Fourier transforms of the sample sinc functions

(b) Sum of the functions in (a), the illumination function

Figure 4.41 The individual inverse Fourier transforms and their normalised sum, the illumination function.

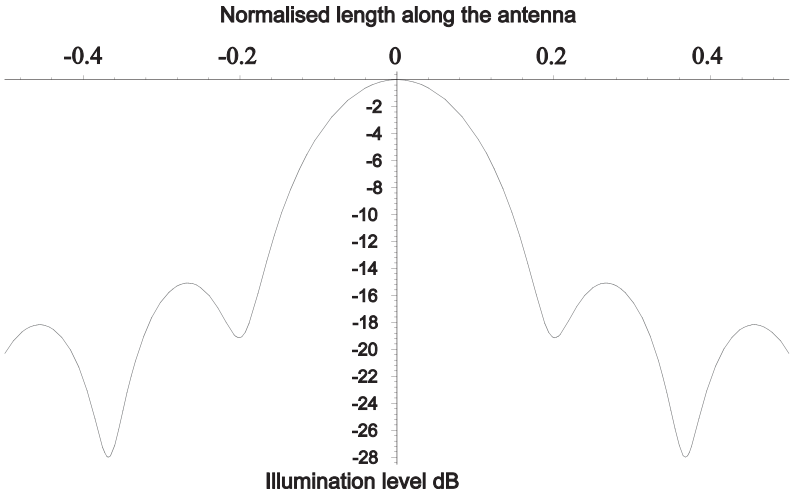

Figure 4.42 The amplitude distribution along the aperture of the antenna.

The sum shows that the inverse Fourier transform curves rotate in unison near the centre of Figure 4.41(a) and tend to cancel near the ends. The amplitude of the illumination function is traditionally plotted in decibels in Figure 4.42.

The phase characteristic in Figure 4.41 shows that the centre of the beam is offset from the normal to the antenna and the linear term may be reduced by mechanically turning the antenna in elevation.

4.5
Conversion of Analogue Signals to Digital Words

The first stage in digital processing is to convert the signals to digital form so that there is as little distortion as possible. The number of binary bits chosen determines the accuracy and dynamic range for the converter and the sampling interval determines its bandwidth.

4.5.1
Dynamic Range

The dynamic range of signals that can be converted depends on the number of characters used in the word describing the number. The characters are normally binary bits. As an example 8 bits can represent integers from 0 to 127. Negative values can be obtained by offsetting the number representing zero, normally by letting the left hand, or most significant bit (MSB) be used for the sign (normally 0 for positive and 1 for negative). There are two conventions for this, ones complement and twos complement, and these are shown in Table 4.5 for numbers with three bits.

Table 4.5 Conventions for the representation of binary numbers

Binary representation	Integer value	Ones complement with negative values	Twos complement with negative values
011	3	3	3
010	2	2	2
001	1	1	1
000	0	+0	0
111	7	–0	–1
110	6	–1	–2
101	5	–2	–3
100	4	–3	–4

4.5.2
Dynamic Range in Vector Systems

Whereas the dynamic range for all signals in polar notation, (r, θ), is the same, the space for vectors in Cartesian coordinates allows larger values in the corners of Figure 4.43 thus an extra bit may be necessary.

Figure 4.44 shows the staircase characteristic for the analogue to digital converter. Obviously the smallest value that can be converted is determined by the size of the step and the largest value by the number of steps. Errors occur when the steps are not the same size or are, in extreme cases, missing. Signals do not have a real zero value as they are contaminated with noise and their amplitude and quality is measured by their signal-to-noise ratio. There is always an error represented by the saw-

tooth form at the bottom of Figure 4.44, where the amplitude is the step size. The standard deviation is thus the step size divided by $\sqrt{12}$.

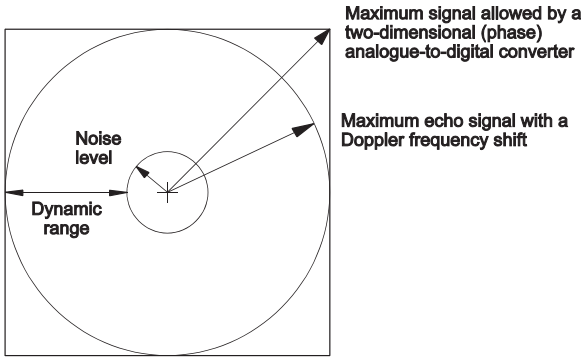

Figure 4.43 The dynamic range depends on the phase angle with Cartesian vectors [Source: Meikle, H.D., *Modern Radar Systems*, Norwood, Massachusetts: Artech House, 2001].

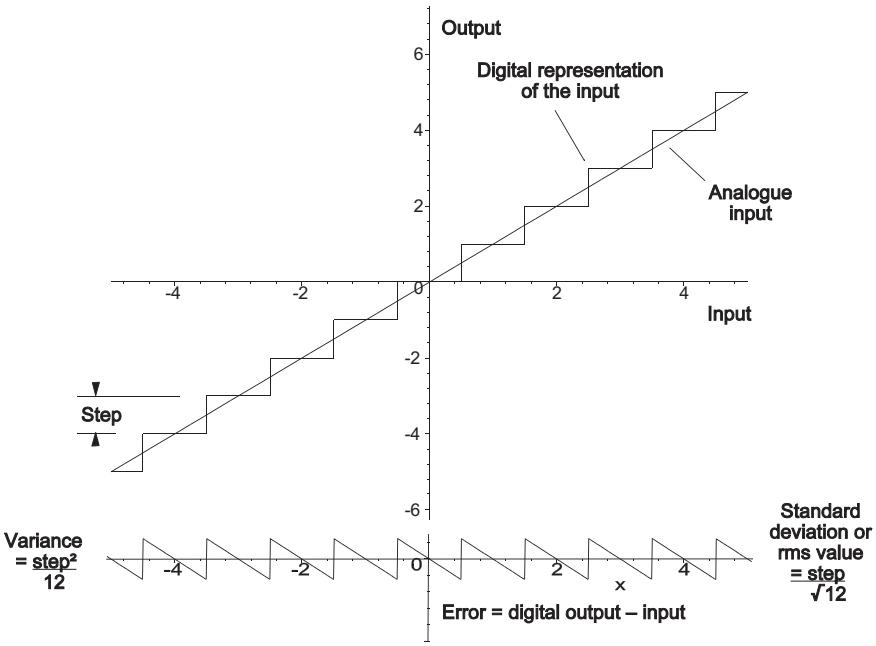

Figure 4.44 The steps in the analogue to digital converter characteristic and the additional noise [Source: Meikle, H.D., *Modern Radar Systems*, Norwood, Massachusetts: Artech House, 2001].

4.5.3
Quantisation Noise

The extra quantisation noise reduces the signal to noise ratio by

$$L_{quant} = 1 + \frac{1}{Quantisation\ variance} \tag{25}$$

$$= 10 \log_{10}\left(1 + \frac{1}{12}\,\frac{1}{2^q}\right) \qquad \text{dB}$$

and this is shown in Figure 4.45.

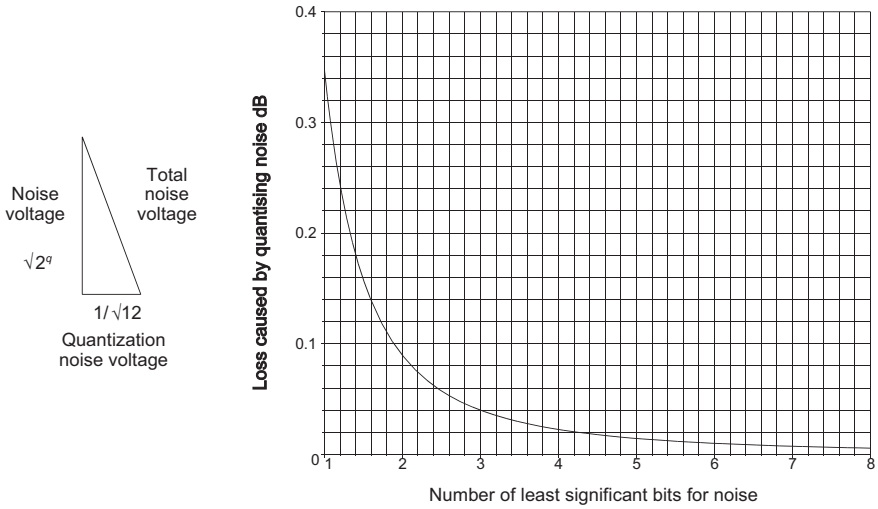

Figure 4.45 The loss of signal-to-noise ratio caused by quantising loss [Source: Meikle, H.D., *Modern Radar Systems*, Norwood, Massachusetts: Artech House, 2001].

4.5.4
Conversion Errors

The principal errors for conversion for vector or two-phase systems are:

- The zero of each converter has an offset error;
- The gain in each channel is not the same for two-phase converters;
- There is a phase or timing error in the sampling so that the phases are not exactly 90 degrees apart in a two-phase system.

There are a number of methods for finding the error and both parametric and nonparametric methods are used. A constant alternating test signal is applied to each converter that provides a large number of samples, *N*, the samples are added,

and the mean is the offset voltage. In a two-phase converter this is carried out for each phase I and Q.

The first step is to remove the direct voltage offset or zero phase sequence component shown in Figure 4.46.

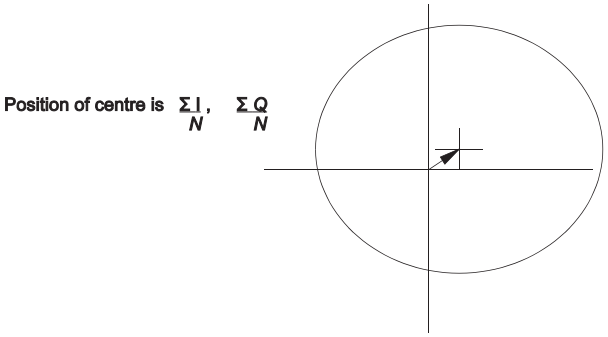

Figure 4.46 The estimation of the direct voltage error or zero phase sequence component.

Having found the direct voltage offset, it may be removed from the sums for each quadrant, namely $I' = I - I_{\text{offset}}$ and $Q' = Q - Q_{\text{offset}}$.

The corrected I' and Q' values are grouped into sectors as shown in Figure 4.47.

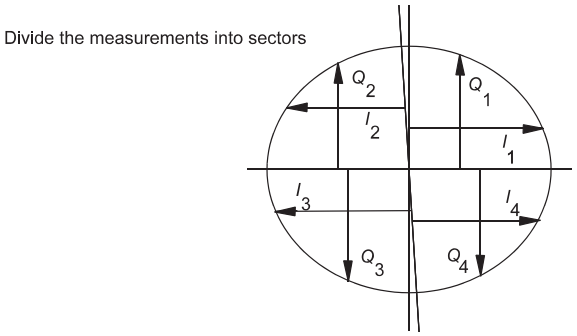

Figure 4.47 The division of the I' and Q' values into sectors.

For two-phase converters differences in the gains in each channel distort a constant rotating vector from a circle into an ellipse with an eccentricity ε

$$\varepsilon^2 = \frac{(\Sigma\,|I'|)^2 - (\Sigma\,|Q'|)^2}{(\Sigma\,|I'|)^2 + (\Sigma\,|Q'|)^2} \tag{26}$$

The phase error, ϕ, is derived by the difference in the number of samples in the diagonally opposite sectors in Figure 4.48(b).

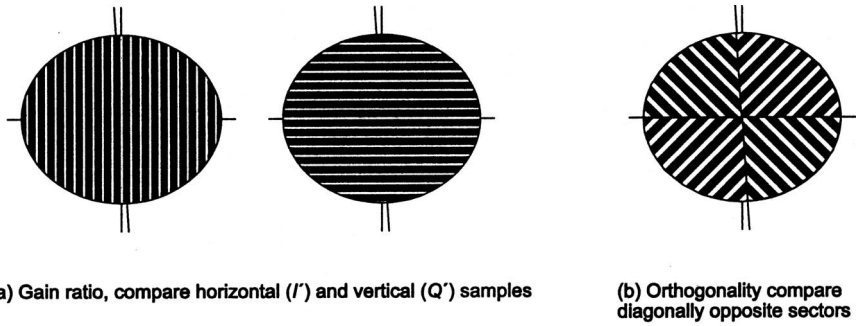

Figure 4.48 The division into sectors to estimate gain and orthogonality errors.

Nonparametric methods have taken hold as they use integers and need much less calculating power and rely on the number and depend on the lengths of the arcs in the four segments estimated from counts of the signs of the data. The test signal is either a continuous rotating voltage or sampled Gaussian noise.

4.5.5
Image Frequency or Negative Phase Sequence Component Power

The image frequency or negative phase sequence power component is the sum of the components caused by amplitude imbalance and lack of orthogonality between the two phases, namely.

$$\text{Image frequency power ratio} = \frac{\phi^2 + \varepsilon^2}{4}$$
$$= 10 \log_{10} \left(\frac{\phi^2 + \varepsilon^2}{4} \right) \text{ dB} \qquad (27)$$

This component is responsible for extra detections in radar and sonar systems and reduces the ability to reject clutter. In applications where the image frequency signal is a problem, the parameters obtained by measuring ε and ϕ may be used to correct the signals before processing.

References

1 Woodward, P.M., *Probability and Information Theory with Applications to Radar,* 2nd edn, Pergamon Press, Oxford, 1964.

2 Bracewell, R.N., *The Fourier Transform and its Applications*, McGraw-Hill, New York 1978.

3 Cooley, J.W. and J.W. Tukey, An algorithm for the machine calculation of complex Fourier series, American Mathematical Society from the *Mathematics of Computation*, Vol. 19, no. 90, pp. 297–301, 1965.

4 Elliott, D.F., and K.R. Rao, *Fast Transforms*, Academic Press, Orlando, Florida, 1982.

5 Skillman, W.A., *Radar Calculations using the TI-59 Programmable Calculator,* Artech House, Dedham, Massachusetts, 1983.

6 Skolnik, M.I., *Radar Handbook*, McGraw-Hill, New York, 1990.

7 Weisstein, E.W., *CRC Concise Encyclopedia of Mathematics*, Boca Raton, Florida: Chapman and Hall/CRC, Boca Raton, Florida, 1999.

8 Jury, E.I., *Theory and Application of the z-Transform Method*, John Wiley and Sons, New York, 1964.

9 Bozic, S.M., *Digital and Kalman Filtering*, Edward Arnold, London, 1979.

5
Tapering Functions

This book uses the simple English expression *tapering function*, other names are:

- Apodization function – Greek?;
- Weighting function – from statistics;
- Windowing function – one sees only part of the outside through a window.

Common linear tapering functions are described in this chapter used to "clean up" the Fourier transforms of limited samples. Though tapering functions may not have a use in statistics, Table 5.1 has a statistics column for completeness (refer to Chapter 6).

In electrical engineering, tapering functions are used, amongst others, for:

- The design of antenna patterns;
- The design of finite impulse response (FIR) filters;
- Spectral analysis.

The examples that follow were first published in book form in [1], extended in [2], recalculated and plotted with greater accuracy by machine and extended in [3], and here they are presented with less accuracy to fit the smaller page size. In contrast to [1] and [3] that show circular and odd functions, only even linear functions are treated here.

Tapering functions shown here are purely real and do not benefit from the vector representation used elsewhere in this book. Taylor and others derived a number of general rules [4, p. 698] for tapering functions, namely

- Symmetric distributions give lower sidelobes;
- $H(q')$ should be an even entire function of q';
- A distribution with a pedestal produces a sidelobe envelope falling off as $1/q'$ and is more efficient;
- A distribution going linearly to zero produces a far sidelobe envelope falling off as $1/q'^2$.

Tapering functions are used so widely, so that for general use common conventions and normalisation must be used.

A New Twist to Fourier Transforms. Hamish D. Meikle

ISBN: 3-527-40441-4

5.1
Conventions and Normalisation

The notation used is similar to that in [1, 3] and uses the *–f* convention. The neutral notation used is

$$\mathrm{H}(q) \;=\; \int_{-\infty}^{+\infty} \mathrm{h}(p)\, \exp(-j2\pi pq)\, \mathrm{d}p \tag{1}$$

and the inverse is

$$\mathrm{h}(p) \;=\; \int_{-\infty}^{+\infty} \mathrm{H}(q)\, \exp(+j2\pi pq)\, \mathrm{d}q \tag{2}$$

The normalised variables are shown with primes so that

$$\mathrm{H}(q') \;=\; \int_{-\infty}^{+\infty} \mathrm{h}(p')\, \exp(-j2\pi p' q')\, \mathrm{d}p' \tag{3}$$

and its inverse is

$$\mathrm{h}(p') \;=\; \int_{-\infty}^{+\infty} \mathrm{H}(q')\, \exp(+j2\pi p' q')\, \mathrm{d}q' \tag{4}$$

Tapering functions arose from the wish to "clean up" the results of Fourier transforms (for example von Hann or Hanning) and were applied to the design of the highly directional antennae for radars, amongst others. Approximations to the tapering functions used are:

- $(1 - 4p^2)^{\mathrm{n}}$ illumination;
- cosine to the power *n* illumination;
- Cosine on a pedestal;
- Truncated Gaussian.

Planar arrays gave the opportunity to control the illumination from a surface more accurately using numerically controlled machines to cut the radiating slots. Examples are Hamming, Blackman, and Blackman-Harris tapering.

A major improvement in reducing sidelobe levels came with Dolph's use of Chebyshev polynomials for antenna design (see Section 5.2.7). Though a significant development for discrete arrays, the reduced sidelobes are constant and extend, theoretically, to ±∞. Taylor combined the Dolph-Chebyshev pattern with a $\sin x/x$ pattern for a continuous array illumination with still smaller distant sidelobes.

Radio transmitters work most efficiently at full power and as sideband control in radar transmitter waveforms became important to reduce interference to other users of the frequency band shaping the pulse became important. The simplest for pulse transmitters, is trapezoidal shaping followed by cosine and sine squared pulse flanks that have too many parameters to be able to be shown with a small number of curves.

Table 5.1 Conventions and symbols

	Antenna	Waveform *f* convention	Spectrum	Statistics +ω convention
Width	w, m	τ, s	B, Hz	σ
Width limits	$-\frac{w}{2} \,..\, +\frac{w}{2}$	$-\frac{\tau}{2} \,..\, +\frac{\tau}{2}$	$-\frac{B}{2} \,..\, +\frac{B}{2}$	
p	x m	t, s	f, Hz	x
p'	$p' = x' = \frac{x}{w}$	$p' = t' = \frac{t}{\tau}$	$p' = f' = \frac{f}{B}$	
Functions	$g(x)$, $g(x')$	$h(t)$, $h(t')$	$H(f)$, $H(f')$	$p(x)$
		... transform to ...		
q	u, m^{-1}	f, Hz	t, s	ξ
q'	$q' = u' = wu$	$q' = f' = f\tau$	$q' = t' = tB$	
	$q' = u' = \frac{w}{\lambda} \sin\theta$			
Functions	$F(u)$, $F(u')$	$H(f)$, $H(f')$	$h(t)$, $h(t')$	$C(\xi)$

With tapering, the energy is partially used in order to achieve lower sidelobes, for example, and results in lower gain. Other effects, such as wider main lobe are discussed in the next section.

5.2
Parameters used with Tapering Functions

The parameters are discussed in terms of antenna and signal processing theory, principally used in communications and radar. They are given here as normalised ratios and in decibels.

5.2.1
Parameters *A* and *C*

Parameters A and C represent the (loss of) gain when a tapering is used.

Parameter A is the *effective length* of an antenna after tapering (the vector sum or integral of the voltages along an antenna) or the *coherent voltage gain* (vector sum) in a finite impulse response (FIR) filter, as examples. In terms of normalised variables

$$A = \int_{-\frac{1}{2}}^{+\frac{1}{2}} h(p')\, dp' \tag{5}$$

Parameter C is the sum of the powers along the length of an antenna or at the summing point of a finite impulse response filter, or *incoherent power gain*, namely

$$C = \int_{-\frac{1}{2}}^{+\frac{1}{2}} \Big(h(p') \Big)^2 \, \mathrm{d}p' \tag{6}$$

The equation also represents the sum of noise powers.

5.2.2
Efficiency Parameter η

The *efficiency* of an antenna or the *processing gain* of a filter, η, is the ratio of the square of the sum of the voltages divided by the sum of the powers.

$$\eta = \frac{A^2}{C} \tag{7}$$

5.2.3
Noise Width

When tapering is used in a filter, both the signal power and the noise power are reduced by filtering to affect the signal-to-noise ratio by the factor

$$\theta_n, \; t_n, \; B_n = \frac{C}{A^2} \tag{8}$$

5.2.4
Half-power Width

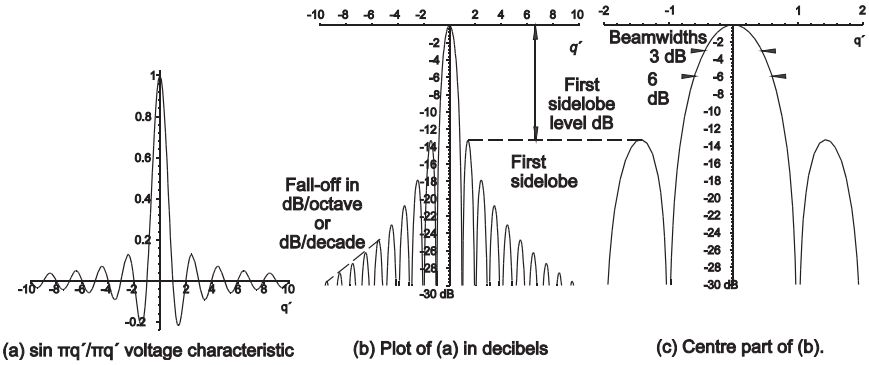

Figure 5.1 Sidelobes and fall-off for a sinc($\pi q'$) function.

This is the traditional measure of an antenna beamwidth and is also used for filters (Figure 5.1). The value is measured or found by solving the equation the voltage pattern or characteristic at the square root of two points or the equation for the

power characteristic at the 3 dB points. The width is from one side of the characteristic to the same point on the other side.

5.2.5
Parameters *D* and *G*

The accuracy in estimating the angle of signals entering an antenna or the position in time of a pulse depends on the standard deviation of the characteristic [5] or the root mean square (rms) width. The parameters *D* and *G* are used in calculation.

$$D = \int_{-\frac{1}{2}}^{+\frac{1}{2}} \left(\frac{\mathrm{d}h(p')}{\mathrm{d}p'} \right)^2 \mathrm{d}p' \tag{9}$$

$$G = \int_{-\frac{1}{2}}^{+\frac{1}{2}} \left(p' h(p') \right)^2 \mathrm{d}p' \tag{10}$$

5.2.6
Root Mean Square (rms) Width in Terms of *p*′

The root mean square width of the original function is given by

$$\Theta,\ \tau_{\mathrm{rms}},\ B_{\mathrm{rms}} = \sqrt{\frac{D}{C}} \tag{11}$$

5.2.7
Root Mean Square (rms) Width in Terms of *q*′

The root mean square width of the Fourier transform is

$$\mathscr{L} = 2\pi\sqrt{\frac{G}{C}} \tag{12}$$

5.2.8
First Sidelobe or Sideband Height

The first sidelobe or sideband height is the ratio of the height of the main lobe to the first sidelobe. This factor is critical to discriminate between a large spectral component and a smaller component near it.

5.2.9
Fall-off

When a line is drawn along the peaks of the far sidelobes, its slope in terms of decibels per octave or decade (in frequency) is a measure of the response to far sidelobes (Figure 5.1).

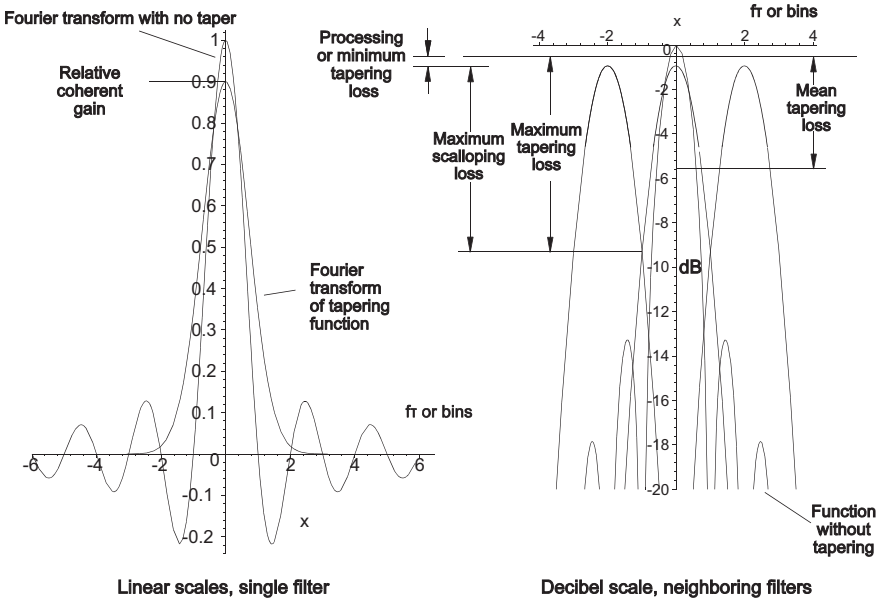

Figure 5.2 Gains and losses with adjacent filters using tapering functions. [Source: Meikle, H.D., *Modern Radar Systems*, Artech House, Norwood, Massachusetts, 2001.]

5.2.10
Scalloping and Worst Case Processing Losses

When a bank of filters are used for filtering and are spaced at the resolution width of the filters, the signals falling between the centre frequencies of the filters are subject to an additional loss. The shape of this characteristic is similar to the outside of a scallop shell (used as a trademark by Shell), hence its name. When the scalloping loss at the minimum point is added to the processing loss it becomes the worst case processing loss.

5.2.11
Spectral Leakage or Two-tone Characteristics

When a discrete transform is used not all frequency components fit the bin frequencies (see also Section 4.1). Later in this chapter examples are shown for indication when there are two signals with the major signal being moved between the 10th and 11th bin and a minor signal in the 16th bin in a filter having 100 bins. The examples are for two amplitude ratios: 20 dB and 40 dB to be consistent with [2].

5.3
Other names for tapering functions

Tapering functions are used in many branches of learning with a number of them being called different names shown in Table 5.2.

Table 5.2 Other names used for tapering functions

Name	Used here	Section
Bartlet	Triangular	5.2.1
Blackman		5.2.5
Blackman-Harris		5.2.5
Bochner	Parabolic	5.2.2
Chebyshev	Dolph-Chebyshev	5.2.7
Dirichlet	Rectangular	5.2.1
Frejer	Triangular	5.2.1
Hamming		5.2.3
von Hann	Cos^2	5.2.3
Hanning	Cos^2	5.2.3
Parzen	Parabolic	5.2.2
Raised cosine	Cosine on pedestal	5.2.4
Riesz	Parabolic	5.2.2
Weierstrass	Gaussian	5.2.6

5.4
Tapering Functions

5.4.1
Trapezoidal Tapering

Trapezoidal tapering is a simple form of tapering to reduce the sidelobes of an antenna or to reduce the sidebands of a pulse transmitter. The parameter k is the flat portion of the tapering over half the antenna length or the transmitter pulse time. Thus $k = 0$ is for triangular tapering and $k = 0.5$ for uniform tapering.

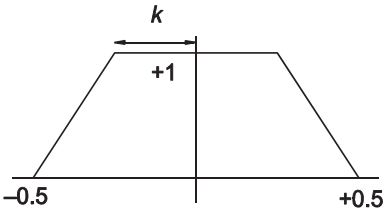

Figure 5.3 Trapezoidal function. [Source: Meikle, H.D., *Modern Radar Systems*, Artech House, Norwood, Massachusetts, 2001.]

The trapezoidal function is given by

$$h(p') = \frac{p'+0.5}{0.5-k} \text{ when } p' < k$$

$$1 \qquad \text{when } p^2 < k^2 \tag{13}$$

$$\frac{0.5-p'}{0.5-k} \text{ when } p' > k$$

The closed form for the Fourier transform is

$$H(q') = \frac{\sin[\pi\, q'\, (0.5+k)]}{\pi\, q'\, (0.5+k)} \frac{\sin[\pi\, q'\, (0.5-k)]}{\pi\, q'\, (0.5-k)} \tag{14}$$

The principal parameters are shown in Table 5.3.

Table 5.3 Table of values for trapezoidal tapering

	Values of *k*					
	0.0	**0.1**	**0.2**	**0.3**	**0.4**	**0.5**
	Triangular					**Uniform**
A, effective length, *coherent gain*	0.50	0.60	0.70	0.80	0.90	1.00
A, dB	–6.02	–4.44	–3.10	–1.94	–0.92	0.00
C, effective power, *power gain*	0.33	0.47	0.60	0.73	0.87	1.00
C, dB	–4.77	–3.31	–2.22	–1.35	–0.62	0.00
D	4.00	5.00	6.67	10.00	20.00	0.00
G	0.01	0.01	0.02	0.03	0.05	0.08
Efficiency η, *processing gain*	0.75	0.77	0.82	0.87	0.93	1.00
Efficiency η, *processing gain*, dB	–1.25	–1.13	–0.88	–0.59	–0.29	0.00
Noise beamwidth	1.33	1.30	1.22	1.15	1.07	1.00
Half-power beamwidth	1.28	1.25	1.17	1.08	0.98	0.89
RMS beamwidth	3.46	3.27	3.33	3.69	4.80	0.00
RMS aperture	0.99	1.05	1.18	1.36	1.58	1.81
First sidelobe, dB	–26.52	–28.76	–18.99	–15.13	–13.62	–13.26
Falloff dB/octave	–12.00					–6.00
Scalloping loss	0.81	0.80	0.78	0.74	0.70	0.64
Scalloping loss, dB	–1.82	–1.91	–2.15	–2.56	–3.15	–3.92
Worst case loss	0.70	0.71	0.71	0.70	0.67	0.64
Worst case loss, dB	–3.07	–3.03	–3.03	–3.15	–3.44	–3.92

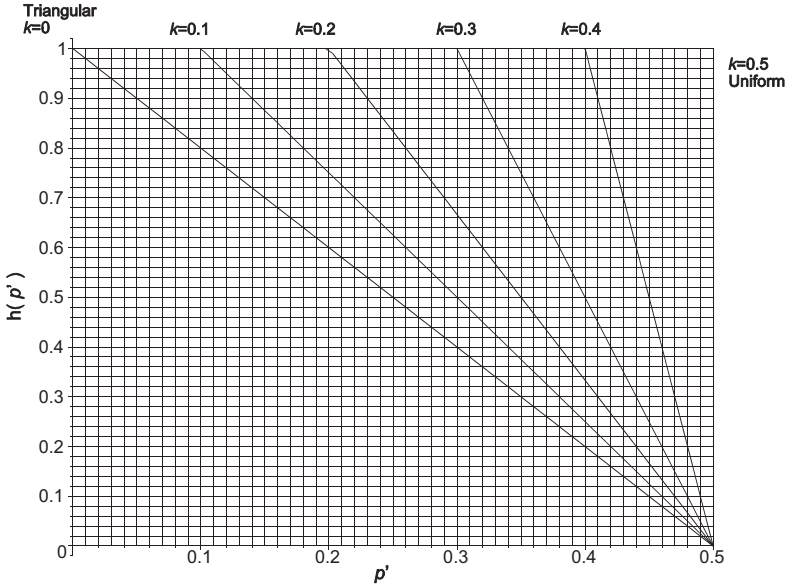

Figure 5.4 The trapeziodal tapering functions for $k = 0$ for triangular tapering to $k = 0.5$ for uniform tapering. [Source: Meikle, H.D., *Modern Radar Systems*, Artech House, Norwood, Massachusetts, 2001.]

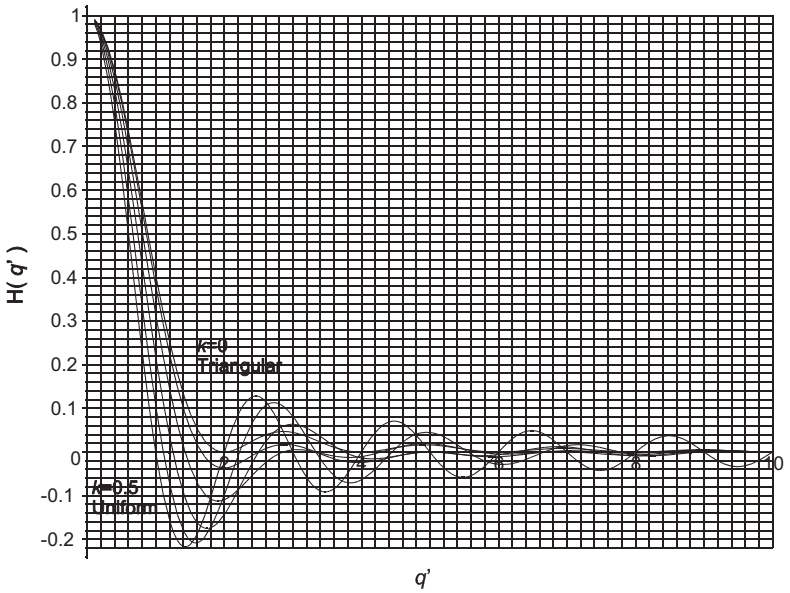

Figure 5.5 The Fourier transforms for trapezoidal tapering for $k = 0$ for triangular tapering, $k = 0.1$, 0.2, 0.3, 0.4, and $k = 0.5$ for uniform tapering. [Source: Meikle, H.D., *Modern Radar Systems*, Artech House, Norwood, Massachusetts, 2001.]

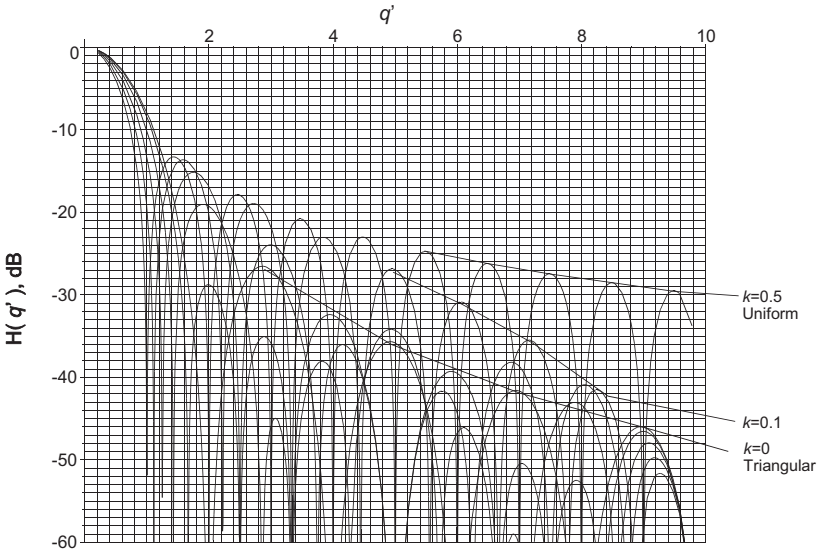

Figure 5.6 The Fourier transforms in decibels for trapezoidal tapering for $k = 0$ for triangular tapering, $k = 0.1$, 0.2, 0.3, 0.4, and $k = 0.5$ for uniform tapering. [Source: Meikle, H.D., *Modern Radar Systems*, Artech House, Norwood, Massachusetts, 2001.]

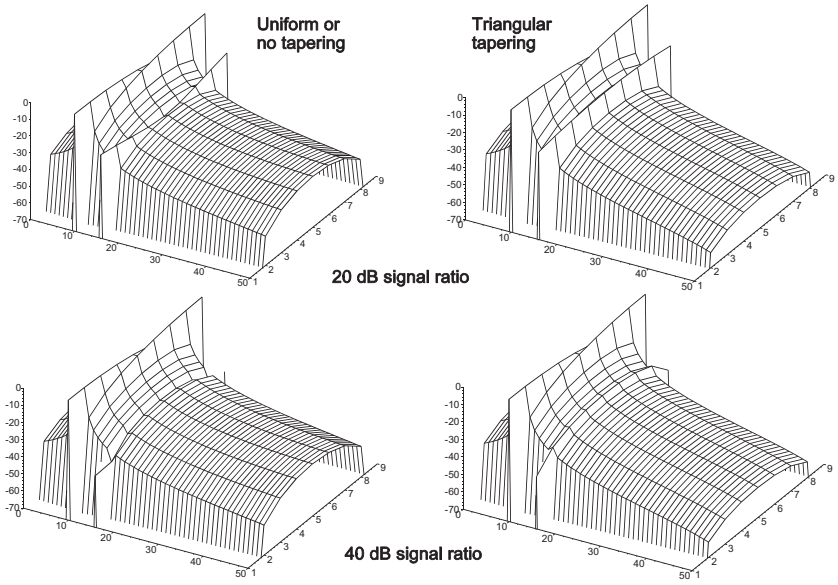

Figure 5.7 Examples of the spectral leakage or two-tone characteristics for a 100 sample filter as the major signal frequency is varied from bin 10 to bin 11. The minor signal, 20 dB or 40 dB smaller, is in bin 16. [Source: Meikle, H.D., *Modern Radar Systems*, Artech House, Norwood, Massachusetts, 2001.]

Figure 5.7 shows an example of the effects of sampling on spectral leakage or two-tone characteristics when the discrete Fourier transform is used for 100 samples. The minor signal has a frequency corresponding to the 16th bin, and the major signal has its frequency varied between the 10th and 11th bins.

The worst case occurs when the major signal has a frequency corresponding to 10.5 bins, in Figure 5.7. This case is illustrated in Figure 5.8.

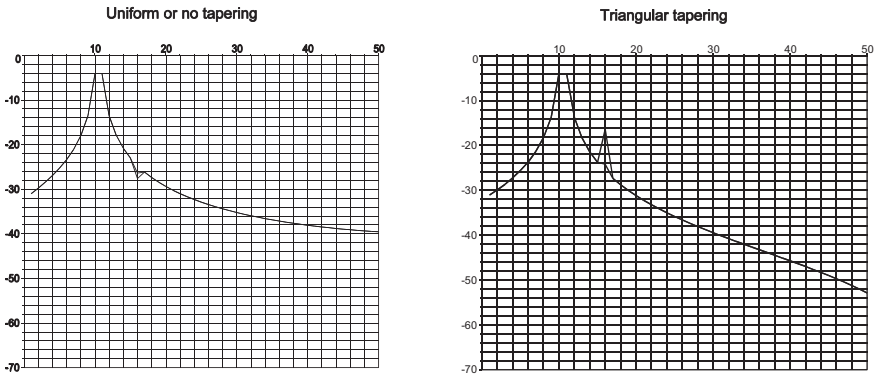

Figure 5.8 Worst case masking of the minor signal with uniform or no weighting and triangular weighting. [Source: Meikle, H.D., *Modern Radar Systems*, Artech House, Norwood, Massachusetts, 2001.]

5.4.2 $(1 - 4p'^2)^n$ Tapering

The tapering function is given by h $(p') = (1 - 4p'^2)^n$ and examples are shown in Table 5.4 and Figure 5.9.

Table 5.4 Table of values for $(1 - 4p'^2)^n$ tapering

	Power of *n*					
	0 Uniform	**1** Parabolic	**2**	**3**	**4**	**5**
A, effective length, *coherent gain*	1.00	0.67	0.53	0.46	0.41	0.37
A, dB	0.00	–3.52	–5.46	–6.80	–7.82	–8.65
C, effective power, *incoherent power gain*	1.00	0.53	0.41	0.34	0.30	0.27
C, dB	0.00	–2.73	–3.91	–4.67	–5.24	–5.68
D (see Section 5.1)	0.00	5.33	4.88	5.32	5.82	6.31
G (see Section 5.1)	0.08	0.02	0.01	0.01	0.00	0.00
Efficiency η, *processing gain*	1.00	0.83	0.70	0.61	0.55	0.50
Efficiency η, *processing gain,* dB	0.00	–0.79	–1.55	–2.13	–2.59	–2.97
Noise beamwidth	1.00	1.20	1.43	1.63	1.81	1.98
Half-power beamwidth	0.89	1.16	1.37	1.56	1.73	1.89
RMS beamwidth	0.00	3.16	3.46	3.95	4.41	4.83
RMS aperture	1.81	1.19	0.95	0.81	0.72	0.66
First sidelobe dB	–13.26	–21.29	–27.72	–33.35	–38.48	–43.27
Falloff dB/octave	–6.00	–12.00	–18.00	–24.00	–30.00	–36.00
Scalloping loss	0.64	0.77	0.84	0.87	0.89	0.91
Scalloping loss dB	–3.92	–2.22	–1.56	–1.21	–0.98	–0.83
Worst case loss	0.64	0.71	0.70	0.68	0.66	0.65
Worst case loss, dB	–3.92	–3.02	–3.11	–3.33	–3.57	–3.80

Closed forms for the Fourier transform are shown in Table 5.5.

Table 5.5 Closed forms for the Fourier transforms for the first three values of *n* for $(1 - 4p'^2)^n$ tapering

Tapering function	Fourier transform
$\left(1 - 4p'^2\right)^0$	$\frac{\sin(\pi q')}{\pi q'}$
$\left(1 - 4p'^2\right)^1$	$-2\frac{\cos(\pi q')\pi q' - \sin(\pi q')}{\pi^3 q'^3}$
$\left(1 - 4p'^2\right)^2$	$-8\frac{\sin(\pi q')\pi^2 q'^2 + 3\cos(\pi q')\pi q' - 3\sin(\pi q')}{\pi^5 q'^5}$

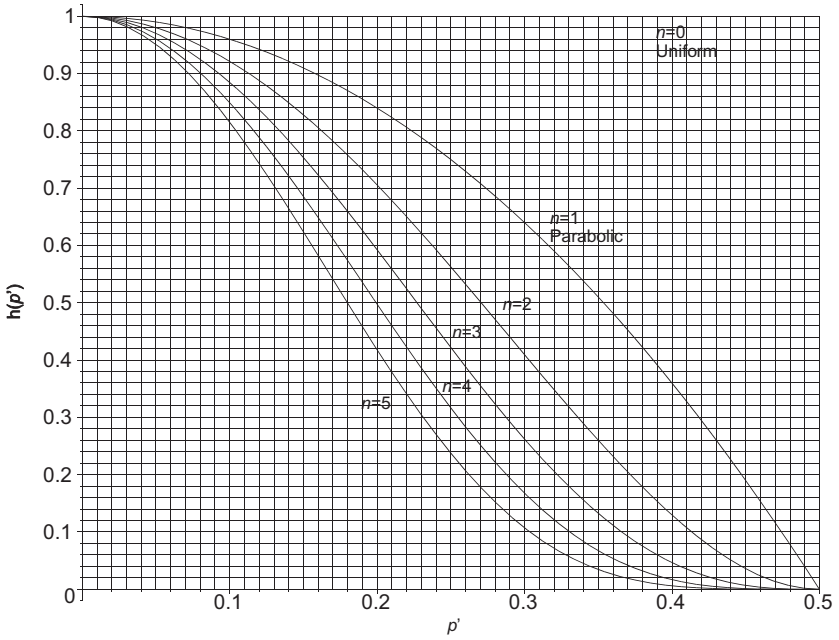

Figure 5.9 $(1 - 4p'^2)^n$ tapering functions for n from 0 to 5. [Source: Meikle, H.D., *Modern Radar Systems*, Artech House, Norwood, Massachusetts, 2001.]

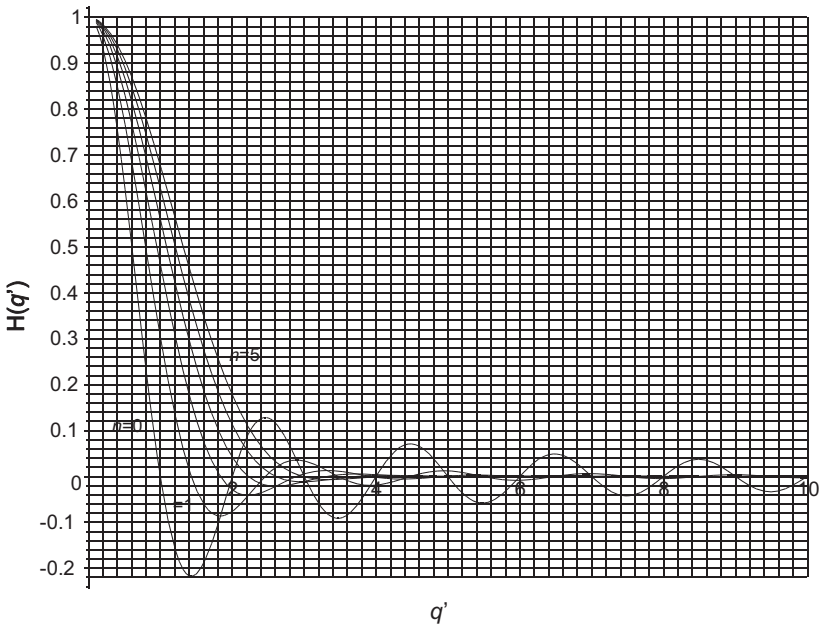

Figure 5.10 Fourier transforms for $(1 - 4p'^2)^n$ tapering for n from 0 to 5. [Source: Meikle, H.D., *Modern Radar Systems*, Artech House, Norwood, Massachusetts, 2001.]

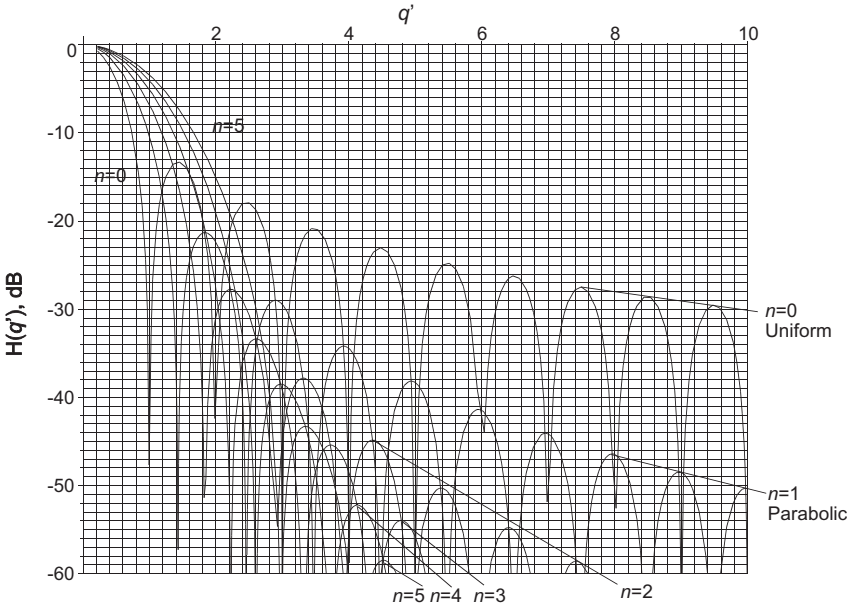

Figure 5.11 Fourier transforms in decibels for $(1 - 4p'^2)^n$ tapering for n from 0 to 5. [Source: Meikle, H.D., *Modern Radar Systems*, Artech House, Norwood, Massachusetts, 2001.]

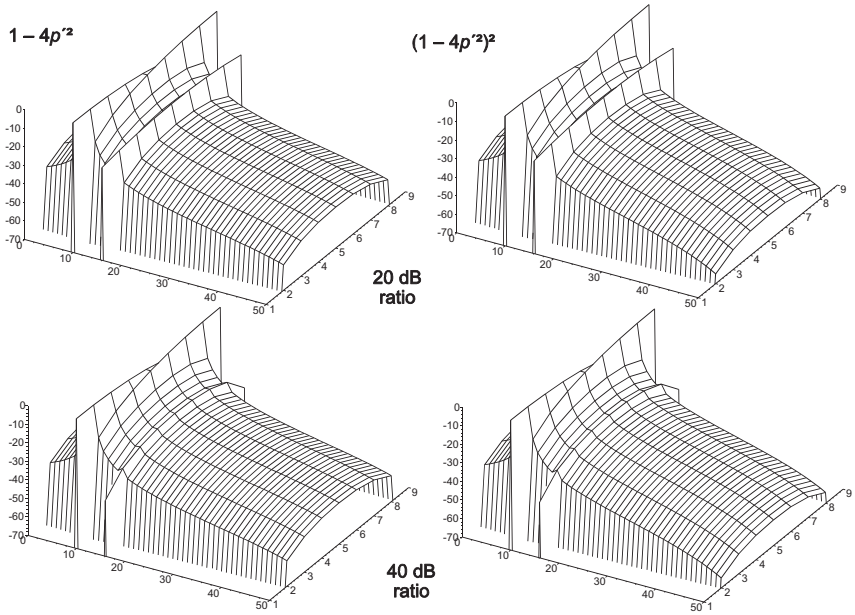

Figure 5.12 Examples of the spectral leakage or two-tone characteristics for a 100 sample filter as the major signal frequency is varied from bin 10 to bin 11. The minor signal, 20 dB or 40 dB smaller, is in bin 16. [Source: Meikle, H.D., *Modern Radar Systems*, Artech House, Norwood, Massachusetts, 2001.]

Figure 5.12 shows an example of the effects of sampling on spectral leakage, or two-tone characteristics, when the discrete Fourier transform is used for 100 samples. The minor signal has a frequency corresponding to the 16th bin, and the major signal has its frequency varied between the 10th and 11th bins.

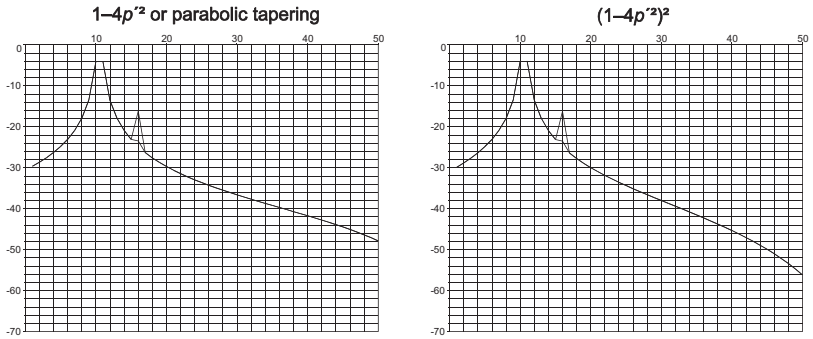

Figure 5.13 Worst case masking of the minor signal with parabolic and $(1 - 4p'^2)^2$ tapering. [Source: Meikle, H.D., *Modern Radar Systems*, Artech House, Norwood, Massachusetts, 2001.]

5.4.3 Cosine to the Power *n* Tapering

The tapering function is $\cos^n \pi p'$, and examples are shown in Figure 5.14 and Table 5.6.

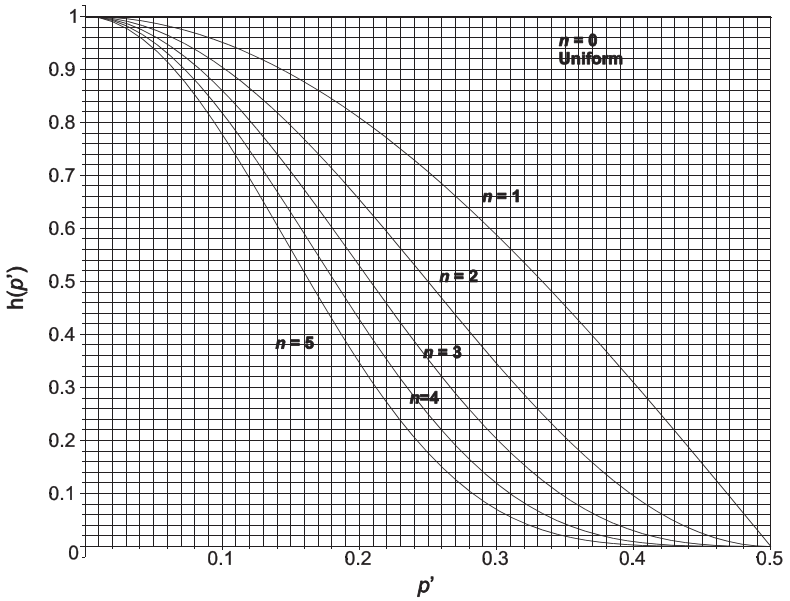

Figure 5.14 Cosine to the power *n* tapering functions for $n = 0, 1, 2, 3, 4$, and 5. [Source: Meikle, H.D., *Modern Radar Systems*, Artech House, Norwood, Massachusetts, 2001.]

Table 5.6 Table of values for cosine to the power *n* tapering

	Power of *n*					
	0	**1**	**2**	**3**	**4**	**5**
	Uniform	**Cosine**	**Cosine^2, von Hann, Hanning**	**Cosine^3**	**Cosine^4**	**Cosine^5**
A, effective length, *coherent gain*	1.00	0.64	0.50	0.42	0.38	0.3
A, dB	0.00	–3.92	–6.02	–7.44	–8.52	–9.4
C, effective power, *incoherent power gain*	1.00	0.50	0.38	0.31	0.27	0.2
C, dB	0.00	–3.01	–4.26	–5.05	–5.63	–6.1
D (see Section 5.1)	0.00	4.93	4.93	5.55	6.17	6.7
G (see Section 5.1)	0.08	0.02	0.01	0.00	0.00	0.0
Efficiency η, *processing gain*	1.00	0.81	0.67	0.58	0.51	0.5
Efficiency η, *processing gain*, dB	0.00	–0.91	–1.76	–2.39	–2.89	–3.3
Noise beamwidth	1.00	1.23	1.50	1.73	1.94	2.1
Half-power beamwidth	0.89	1.19	1.44	1.66	1.85	2.0
RMS beamwidth	0.00	3.14	3.63	4.21	4.75	5.2
RMS aperture	1.81	1.14	0.89	0.75	0.67	0.6
First sidelobe, dB	–13.26	–23.00	–31.47	–39.30	–46.74	–53.9
Falloff dB/octave	–6	–12	–18	–24	–30	–36
Scalloping loss	0.64	0.79	0.85	0.88	0.91	0.9
Scalloping loss dB	–3.92	–2.10	–1.42	–1.08	–0.86	–0.7
Worst case loss	0.64	0.71	0.69	0.67	0.65	0.6
Worst case loss, dB	–3.92	–3.01	–3.18	–3.47	–3.75	–4.0

Closed forms for the Fourier transform are given in Table 5.7.

Table 5.7 Fourier transforms for cosine to the power *n* tapering.

Tapering function	**Fourier transform**
$\cos^0 \pi p'$	$\frac{\sin(q')}{q'}$
$\cos^1 \pi p'$	$\frac{\cos(q')}{1-\left(2\frac{q'}{\pi}\right)^2}$
$\cos^2 \pi p'$	$\frac{\sin(q')}{q'}\,\frac{1}{1-\left(\frac{q'}{\pi}\right)^2}$
$\cos^3 \pi p'$	$\frac{9\cos(q')}{16\left(\frac{q'}{\pi}\right)^4-40\left(\frac{q'}{\pi}\right)^2+9}$

Tapering function	Fourier transform
$\cos^4 \pi p'$	$\frac{\sin(q')}{q'} \frac{4}{\left(\frac{q'}{\pi}\right)^4 - 5\left(\frac{q'}{\pi}\right)^2 + 4}$
$\cos^5 \pi p'$	$\frac{-225\cos(q')}{64\left(\frac{q'}{\pi}\right)^6 - 560\left(\frac{q'}{\pi}\right)^4 + 1036\left(\frac{q'}{\pi}\right)^2 - 225}$

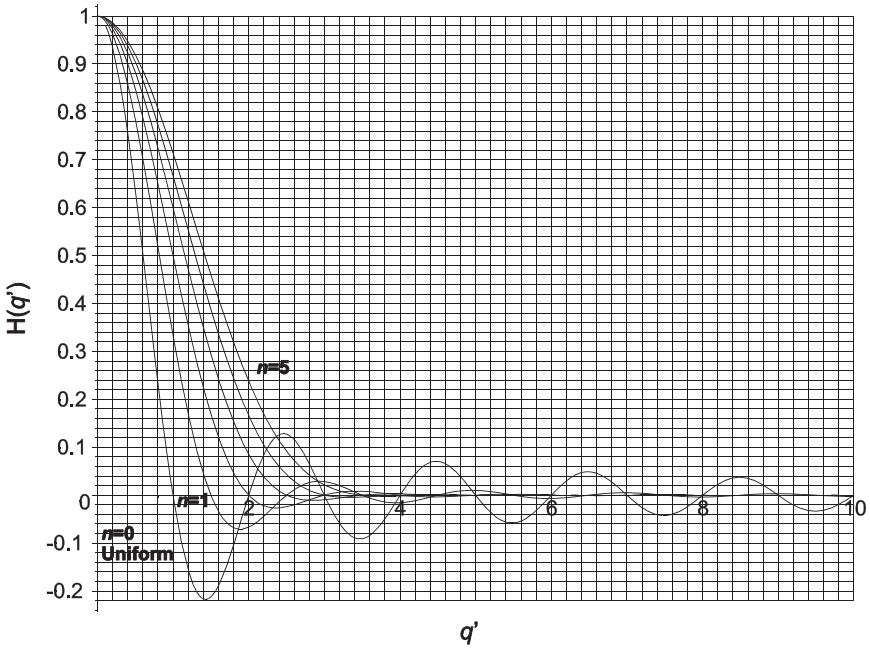

Figure 5.15 Fourier transforms of the cosine to the power *n* tapering functions for $n = 0, 1, 2, 3, 4$, and 5. [Source: Meikle, H.D., *Modern Radar Systems*, Artech House, Norwood, Massachusetts, 2001.]

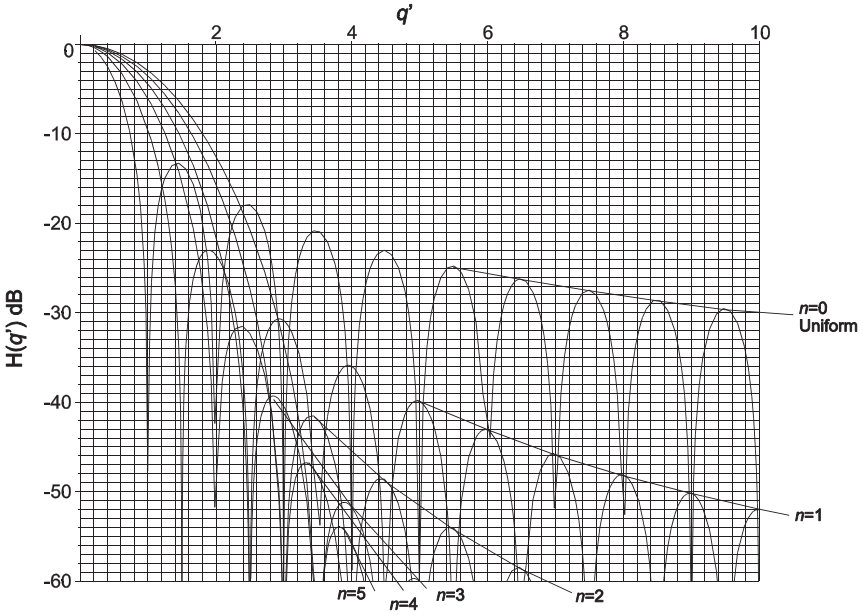

Figure 5.16 Fourier transform in decibels for cosine to the power n tapering for $n = 0, 1, 2, 3, 4,$ and 5. [Source: Meikle, H.D., *Modern Radar Systems*, Artech House, Norwood, Massachusetts, 2001.]

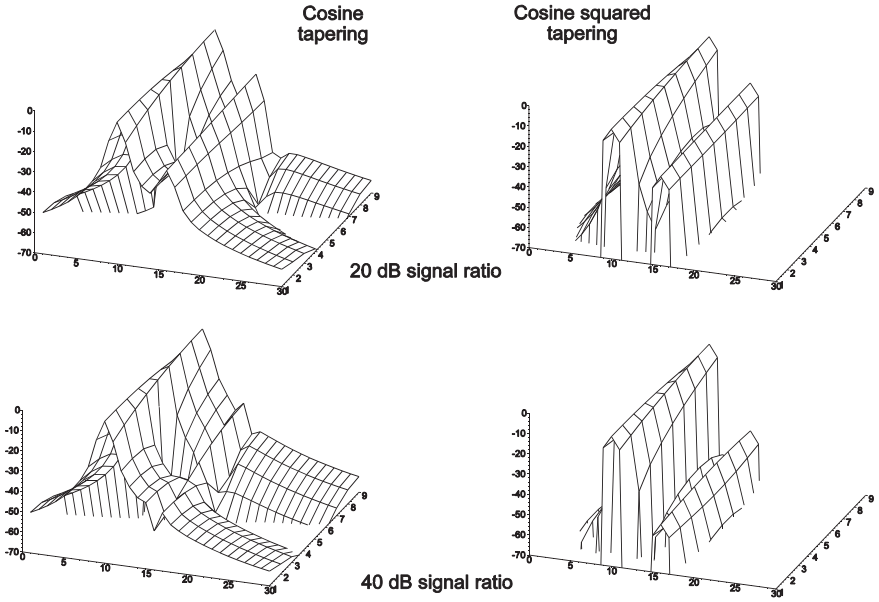

Figure 5.17 Examples of the spectral leakage or two-tone characteristics for a 100 sample filter as the major signal frequency is varied from bin 10 to bin 11. The minor signal, 20 dB or 40 dB smaller, is in bin 16. [Source: Meikle, H.D., *Modern Radar Systems*, Artech House, Norwood, Massachusetts, 2001.]

Figure 5.17 shows an example of the effects of sampling on spectral leakage, or two-tone characteristics, when the discrete Fourier transform is used for 100 samples. The minor signal has a frequency corresponding to the 16th bin, and the major signal has its frequency varied between the 10th and 11th bins.

The worst cases occur with the major signal at the bin frequency, and the worst cases in Figure 5.16 are shown in Figure 5.18.

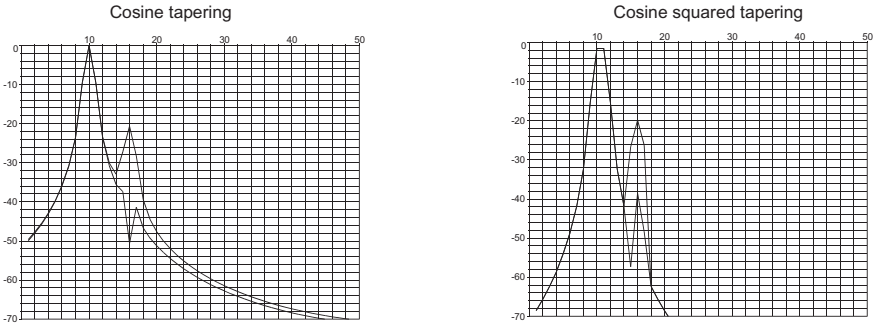

Figure 5.18 Worst case masking of the minor signal with cosine and cosine squared tapering. [Source: Meikle, H.D., *Modern Radar Systems*, Artech House, Norwood, Massachusetts, 2001.]

5.4.4
Cosine on a Pedestal Tapering

The tapering function is given by the edge value k in the function $k + (1 - k)\cos\pi\ p'$ and shown in Figure 5.19 with the calculated values in Table 5.8.

Table 5.8 Table of values for cosine on a pedestal tapering

Edge value	**0.5**	**0.3**	**0.2**	**0.1**	**0.05**	**0.03**
Edge value, dB	**–6.00**	**–10.50**	**–14.00**	**–20.00**	**–26.00**	**–30.50**
A, effective length, *coherent gain*	0.82	0.75	0.71	0.67	0.65	0.65
A, dB	–1.74	–2.55	–2.98	–3.44	–3.68	–3.77
C, effective power, *incoherent power gain*	0.69	0.60	0.56	0.53	0.51	0.51
C, dB	–1.59	–2.20	–2.49	–2.76	–2.89	–2.94
D (see Section 5.1)	1.23	2.42	3.16	4.00	4.45	4.64
G (see Section 5.1)	0.04	0.03	0.02	0.02	0.02	0.02
Efficiency η, *processing gain*	0.97	0.92	0.89	0.86	0.83	0.82
Efficiency η, *processing gain*, dB	–0.15	–0.35	–0.49	–0.68	–0.79	–0.84
Noise beamwidth	1.04	1.08	1.12	1.17	1.20	1.21
Half-power beamwidth	0.98	1.04	1.08	1.13	1.16	1.17
RMS beamwidth	1.33	2.00	2.37	2.75	2.94	3.02
RMS aperture	1.51	1.36	1.28	1.21	1.17	1.16
First sidelobe, dB	–17.65	–20.29	–21.65	–22.72	–22.99	–23.03
Falloff dB/octave	–10.00					–12.00
Scalloping loss	0.69	0.73	0.74	0.76	0.77	0.78
Scalloping loss, dB	–3.17	–2.79	–2.58	–2.35	–2.22	–2.17
Worst case loss	0.68	0.70	0.70	0.71	0.71	0.71
Worst case loss, dB	–3.32	–3.14	–3.07	–3.03	–3.01	–3.01

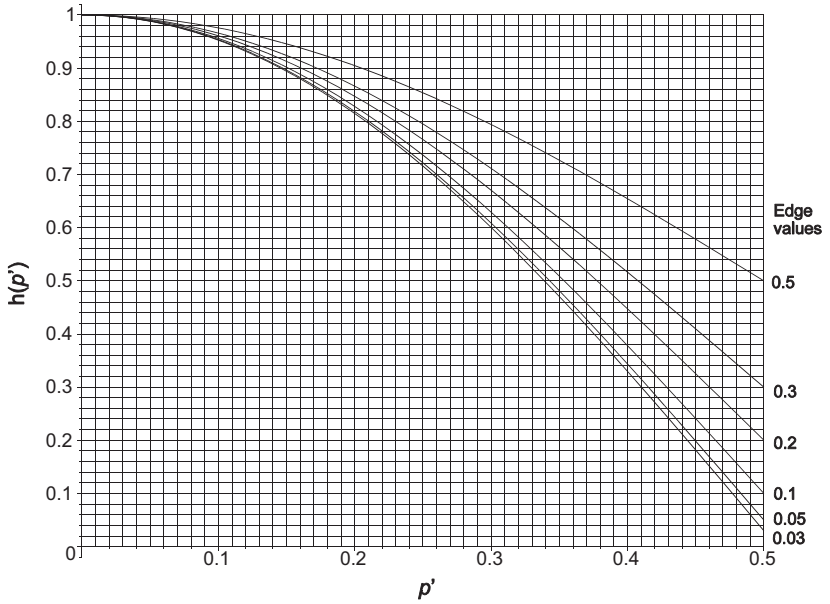

Figure 5.19 Cosine on pedestal tapering with edge values *k* from 0.5 to 0.03. [Source: Meikle, H.D., *Modern Radar Systems*, Artech House, Norwood, Massachusetts, 2001.]

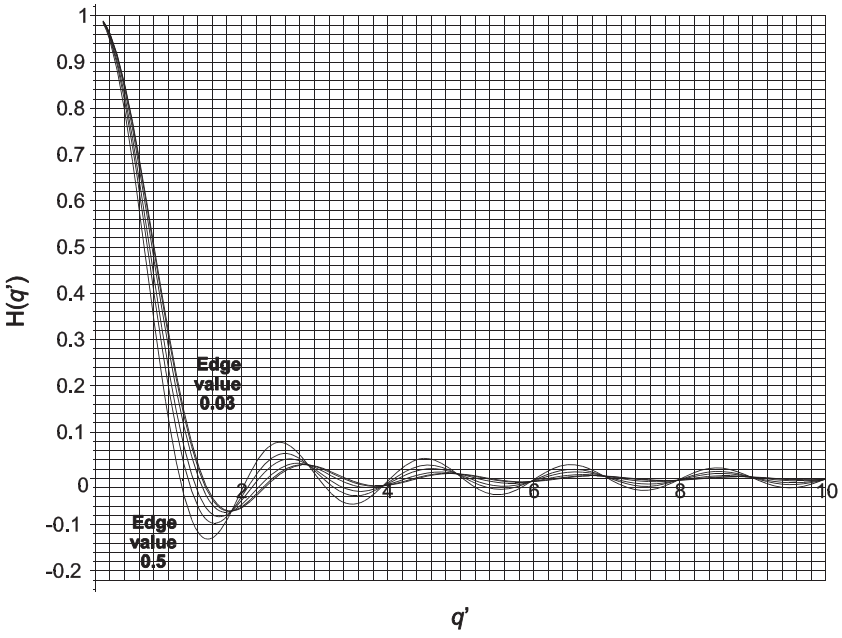

Figure 5.20 Fourier transforms for cosine on pedestal illumination with edge values *k* from 0.5 to 0.03. [Source: Meikle, H.D., *Modern Radar Systems*, Artech House, Norwood, Massachusetts, 2001.]

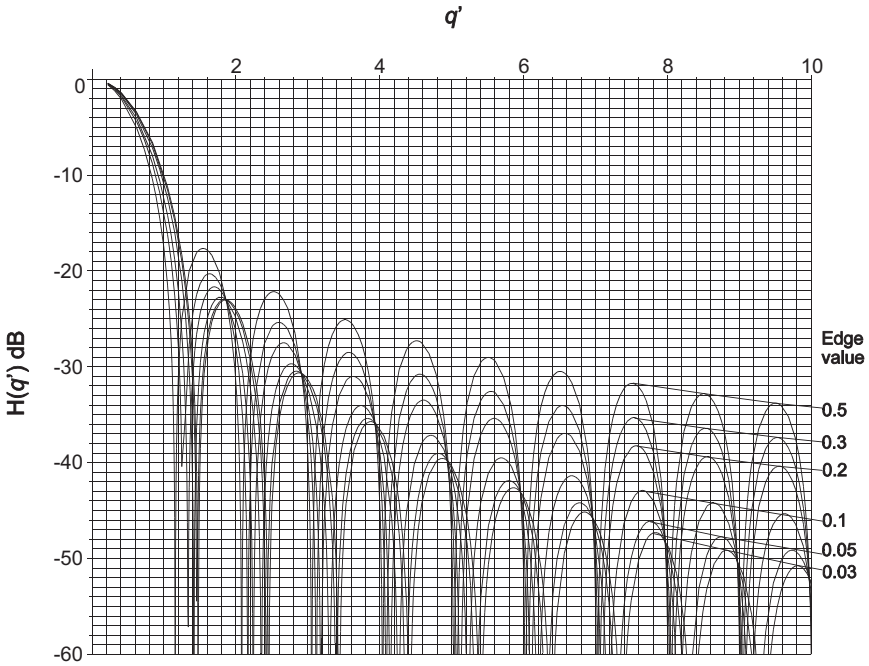

Figure 5.21 Fourier transforms in decibels for cosine on pedestal tapering with edge values k from 0.5 to 0.03. [Source: Meikle, H.D., *Modern Radar Systems*, Artech House, Norwood, Massachusetts, 2001.]

The closed form for the Fourier transform is

$$H(q') = \frac{4kq'^2 \sin(\pi q') - k \sin(\pi q') + 2kq' \cos(\pi q') - 2q' \cos(\pi q')}{\pi q' (4q'^2 - 1)\left(k + \frac{2}{\pi} - \frac{2k}{\pi}\right)} \tag{15}$$

Figure 5.22 shows an example of the effects of sampling on spectral leakage, or two-tone characteristics, when the discrete Fourier transform is used for 100 samples. The minor signal has a frequency corresponding to the 16th bin, and the major signal has its frequency varied between the 10th and 11th bins.

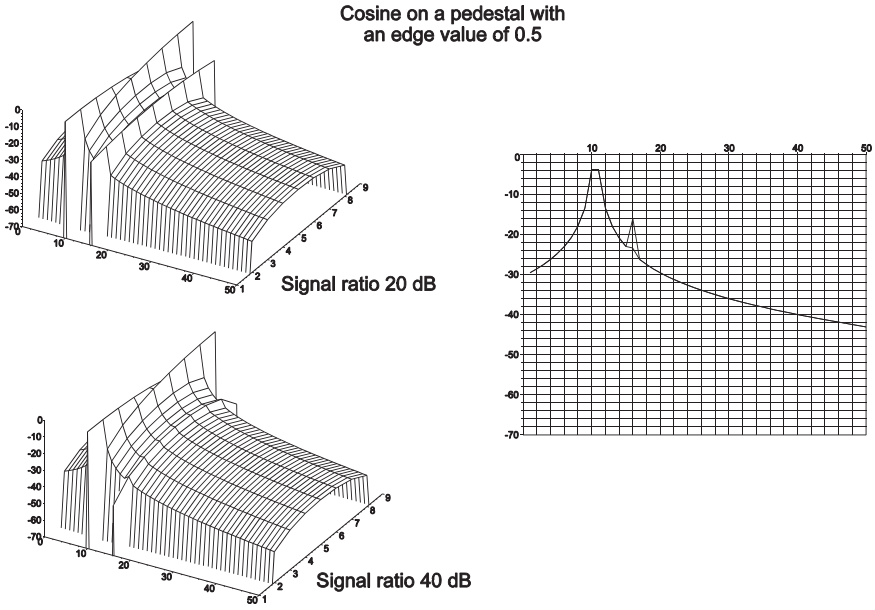

Figure 5.22 Examples of the spectral leakage or two-tone characteristics for a 100 sample filter as the major signal frequency is varied from bin 10 to bin 11. The minor signal, 20 dB or 40 dB smaller, is in bin 16. [Source: Meikle, H.D., *Modern Radar Systems*, Artech House, Norwood, Massachusetts, 2001.]

5.4.5
Hamming, Blackman, and Blackman-Harris Tapering

These functions look like truncated Gaussian functions on a pedestal and the Fourier transforms all have closed forms with low sidelobes. The aperture functions are given in Figure 5.23, Tables 5.9 and 5.11 [2] [6, Appendix B].

Table 5.9 The aperture functions for Hamming and Blackman tapering

Name	Aperture function
Hamming	$h(p') = 0.54 + 0.46 \cos(2\pi p')$
Exact Hamming	$h(p') = \frac{25}{46} + \frac{21}{46} \cos(2\pi p')$
Blackman	$h(p') = 0.42 + 0.5 \cos(2\pi p') + 0.88 \cos(4\pi p')$
Exact Blackman	$h(p') = \frac{3969}{9304} + \frac{1155}{2326} \cos(2\pi p') + \frac{715}{9304} \cos(4\pi p')$

Table 5.10 The aperture functions for Blackman-Harris tapering

Name	Aperture function
Blackman-Harris 2 terms	$h(p') = 0.5386 + 0.4614 \cos(2\pi p')$
Blackman-Harris 3 terms, 67 dB	$h(p') = 0.4232 + 0.4976 \cos(2\pi p') + 0.07922 \cos(4\pi p')$
Blackman-Harris 3 terms, 61 dB	$h(p') = 0.4496 + 0.4936 \cos(2\pi p') + 0.05677 \cos(4\pi p')$
Blackman-Harris 4 terms, 92 dB	$h(p') = 0.3588 + 0.4883 \cos(2\pi p') + 0.1413 \cos(4\pi p') + 0.01168 \cos(6\pi p')$
Blackman-Harris 4 terms, 74 dB	$h(p') = 0.4024 + 0.4980 \cos(2\pi p') + 0.09831 \cos(4\pi p') + 0.00122 \cos(6\pi p')$

Values calculated from the aperture functions in Tables 5.9 and 5.10 are shown in Table 5.11.

Table 5.11 Table of values for Hamming, Blackman, and Blackman-Harris tapering

	Hamming		Blackman		Blackman-Harris				
					2 term	3 terms		4 terms	
	Exact		Exact			67 dB	61 dB	92 dB	74 dB
A, effective length, *coherent gain*	0.54	0.54	0.42	0.43	0.54	0.42	0.45	0.36	0.40
A, dB	–5.35	–5.30	–7.54	–7.40	–5.38	–7.47	–6.94	–8.90	–7.91
C, effective power gain, *incoherent gain*	0.40	0.40	0.30	0.31	0.40	0.31	0.33	0.26	0.29
C, dB	–4.01	–3.98	–5.16	–5.11	–4.02	–5.14	–4.87	–5.88	–5.36
D (see Section 5.1)	4.18	4.11	5.44	5.33	4.20	5.38	5.06	6.31	5.66
G (see Section 5.1)	0.01	0.01	0.00	0.00	0.01	0.00	0.01	0.00	0.00
Efficiency, η, *processing gain*	0.73	0.74	0.58	0.59	0.73	0.59	0.62	0.50	0.56
Efficiency, η, *processing gain*, dB	–1.34	–1.31	–2.37	–2.29	–1.36	–2.33	–2.07	–3.02	–2.54
Noise beamwidth	1.36	1.35	1.73	1.69	1.37	1.71	1.61	2.00	1.80
Half-power beamwidth	1.30	1.29	1.64	1.61	1.31	1.62	1.53	1.90	1.71
RMS beamwidth	3.24	3.21	4.23	4.16	3.26	4.19	3.94	4.94	4.41
RMS aperture	0.96	0.97	0.75	0.76	0.96	0.75	0.80	0.64	0.71
First sidelobe dB	–44.04	–46.01	–58.11	–69.41	–43.29	–70.83	–74.52	–92.01	–66.42
Maximum sidelobe, dB	–42.68	–41.69	–58.11	–68.24	–43.12	–70.83	–62.05	–92.01	–66.42
Falloff dB/octave	–6.00	–6.00	–18.00	–6.00	–6.00	–6.00	–6.00	–6.00	–6.00
Scalloping loss	0.82	0.81	0.88	0.88	0.82	0.88	0.86	0.91	0.89
Scalloping loss dB	–1.75	–1.78	–1.10	–1.15	–1.74	–1.13	–1.27	–0.83	–1.02
Worst case loss	0.70	0.70	0.67	0.67	0.70	0.67	0.68	0.64	0.66
Worst case loss, dB	–3.10	–3.09	–3.47	–3.44	–3.10	–3.45	–3.34	–3.85	–3.56

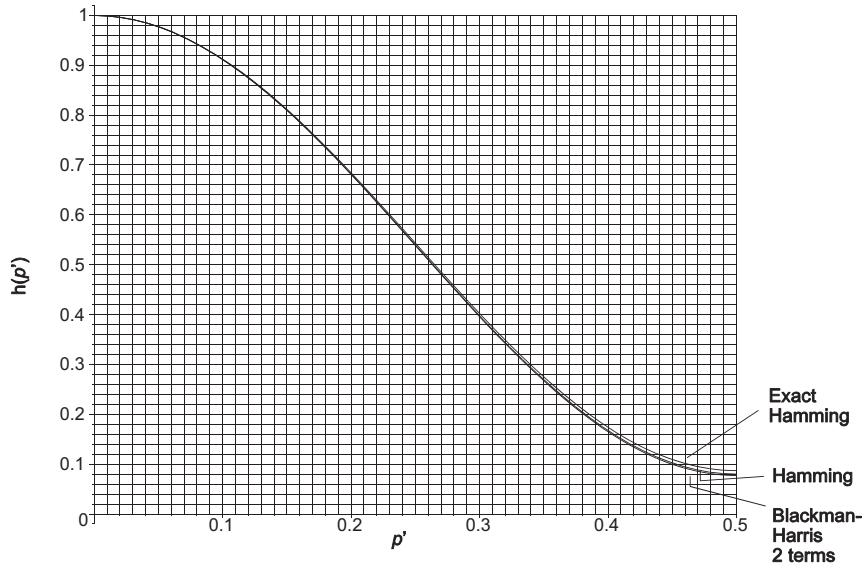

Figure 5.23 Hamming, exact Hamming, and Blackman-Harris tapering function with two terms. [Source: Meikle, H.D., *Modern Radar Systems*, Artech House, Norwood, Massachusetts, 2001.]

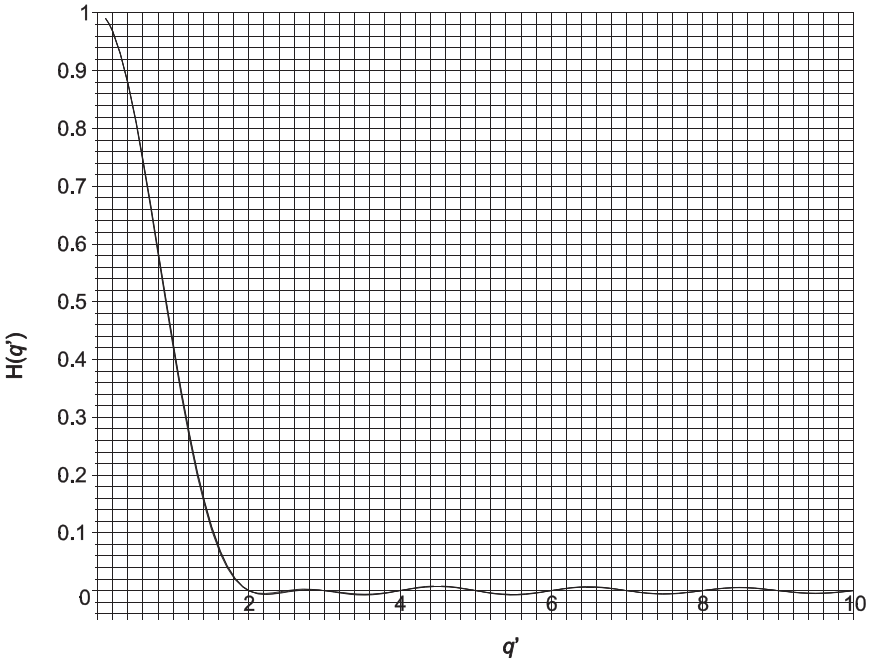

Figure 5.24 Hamming, exact Hamming, and two term Blackman-Harris Fourier transforms. The curves are too close to separate. [Source: Meikle, H.D., *Modern Radar Systems*, Artech House, Norwood, Massachusetts, 2001.]

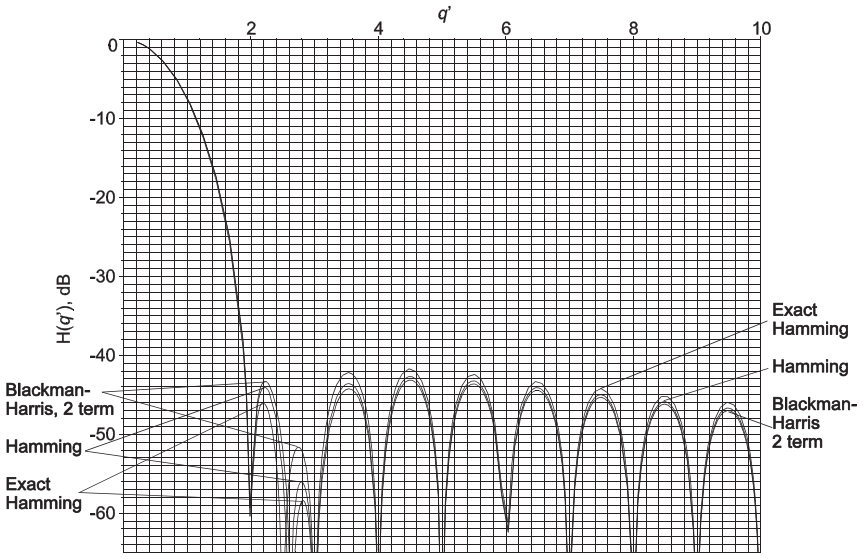

Figure 5.25 Hamming, exact Hamming, and two term Blackman-Harris Fourier transforms in decibels. [Source: Meikle, H.D., *Modern Radar Systems*, Artech House, Norwood, Massachusetts, 2001.]

The closed forms for the Fourier transforms are given in Table 5.12.

Table 5.12 Fourier transforms for the Hamming, exact Hamming, and two term Blackman-Harris aperture functions

Aperture function	Fourier transform
Hamming	$H(q') = \dfrac{-2(0.01273q'^2 - 0.08594)\ \sin(\pi\ q')}{q'\ (q'^2 - 1)}$
Exact Hamming	$H(q') = \dfrac{-2\ \left(-\frac{q'^2}{23} + \frac{25}{92}\right)\ \sin(\pi\ q')}{\pi\ q'\ (q'^2 - 1)}$
Two term Blackman-Harris	$H(q') = \dfrac{-2\ (-0.01227q'^2 + 0.08571)\ \sin(\pi\ q')}{q'\ (q'^2 - 1)}$

Figure 5.26 shows an example of the effects of sampling on spectral leakage, or two-tone characteristics, when the discrete Fourier transform is used for 100 samples. The minor signal has a frequency corresponding to the 16th bin, and the major signal has its frequency varied between the 10th and 11th bins.

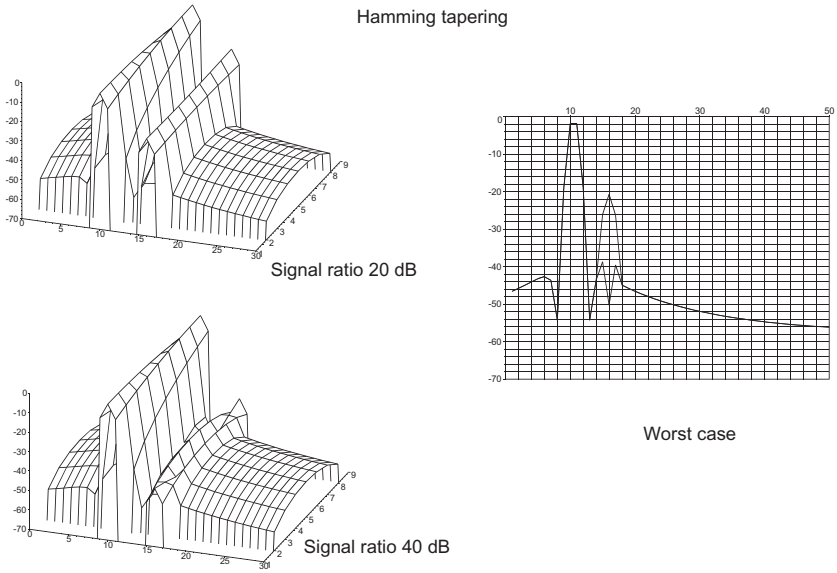

Figure 5.26 Examples of the spectral leakage, or two-tone characteristics, for a 100 sample filter with Hamming tapering as the major signal frequency is varied from bin 10 to bin 11. The minor signal, 20 dB or 40 dB smaller, is in bin 16. [Source: Meikle, H.D., *Modern Radar Systems*, Artech House, Norwood, Massachusetts, 2001.]

5.4.5.1 **Blackman and Exact Blackman**

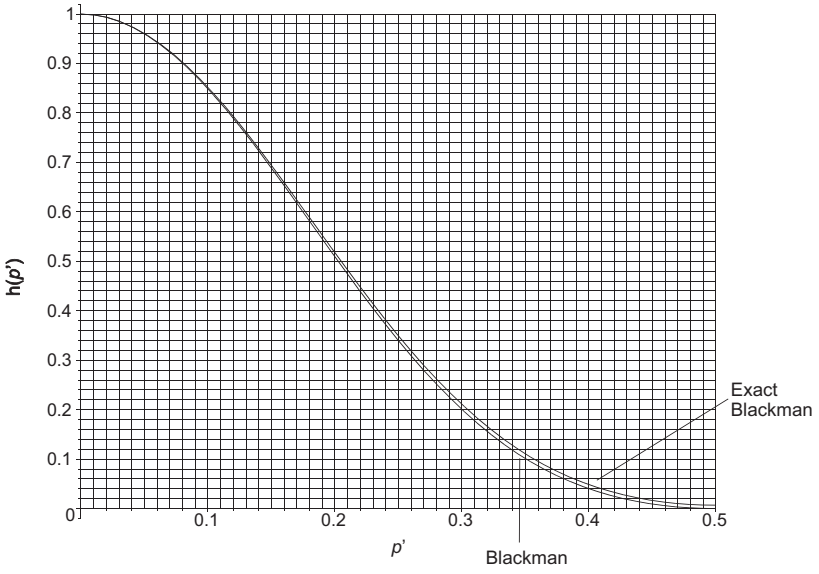

Figure 5.27 Blackman and exact Blackman tapering functions. [Source: Meikle, H.D., *Modern Radar Systems*, Artech House, Norwood, Massachusetts, 2001.]

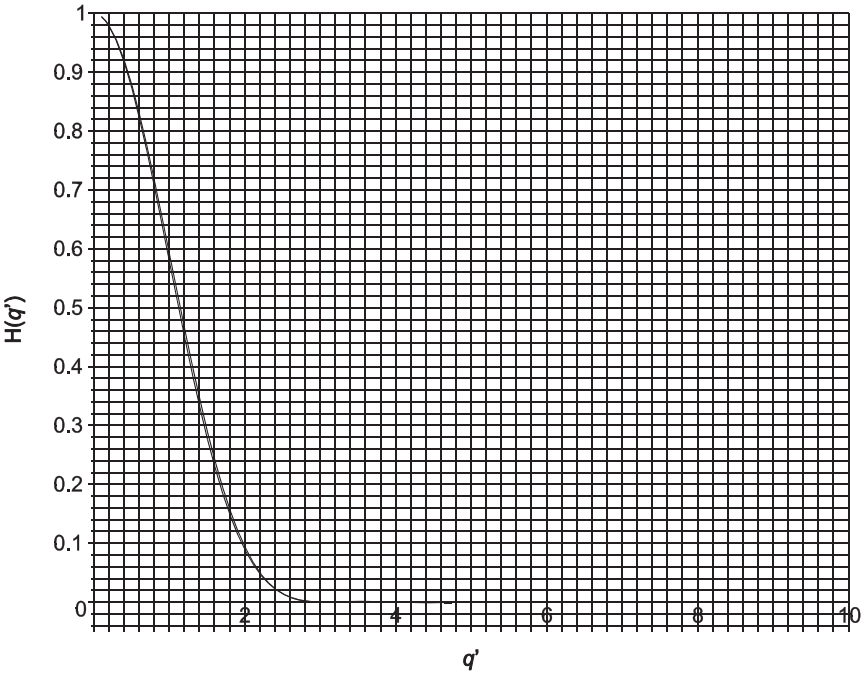

Figure 5.28 Blackman and exact Blackman Fourier transforms. The curves are too close to separate. [Source: Meikle, H.D., *Modern Radar Systems*, Artech House, Norwood, Massachusetts, 2001.]

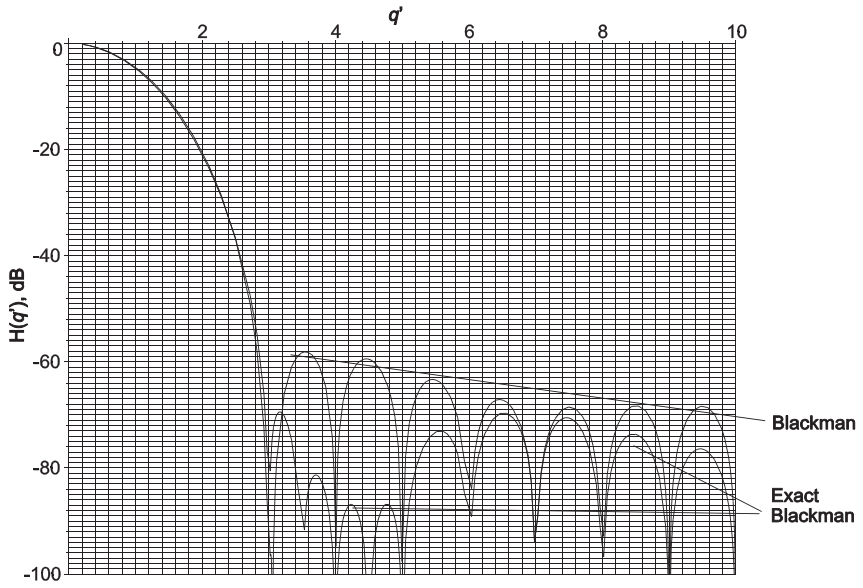

Figure 5.29 Blackman and exact Blackman Fourier transforms in decibels. [Source: Meikle, H.D., *Modern Radar Systems*, Artech House, Norwood, Massachusetts, 2001.]

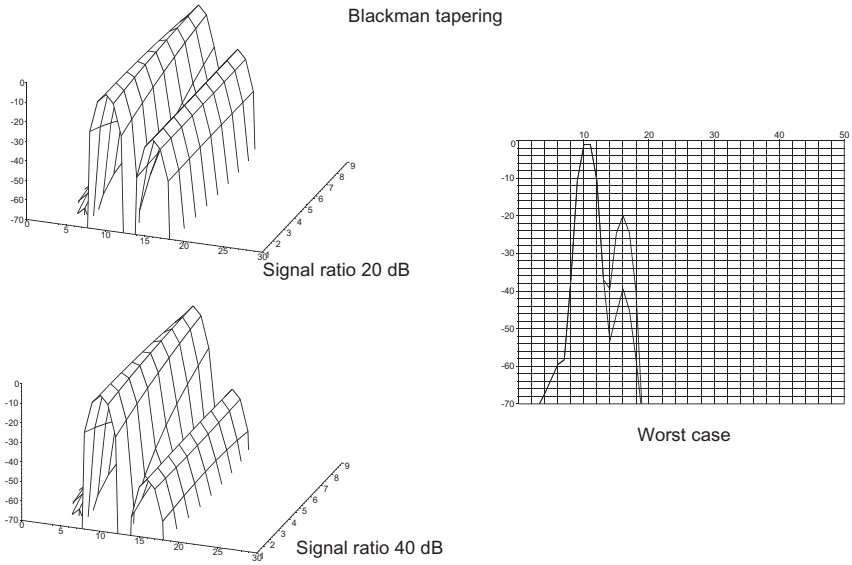

Figure 5.30 Examples of the spectral leakage, or two-tone characteristics, for a 100 sample filter with Blackman tapering as the major signal frequency is varied from bin 10 to bin 11. The minor signal, 20 dB or 40 dB smaller, is in bin 16. [Source: Meikle, H.D., *Modern Radar Systems*, Artech House, Norwood, Massachusetts, 2001.]

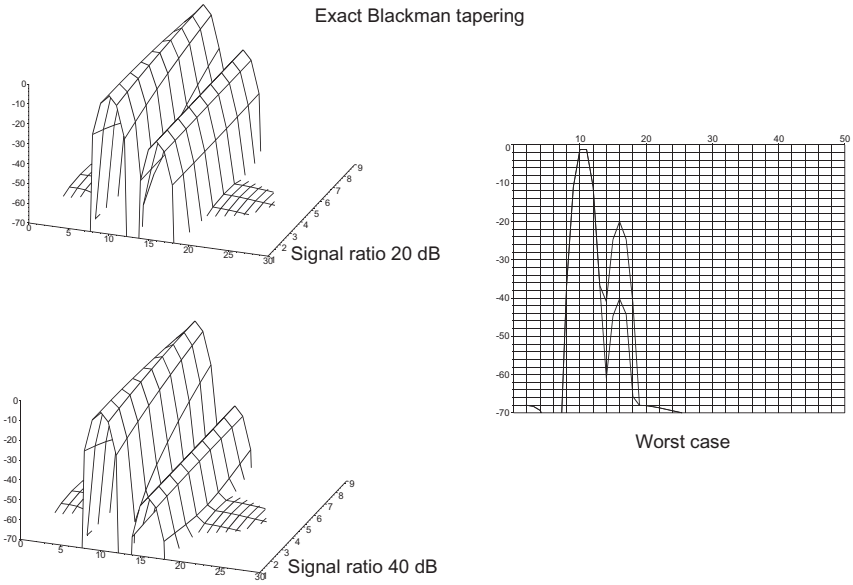

Figure 5.31 Examples of the spectral leakage, or two-tone characteristics, for a 100 sample filter with exact Blackman tapering as the major signal frequency is varied from bin 10 to bin 11. The minor signal, 20 dB or 40 dB smaller, is in bin 16. [Source: Meikle, H.D., *Modern Radar Systems*, Artech House, Norwood, Massachusetts, 2001.]

Figures 5.30 and 5.31 show an example of the effects of sampling on spectral leakage, or two-tone characteristics, when the discrete Fourier transform is used for 100 samples. The minor signal has a frequency corresponding to the 16th bin, and the major signal has its frequency varied between the 10th and 11th bins.

Closed forms for the Fourier transforms are given in Table 5.12.

Table 5.13 Fourier transforms for Blackman and exact Blackman tapering

Name	Fourier transform
Blackman	$H(q') = \dfrac{-2\,(0.02865^{\prime 2} - 0.2674)\,\sin(\pi\, q')}{q'\,(q'^2 - 4)\,(q'^2 - 1)}$
Exact Blackman	$H(q') = \dfrac{-2\left(-\frac{4q'^4}{1163} + \frac{130q'^2}{1163} - \frac{3969}{4652}\right)\sin(\pi\, q')}{\pi\, q'\,(q'^2 - 4)\,(q'^2 - 1)}$

5.4.5.2 **Blackman-Harris tapering**

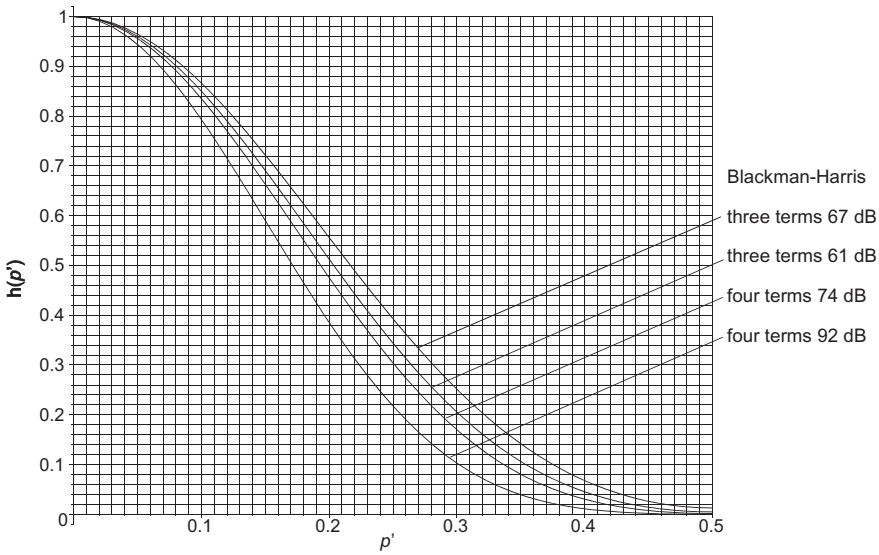

Figure 5.32 Blackman-Harris tapering functions. [Source: Meikle, H.D., *Modern Radar Systems*, Artech House, Norwood, Massachusetts, 2001.]

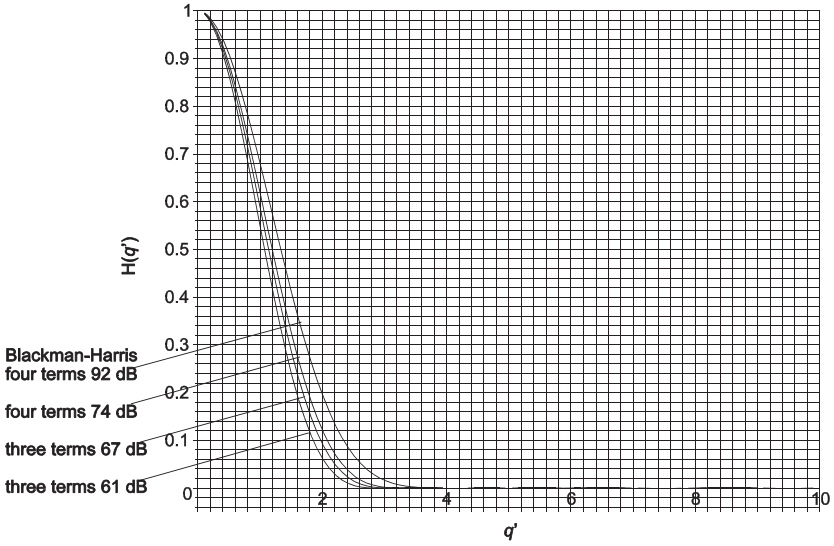

Figure 5.33 Blackman-Harris Fourier transforms. [Source: Meikle, H.D., *Modern Radar Systems*, Artech House, Norwood, Massachusetts, 2001.]

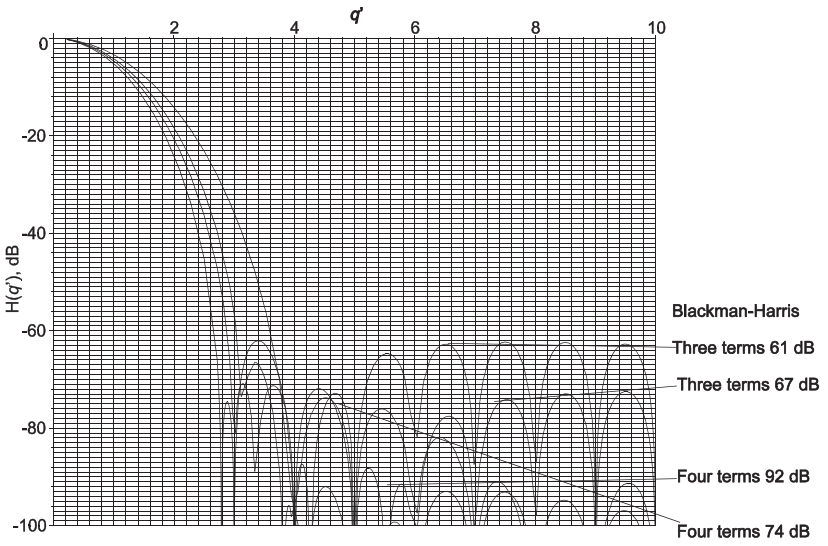

Figure 5.34 Blackman-Harris Fourier transforms in decibels. [Source: Meikle, H.D., *Modern Radar Systems*, Artech House, Norwood, Massachusetts, 2001.]

Figures 5.35 and 5.36 show an example of the effects of sampling on spectral leakage, or two-tone characteristics, when the discrete Fourier transform is used for 100 samples. The minor signal has a frequency corresponding to the 16th bin, and the major signal has its frequency varied between the 10th and 11th bins.

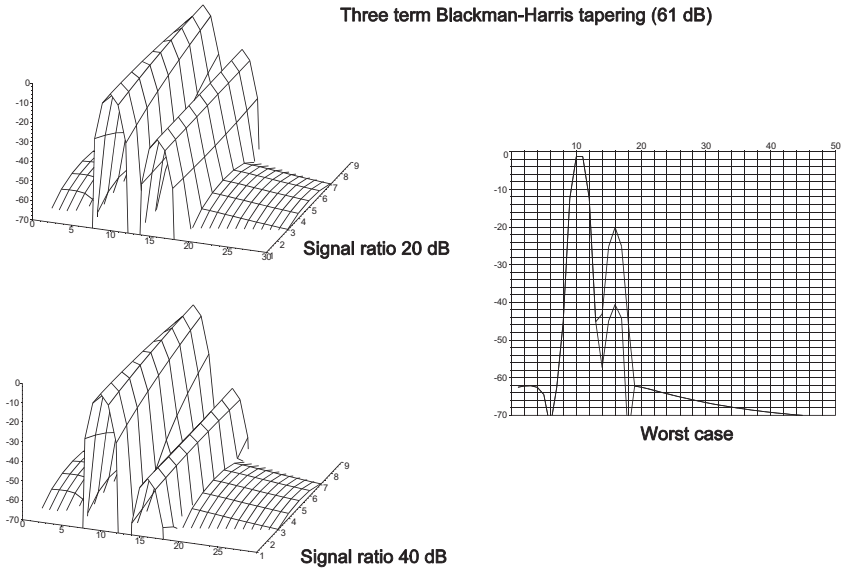

Figure 5.35 Examples of the spectral leakage, or two-tone characteristics, for a 100 sample filter with three term Blackman-Harris 61 dB sidelobe tapering as the major signal frequency is varied from bin 10 to bin 11. The minor signal, 20 dB or 40 dB smaller, is in bin 16. [Source: Meikle, H.D., *Modern Radar Systems*, Artech House, Norwood, Massachusetts, 2001.]

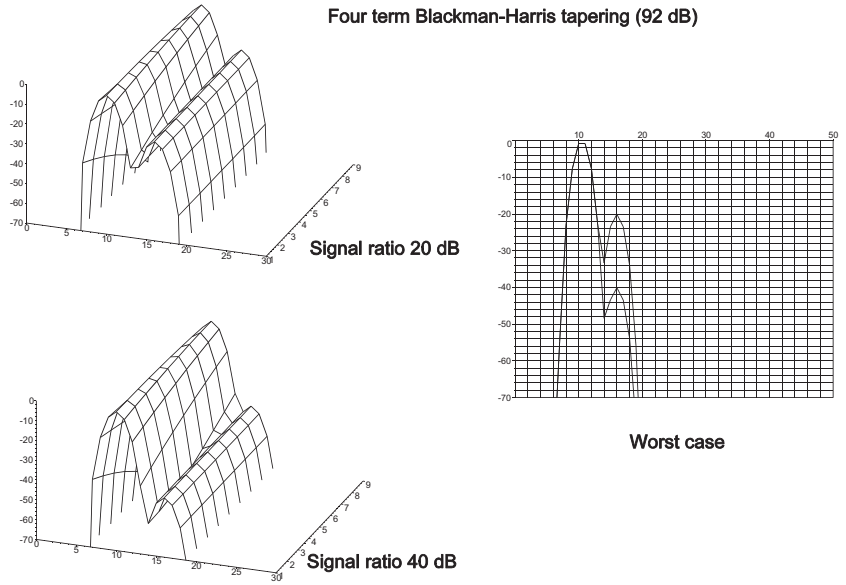

Figure 5.36 Examples of the spectral leakage, or two tone-characteristics, for a 100 sample filter with four term Blackman-Harris 92 dB sidelobe tapering as the major signal frequency is varied from bin 10 to bin 11. The minor signal, 20 dB or 40 dB smaller, is in bin 16. [Source: Meikle, H.D., *Modern Radar Systems*, Artech House, Norwood, Massachusetts, 2001.]

Closed forms for the Fourier transforms are shown in Table 5.13, more accurate forms are available in [6, Appendix B].

Table 5.14 Fourier transforms of examples of Blackman-Harris functions

Function name	Fourier transform
Blackman-Harris three terms 67 dB	$\frac{H(q') = -2(-0.0007799q'^4+0.03265q'^2-0.2694)\ sin(\pi\ q')}{q'\ (q'^2-4)(q'^2-1)}$
Blackman-Harris three terms 61 dB	$\frac{H(q') = -2\ (-0.002024q'^4+0.05255q'^2-0.2862)\ sin(\pi\ q')}{q'\ (q'^2-4)(q'^2-1)}$
Blackman-Harris four terms 92 dB	$\frac{H(q') = -2.(-0.000009549q'^6+0.004636q'^4-0.1949q'^2+2.0555)\ sin(\pi\ q')}{q'\ (q'^2-4)(q'^2-1)(q'^2-9)}$
Blackman-Harris four terms 74 dB	$\frac{H(q') = -2(-0.0002355q'^6+0.02172q'^4-0.4249q'^2+2.3056)\ sin(\pi\ q')}{q'\ (q'^2-4)(q'^2-1)(q'^2-9)}$

5.4.6 Truncated Gaussian tapering

The tapering function is $\exp(-2\ln(2)\ (n\,p')^2)$ and examples are shown in Figure 5.37.

Table 5.15 Table of values for a number of truncated Gaussian tapering functions

	Value of *n*				
	1	**1.7**	**2.4**	**2.8**	**3.2**
Edge illumination, dB	–3.01	–8.70	–17.34	–23.60	–30.83
A, effective length, *coherent gain*	0.90	0.75	0.60	0.53	0.47
A, dB	–0.96	–2.54	–4.46	–5.56	–6.62
C, effective power, *incoherent power gain*	0.81	0.60	0.44	0.38	0.33
C, dB	–0.92	–2.23	–3.55	–4.20	–4.78
D (see Section 5.1)	0.43	1.85	3.38	4.08	4.71
G (see Section 5.1)	0.06	0.03	0.01	0.01	0.01
Efficiency η, *processing gain*	0.99	0.93	0.81	0.73	0.66
Efficiency η, *processing gain*, dB	–0.04	–0.30	–0.91	–1.36	–1.84
Noise beamwidth	1.01	1.07	1.23	1.37	1.53
Half-power beamwidth	0.93	1.02	1.18	1.30	1.45
RMS beamwidth	0.73	1.76	2.77	3.28	3.76
RMS aperture	1.65	1.38	1.09	0.95	0.83
First sidelobe, dB	–15.43	–20.70	–31.86	–39.15	–
Falloff dB/octave	–6.00	–6.00	–6.00	–6.00	–6.00
Scalloping loss	0.67	0.72	0.78	0.82	0.85
Scalloping loss, dB	–3.51	–2.86	–2.13	–1.75	–1.43
Worst case loss	0.66	0.69	0.71	0.70	0.69
Worst case loss, dB	–3.56	–3.17	–3.04	–3.11	–3.26

$2\ln(2) = 1.386$ is the scaling factor to make the tip of a Gaussian approximate to a $\sin x/x$ function with the same half-power beamwidth.

The closed form for the Fourier transform is

$$H(q') = \frac{\sqrt{\pi}\, e^{-\frac{\pi^2 q'^2}{2\ln(2)n^2}} \left[\operatorname{erf}\left(\frac{j2\pi q' + \ln(2)n^2}{2n\sqrt{2\ln(2)}}\right) - \operatorname{erf}\left(\frac{j2\pi q' - \ln(2)n^2}{2n\sqrt{2\ln(2)}}\right)\right]}{n\sqrt{2\ln(2)}} \tag{16}$$

where $\operatorname{erf}(x)$ denotes the Gaussian error function, $\int_x^\infty e^{-x^2}\, dx$.

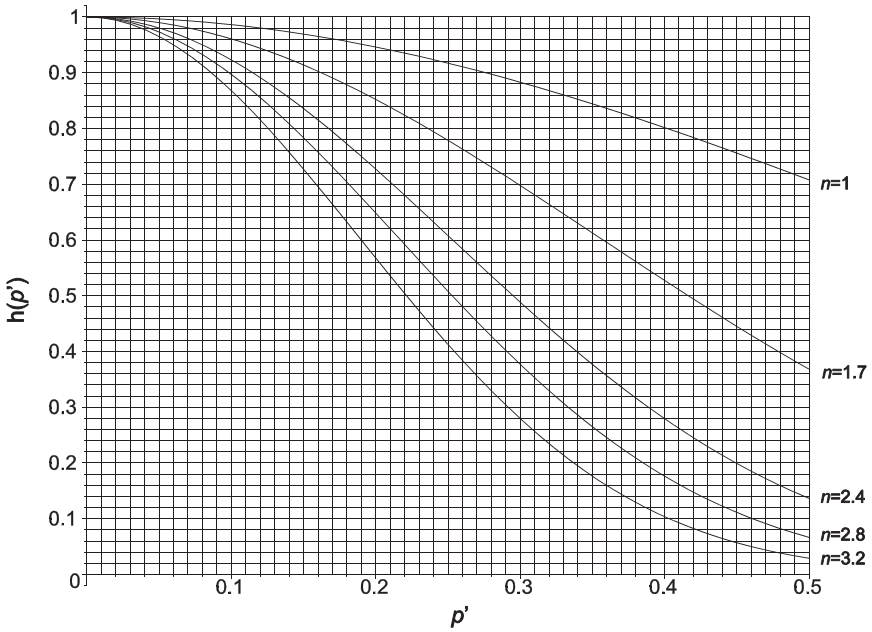

Figure 5.37 Truncated Gaussian tapering function. [Source: Meikle, H.D., *Modern Radar Systems*, Artech House, Norwood, Massachusetts, 2001.]

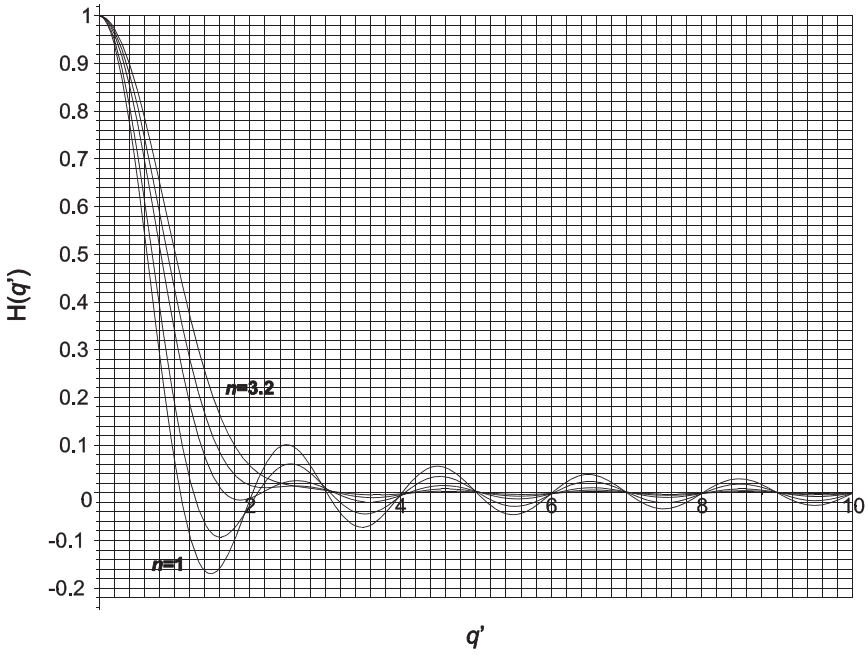

Figure 5.38 Fourier transforms for truncated Gaussian tapering for $n = 1, 1.7, 2.4, 2.8, 3.2$. [Source: Meikle, H.D., *Modern Radar Systems*, Artech House, Norwood, Massachusetts, 2001.]

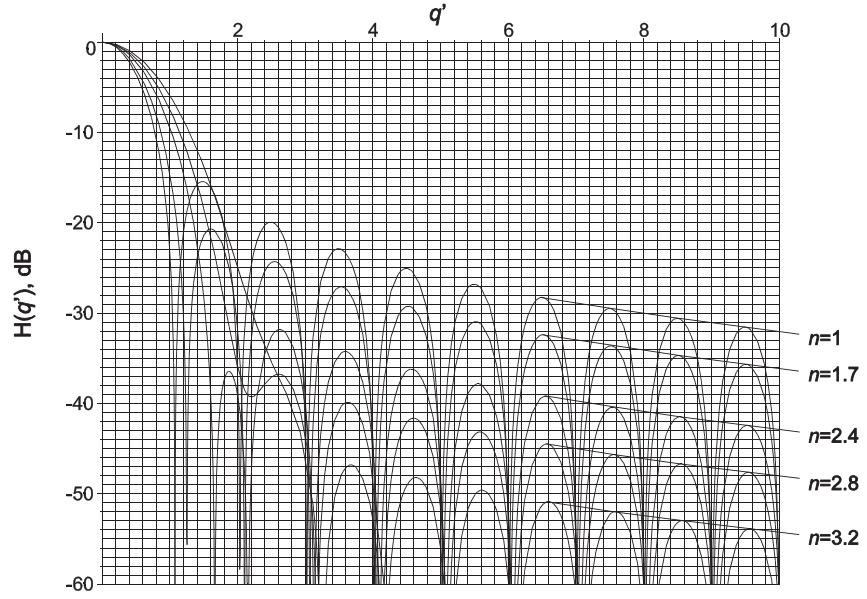

Figure 5.39 Fourier transforms in decibels for truncated Gaussian tapering for $n = 1, 1.7, 2.4, 2.8, 3.2$. [Source: Meikle, H.D., *Modern Radar Systems*, Artech House, Norwood, Massachusetts, 2001.]

Figure 5.40 shows an example of the effects of sampling on spectral leakage, or two-tone characteristics, when the discrete Fourier transform is used for 100 samples. The minor signal has a frequency corresponding to the 16th bin and the major signal has its frequency varied between the 10th and 11th bins.

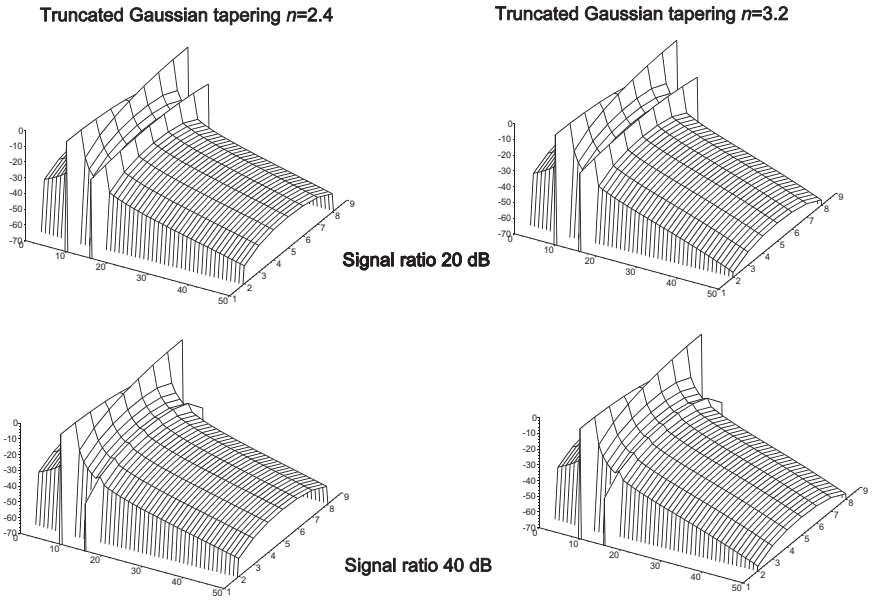

Figure 5.40 Examples of the spectral leakage, or two-tone characteristics for a 100 sample filter as the major signal frequency is varied from bin 10 to bin 11. The minor signal, 20 dB or 40 dB smaller, is in bin 16. [Source: Meikle, H.D., *Modern Radar Systems*, Artech House, Norwood, Massachusetts, 2001.]

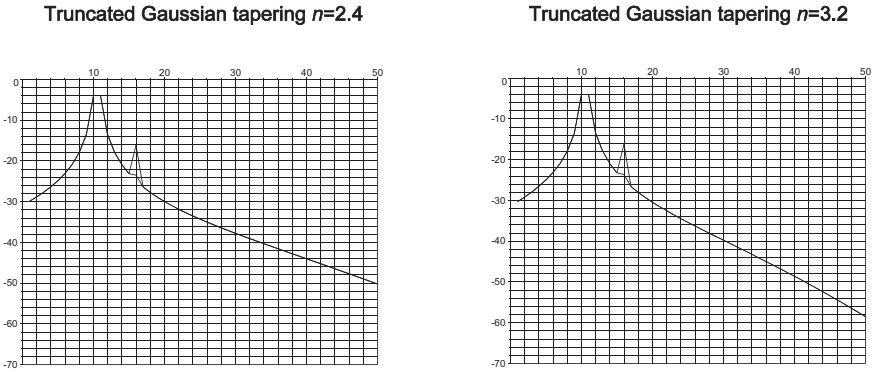

Figure 5.41 Worst case masking of the minor signal with two cases of truncated Gaussian tapering. [Source: Meikle, H.D., *Modern Radar Systems*, Artech House, Norwood, Massachusetts, 2001.]

5.4.7

Dolph-Chebyshev Tapering with 10 Discrete Samples

A use of Chebyshev (Чебышев) polynomials is to economise expressions for the calculation of functions. The function is scaled to lie between ±1 and the error has a constant ripple within this region. Chebyshev polynomials of the first kind, order n are given by [6, p.537]

$$T_n(x) = \begin{cases} -1^n \cosh(n \operatorname{arccosh}|x|) & x < -1 \\ \cos(n \arccos x) & -1 < x < 1 \\ \cosh(n \operatorname{arccosh} x) & x > 1 \end{cases} \tag{17}$$

The first seven polynomials are plotted in Figure 5.42.

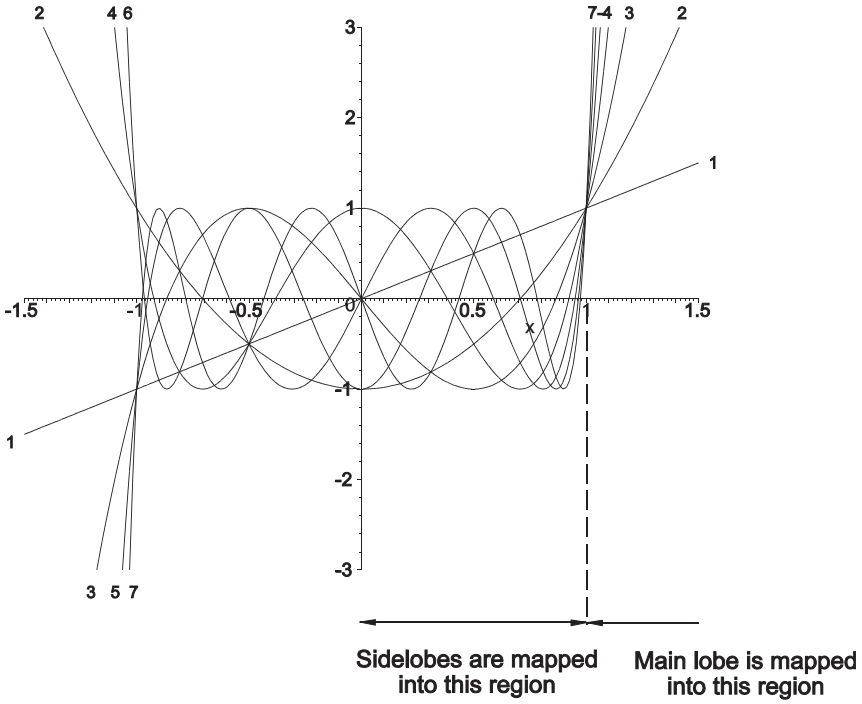

Figure 5.42 Plots of the first seven Chebyshev polynomials of the first kind. [Source: Meikle, H.D., *Modern Radar Systems*, Artech House, Norwood, Massachusetts, 2001.]

Considering discrete antenna arrays with N elements, Dolph mapped the sidelobes into the region 0 to 1 where the Chebyshev polynomial of order N–1 oscillates between ±1, and the main lobe beyond +1 where the polynomial increases almost exponentially. Equating the peak of the main lobe to unity, the oscillating polyno-

mial between 0 and 1 represents the sidelobe level with $n-1$ peaks between ±1. The abscissa x_0 is found by solving for x in Equation (17) with the right-hand side equated to the voltage sidelobe level ratio, R, namely

$$q_0 = \cosh \frac{\operatorname{arccosh} R}{N-1} \tag{18}$$

R is usually expressed as the sidelobe level, SLL, in decibels

$$R = 10^{\frac{SLL}{20}} \tag{19}$$

The characteristic, in the case of antennae, the voltage pattern, $\mathrm{H}(q')$ is given by

$$\begin{aligned} \mathrm{H}(q') &= T_{N-1}(q_0 \cos \pi q') \\ &= \cos\Big((N-1) \arccos(q_0 \cos \pi q')\Big) \end{aligned} \tag{20}$$

where $q' = \frac{w}{\lambda} \sin \theta$;
w is the width of the antenna;
λ is the wavelength in the same units;
θ is the angle to the normal of the antenna.

The tapering values for each element are found from the inverse transform, one version is [7] [3, Appendix B]

$$W[K] = \frac{N-1}{N-K} \sum_{S=0}^{K-2} \frac{(K-2)!(N-K)!\alpha^{S+1}}{S!\ (K-2-S)!\ (S+1)!\ (N-K-S-1)!} \tag{21}$$

where $\alpha = \left[\tanh \frac{\operatorname{arccosh}(R)}{N-1}\right]^2$;
$W[1] = W[K]$
N is the number of samples or elements.

The tapering values for each element, or weights, are normalised to unity at the centre in Figure 5.43.

The same applies to finite impulse response filters that use the sum of N tapered signals.

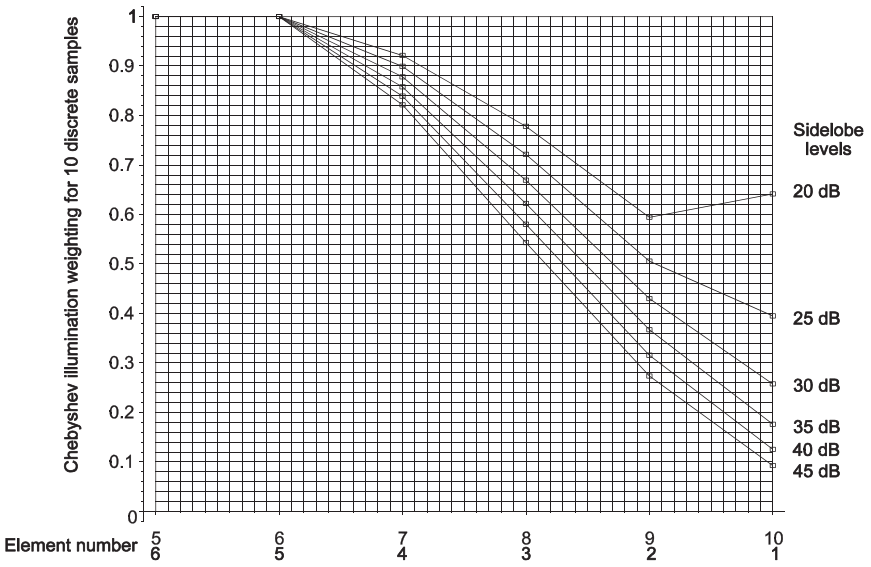

Figure 5.43 The points show the weights for Dolph-Chebyshev tapering with 10 discrete samples. [Source: Meikle, H.D., *Modern Radar Systems*, Artech House, Norwood, Massachusetts, 2001.]

Table 5.16 Table of values for Chebyshev tapering with 10 elements

	Sidelobe level, dB					
	20.0	**25.0**	**30.0**	**35.0**	**40.0**	**45.0**
A, effective length, *coherent gain*	0.79	0.70	0.65	0.60	0.57	0.55
A, dB	–2.08	–3.05	–3.78	–4.37	–4.85	–5.25
C, effective power, *incoherent power gain*	0.64	0.55	0.49	0.46	0.43	0.41
C, dB	–1.91	–2.61	–3.06	–3.39	–3.65	–3.87
D (see Section 5.1)	–	–	–	–	–	–
G (see Section 5.1)	–	–	–	–	–	–
Efficiency η, *processing gain*	0.96	0.90	0.85	0.80	0.76	0.73
Efficiency η, *processing gain*, dB	–0.17	–0.43	–0.72	–0.98	–1.20	–1.39
Noise beamwidth	1.04	1.11	1.18	1.25	1.32	1.38
Half-power beamwidth	0.97	1.06	1.14	1.20	1.26	1.32
RMS beamwidth	–	–	–	–	–	–
RMS aperture	–	–	–	–	–	–
First sidelobe, dB	19.73	24.91	29.97	34.99	40.00	45.00
Falloff dB/octave	0.00	0.00	0.00	0.00	0.00	0.00
Scalloping loss	0.69	0.74	0.77	0.79	0.81	0.82
Scalloping loss, dB	–3.18	–2.67	–2.31	–2.06	–1.86	–1.71
Worst case loss	0.68	0.70	0.71	0.71	0.70	0.70
Worst case loss, dB	–3.35	–3.10	–3.03	–3.03	–3.06	–3.10

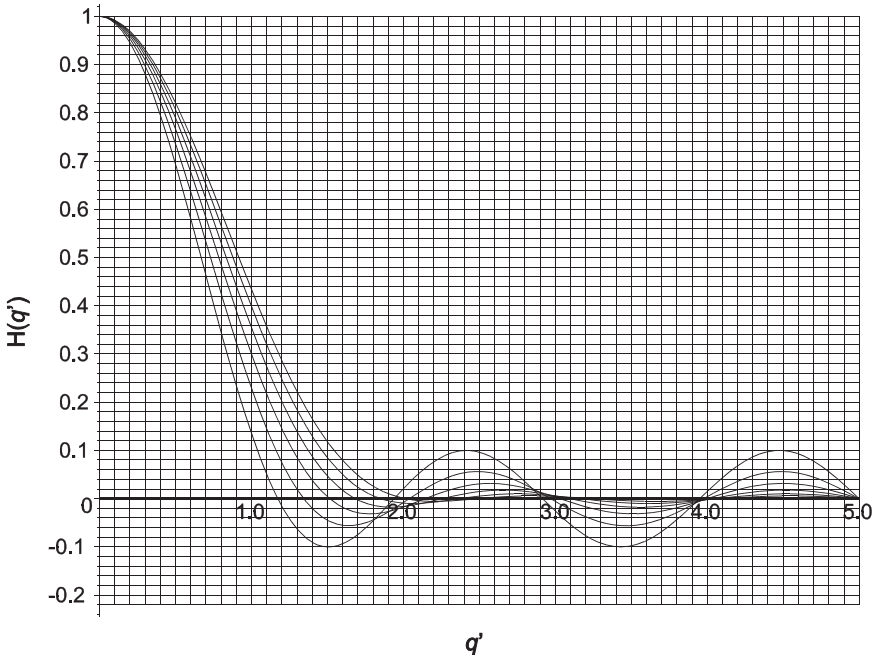

Figure 5.44 Fourier transform for Dolph-Chebyshev tapering with discrete 10 elements.
[Source: Meikle, H.D., *Modern Radar Systems*, Artech House, Norwood, Massachusetts, 2001.]

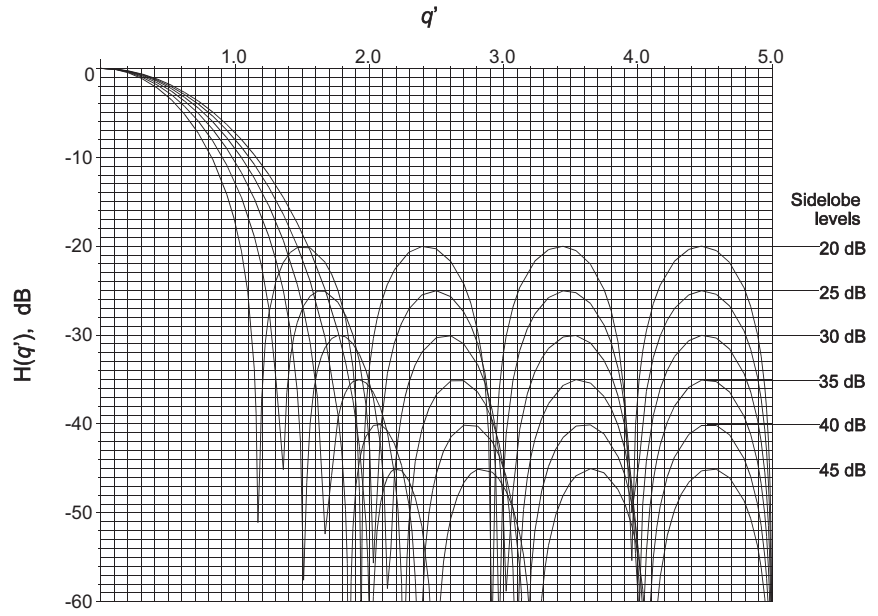

Figure 5.45 Fourier transform decibels for Dolph-Chebyshev tapering with discrete 10 elements.
[Source: Meikle, H.D., *Modern Radar Systems*, Artech House, Norwood, Massachusetts, 2001.]

Figure 5.46 shows an example of the effects of sampling on spectral leakage, or two-tone characteristics, when the discrete Fourier transform is used for 100 samples. The minor signal has a frequency corresponding to the 16th bin, and the major signal has its frequency varied between the 10th and 11th bins.

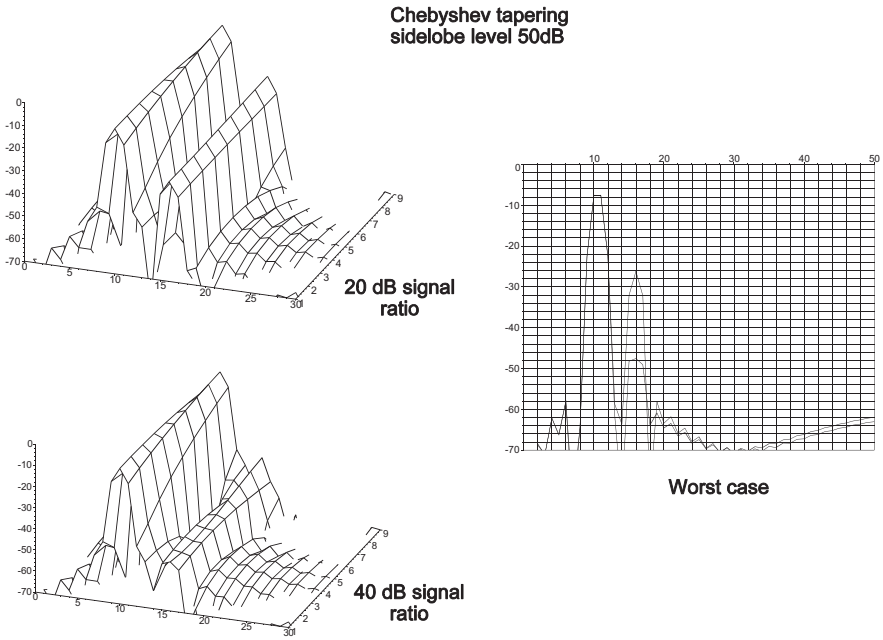

Figure 5.46 Examples of the spectral leakage or two-tone characteristics for a 100 sample filter as the major signal frequency is varied from bin 10 to bin 11. The minor signal, 20 dB or 40 dB smaller, is in bin 16. [Source: Meikle, H.D., *Modern Radar Systems*, Artech House, Norwood, Massachusetts, 2001.]

5.4.8
Taylor Tapering

Taylor extended the Dolph-Chebyshev tapering to continuous functions by modelling the near sidelobes, *SLL* dB, on the Chebyshev characteristic and the far sidelobes on the sinc function ($\sin x/x$) [6, p. 543] [4, p. 719]. Figure 5.47 shows a comparison of $\text{sinc}(\pi q')$, Chebyshev, and Taylor characteristics.

Figure 5.47 shows that the Chebyshev sidelobes do not have the same number and positions as the $\text{sinc}(\pi x)$ function. So that the two types of characteristic 'fit', Taylor changed the modelling expression to

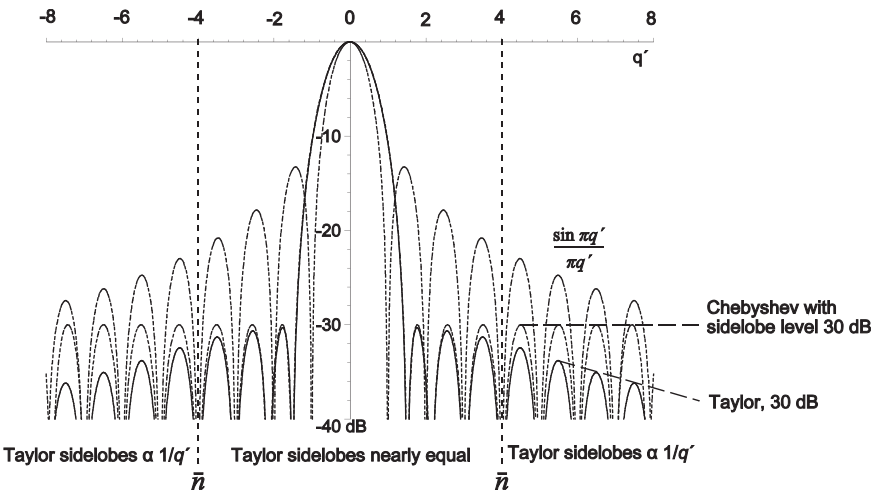

Figure 5.47 A comparison between sinc $\pi q'$, Chebyshev, and Taylor patterns.

$$\mathrm{H}(q') = \cosh\left(\pi\sqrt{A_t^2 - q'^2}\right) \quad \text{for } q' < A \text{ main beam}$$

$$\text{or } \cos\left(\pi\sqrt{q'^2 - A_t^2}\right) \quad \text{for } q' > A \text{ sidelobe} \tag{22}$$

where q' is the variable and, for antennae, $q' = \frac{w}{\lambda}\sin\theta$;
w is the antenna width;
λ is the wavelength in the same units;
A_t is a constant controlling the characteristic and is defined later.

The value of A_t, as with the Chebyshev characteristic, has the value of $\mathrm{H}(q')$ when $q' = 0$, namely

$$R = \cosh\pi A_t \quad \text{or} \quad A_t = \frac{\operatorname{arccosh}(R)}{\pi} \tag{23}$$

where, as with Chebyshev tapering, the sidelobe voltage ratio, R, is

$$R = 10^{\frac{SLL}{20}} \text{ voltage ratio} \tag{24}$$

The zeroes for the sinc $\pi q'$part of the characteristic occur at integer values of $q'$and the last zero of the inner characteristic must occur at an integer value, or $q' = \bar{n}$. The smallest value of $\bar{n}$ is found from

$$\bar{n}_{\text{minimum}} = 2A^2 + \frac{1}{2} \tag{25}$$

For the Taylor sidelobe characteristic with a sidelobe level of 30 dB in Figure 5.47, $R = \sqrt{10000}$, $A_t = 1.32$, and $\bar{n}_{\text{minimum}} = 3.98$ that forces $\bar{n}$ to at least 4. The value σ_d,

the dilation factor, is used to scale q' so that when $q' = \bar{n}$ the zeroes of both characteristics coincide. The zeroes occur at

$$\begin{aligned} z(n) &= \pm\,\sigma\sqrt{A_t^{\,2} + \left(n - \frac{1}{2}\right)^2} \quad \text{for } 1 \le n \le \overline{n} \\ &= \pm\, n \qquad\qquad\qquad\qquad\quad \text{for } \overline{n} \le n \le \infty \end{aligned} \tag{26}$$

where n is an integer.

At the points of the common zero $z(n) = \bar{n}$, so that

$$\sigma_d = \frac{\overline{n}}{\sqrt{A_t^{\,2} + (\overline{n} - 0.5)^2}} \tag{27}$$

The tapering function is found by the inverse Fourier transform, one form is given by the Fourier series and illustrated in Figure 5.48 [4, p. 721].

$$h(p') = 1 + 2\sum_{n=1}^{\overline{n}-1} F_n \cos(2\,\pi\, n\, p') \tag{28}$$

$$H(q') = \frac{\sin(\pi q')}{\pi q'} \prod_{n=1}^{\bar{n}-1} \frac{1 - \dfrac{q'^2}{z(n)^2}}{1 - \dfrac{q'^2}{n^2}} \tag{29}$$

where

$$F_n = \frac{[(\bar{n}-1)!]^2}{(\bar{n}-1+n)!\;(\bar{n}-1-n)!} \prod_{m=1}^{\bar{n}-1} 1 - \frac{n^2}{z_m^2} \tag{30}$$

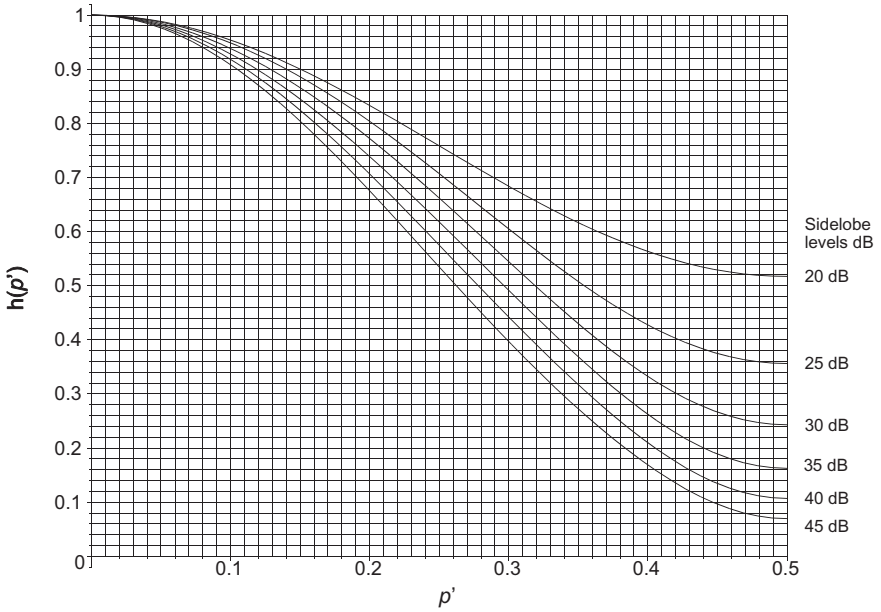

Figure 5.48 Taylor tapering functions for sidelobe levels from 20 dB to 45 dB. [Source: Meikle, H.D., *Modern Radar Systems*, Artech House, Norwood, Massachusetts, 2001.]

Table 5.17 Table of values for examples of Taylor tapering

	Sidelobe level, dB					
	20	**25**	**30**	**35**	**40**	**45**
$\bar{n}$	2	3	4	5	6	8
A, effective length, *coherent gain*	0.76	0.69	0.64	0.60	0.57	0.54
A, dB	–2.40	–3.19	–3.85	–4.43	–4.94	–5.40
C, effective power, *incoherent power gain*	0.60	0.53	0.48	0.45	0.42	0.39
C, dB	–2.18	–2.74	–3.16	–3.50	–3.79	–4.05
D (see Section 5.1)	–	–	–	–	–	–
G (see Section 5.1)	0.03	0.02	0.02	0.01	0.01	0.01
Efficiency η, *processing gain*	0.95	0.90	0.85	0.81	0.77	0.73
Efficiency η, *processing gain*, dB	–0.21	–0.45	–0.69	–0.93	–1.15	–1.36
Noise beamwidth	1.05	1.11	1.17	1.24	1.30	1.37
Half-power beamwidth	0.99	1.06	1.12	1.19	1.25	1.31
RMS beamwidth	–	–	–	–	–	–
RMS aperture	1.45	1.29	1.17	1.08	1.01	0.96
First sidelobe, dB	–20.70	–25.46	–30.31	–35.22	–40.16	–45.13
Falloff dB/octave	–	–	–	–	–	–
Scalloping loss	0.70	0.74	0.76	0.78	0.80	0.82
Scalloping loss, dB	–3.05	–2.66	–2.36	–2.11	–1.91	–1.74
Worst case loss	0.69	0.70	0.70	0.70	0.70	0.70
Worst case loss dB	–3.26	–3.11	–3.05	–3.04	–3.06	–3.10

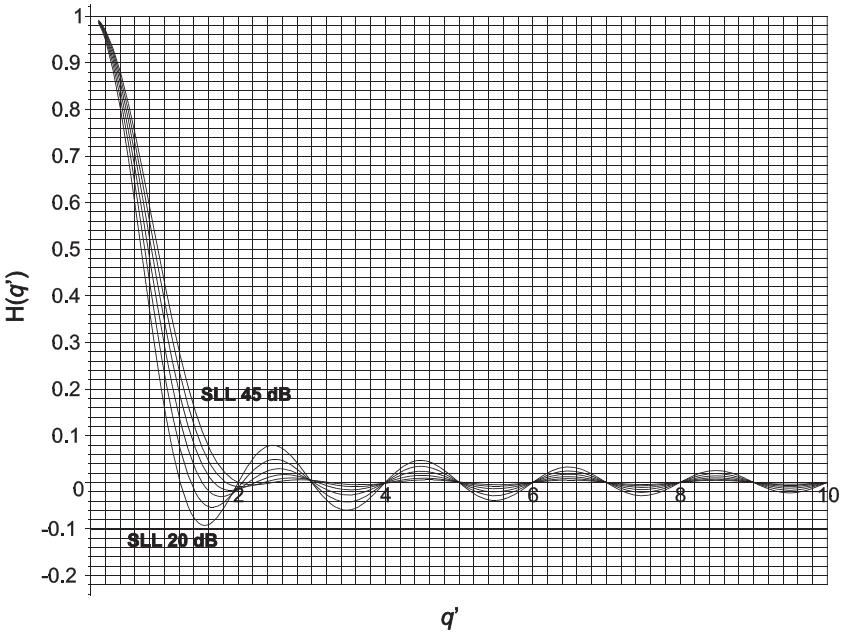

Figure 5.49 Fourier transforms for Taylor tapering functions with sidelobe levels between 20 dB and 45 dB. [Source: Meikle, H.D., *Modern Radar Systems*, Artech House, Norwood, Massachusetts, 2001.]

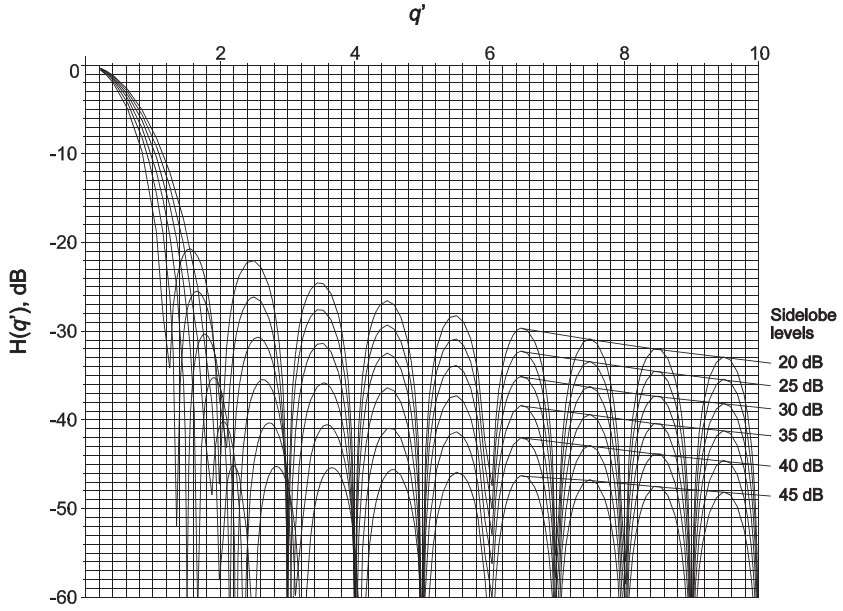

Figure 5.50 Fourier transforms in decibels for Taylor tapering functions with sidelobe levels between 20 dB and 45 dB. [Source: Meikle, H.D., *Modern Radar Systems*, Artech House, Norwood, Massachusetts, 2001.]

Figure 5.51 shows an example of the effects of sampling on spectral leakage or two-tone characteristics when the discrete Fourier transform is used for 100 samples. The minor signal has a frequency corresponding to the 16th bin, and the major signal has its frequency varied between the 10th and 11th bins.

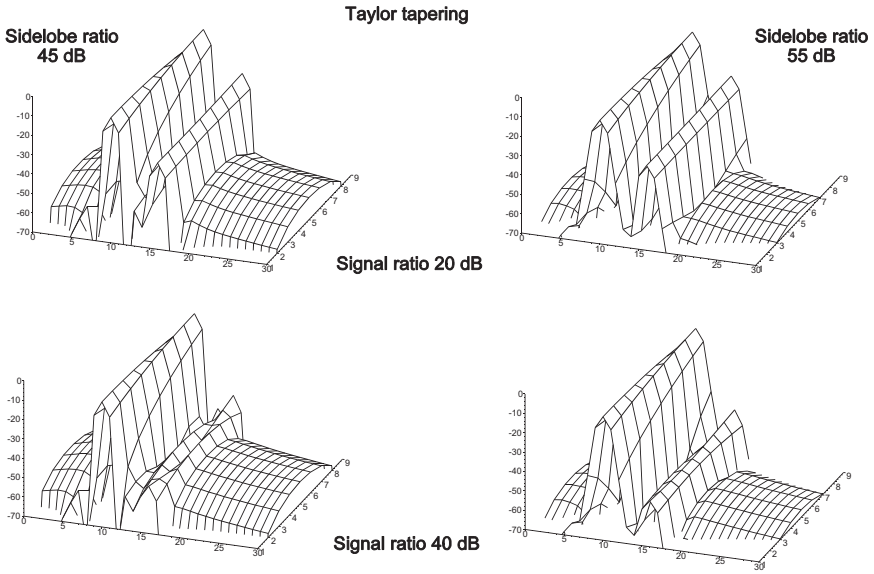

Figure 5.51 Examples of the spectral leakage, or two-tone characteristics, for a 100 sample filter as the major signal frequency is varied from bin 10 to bin 11. The minor signal, 20 dB or 40 dB smaller, is in bin 16. [Source: Meikle, H.D., *Modern Radar Systems*, Artech House, Norwood, Massachusetts, 2001.]

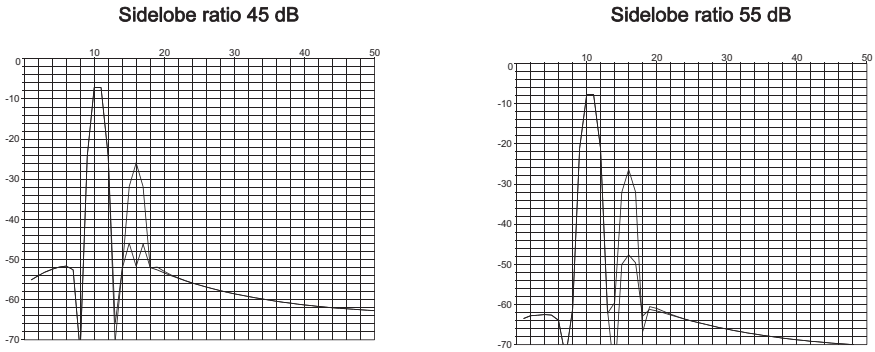

Figure 5.52 Worst case masking of the minor signal with two cases of Taylor tapering. [Source: Meikle, H.D., *Modern Radar Systems*, Artech House, Norwood, Massachusetts, 2001.]

References

1 Barton, D.K., and H.W. Ward, *Handbook of Radar Measurement*, Prentice-Hall, Englewood Cliffs, New Jersey, 1969.

2 Harris, F.J., On the use of windows for harmonic analysis with the discrete Fourier transform, *Proceedings of the IEEE, Vol. 66* pp. 51 – 83, 1978.

3 Meikle, H.D., *Modern Radar Systems*, Artech House, Norwood, Massachusetts, 2001.

4 Rudge, A.W., K. Milne, A.D. Olver, and P. Knight, *The Handbook of Antenna Design*, Peter Peregrinus, London, 1986.

5 Woodward, P.M., *Probability and Information Theory with Applications to Radar,* 2nd edn, Pergamon Press, Oxford, 1964.

6 Stutzman, W.L.and G.A. Thiele, *Antenna Theory and Design*, Wiley, New York, 1981.

7 Skillman, W.A., *Radar Calculations using the TI-59 Programmable Calculator*, Artech House, Dedham, Massachusetts, 1983.

6
Fourier Transforms in Statistics

The primary use of Fourier transforms in statistics is to find what happens to the sums of samples taken from different probability distributions. Examples are the probability distribution of signal plus noise in communications and the total waiting time for a number of queues in queueing theory. Fourier transforms, being integrals of complex functions, are difficult to visualise and statisticians have tried to avoid them, there being no physical example of the spatial spiral functions involved. This chapter describes the concepts of probability distribution functions, the moments of probability distribution functions, moment generating functions, and the relationships leading to Fourier transforms.

Statisticians use the +omega convention for Fourier transforms as mentioned in Section 3.2. *In this chapter the symbol i is used for* $\sqrt{-1}$ *to indicate that the +omega convention is used.*

6.1
Basic Statistics

When, for example, the lengths of parts after a manufacturing process are measured all will have a slightly different length. Quality may be controlled by making a cross corresponding to the length found on a chart shown in Figure 6.1. If the part is supposed to be 10 cm long and the abscissa is in tenths of a centimetre, it can be seen that the greatest number of the crosses occur at 10.2 cm. Obviously there is a systematic error occurring and the other problem is the accuracy of the cutting process that is given by the width of the heap. Statisticians have developed methods of measuring the positions and shapes of these heaps that are the basic definitions in statistics.

The first step is to find the average error of the 127 parts measured in Figure 6.1. At school we learn to add all the lengths, x_k together and divide by the number of lengths, N, or mathematically

$$\text{Average, } m = \frac{\Sigma\, x_k}{N} \tag{1}$$

A New Twist to Fourier Transforms. Hamish D. Meikle

ISBN: 3-527-40441-4

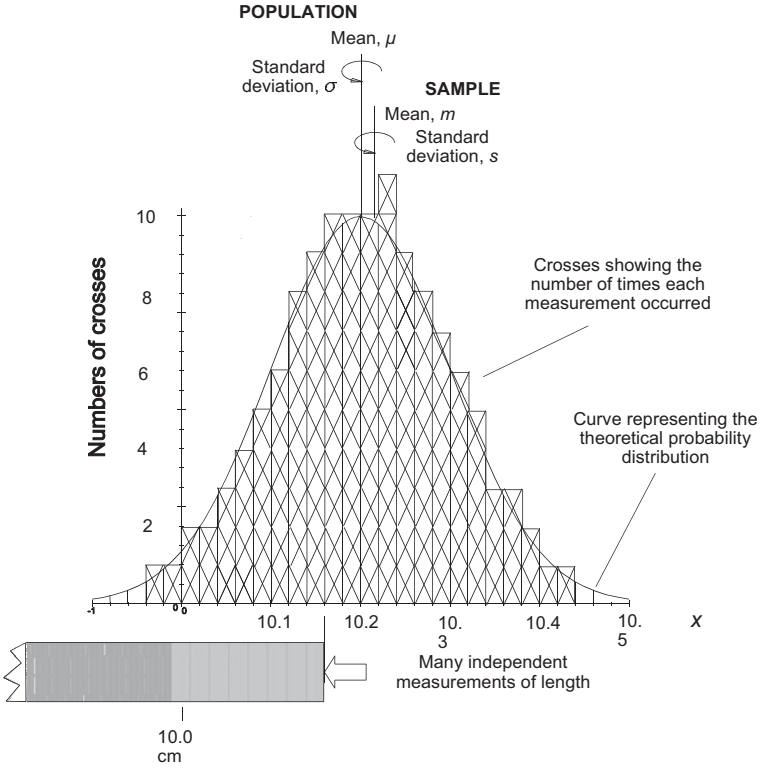

Figure 6.1 The results of collecting the measurements of lengths after a manufacturing process [After: Meikle, H.D., *Modern Radar Systems*, Norwood, Massachusetts: Artech House, 2001]

In Figure 6.1 the sum for each column of crosses may be found by multiplying the number of crosses in the kth column, y_k (representing the area of the column) by the length x_k represented by the column, say $y_k\, x_k$. The average becomes

$$\text{Average, } m = \frac{\sum_{1}^{n} y_k x_k}{N} \tag{2}$$

where n is the number of columns.

The total number of points comprising the area under the histogram is

$$N = \sum_{k=1}^{n} y_k \tag{3}$$

So that the average may be expressed as

$$\text{Average, } m_1 = \frac{\sum_{k=1}^{n} x_k y_k}{\sum_{k=1}^{n} y_k} \tag{4}$$

If the column widths of the histogram approach dx that approaches zero, the histogram becomes a smooth curve and the average becomes

$$\text{Population average, } \mu_1 = \frac{\int xy\,\mathrm{d}x}{\int y\,\mathrm{d}x} \tag{5}$$

where the integration takes place over all valid values of x.

For those who are familiar with mechanics, the expression above will be recognised as that for the centre of gravity or first moment of area.

The cumulative diagram, for example Figure 6.2, is often used to estimate the ranges of the measured parts in the sample. The first quarter is called the first quartile, the half-way point is named the median, the 80% point is the 80th percentile, and so on.

A histogram is often called the distribution of the frequencies of occurrences of the individual measurement values, or frequency distribution. When the y scale is changed so that $\sum_{k=1}^{n} y_k = 1$ or $\int y\,\mathrm{d}x = 1$, then the y scale represents the probability of that measurement occurring and the curve becomes the probability distribution. Its mathematical representation its the probability distribution function (often abbreviated to p.d.f.).

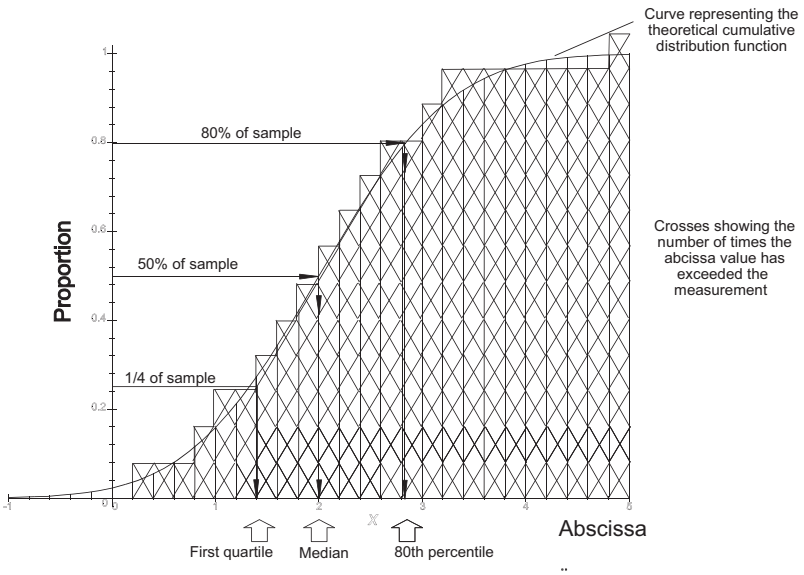

Figure 6.2 The cumulative plot of Figure 6.1 showing a quartile, the median, and a percentile [After: Meikle, H.D., *Modern Radar Systems*, Norwood, Massachusetts: Artech House, 2001].

Thus the average of a small number of samples is an estimate of the average of the population. In the rest of the text Roman letters are used for sample estimates and Greek letters for the population parameters.

The estimate of the width of the pile is more difficult as the sum of the differences of the measurements from the mean is zero. The positive and negative signs may be eliminated by taking the squares of these differences, namely

$$\text{Variance, } s^2 = \frac{\sum_{k=1}^{n}(x_k - m)^2 y_k}{N} = \frac{\sum_{k=1}^{n}(x_k - m)^2 y_k}{\sum_{k=1}^{n} y_k} \tag{6}$$

The positive square root of the variance is called the standard deviation in the literature in English. In other languages the variance is sometimes mentioned as $\pm s$.

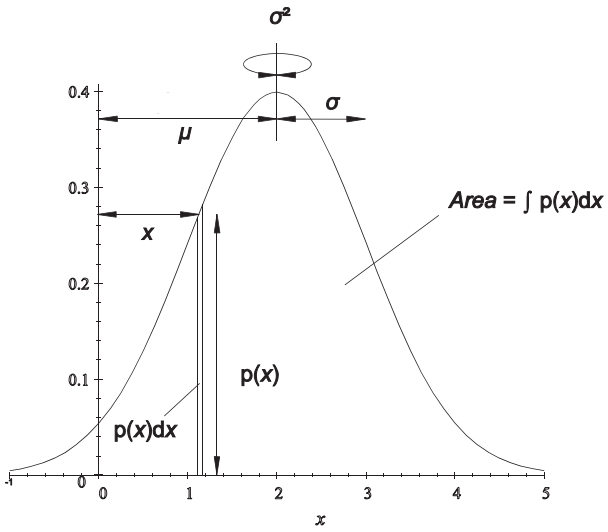

Figure 6.3 The first two moments of a Gaussian distribution [Source: Meikle, H.D., *Modern Radar Systems*, Norwood, Massachusetts: Artech House, 2001]

Expanding Equation (6)

$$\begin{aligned} s^2 &= \frac{1}{N}\left(\sum x_k^2 y_k - 2m\sum x_k y_k + m^2\right) \\ &= \frac{1}{N}\sum x_k^2 y_k - m^2 \end{aligned} \tag{7}$$

The expression shows that the sum of the squares of the differences is at a minimum when taken from the mean. As with the average, this is analogous to the moment of inertia and the second moment of area in mechanics. The common expression to calculate the variance from sample data is

$$s^2 = \frac{N\sum_{k=1}^{N} x_k^2 - \left(\sum_{k=1}^{N} x_k\right)^2}{N(N-1)} \tag{8}$$

The calculated mean has an error when compared to the population mean (see Figure 6.1) and the N–1 in the denominator corrects (increases) the value of the variance to reflect this error.

The variance and standard deviation of the sample mean, s_m, is given by [1, p. 146]

$$s_m^2 = \frac{s^2}{N} \text{ or } s_m = \frac{s}{\sqrt{N}} \tag{9}$$

Chebyshev's inequality [1, p. 148] [2, p. 226] [4, p. 32] gives an outside limit for the estimates of the mean, regardless of the probability distribution

$$\text{Probability that } \left(|m_1 - \mu_1| \le h\sigma\right) \ge 1 - \frac{1}{h^2} \tag{10}$$

where h>0 and preferably h>1.

For example, the probability that m_1 will be within three standard deviations of the true mean μ_1 is better than 88.89%.

6.1.1 Higher Moments

In their quest to find numbers as measurements of the shapes of statistical heaps (or distributions), statisticians use the higher moments. The rth moment about the mean, m_1, is given by

$$m_r = \frac{1}{N}\sum_{k=1}^{N}(x_k - m_1)^r \tag{11}$$

Table 6.1 Measures of skewness

Name	Equation	Reference
Fisher	$\gamma_1 = \frac{\mu_3}{\sigma^3}$	[3, p. 650]
Pearson	$\beta_1 = \left\lvert\frac{\mu_3}{\sigma^3}\right\rvert^2 = \gamma_1^2$	[3, p. 1652]
Pearson mode	$\frac{\text{mean} - \text{mode}}{\text{standard deviation}}$	[4, p. 15]

Statisticians use the third moment as a measure of the skewness of a probability distribution. Skewness is relatively rarely used and a number of statisticians have given their names to the measures, some of which are shown in Table 6.1. Luckily the notation is relatively standard.

The spikiness of the heap is called the *kurtosis*. Pearson [3 p. 1009][5, p. 46] gives kurtosis as

$$\beta_2 = \frac{\mu_4}{\mu_2^2} = \frac{\mu_4}{\sigma^4} \tag{14}$$

Fisher [3, p. 1009] gives an excess kurtosis as $\gamma_2 = \beta_2 - 3$, but sometimes the word *excess* is omitted.

Commonly only the first four moments of a distribution are used to measure the position, width, and shape of a distribution and the remaining moments are not used.

6.1.2 Moment Generating Functions

The moment generating function (often abbreviated to m.g.f) may be considered to be an expression containing all the moments of a probability distribution function, $p(x)$. The moment generating function about the origin is a function of t [4, p. 86]

$$M(t) = \int p(x)\, e^{tx} dx \tag{16}$$

where the integration takes place over all valid values of x.

If the exponential function is expanded as a Maclaurin series

$$M_0(t) = 1 + \mu_1' t + \frac{\mu_2' t^2}{2!} + \frac{\mu_3' t^3}{3!} + \ldots \tag{17}$$

where $\mu_r' = \int x^r\, p(x)\, dx$ is the rth moment about the origin and the integration takes place over all valid values of x.

The moment generating function about a point a is given by

$$\begin{aligned} M(t) &= \int p(x)\, e^{t(x-a)} dx \\ &= e^{-at} M_0(t) \end{aligned} \tag{18}$$

Nevertheless the moment generating function does not define a probability distribution function uniquely as does the Fourier transform, conventionally called the characteristic function in statistics, $C(\xi)$ given by

$$C(\xi) = \int_{-\infty}^{+\infty} p(x)\ \exp(+i\ \xi x)\ dx \tag{19}$$

where x is the variable for the probability distribution function;
$p(x)$ is the probability distribution function;
ξ is the variable in the characteristic function;
$C(\xi)$ is the characteristic function;
i is $\sqrt{-1}$ to be compatible with statistics texts.

Where the distribution only exists between two values of x then the limits of integration are set to these values.

The inverse Fourier transform, also called the anticharacteristic function in statistics, is given by (omega convention)

$$p(x) = \frac{1}{2\pi} \int_{-\infty}^{+\infty} C(\xi)\ \exp(-i\xi x)\ d\xi \tag{20}$$

The range of ξ in characteristic functions extends from minus to plus infinity.

The relationships between the moments and the derivatives of the Fourier transform using the f convention was discussed in Section 3.4.5. Repeating Equation (85) of Chapter 3 and differentiating Equation (19) with respect to ξ

$$\begin{aligned} C'(\xi) &= \frac{d}{d\xi} \int p(x)\ \exp(+ix\xi)\ dx \\ &= i \int x\ p(x)\ \exp(+ix\xi)\ dx \end{aligned} \tag{21}$$

where the integration takes place over all valid values of x.

Setting $\xi = 0$ the derivative becomes

$$C'(0) = i \int x\ p(x)\ dx \tag{22}$$

and the first moment about the origin is

$$\mu_1' = \frac{C'(0)}{i} \tag{23}$$

Notice that when the +omega convention is used there is no power of 2π in the divisor (see Section 3.4.5) and the moment is given directly. Extending to the rth moment

$$\mu_r' = \frac{C^r(0)}{i^r} \tag{24}$$

Taking an example with a Gaussian or normal probability density function with a mean of 2 and a standard deviation of unity in Figure 6.4(a),

$$p(x) = \frac{1}{\sqrt{2\pi}}\ \exp\left(-\frac{(x^2-2)^2}{2}\right) \tag{25}$$

its Fourier transform using the omega convention is shown in Figure 6.4(b).

$$C(\xi) = \exp\left(i2\xi - \frac{x^2}{2}\right)$$
$$C(0) = 1 \tag{26}$$

where C(0) is the area under the probability distribution function curve.

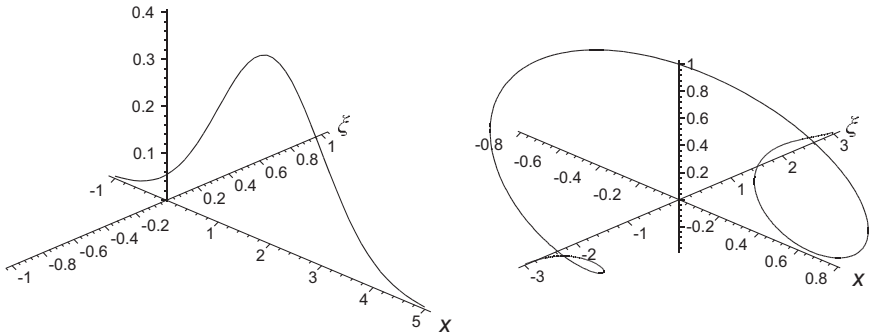

(a) Gaussian or normal distribution
Mean = 2
Standard deviation = 1

(b) Fourier transform of the Gaussian distribution in (a)

Figure 6.4 The Gaussian or normal distribution and its characteristic function used in the example.

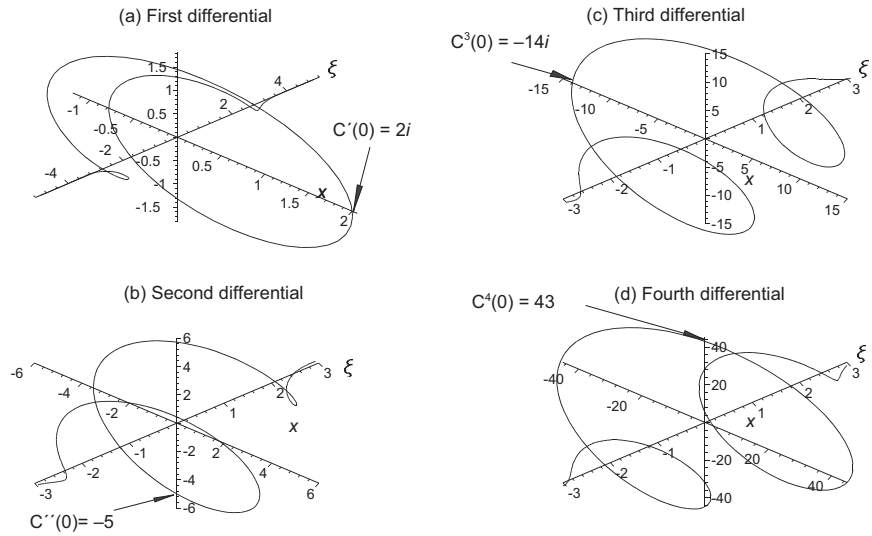

Figure 6.5 The first four derivatives of the characteristic function.

The first derivative is

$$\begin{aligned} C'(\xi) &= (i2 - \xi)\ \exp\left(i2\xi - \frac{\xi^2}{2}\right) \\ C'(0) &= 2i \end{aligned} \tag{27}$$

The first differential in the $\xi = 0$ plane represents the number of turns per unit that locates the mean. Vector multiplication rules give the turns per unit of the product of two characteristic functions as the sum of the turns per unit of the two factors. Taking anti–characteristic functions the mean of the combined probability distribution function is the sum of the means of the individual probability distribution functions.

Similarly, the higher derivatives represent accelerations of the numbers of turns per unit. These also add to give the sums of higher moments as shown in the example at the end of the chapter.

The expressions for the higher derivatives are too large for these pages. Summarising

$$\begin{aligned} C''(0) &= -5 & m_2' &= 5 \\ C'''(0) &= -14i & m_3' &= 14 \\ C^4(0) &= 43 & m_4' &= 43 \end{aligned} \tag{28}$$

The moments about the mean, skew, and kurtosis may be calculated from Table 3.2.

$$\begin{aligned} \mu_2 &= \mu_2' - (\mu_1')^2 \\ &= 5 - 2^2 = 1 \\ \mu_3 &= \mu_3' - 3\mu_2'\mu_1' + (\mu_1')^3 \\ &= 14 - 3 \times 5 \times 2 + 2 \times 8 = 0 \\ \mu_4 &= \mu_4' - 4\mu_3'\mu_1' + 6\mu_2'(\mu_1')^2 - 3(\mu_1')^4 \\ &= 43 - 4 \times 14 \times 2 + 6 \times 5 \times 4 - 3 \times 16 = 3 \end{aligned} \tag{29}$$

The skew and kurtosis are

$$\begin{aligned} \text{Skew} &= \frac{\mu_3}{(\mu_2)^2} = \frac{0}{1} = 0 \\ \text{Kurtosis} &= \frac{\mu_4}{(\mu_2)^2} = \frac{3}{1} = 3 \end{aligned} \tag{30}$$

The values obtained in Equation (29) are those to be expected from a Gaussian or normal distribution.

6.2
Properties of Characteristic Functions

Section 3.4 describes the properties of Fourier transforms using the f convention and this section describes them for characteristic functions, Fourier transforms using the omega convention.

6.2.1
Linearity – Addition, Subtraction, and Scaling

Linearity does not change with the convention, namely

- Addition
  $p(x) + q(x)$ has the characteristic function $C(\xi) + D(\xi)$
- Multiplication by a constant
  $a\ p(x)$ has the characteristic function $aC(\xi)$
- Scaling
  $p(a\ x)$ has the characteristic function $\frac{1}{|a|}\ C\left(\frac{\xi}{a}\right)$

6.2.2
Multiplication

Multiplication, as in Section 3.4, is of three types

- Multiplication of the characteristic function with a helix to shift the mean.
  $p(x \pm m)$ has the characteristic function $C(\xi)\ \exp(\mp\ i\ \xi\ m)$
  The converse of multiplying the probability distribution function by a helix does not occur as probability distribution functions are purely real.
- Multiplication of the characteristic functions – convolution
  Convolution is the most common use of the Fourier transform, or characteristic function, in statistics. Convolution is used to find the probability distribution functions of the sums of random processes and an example is given at the end of this chapter.
  After multiplication the inverse transform can be found to calculate the mean, standard deviation, and the percentiles.
- Multiplication with a complex conjugate – correlation
  Figure 3.12 shows the correlation of two Gaussian distributions. The remaining curve is displaced by the lag, or the difference in means. Normally the means of the two distributions are known and it is much easier to subtract them directly.

Table 6.2 gives a summary of characteristic function properties [4, p. 24]

Table 6.2 Summary of properties of characteristic functions

Property	Probability function domain, p(*x*)	Characteristic function domain, C(ξ)
Linearity	$a\ \mathrm{p}(x) + b\ \mathrm{q}(x)$	$a\ \mathrm{C}(\xi) + \mathrm{D}(\xi)$
Scaling	$\mathrm{p}(a\ x)$	$\frac{1}{\lvert a\rvert}\ \mathrm{C}\left(\frac{\xi}{a}\right)$
Sign change	$\mathrm{p}(-x)$	$\mathrm{C}(-\xi)$
Complex conjugation	$\mathrm{p}^*(x)$	$\mathrm{C}^*(-\xi)$
Shift of mean	$\mathrm{p}(x \pm m)$	$\exp(\mp\ m\ \xi)\ \mathrm{C}(\xi)$
Differentiation in probability function domain	$\frac{\mathrm{d}}{\mathrm{d}t}\ \mathrm{p}(x)$	$i\ \xi\ \mathrm{C}(\xi)$
Differentiation in characteristic function domain	$i\ x\ \mathrm{p}(x)$	$\frac{\mathrm{d}}{\mathrm{d}\xi}\ \mathrm{C}(\xi)$
Convolution in probability function domain	$\mathrm{p}(x)\ *\ \mathrm{q}(x)$	$\mathrm{C}(\xi)\ \mathrm{D}(\xi)$
Convolution in characteristic function domain	$\mathrm{p}(x)\ \mathrm{q}(x)$	$\mathrm{C}(\xi)\ *\ \mathrm{D}(\xi)$

6.3 Characteristic Functions of Some Continuous Distributions

Unlike spectra and antenna patterns, characteristic functions look very similar and are not useful for statistical estimations: their only use is a stepping stone in convolution. The distributions are treated, where possible in families.

6.3.1 Uniform Distribution

The uniform distribution is the chance that particular numbers are drawn from a drum containing one ball for each number, as in lotteries [2, p. 220]. Examples of the distribution are shown in Figure 6.6 and are given by

$$\begin{aligned} \mathrm{p}(x) &= \frac{1}{b-a} \text{ where } a < x < b \\ &= 0 \quad \text{elsewhere} \end{aligned} \tag{31}$$

The characteristic function, an example is shown in Figure 6.7, is

$$\mathrm{C}(\xi) = \frac{\exp(ib\xi) - \exp(ia\xi)}{i\xi(b-a)} = \frac{2\ \sin\frac{b-a}{2}\ \xi}{(b-a)\ \xi}\ \exp\left(i\frac{a+b}{2}\xi\right) \tag{32}$$

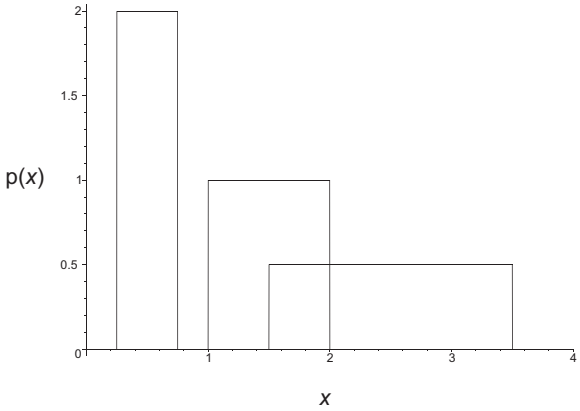

Figure 6.6 Three examples of the uniform probability distribution function.

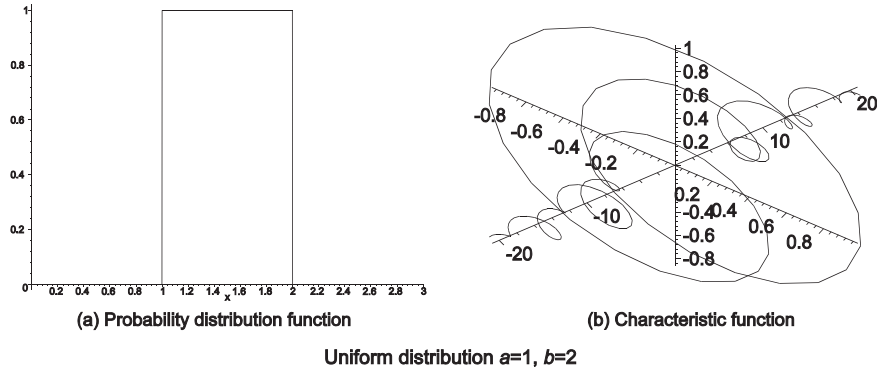

Figure 6.7 A uniform probability distribution function and its characteristic function.

The moment generating function is

$$\mathrm{M}(t) = \frac{e^{tb} - e^{ta}}{t(b-a)} \tag{33}$$

The moments may be obtained either directly or from the characteristic function. The central moments, about the mean, are

$$\begin{aligned} \text{Mean} &= m_1 = \frac{a+b}{2} \\ \text{Variance} &= m_2 = \frac{(b-a)^2}{12} \\ \text{Standard deviation} &= s = \frac{b-a}{2\sqrt{3}} \end{aligned} \tag{34}$$

The skew and kurtosis are

$$\begin{aligned} \text{Skew} &= 0 \\ \text{Kurtosis} &= \frac{9}{5} = 1.80 \end{aligned} \tag{35}$$

Note that the *excess kurtosis* is 1.8 – 3 = –1.2.

6.3.2 Gaussian or Normal Distribution Family

The Gaussian distribution is so common that it is called the *normal* distribution in many English texts [example 2, p. 220] and examples are illustrated in Figure 6.8. When the mean is μ and the standard deviation is σ, it is given by

$$p(x) = \frac{1}{\sigma\sqrt{2\pi}} \exp\left(-\frac{(x-\mu)^2}{2\sigma^2}\right) \quad \text{where } \sigma > 0 \tag{36}$$

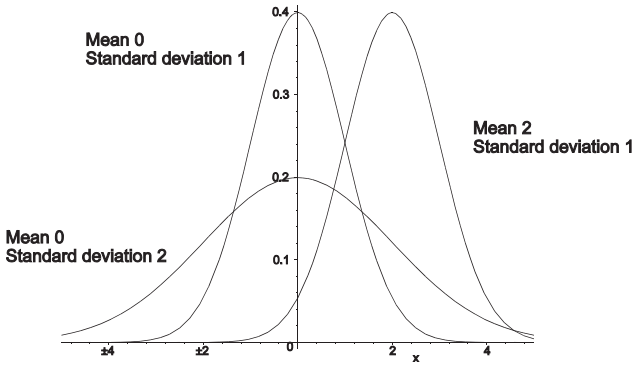

Figure 6.8 Examples of Gaussian or normal probability distribution functions.

The characteristic function, see Figure 6.9, is

$$C(\xi) = \exp\left(i\mu\xi - \frac{\xi^2\sigma^2}{2}\right) \tag{37}$$

The moment generating function is

$$M(t) = \exp\left(t\mu + \frac{t^2\sigma^2}{2}\right) \tag{38}$$

The moments may be obtained either directly or from the characteristic function. The first two central moments, μ and σ define the distribution. The skew is zero and the kurtosis is 3.

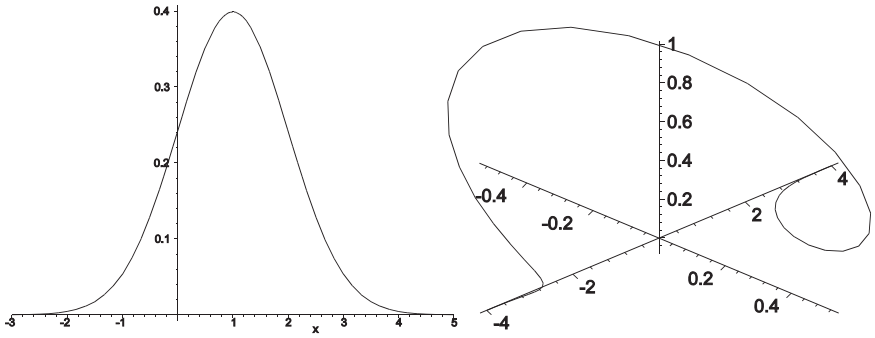

(a) Gaussian or normal distribution μ=1, σ=1 (b) Characteristic function of (a)

Figure 6.9 An example of a Gaussian or normal probability distribution function and its characteristic function.

Related distributions are:

- Log-normal [5, p. 99], Distribution of the product of Gaussian random variables
- Rayleigh [5, p. 100] and Rice distributions described in the next paragraphs.

6.3.2.1 **Rayleigh Distribution**

If two Gaussian distributions are taken in two orthogonal dimensions, their product is the joint probability and looks like the heap shown in Figure 6.10. The mathematical expression is

$$\begin{aligned} \mathrm{p}(x,y) &= \frac{1}{2\pi\sigma^2}\,\exp\left(-\frac{1}{2}\left(\frac{x}{\sigma}\right)^2\right)\exp\left(-\frac{1}{2}\left(\frac{y}{\sigma}\right)^2\right) \\ &= \frac{1}{2\pi\sigma^2}\,\exp\left(-\frac{x^2+y^2}{2\sigma^2}\right) \end{aligned} \tag{39}$$

where x is the variable along the x axis;
y is the variable along the y axis;
σ is the standard deviation of both distributions

The Rayleigh distribution is the probability distribution taken along a radius in Figure 6.10, that is in polar coordinates. Changing to polar coordinates, $r^2 = x^2 + y^2$, and integrating the elements over a circle of radius r, we have

$$\begin{aligned} \mathrm{p}_{\text{Rayleigh}}(r) &= \int_0^{2\pi} r\mathrm{p}(r)\;\theta\;\mathrm{d}\theta \\ &= \frac{r}{\sigma^2}\,\exp\left(-\frac{r^2}{2\sigma^2}\right) \end{aligned} \tag{40}$$

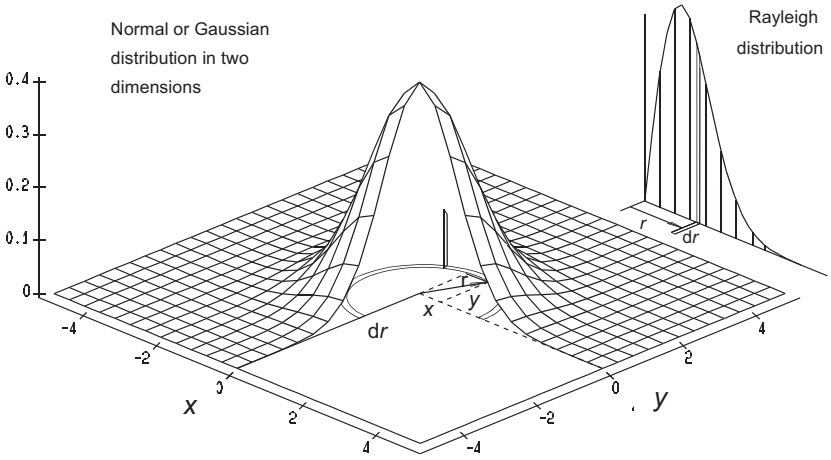

Figure 6.10 The shape of the joint probability distribution of two orthogonal Gaussian distributions. [Source: Meikle, H.D., *Modern Radar Systems*, Norwood, Massachusetts: Artech House, 2001.]

Maple calculates the characteristic function as

$$C(\xi) = 1 + i\xi\sigma\sqrt{\frac{\pi}{2}}\exp\left(-\frac{\xi^2\sigma^2}{2}\right)\left(1 + \operatorname{erf}\left(\frac{i\xi\sigma}{\sqrt{2}}\right)\right) \tag{41}$$

where ξ is the variable

i is $\sqrt{-1}$.

$$\operatorname{erf}(x) = \frac{2}{\sqrt{\pi}}\int_0^x \exp(-t^2)\,dt$$

An example is shown in Figure 6.11.

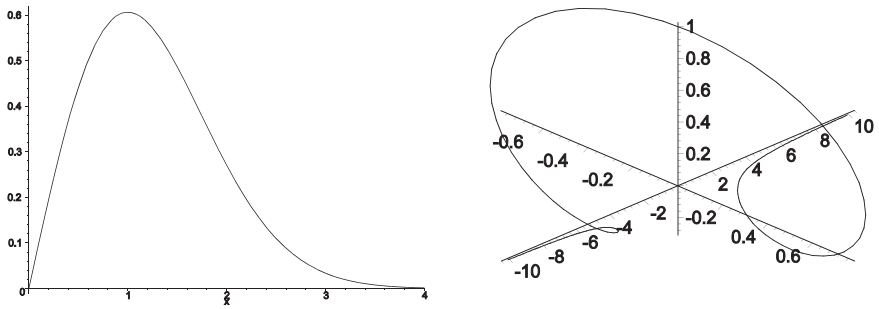

(a) Rayleigh distribution, $\sigma = 1$ (b) Characteristic function of (a)

Figure 6.11 An example of the Rayleigh probability density function and its characteristic function.

The moments of the Rayleigh distribution may be obtained from the characteristic function or directly. If σ is the standard deviation of the component Gaussian distributions then

$$\begin{aligned}
\mu &= \sqrt{\frac{\pi}{2}}\,\sigma \\
\text{variance} &= 2\sigma^2 \text{ about the origin} \\
\mu_2 &= \left(2 - \frac{\pi}{2}\right)\sigma^2 \text{ about the mean} \\
\mu_3 &= \sqrt{\frac{\pi}{2}}\,(3 + \pi)\,\sigma^3 \\
\text{skewness} &= \frac{3}{8}\sqrt{\frac{\pi}{2}}\,\frac{1}{\sigma^3} \\
\mu_4 &= \left(8 - \frac{3\pi^2}{4}\right) \\
\text{kurtosis} &= 2
\end{aligned} \tag{42}$$

Some of these are shown in Figure 6.12 that has an abscissa in terms of σ.

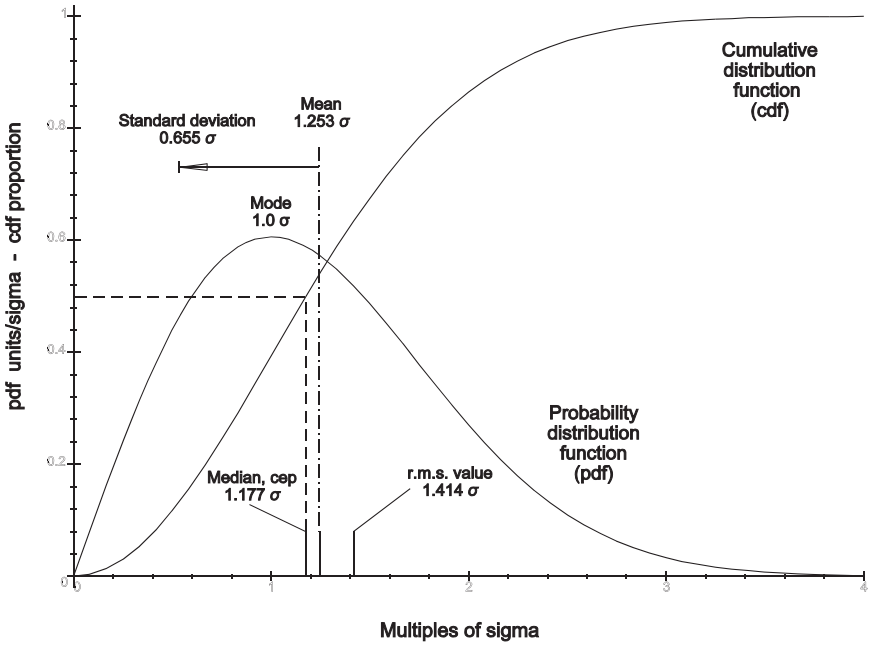

Figure 6.12 The Rayleigh distribution [Source: Meikle, H.D., *Modern Radar Systems*, Norwood, Massachusetts: Artech House, 2001].

The Rayleigh probability distribution function is a special form of the Weibull distribution with $\eta = 1$ and σ is scaled by $\sqrt{2}$

The cumulative distribution is

$$\begin{aligned} P(r) &= 1 - \exp\left(-\frac{r^2}{2\sigma^2}\right) \quad \text{for } r > 0 \\ &= 0 \qquad\qquad\qquad\quad \text{elsewhere} \end{aligned} \tag{43}$$

Many phenomena follow the Rayleigh distribution and for some the distribution is required in terms of power ratio or $X = r^2/2\sigma^2$. Substituting we have

$$p(r)\,dr = \exp(-X)\,d(X) \tag{44}$$

remembering that $dr/dX = r/\sigma^2$. This is a negative exponential distribution or a gamma distribution with a shape factor, η, of unity (see Section 6.3.4).

6.3.2.2 **Rice Distribution**

The Rice distribution is a Rayleigh distribution offset from the origin by the amounts μ_x and μ_y as shown in Figure 6.13.

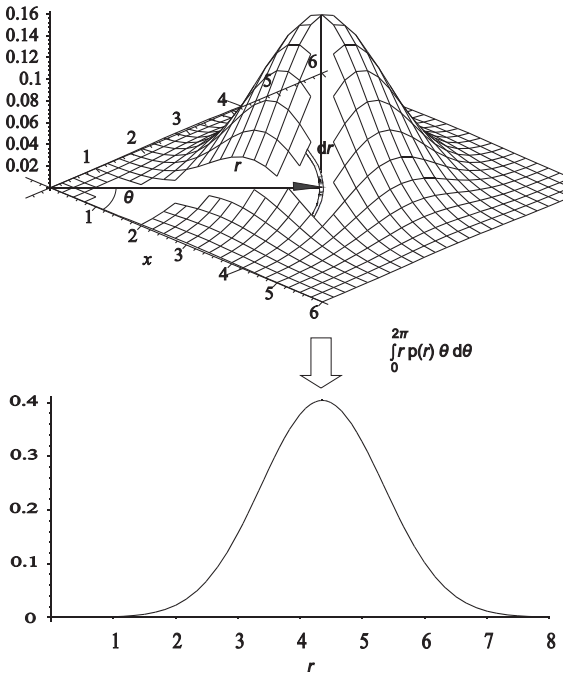

Figure 6.13 The derivation of the Rician distribution.

The distribution is thus the joint probability of two orthogonal Gaussian distributions, namely

$$\begin{aligned} p(x,\ y) &= \frac{1}{2\pi\sigma^2}\ \exp\left(-\frac{1}{2}\left(\frac{x-\mu_x}{\sigma}\right)^2\right)\exp\left(-\frac{1}{2}\left(\frac{y-\mu_y}{\sigma}\right)^2\right) \\ &= \frac{1}{2\pi\sigma^2}\ \exp\left(-\frac{x^2+y^2-2(x\mu_x+y\mu_y)+\mu_x^2+\mu_y^2}{2\sigma^2}\right) \end{aligned} \tag{45}$$

Converting to polar coordinates centred at the origin we replace x with $r\cos\theta$, y with $r\sin\theta$, ${\mu_x}^2+{\mu_y}^2$ with S^2 and we have

$$\begin{aligned} p(r) &= \frac{1}{2\pi\sigma^2}\ \exp\left(-\frac{r^2-2r(\mu_x\cos\theta+\mu_y\sin\theta)+S^2}{2\sigma^2}\right) \\ &= \frac{1}{2\pi\sigma^2}\ \exp\left(-\frac{r^2+S^2}{2\sigma^2}\right)\ \exp\left(\frac{2r}{\sigma^2}(\mu_x\cos\theta+\mu_y\sin\theta)\right) \end{aligned} \tag{46}$$

The expression $\mu_x\cos\theta+\mu_y\sin\theta$ may be rewritten as $\sqrt{\mu_x^2+\mu_y^2}\cos(\theta+\alpha)$ or $S\cos(\theta+\alpha)$ with $\alpha=\arctan(\mu_y/\mu_x)$

$$p(r) = \frac{1}{2\pi\sigma^2}\ \exp\left(-\frac{r^2+S^2}{2\sigma^2}\right)\ \exp\left(\frac{rS\cos(\theta+\alpha)}{\sigma^2}\right) \tag{47}$$

The Rician distribution is given by the probability taken over a whole circle of radius r, it is immaterial where the circle starts and finishes (α), namely [6, Eq. 3.10–11]

$$\begin{aligned} P_{\text{Rice}}(r) &= \int_0^{2\pi} rp(r)\ \theta\ d\theta \\ &= \frac{1}{2\pi\sigma^2}\exp\left(-\frac{r^2+S^2}{2\sigma^2}\right)\int_0^{2\pi}\exp\left(\frac{rS}{\sigma^2}\cos(\theta+\alpha)\right)d\theta \\ &= \frac{r}{\sigma^2}\exp\left(-\frac{r^2+S^2}{2\sigma}\right)I_0\left(\frac{rS}{\sigma^2}\right) \end{aligned} \tag{48}$$

using the Bessel function [7, Eq. 9.6.16, p. 376] $I_0(z) = \frac{1}{\pi}\int_0^{\pi}\exp(\pm z\cos\theta)\ d\theta$.

Examples of the Rice distribution are shown in Figure 6.14, note that when $S=0$ then this is the Rayleigh distribution.

More commonly the Rice distribution is used in electrical engineering in terms of electrical power, X replaces $r^2/2\sigma^2$, R replaces $S^2/2\sigma^2$, and the Jacobean is r/σ^2.

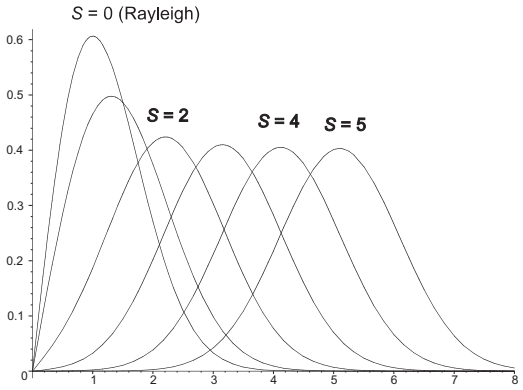

Figure 6.14 Examples of the Rice distribution with $\sigma = 1$.

$$p(X) = \exp(-(X+R))\ I_0\left(\sqrt{4XR}\ \right) \tag{49}$$

It has the characteristic function, an example is shown in Figure 6.15.

$$C(\xi) = \frac{i\ \exp\left(-\frac{R\xi}{i+\xi}\right)}{i+\xi} \tag{50}$$

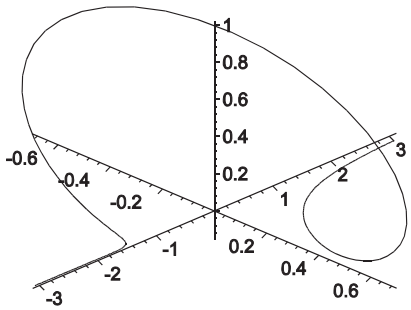

Figure 6.15 An example of the characteristic function of a Rice distribution in terms of power ($X = 3$).

The first two moments (either directly or using the characteristic function) are

$$\begin{aligned} \text{First moment} &= 1 + X \\ \text{Second moment} &= 2 + 4X + X^2 \\ \text{Variance} &= 1 + 2X \end{aligned} \tag{51}$$

The higher moments are outside the scope of this book.

6.3.3 Cauchy Distribution

The Cauchy distribution [5, p. 101] has long tails and is the distribution of the quotients of Gaussian variables. An example is shown in Figure 6.16 and is given by

$$p(x) = \frac{1}{\pi\sigma\left(1 + \left(\frac{x-\mu}{\sigma}\right)^2\right)} \quad \text{where } \sigma > 0 \tag{52}$$

where μ is the median and also the mode;
σ is half the width where $p(x)$ is half the peak value

The integrals for the moments do not converge so that the terms mean and standard deviation are not appropriate and there are no higher moments.

The characteristic function is given by [3, p. 207] and an example is shown in Figure 6.16.

$$\begin{aligned} C(\xi) &= \int_{-\infty}^{+\infty} p(x)\, \exp(ix\xi)\, dx \\ &= \frac{\exp(-\mu\xi)}{\pi} \int_{-\infty}^{+\infty} \frac{\cos(\sigma x\xi)}{1 + (\sigma x)^2} dx \\ &= \exp(-i\mu\xi - \sigma|\xi|) \end{aligned} \tag{53}$$

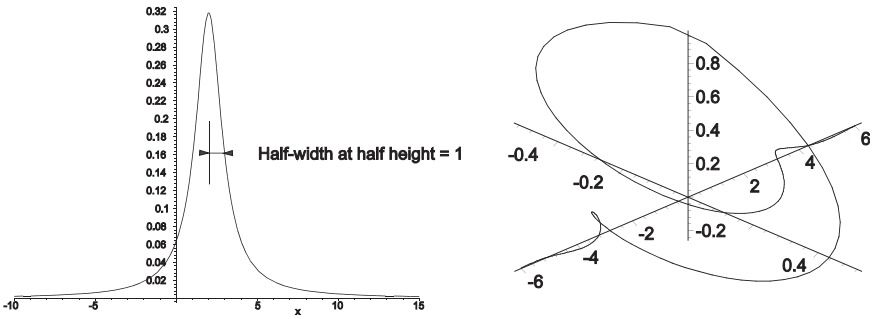

Figure 6.16 An example of the Cauchy probability distribution function with $\mu = 2$ and $\sigma = 1$.

6.3.4
Gamma Family

The gamma family [2, p. 220] [5, p. 83] contains a number of distributions based on the gamma distribution, given by

$$p(x) = \frac{\lambda}{\Gamma(\eta)}(\lambda x)^{\eta-1}\ e^{-\lambda x} \tag{54}$$

where η is the shape factor;
λ is the scale factor

Examples of gamma distribution curves are shown in Figure 6.17.
The characteristic function is given by, an example is shown in Figure 6.18.

$$C(\xi) = \left(1 - \frac{i\xi}{\lambda}\right)^{-\eta} \tag{55}$$

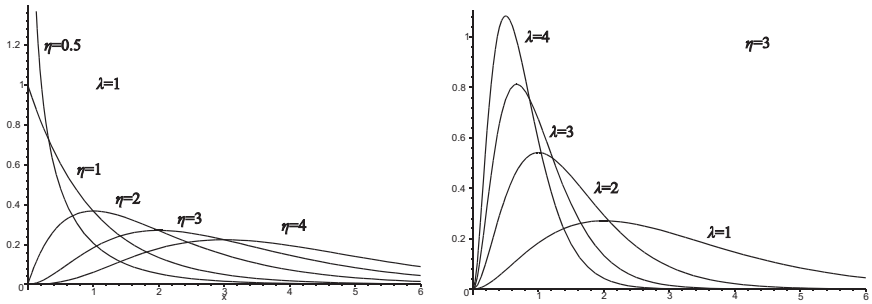

Figure 6.17 Examples of the gamma probability distribution function.

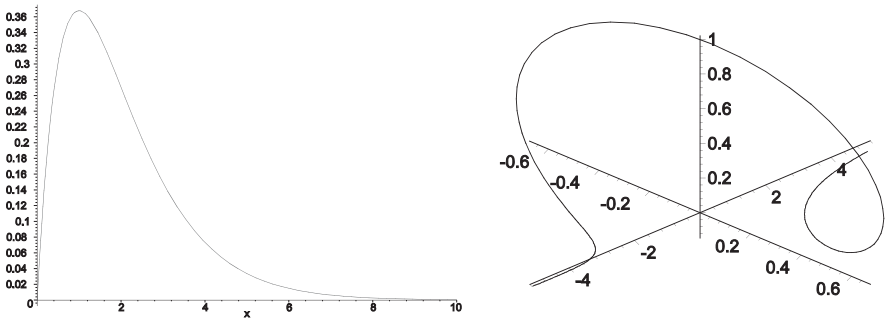

(a) Gamma probability density function η=1, λ=1 **(b) Characteristic function of (a)**

Figure 6.18 An example of the gamma probability distribution function and its characteristic function.

From an inspection of the form of the characteristic function it can be seen that the result of the addition of gamma variates with the same scale factor, λ, is a gamma variate with a form factor, η, that is the sum of the individual form factors.

The moment generating function is given by

$$\mathrm{M}(t) = \left(1 - \frac{t}{\lambda}\right)^{-\eta} \tag{56}$$

The central moments may be obtained from the characteristic function or directly

$$\begin{aligned} \text{Mean} &= m_1 = \frac{\eta}{\lambda} \\ \text{Variance} &= m_2 = \frac{\eta}{\lambda^2} \\ \text{Standard deviation} &= \frac{\sqrt{\eta}}{\lambda} \end{aligned} \tag{57}$$

and the higher moments, skew and kurtosis, are

$$\begin{aligned} \text{Skew} &= \frac{2}{\sqrt{\eta}} \\ \text{Kurtosis} &= \frac{3(\eta+2)}{\eta} \end{aligned} \tag{58}$$

The mode is $\dfrac{\eta - 1}{\lambda}$.

The moment generating function is given by

$$\mathrm{M}(t) = \left(1 - \frac{t}{\lambda}\right)^{-\eta} \tag{59}$$

In an alternative form of the gamma distribution, the scale factor λ is replaced by $1/b$ which is useful as b corresponds to signal-to-noise ratios, for example. Then the probability distribution and characteristic functions are given by

$$\mathrm{p}(x) = \frac{1}{b\Gamma(\eta)} \left(\frac{x}{b}\right)^{\eta-1} \exp\left(-\frac{x}{b}\right) \tag{60}$$

where $b = 1/\lambda$.

The characteristic function is

$$\mathrm{C}(\xi) = (1 - ib\xi)^{-\eta} \tag{61}$$

Other members of the gamma distribution family are [5, p.90]

- Negative exponential distribution

This is a gamma distribution with $\eta = 1$ and is given by

$$\mathrm{p}(x) = \lambda \exp(-\lambda x) \tag{62}$$

It has a simple cumulative distribution function

$$\mathrm{P}(x) = 1 - \exp(-\lambda x) \tag{63}$$

and characteristic function

$$C(\xi) = \frac{1}{1 - \frac{i\xi}{\lambda}} \tag{64}$$

- The Erlangian distribution is used in queueing theory, for example, in telephone exchanges and is a gamma distribution where η is restricted to integers, n.
- The chi-square distribution [2, p. 181] is a special case with $\lambda = 1/2\sigma^2$ and $n = 2\eta$, an integer called the number of degrees of freedom, namely,

$$p(x) = \frac{1}{2^{\frac{\nu}{2}}\sigma^{\nu}\Gamma\left(\frac{\nu}{2}\right)} x^{\frac{\nu}{2}-1} \exp\left(-\frac{x^2}{2\sigma^2}\right) \quad \text{when } x > 0 \tag{65}$$

The characteristic function is

$$C(\xi) = \frac{1}{(1 - i2\sigma^2\xi)^{\frac{\nu}{2}}} \tag{66}$$

6.3.5 Beta Family

The beta distribution of the first kind [5, p. 91] is limited to the range zero to unity. The scale is limited and many shapes are possible with the two shape parameters η and γ as shown in Figures 6.19 and 6.20. The beta probability distribution function is given by

$$\begin{aligned} p(x) &= \frac{\Gamma(\gamma + \eta)}{\Gamma(\gamma)\Gamma(\eta)} x^{\gamma-1} (1 - x)^{\eta-1} \quad \text{when } x > 0 \\ &= 0 \qquad\qquad\qquad\qquad\quad \text{elsewhere} \end{aligned} \tag{67}$$

where γ and η are the shape factors and both are greater than zero.

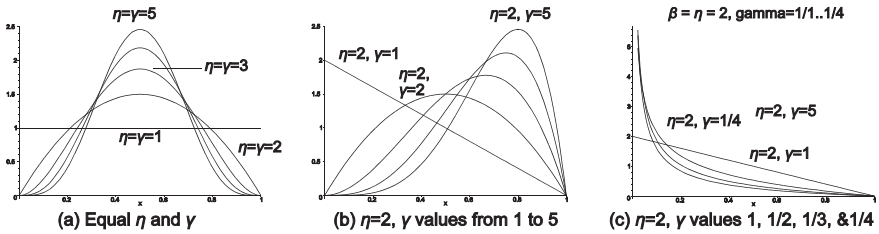

Figure 6.19 Examples of the beta probability distribution function.

The characteristic function is given by [3, p. 125]

$$C(\xi) \;=\; {}_1F_1(\gamma,\ \gamma+\eta,\ i\xi) \tag{68}$$

where ${}_1F_1(a,\ b;\ x)$ is the confluent hypergeometric or Kummer's function of the first kind [3, p. 297] [7, p. 504] given by

$${}_1F_1(a;\ b;\ z) = 1 + \frac{a}{b}\ z + \ \frac{a(a+1)}{b(b+1)}\ \frac{z^2}{2!}\ +\ \ldots \tag{69}$$

A more interesting example with $\eta = \gamma = 0.5$ is shown in Figure 6.20. The curve is given by $J_0\left(\frac{\xi}{2}\right)\ \exp\left(-i\frac{\xi}{2}\right)$.

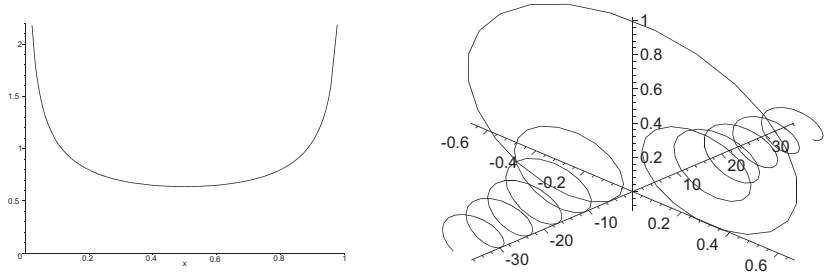

(a) Beta probability distribution function $\eta = \gamma = 0.5$ (b) Characteristic function of (a) $\eta = \gamma = 0.5$

Figure 6.20 An example of the beta probability distribution function and its characteristic function.

The central moments may be obtained from the characteristic function or directly and are given by

$$\begin{aligned} \text{Mean} \;&=\; \frac{\gamma}{\eta+\gamma} \\ \text{Variance} \;&=\; \frac{\eta\gamma}{(\eta+\gamma)^2(\eta+\gamma+1)} \end{aligned} \tag{70}$$

The skew and kurtosis are [5, p. 128]

$$\begin{aligned} \text{Skew} \;&=\; \frac{2(\eta-\gamma)\sqrt{(\eta+\gamma+1)}}{\sqrt{\eta\gamma}(\eta+\gamma+2)} \\ \text{Kurtosis} \;&=\; \frac{3(\eta+\gamma+1)\left(2(\eta+\gamma)^2+\eta\gamma(\eta+\gamma-6)\right)}{\eta\gamma(\eta+\gamma+2)(\eta+\gamma+3)} \end{aligned} \tag{71}$$

The mode occurs at [3, p. 125] $\dfrac{\eta-1}{\eta+\gamma-2}$

The distributions shown below are also members of the beta distribution family

- Uniform distribution $\eta = \gamma = 1$.
- Parabolic distribution $\eta = \gamma = 2$.

The beta probability density function of the second kind [4, p. 156] is given by

$$p(x) = \frac{\Gamma(\gamma+\eta)}{\Gamma(\gamma)\ \Gamma(\eta)}\ \frac{x^{\gamma-1}}{(1+x)^{\eta+\gamma}} \tag{72}$$

where x is in the range from zero to infinity with γ and η as parameters. An example is shown in Figure 6.21.

The characteristic function is given by [using Maple V]

$$C(\xi) = \frac{\Gamma(\gamma+\eta)\ \Gamma(-\eta)}{\xi\ \Gamma(\gamma)\ \Gamma(\eta)}\ (i\xi)^{\eta}\ {}_1F_1(\gamma+\eta;\ \eta+1;\ i\xi) \tag{73}$$

An example is shown in Figure 6.21.

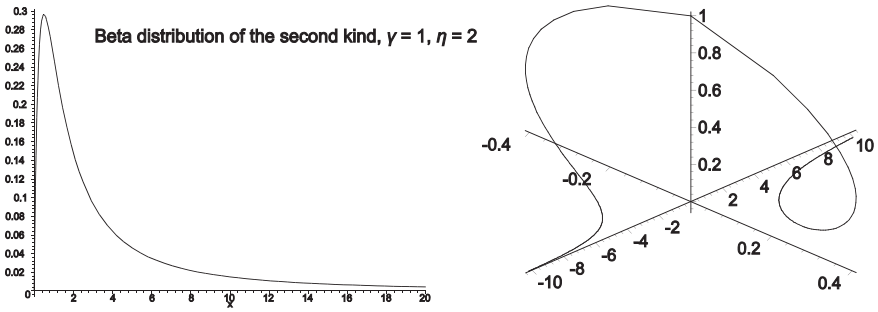

Figure 6.21 An example of the beta probability distribution function of the second kind $\gamma = 1$ and $\eta = 2$ with its characteristic function.

The *r*th moment about the origin may be obtained from the characteristic function or directly and is given by

$$\mu_r' = \frac{\Gamma(\eta-r)\ \Gamma(r+\gamma)}{\Gamma(\gamma)\ \Gamma(\eta)} \tag{74}$$

and the first four moments about the origin are

$$\begin{aligned}
\mu_0 &= 1 \\
\mu_1' &= \frac{\gamma}{\eta-1}, \\
\mu_2' &= \frac{\gamma\ (\gamma+1)}{(\eta-2)\ (\eta-1)} \\
\mu_3' &= \frac{\gamma\ (\gamma+1)\ (\gamma+2)}{(\eta-3)\ (\eta-2)\ (\eta-1)} \\
\mu_4' &= \frac{\gamma\ (\gamma+1)\ (\gamma+2)\ (\gamma+3)}{(\eta-4)\ (\eta-3)\ (\eta-2)\ (\eta-1)}
\end{aligned} \tag{75}$$

The mean and variance are

$$\begin{aligned} \text{Mean} &= \mu_1 = \frac{\gamma}{\eta-1} \\ \text{Variance} &= \mu_2 = \frac{\gamma\,(\gamma+\eta-1)}{(\eta-2)\,(\eta-1)^2} \end{aligned} \tag{76}$$

The third moment about the mean is

$$\mu_3 = \frac{2\,\gamma\,(2\gamma^2+3\gamma\eta-3\gamma+\eta^2-2\eta+1)}{(\eta-3)\,(\eta-2)\,(\eta-1)^3} \tag{77}$$

and the skew is

$$\text{Skew} = \frac{2(\eta-1)^3\,(\eta-2)^2\,(2\gamma+\eta-1)}{\gamma^2\,(\gamma+\eta-1)^2\,(\eta-3)} \tag{78}$$

The expression for the kurtosis is too large for the page.

Both 'Student's' t distribution function and Fisher's F distribution function are beta functions of the second kind.

- 'Student's' *t* distribution [2, p. 180] [3, p. 1751] [4, p. 186]
  The expression x^2/ν is a beta probability density function of the second kind (β_2 ($^1/_2$, $\nu/2$)) and may be found by substituting $\gamma = {}^1/_2$, $\eta = \nu/2$ in Equation (73). The symbol ν is the number of degrees of freedom, an integer. When $\nu = 1$ this is the Cauchy distribution.

$$p(x) = \frac{\Gamma\left(\frac{\nu+1}{2}\right)}{\sqrt{\pi\nu}\,\Gamma\left(\frac{\nu}{2}\right)} \frac{1}{\left(1+\frac{x^2}{\nu}\right)^{(\nu+1)/2}} \quad \text{when } x > 0 \tag{79}$$

- Fisher's F distribution [3, p. 651] [4, p. 199]
  The expression for $x = \nu_1\,F\,/\,\nu_2$ is a beta probability distribution function of the second kind (β_2 ($^1/_2\nu_1$, $^1/_2\,\nu_2$)) that may be found by substituting $\gamma = \nu_1/2$ and $\eta = \nu_2/2$. The symbols ν_1 and ν_2 are the numbers of degrees of freedom.

$$p(x) = \frac{\Gamma\left(\frac{\nu_1+\nu_2}{2}\right)}{\Gamma\left(\frac{\nu_1}{2}\right)\,\Gamma\left(\frac{\nu_2}{2}\right)} \frac{x^{\nu_1/2-1}}{(1+x)^{(\nu_1+\nu_2)/2}} \tag{80}$$

6.3.6 Weibull Distribution

The Weibull distribution [5, p. 108] is used as a model in the science of life testing and as a model of radar clutter. The Weibull probability distribution function is given by

$$\begin{aligned} p(x) &= \frac{\eta}{\sigma}\left(\frac{x}{\sigma}\right)^{\eta-1} \exp\left(-\left(\frac{x}{\sigma}\right)^{\eta}\right) \quad \text{when } x > 0 \\ &= 0 \qquad\qquad\qquad\qquad\qquad \text{elsewhere} \end{aligned} \tag{81}$$

Examples are shown in Figure 6.22.

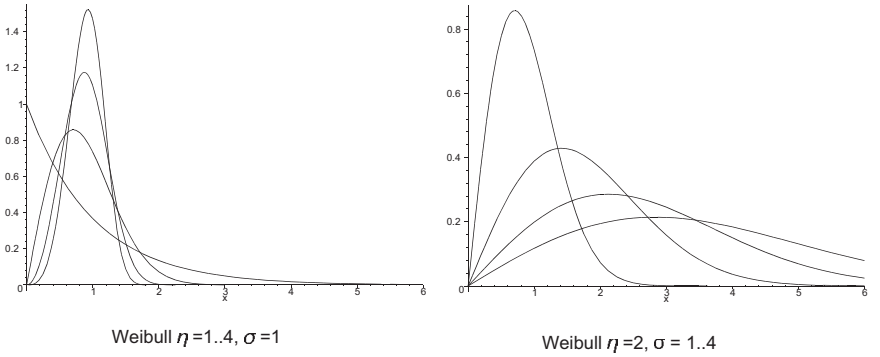

Figure 6.22 Examples of the Weibull probability distribution function.

The cumulative distribution function is given by [5, p. 109]

$$P(x) = 1 - \exp\left(-\left(\frac{x}{\sigma}\right)^{\eta}\right) \quad \text{where } x > 0 \tag{82}$$

The characteristic function in Figure 6.23 has been obtained by numerical integration.

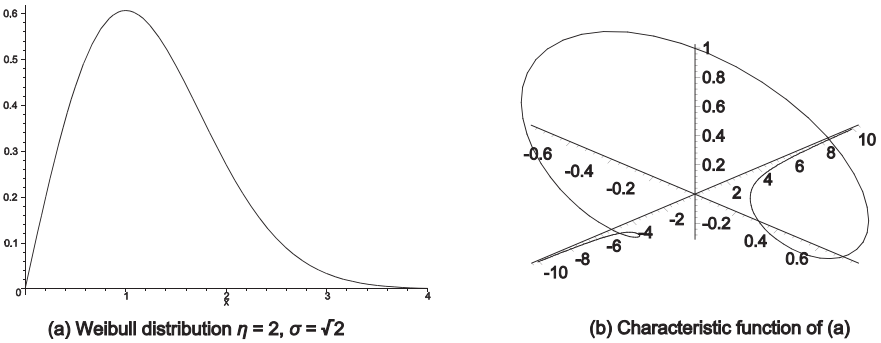

Figure 6.23 An example of the Weibull probability density function and its characteristic function.

The central moments may be obtained from the characteristic function or directly and are

$$\begin{aligned} \text{Mean} &= \sigma\Gamma\left(\frac{1}{\eta} + 1\right) \\ \text{Variance} &= \sigma^2\left(\Gamma\left(\frac{2}{\eta} + 1\right) - \left(\Gamma\left(\frac{1}{\eta} + 1\right)\right)^2\right) \end{aligned} \tag{83}$$

The expressions for skew and kurtosis are too large for this page see [5, p. 132].

6.3.6.1.2 Rayleigh distribution

The Rayleigh probability distribution function is a special form of the Weibull distribution with $\eta = 1$ and σ is scaled by $\sqrt{2}$, namely

$$p(x) = \frac{x}{\sigma^2} \exp\left(-\frac{x^2}{2\sigma^2}\right) \tag{84}$$

The cumulative distribution is

$$\begin{aligned} P(x) &= 1 - \exp\left(-\frac{^2}{2\sigma^2}\right) \quad \text{for } x > 0 \\ &= 0 \qquad\qquad\qquad\qquad\quad \text{elswhere} \end{aligned} \tag{85}$$

Maple calculates the characteristic function as

$$C(\xi) = 1 + \frac{i\xi\sigma\sqrt{\pi}}{\sqrt{2}} \exp\left(-\frac{\xi^2\sigma^2}{2}\right)\left(1 + \operatorname{erf}\left(\frac{i\xi\sigma}{\sqrt{2}}\right)\right) \tag{86}$$

6.4 Characteristic Functions of Some Discrete Distributions

Discrete probability distribution functions are valid only at integer values of x. The characteristic function is the discrete Fourier transform

$$C(\xi) = \sum_x p(x) \exp(ix\xi) \tag{87}$$

where $C(\xi)$ is the characteristic function with variable ξ;
$p(x)$ is the probability distribution function;
x is an integer and the sum is for all valid values of x;
i is $\sqrt{-1}$.

The use of a sum and unity spacing for the values of x gives an unambiguous range for the characteristic function of $\pm\pi$ about the ξ axis. Beyond $\pm\pi$ the characteristic function curve repeats itself each 2π as would be expected if the omega convention was used in Section 4.2. For this reason, the characteristic functions of discrete probability distributions are shown only between the limits $\pm\pi$.

This section discusses a number of discrete probability distributions and their characteristic functions. The literature uses a number of different conventions, one of which is used here. As the letter p is used for probability function, in this section, the variable q is used for the probability of an individual trial.

6.4.1 Binomial Distribution

The binomial distribution [2, p. 179] [3, p. 138] [5, p. 138] is the probability distribution function of the results of n samples or trials with alternative outcomes each

having an individual probability q (note that q is used as the parameter to avoid confusion with the function p). The value of n is small compared with the population size and the sampling takes place with replacement. An example with $q = 0.75$ and $n = 10$ is shown in Figure 6.24(a) It is given by

$$\mathrm{p}(x) \;=\; \frac{n!}{x!(n-x)!}\; q^{x}\; (1-q)^{n-x} \quad x = \;1,\; 2,\; ..,\; n \tag{88}$$

The sample drawn at random must be replaced before the next draw.
The characteristic function is][2, p. 218][[3, p. 138][7, p. 929]

$$\mathrm{C}(\xi) \;\;=\;\; (q\,\exp(i\xi) \;+\; 1 \;-\; q)^{n} \tag{89}$$

An example is shown in Figure 6.24(b).

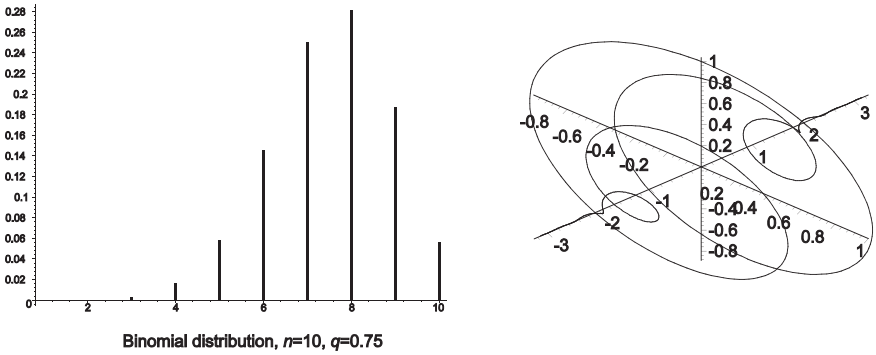

Figure 6.24 An example of the probability distribution function of the binomial distribution and its characteristic function.

The moment generating function is [2, p. 218] [3, p. 138] [7, p. 929]

$$\mathrm{M}(t) \;\;=\;\; (q\,\exp(t) \;+\; 1 \;-\; q)^{n} \tag{90}$$

The moments about the origin may be obtained from the characteristic function or directly and are

$$\begin{aligned} \text{Mean} \;&=\; nq \\ \text{Variance} \;&=\; nq(1-q) \end{aligned} \tag{91}$$

The skewness and kurtosis are given by

$$\begin{aligned} \text{Skew} \;&=\; \frac{1-2p}{\sqrt{nq(1-q)}} \\ \text{Kurtosis} \;&=\; 3 \;+\; \frac{1-6q(1-q)}{nq(1-q)} \end{aligned} \tag{92}$$

The Bernoulli distribution is a special case of the binomial distribution with $n = 1$ [2, p. 167] [5, p. 167].

6.4.2
Hypergeometric Distribution

The hypergeometric distribution [2, p. 218] [5, p. 151] is the probability distribution function of drawing exactly x white balls in n trials from a population of size N of mixed black and white balls with k white balls. The value of n need not be small compared with the population size. The probability distribution function is given by

$$\mathrm{p}(x) = \frac{k!}{x!(k-x)!} \frac{(N-k)!}{(n-x)!(N-k)-(n-x))!} \frac{1}{\frac{N!}{n!(N-n)!}} \tag{93}$$

where $x < k$;
$n - x < N - k$;
the value q in the binomial distribution is given by $q = k/N$.

Figure 6.25 shows the probability of finding x bad units in a sample of 10 when it is known that there are 8 bad units in the population of 25.

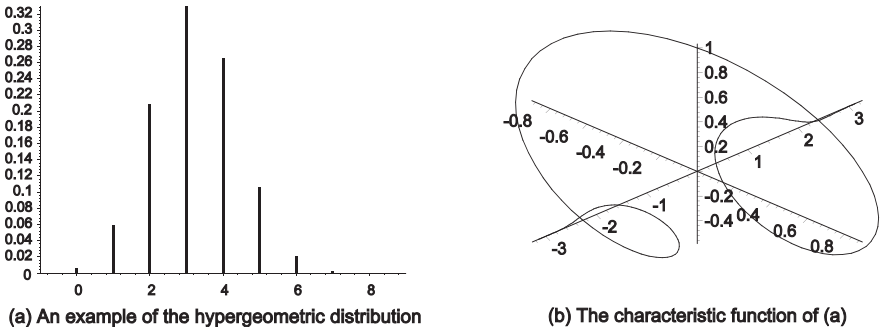

Figure 6.25 An example of the hypergeometric distribution for a sample of 10 in a population of 25 units where 8 are bad, and its characteristic function.

The characteristic function is given by [3, p. 972]

$$\mathrm{C}(\xi) = \frac{(N-k)!}{n!(N-k-n)!} \frac{(N-n)!n!}{N!} \quad {}_2\mathrm{F}_1(-n,\ -k;\ N-k-n+1;\ \exp(i\xi)) \tag{94}$$

where the function ${}_2\mathrm{F}_1(a,\ b;\ c;\ z)$ is the hypergeometric function [3, p. 873] [7, p. 555].

$${}_2\mathrm{F}_1(a,\ b;\ c;\ z) = 1 + \frac{ab}{1!c}\, z + \frac{a(a+1)\ b(b+1)}{2!c(c+1)}\, z^2 \ \ldots \tag{95}$$

An example is shown for $k = 8$, $n = 10$, and $N = 25$ in Figure 6.25(b).

The central moments may be obtained from the characteristic function or directly. The mean and variance are

$$\begin{aligned} \text{Mean} &= \frac{nk}{N} \\ \text{Variance} &= \frac{nk(n-k)(N-n)}{N^2(N-1)} \end{aligned} \tag{96}$$

The skew is

$$\text{Skew} = \frac{(N-2k)\ (N-2n)\ \sqrt{N-1}}{(N-2)\ \sqrt{nk(N-k)\ (N-n)}} \tag{97}$$

The expression for kurtosis is too large for the page.

6.4.3
Pascal, Negative Binomial, and Geometric Distributions

The Pascal probability distribution [5, p. 154] is the probability of having exactly x failures preceding the sth success in $x+s$ trials. It is given by

$$\mathrm{p}(x) = \frac{(x+s-1)!}{x!(s-1)!}\ q^s\ (1-q)^x\ x = 0,\ 1,\ 2,\ .. \tag{98}$$

An example with $s = 5$ and $q = 0.3$ is shown in Figure 6.26.
The characteristic function is [2, p. 218] [3, p. 1221] [7, p. 929]

$$\mathrm{C}(\xi) = \left(\frac{q}{1-(1-q)e^{i\xi}}\right)^s \tag{99}$$

An example of the characteristic function with $s = 5$ and $q = 0.3$ is shown in Figure 6.26.

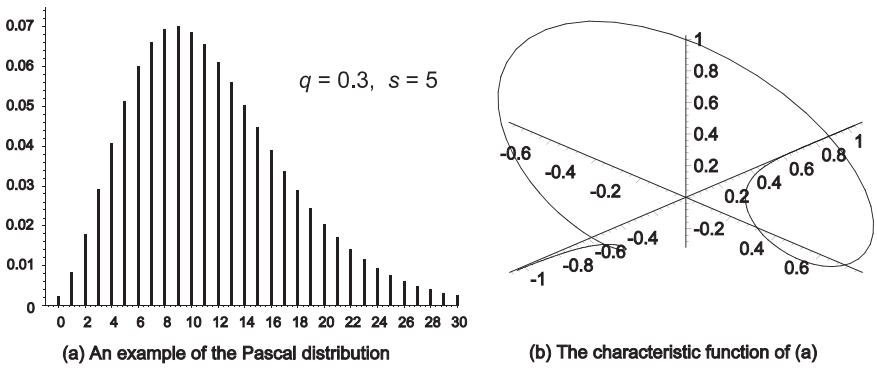

Figure 6.26 An example of the Pascal distribution with $s = 5$ and $q = 0.3$ and its characteristic function.

The moment generating function is [2, p. 218] [3, p. 1221] [7, p. 929]

$$\mathrm{M}(t) = \left(\frac{q}{1-(1-q)e^{t}}\right)^s \tag{100}$$

The central moments may be obtained from the characteristic function or directly, the mean and variance are

$$\begin{aligned} \text{Mean} &= \frac{s(1-q)}{q} \\ \text{Variance} &= \frac{s(1-q)}{p^2} \end{aligned} \tag{101}$$

The skewness and kurtosis are

$$\begin{aligned} \text{Skew} &= \frac{2-q}{\sqrt{s(1-q)}} \\ \text{Kurtosis} &= \frac{q^2 - 6q + 6}{s(1-q)} + 3 \end{aligned} \tag{102}$$

Some authors, for example [5, p. 154] give the negative binomial distribution as the generalisation of the Pascal distribution with the factorials replaced by gamma functions to give a distribution similar to Poisson distribution when events do not occur at a constant rate. The occurrence rate is a gamma distributed random variable.

$$\mathrm{p}(x) = \frac{\Gamma(x+s)}{\Gamma(x+1)\,\Gamma(s)}\, q^s\, (1-q)^x \quad x = 0,\ 1,\ \ldots \tag{103}$$

The *geometric* probability distribution [2, p. 179] [3, p. 781] [5, p. 152] is the probability of having x binomial trials before the first success is achieved. That is there are x–1 failures before this, success occurs at the xth trial and is an example of the Pascal distribution with $s = 1$ and x trials (not x+1). The geometric distribution is given by

$$\mathrm{p}(x) = q(1-q)^{x-1} \tag{104}$$

An example of the geometric distribution with $q = 0.5$ is given in Figure 6.27(a).

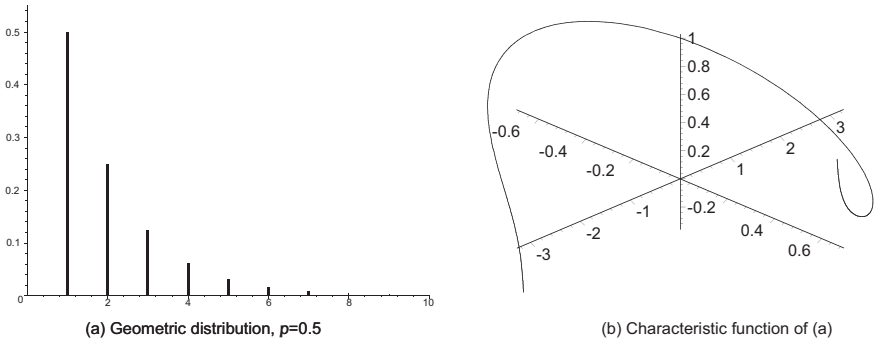

(a) Geometric distribution, p=0.5 (b) Characteristic function of (a)

Figure 6.27 An example of the geometric distribution with $q = 0.5$ and its characteristic function.

The characteristic function is given by [2, p. 218] [3, p. 781]

$$C(\xi) = \frac{qe^{i\xi}}{1-(1-q)e^{i\xi}} \tag{105}$$

An example of the characteristic function with $q = 0.5$ is shown in Figure 6.27(b).
The moment generating function is [2, p. 218] [3, p. 781]

$$M(t) = \frac{qe^{t}}{1-(1-q)e^{t}} \tag{106}$$

The central moments may be obtained from the characteristic function or directly, the mean and variance are

$$\begin{aligned} \text{Mean} &= \frac{1}{q} \\ \text{Variance} &= \frac{1-q}{q^2} \end{aligned} \tag{107}$$

The skew and kurtosis are

$$\begin{aligned} \text{Skew} &= \frac{2-q}{\sqrt{1-q}} \\ \text{Kurtosis} &= \frac{q^2-9q+9}{1-q} \end{aligned} \tag{108}$$

6.4.4
Poisson Distribution

The Poisson probability distribution [2, p. 53] [3, p. 1388] [5, p. 154] is the probability of exactly x independent occurrences during a period of time if events take place independently at a constant rate, λ. The Poisson distribution is given by

$$\begin{aligned} p(x) &= e^{-\lambda}\frac{\lambda^x}{x!} \qquad x = 1,\ 2,\ \ldots \\ &= 0 \qquad\qquad \text{otherwise} \end{aligned} \tag{109}$$

An example with $\lambda = 5$ is shown in Figure 6.28(a).
The Poisson distribution may be derived from the binomial distribution by setting $\lambda = nq$, using the Stirling formula for $n!$ (namely $n! = \sqrt{2\pi n}\, n^n \exp(-n)$), and letting n tend to infinity [4, p. 63]
The characteristic function is given by [2, p. 218][3, p. 1388] [7, p. 929]

$$C(\xi) = \exp\left(\lambda\,(e^{i\xi}-1)\right) \tag{110}$$

The characteristic function for $\lambda = 5$ is shown in Figure 6.28(b).
The moment generating function is [2, p. 218] [3, p. 1388] [7, p. 929]

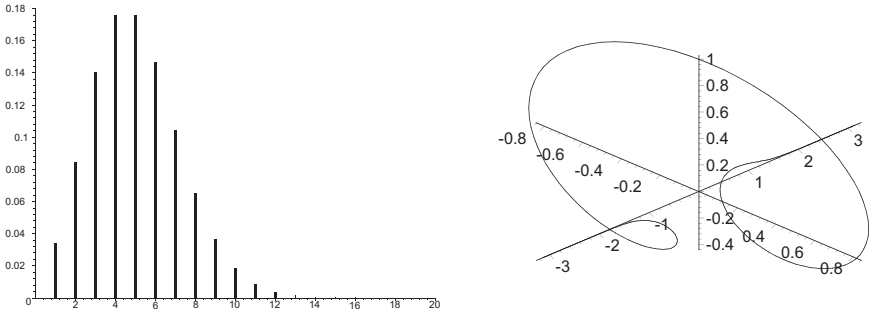

(a) Poisson distribution, λ=5 (b) Characteristic function of (a)

Figure 6.28 An example of the Poisson probability distribution function and its characteristic function.

$$\mathrm{M}(t) \;=\; \exp\Big(\lambda(e^{t}-1)\Big) \tag{111}$$

The central moments may be obtained from the characteristic function or directly. The mean and variance are both λ and the skew and kurtosis are

$$\begin{aligned} \text{Skew} &= \frac{1}{\sqrt{\lambda}} \\ \text{Kurtosis} &= \frac{1+3\lambda}{\lambda} \end{aligned} \tag{112}$$

6.5 An Example from Operational Research

There is an example in [5, p. 227] that can be used to illustrate the use of convolution to estimate the distribution of sums of random variables.

Equipment for repair passes through six stages in a repair facility and records show the statistical distributions of the time taken in hours are those in Table 6.3.

The probability distribution functions and their characteristic functions are shown in Figure 6.29.

Table 6.3 The distribution of test and repair times in each of the six stages

Stage and distribution	Distribution function	Characteristic function
1 Gaussian, $\mu = 10$, $\sigma = 1$	$p_1(x) = \frac{1}{\sqrt{2\pi}} \exp\left(-\frac{(x-10)^2}{2}\right)$	$C_1(\xi) = \exp\left(i10\xi - \frac{\xi^2}{2}\right)$
2 Gaussian, $\mu = 20$, $\sigma = \sqrt{2}$	$p_2(x) = \frac{1}{\sqrt{2\pi}\sqrt{2}} \exp\left(-\frac{(x-20)^2}{2}\right)$	$C_2(\xi) = \exp\left(i20\xi - \xi^2\right)$
3 Gamma, $\eta = 9$, $\lambda = 6$	$p_3(x) = \frac{6^9}{\Gamma(9)} x^8 \exp(-6x)$	$C_3(\xi) = \frac{-10077696}{(-6+i\xi)^9}$
4 Gamma, $\eta = 10$, $\lambda = 1$	$p_4(x) = \frac{1}{\Gamma(10)} x^9 \exp(-x)$	$C_4(\xi) = \frac{1}{(-1+i\xi)^{10}}$
5 Exponential, $\lambda = 5$	$p_5(x) = 5 \exp(-5x)$	$C_5(\xi) = -\frac{5}{-5+i\xi}$
6 Chi-square, $v = 10$	$p_6(x) = \frac{1}{2^5\ \Gamma(5)} x^9 \exp\left(-\frac{x}{2}\right)$	$C_6(\xi) = -\frac{1}{(-1+i2\xi)^5}$

To find the distribution of the total times for equipment to pass through the facility, the characteristic functions are multiplied as in Equation (114) and the result is shown in Figure 6.30.

$$\begin{aligned} C_{\text{total}}(\xi) &= C_1(\xi)\ C_2(\xi)\ C_3(\xi)\ C_4(\xi)\ C_5(\xi)\ C_6(\xi) \\ &= \prod_{k=1}^{6} C_k(\xi) \end{aligned} \tag{114}$$

The probability distribution of the total time is found by taking the anticharacteristic function

$$p_{\text{total}}(x) = \frac{1}{2\pi} \int_{-\infty}^{+\infty} C_{\text{total}}(\xi) \exp(-x\xi)\ d\xi \tag{115}$$

The result has been obtained numerically and is shown in Figure 6.30(b).

The central moments are shown in Table 6.4 with the sums of the moments in the right-hand column.

Figure 6.30(b) shows that the final distribution is skewed and the moments give the skew as $100.10/33.29^{3/2} = 0.521$. The final distribution has a sharper spike than a Gaussian or normal distribution and has a kurtosis of $2055.24/33.29^2 = 1.855$, namely less than the value of 3 for a Gaussian or normal distribution.

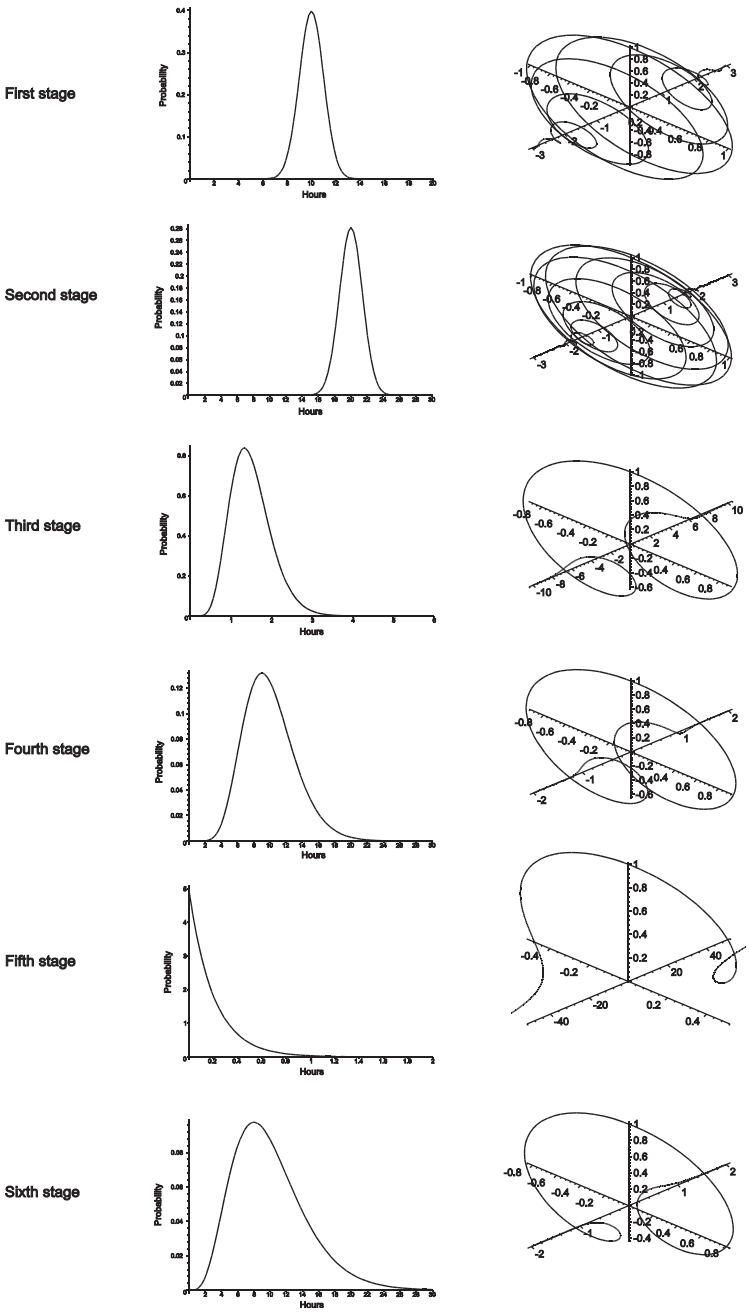

Figure 6.29 The probability distribution functions and their characteristic functions for each of the six test and repair stages. Note that the scales are not uniform.

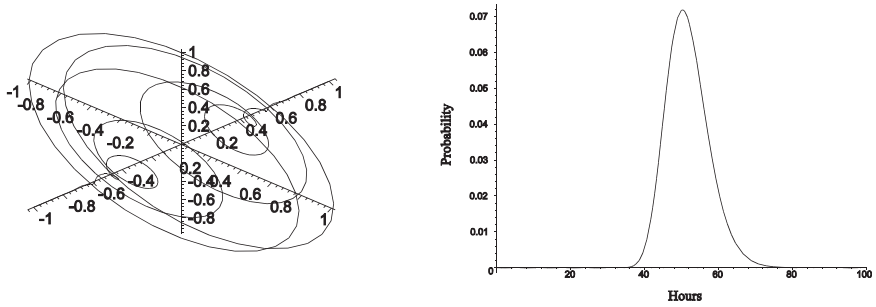

(a) The product of the six characteristic functions (b) The anticharacteristic function of (a)

Figure 6.30 The combined characteristic function for the sum of the times and its anticharacteristic function.

Table 6.4 Table of moments about the mean.

Moment	Stage 1	Stage 2	Stage 3	Stage 4	Stage 5	Stage 6	Total
Area	1	1	1	1	1	1	1
Mean	10	20	1.5	10	0.2	10	51.7
μ_2	1	2	0.25	10	0.04	20	33.29
μ_3	0	0	0.08	20	0.02	80	100.1
μ_4	3	12	0.23	360	0.01	1680	2055.24

Often the values of the percentiles are required, for example, how much time is required for 90% of the throughput. The cumulative distribution function provides the answer, and is given by

$$P(x) = \int_0^q p_{\text{total}}(x)\, dx \tag{116}$$

The cumulative distribution is illustrated in Figure 6.31 and shown as Table 6.5. The table shows that 90% of the throughput is completed in less than 59.3 hours. The median, or 50% point is 51.2 hours.

Table 6.5 Distribution of total time.

Per cent	Time, hours	Per cent	Time, hours	Per cent	Time, hours
5%	43.126	40%	49.814	75%	55.246
10%	44.725	45%	50.510	80%	56.321
15%	45.859	50%	51.211	85%	57.614
20%	46.794	55%	51.928	90%	59.303
25%	47.621	60%	52.672	95%	61.941
30%	48.384	65%	53.458	99%	67.346
35%	49.109	70%	54.307	99.5%	69.483

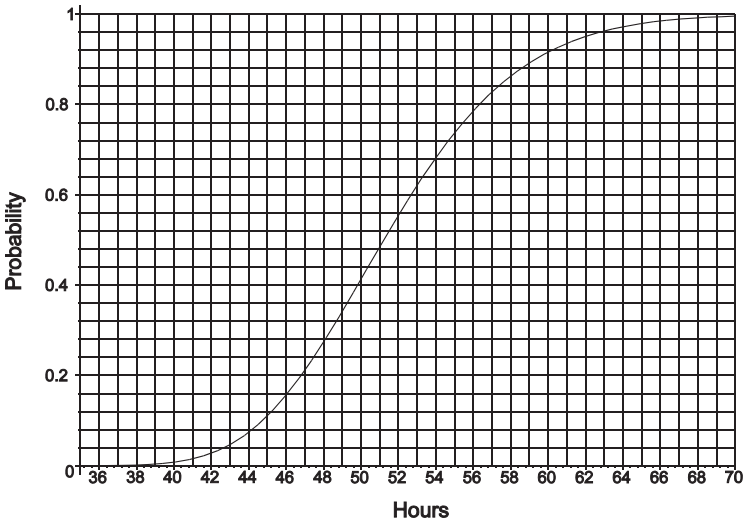

Figure 6.31 The cumulative distribution of the sum of the test and repair times.

References

1 Mood, A.M., F.A. Graybill, *Introduction to the Theory of Statistics*, McGraw-Hill, New York, 1963.

2 Parzen, E., *Modern Probability Theory and its Applications*, John Wiley, New York, 1960.

3 Weisstein, E.W., *CRC Concise Encyclopedia of Mathematics*, Chapman and Hall/CRC, Boca Raton, Florida, 1999.

4 Weatherburn, C.E., *A First Course in Mathematical Statistics*, Cambridge University Press, Cambridge, 1957.

5 Hahn, G.J., and S.S. Shapiro, *Statistical Models in Engineering*, John Wiley, New York, 1967.

6 Rice, S.O., *Mathematical Analysis of Random Noise*, Bell System Technical Journal, Vols. 23 and 24 in N. Wax, *Selected Papers on Noise and Stochastic Processes*, Dover, New York, 1954.

7 Abramowitz, M. and I.A. Stegun, *Handbook of Mathematical Functions*, Dover, New York, 1964.

7
Noise and Pseudo-random Signals

Noise is present in the signals at the outputs of receivers. The noise signals may have entered at the input or been generated in the receiver itself, generally the first stage, as shown in Figure 7.1.

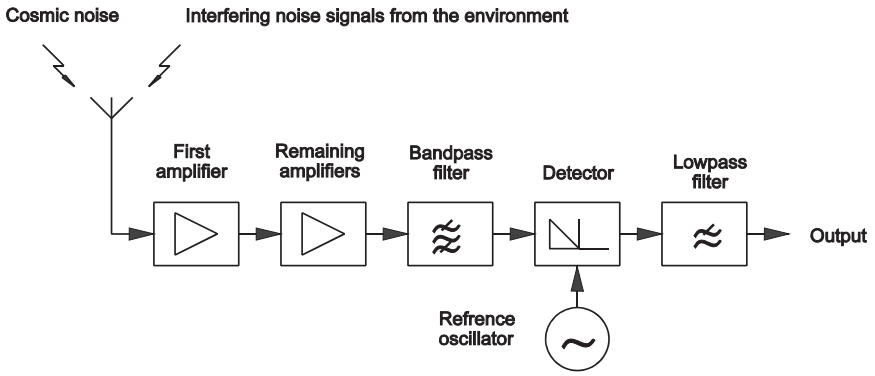

Figure 7.1 A block diagram of a typical receiving system.

The noise at the input is made up of noise from local interfering sources (for example the series commutator motors in vacuum cleaners and electric drills) and cosmic noise from outer space (for example from the sun). Noise generated by the first amplifier is often the limiting factor in the most sensitive of receivers used in radios, radars, and in radio astronomy [1, Chapter 7].

To eliminate outside sources, a resistor matched to the input resistance of the receiver is connected across the input. The noise power generated within a bandwidth B Hz, is

$$\text{Noise power at input} = k\ T\ B\ W \tag{1}$$

where k is Boltzmann's constant 1.38×10^{-23} J/K;
T is the absolute temperature of the resistor in K;
B is the noise bandwidth in Hz.

A New Twist to Fourier Transforms. Hamish D. Meikle

ISBN: 3-527-40441-4

The root mean square voltage of the noise across the resistor, $R\ \Omega$, is

$$\text{Noise voltage across the input} = \sqrt{k\ T\ B\ R}\ \text{V} \tag{2}$$

It is assumed that the filter in the receiver limits the bandwidth to B Hz. When the filter has to reject signal, interference, or noise components that might overload one of the stages, the filter is placed earlier in the train of stages. The amplifiers are not perfect and add their own, internally generated, noise that is greater than the input noise from a resistor, temperature T_{in} multiplied by the amplification factor, A. The expected amplified output noise power from an input resistor at a temperature of T K is

$$\begin{aligned}\text{Output noise power} &= \text{Amplified input noise} \\ &= A\ k\ T_{\text{in}}\ B\end{aligned} \tag{3}$$

In practice the noise power is greater than this and the degradation is accounted for by the noise figure $\overline{NF}$ defined in reference [2] as

$$\overline{NF} = \left.\frac{\text{Noise power out}}{\text{Gain}\times\text{Noise power in}}\right|_{\text{when the input is terminated at 290 K}} \tag{4}$$

When all quantities are referred to the input then

$$\overline{NF}\ \ k\ T_0\ \ B\ A = kT_0\ BA + kT_{\text{eff}}\ BA \tag{5}$$

where T_0 is the temperature of the input resistor, by definition at the standard reference temperature, 290 K [2];

T_{eff} is the effective system temperature referred to the input

Rearranging Equation (7.5) the amplifier has the equivalent temperature T_{eff} referred to the standard input, namely

$$T_{\text{eff}} = T_0\ (\overline{NF} - 1) \tag{6}$$

Noise figures are often given in decibels and typical examples are given in Table 7.1.

Table 7.1 Examples of equivalent noise temperatures, T_{eff} at the inputs of receivers

Noise figure dB	Linear	T_{eff}, K	Example
10.0	10	2610	Crystal diode mixer
3.0	2	290	Transistor amplifier after a transmit-receive switch
0.3	1.07	20.7	Radio astronomy, modern satellite receiver

The amplifier noise dominates in the 10dB and 3dB cases when the receiver is connected to an antenna, whereas galactic noise will dominate in the 0.3 dB case used for radio astronomy.

If n stages of gain A_n and noise figure $\overline{NF}_n$ are cascaded, the equivalent noise temperature at the output referred to the input is

$$T_{\text{eff}} = T_0 + T_0\,(\overline{NF_1} - 1) + \frac{T_0\,(\overline{NF_2} - 1)}{A_1} \tag{7}$$

As long as A_1 is sufficiently large, the noise contribution of the second and remaining stages is small.

The signals in the receiver are alternating current signals at frequencies around a centre frequency f_0 Hz, extending from $f_0 - B/2$ to $f_0 + B/2$. Alternatively a notional carrier signal at the frequency f_0 Hz is modulated with a vector by a vector signal. In the case of noise, the Cartesian, or x and y, coordinates of the vectors have a Gaussian probability density function as shown in Figure 7.2 and this is, loosely, what is seen on an oscilloscope. Though the noise, just described, has equal statistical power density within the bandwidth, called *white* noise (after white light), there are exceptions, such as noise with an amplitude proportional to $1/f$ in the case of transistor audio and video amplifiers. This type of noise is sometimes called *pink* noise.

The minimum duration of the noise pulses is limited by the bandpass filter before the detector and the maximum duration by the nature of the signal. In systems where the content from one pulse width to the next is uncorrelated (radar, digital communications, and so on), the pulse width and thus the bandwidth are defined.

In order to extract the vector value of the modulating signal, its phase is compared to the phase of a reference oscillator (the carrier reinsertion oscillator is used in single-sideband receivers or the coherent oscillator in radars). The output signals may be in Cartesian or polar form shown in Figure 1.3.

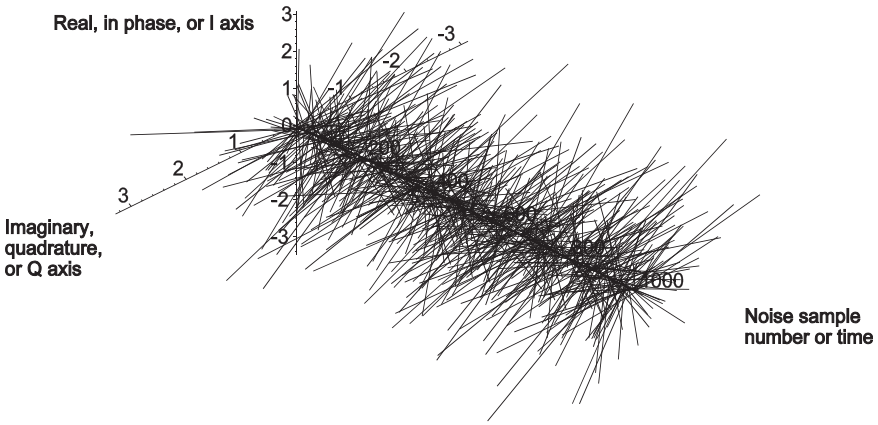

Figure 7.2 Gaussian noise samples demodulated from a (notional) carrier. [Source: Meikle, H.D., *Modern Radar Systems*, Norwood, Massachusetts: Artech House, 2001.]

The Cartesian components of thermal noise have a Gaussian distribution (see Equation (37) in Section 6.3.2].

$$p(x) = \frac{\exp\left(-\frac{x^2}{2\sigma^2}\right)}{\sqrt{2\pi}\sigma} \quad \text{Gaussian distribution} \tag{8}$$

where x is the variable;
the mean is zero (does not appear)
σ is the standard deviation or the root mean square voltage.

In polar form the probability distribution for the amplitude, r, is a Rayleigh distribution (see Section 6.3.2) and the probability distribution for the phase, θ, is uniform over a circle, from zero to 2π radians or 360 degrees.

$$\begin{aligned} p(r) &= \frac{r}{\sigma^2}\exp\left(-\frac{r^2}{2\sigma^2}\right) \quad \text{Rayleigh distribution} \\ p(\theta) &= 1 \quad \text{Uniform distribution } 0 > \theta > 2\pi \end{aligned} \tag{9}$$

where r is the amplitude measured along a radius;
θ is the phase angle from the phase detector;
σ is the standard deviation of one Cartesian component.

A number of such independent noise samples may be plotted in polar vector form and are the same as those in Figure 7.2. The noise is plotted as a vector bar graph of noise samples as the lines joining the noise signals tend to dominate in any illustration. The result is a shaggy bottlebrush [1].

The power in the complex or vector noise waveform may be obtained by multiplying by the complex conjugate, giving the probability distribution function

$$p(r) = \exp(-X) \tag{10}$$

where $X = r^2/2\sigma^2$.

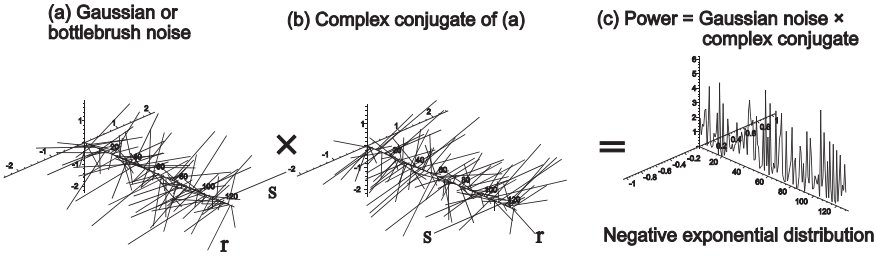

Figure 7.3 The multiplication of a vector noise pulse sequence by its complex conjugate to calculate the power. [Source: Meikle, H.D., Another way of representing echo signals, their spectra, and their statistics, *Proceedings of the German Radar Symposium GRS 2002*, Bonn, Germany, 5th to 9th of September 2002, pp. 509–513].

The main characteristics of Gaussian and Rayleigh noise are shown in Table 7.2.

The original vectors in the illustrations of the bottlebrush are generated from streams of random numbers with a Gaussian distribution, namely

$$\text{Vector}[n_1] \;=\; \text{Rand}[n] \;+\; j\text{Rand}[n+1] \tag{11}$$

where Rand[n] is a number drawn from a list of Gaussian distributed random numbers with zero mean and a standard deviation of unity.

Table 7.2 Comparison of parameters in the Gaussian and Rayleigh distributions

Parameter	Gaussian distribution	Rayleigh distribution
Mean, μ about zero	Here $\mu = 0$	
Root mean square about zero	σ	$\sqrt{2}\sigma$
Mode	0	σ
Mean radial error	0	$\sqrt{\frac{\pi}{2}}\sigma \;=\; 1.2533\ \sigma$
Variance (about mean)	σ^2	$(2 \;-\; \pi/2)\ \sigma^2$
Standard deviation	σ	$\sqrt{(2 \;-\; \pi/2)}\ \sigma \;=\; 0.655\sigma$
Median	Here 0	$\sqrt{2\ \ln\ 2}\sigma \;=\; 1.1774\ \sigma$

For convenience in taking Fourier transforms, the vectors are plotted as bar graph lines in the time domain about epoch zero. The power in one ohm is calculated by multiplying the voltage by its complex conjugate. All sense of phase has been lost to give real power values with a negative exponential distribution

$$p(x) \;=\; \frac{1}{X_0}\exp\left(-\frac{x}{X_0}\right) \tag{12}$$

where the mean power X_0 in 1 Ω is 2 W.

It must be remembered that the above calculation is for the total power in a two-phase circuit with two 1 Ω resistors as a load shown in Figure 7.4.

The power in each phase may be calculated knowing that the root mean square voltage in each phase here is unity (otherwise σ) to dissipate 1 W in each resistor. If the square root of the power is plotted, or the modulus value of the Gaussian vectors, the result is a Rayleigh distribution with a root mean square value of $\sqrt{2}$.

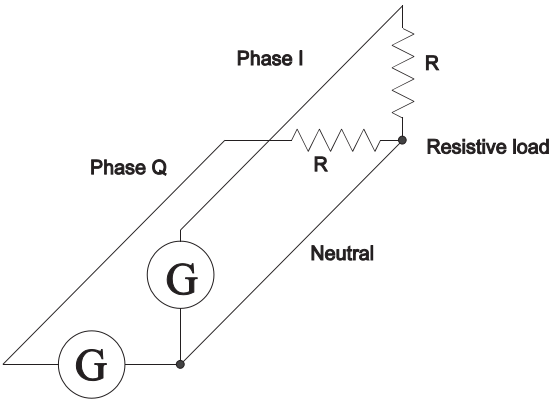

Figure 7.4 A two-phase circuit with Gaussian noise generators, G, and load resistors, R.

7.1 The Fourier Transform of Noise

Noise also has a spectrum. If the noise vector samples are taken each second, then a discrete Fourier transform gives a voltage spectrum valid over 1 Hz. The result is, as in the time domain, a bottlebrush with a Gaussian probability distribution. Each point in the voltage spectrum is the result of the vector sum of twisted Gaussian vectors with a Gaussian distribution in two dimensions as shown in Figure 7.5. By the central limit theorem, these sums also have Gaussian distributions in both dimensions. The power spectrum may be obtained again by multiplying by the complex conjugate of the voltage vector spectrum and the modulus of the voltage spectrum may be found by taking the square root, as in the time domain. If all the points of the discrete power spectrum are added (integrated), the sum is again 2 W to give a spectral density of 2 W/Hz. As in the time domain case, the power spectrum has a negative exponential probability distribution and the voltage spectrum has a Rayleigh distribution.

In order to be able to see individual vectors, a small number of samples, which may or may not be representative, has been shown. When either or both large numbers of samples are considered or more trials are overlaid on each other, the bottlebrushes may be represented by their statistical values as shown in Figure 7.6.

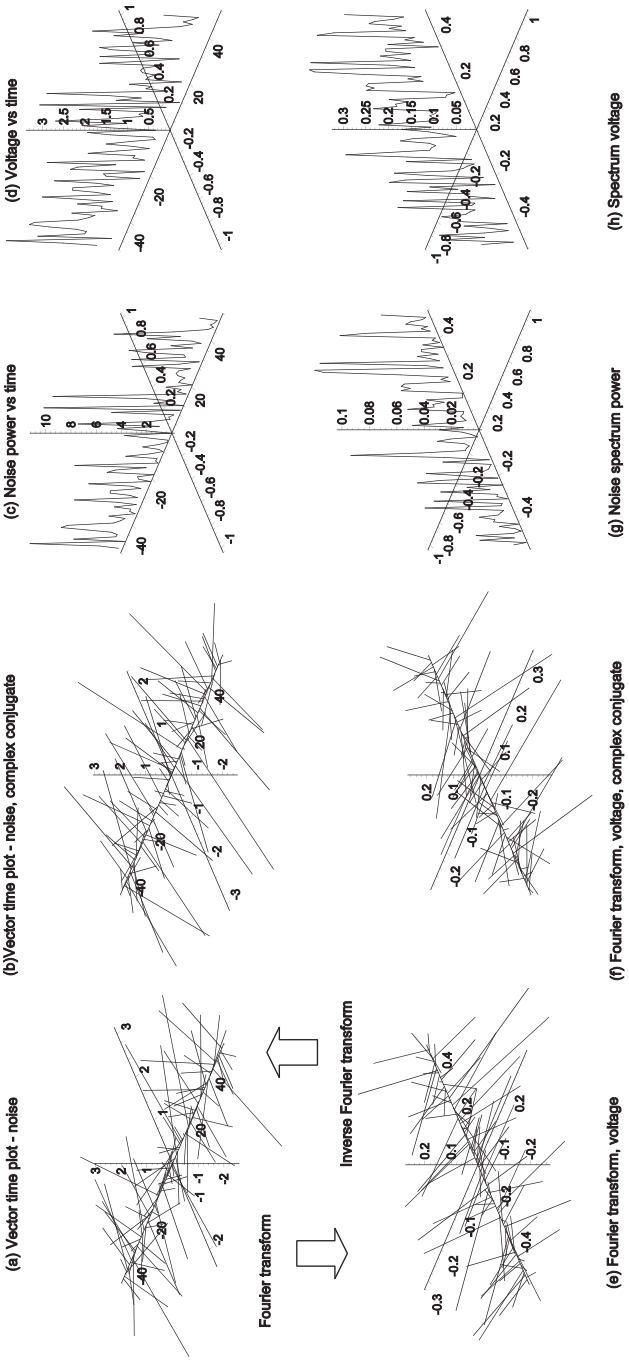

Figure 7.5 Vector representation of noise voltages, their spectra, and the powers in the waveform and spectrum.

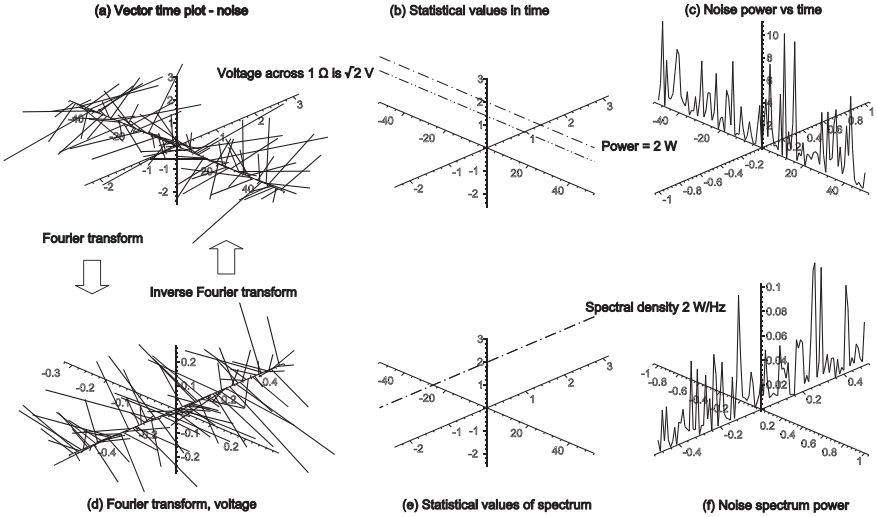

Figure 7.6 The representation of noise samples and their spectra by statistical values.

7.1.1 Optimum Filtering of Signals and Noise

With the use of receivers for radio waves for signals other than voices, music, or television pictures, other methods for determining the best way to filter out noise had to be found. Up to this time the filter width was varied to give the best match for quality or intelligibility. With the advent of radar, the echo signals are copies of the transmitted signal (maybe with a small Doppler frequency shift). Radar transmitters send pulses, normally of constant amplitude, that do not have a simple frequency spectrum for filtering so that mismatch occurs and the problem is to find the shape of filter with the least echo signal loss. One example is given here and others are to be found in references [1, 3, 4].

A pulsed radar signal has a rectangular envelope and, without additional modulation, has a sin x/x shaped spectrum of the form

$$\text{Pulse\_spectrum}(f) = \frac{\sin(\pi f \tau)}{\pi f} \quad \text{(Voltage)} \tag{13}$$

where τ is the width of the rectangular pulse.

The rectangular pulse and its spectrum are shown together in Figure 7.7(a).

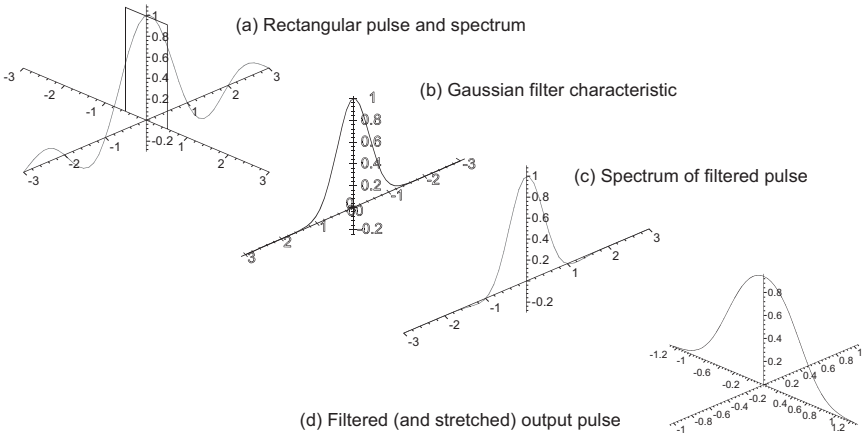

Figure 7.7 A rectangular pulse, its spectrum, and the effects of filtering on the output pulse.

In early British radars the intermediate frequency stages were derived from television receivers with a flat response centred on 45 MHz, the frequency of the BBC's first television transmitter. The problem studied [3 and 4, for example] was the problem to find the optimum rectangular bandpass to give the minimum signal loss for the minimum amount of noise after filtering, or the best signal-to-noise ratio. Later it was found that a filter with a Gaussian shape gave a better compromise of the form, see Figure 7.7(b).

$$\text{Filter\_characteristic}(f) = \exp\left(-\frac{f^2\tau^2\ 2\ \ln(2)}{B^2}\right) \quad \text{(Voltage)} \tag{14}$$

The spectrum of the signal having passed through the filter is the product of the spectrum and the filter characteristic is shown in Figure 7.7(c), namely

$$\text{Filter\_output}(f) = \frac{\sin(\pi f\tau)}{\pi f}\ \exp\left(-\frac{f^2\tau^2\ 2\ \ln(2)}{B^2}\right) \quad \text{(Voltage)} \tag{15}$$

The inverse Fourier transform has been calculated numerically and the pulse shape after filtering is shown in Figure 7.7(d).

The statistical value of the noise spectrum is initially considered to be flat as in Figure 7.6(e) and wider than the significant part of the filter characteristic, so that the output is the same as the filter characteristic. The signal-to-noise ratio is then

$$\text{Signal}-\text{to}-\text{noise ratio} = \frac{\left[\int_{-\infty}^{+\infty} \frac{\sin(\pi f\tau)}{\pi f}\exp\left(-\frac{f^2\tau^2 2\ln(2)}{B^2}\right)\mathrm{d}f\right]^2}{\int_{-\infty}^{+\infty}\left[n\ \exp\left(-\frac{f^2\tau^2\ 2\ln(2)}{B^2}\right)\right]^2\mathrm{d}f} \text{(Power)} \tag{16}$$

If the signal-to-noise ratio is plotted against the bandwidth, B, for a pulse of unity width, then the results are shown in Figure 7.8. The minimum loss of signal-to-noise

ratio occurs when the 3 dB bandwidth is $0.742/\tau$ and the signal energy is reduced to 0.890 of the input energy or a loss of 0.506 dB. In addition to the loss of signal energy, the pulse is stretched, leading to a reduction of range resolution in a radar.

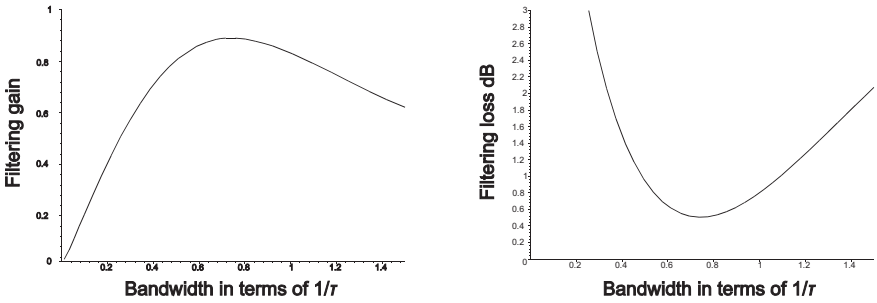

Figure 7.8 The effect of filter bandwidth on signal-to-noise ratio. [Source: Meikle, H.D., *Modern Radar Systems*, Norwood, Massachusetts: Artech House, 2001]

The above is the classical treatment of a matching filter without time delay. In real life the signal takes time to build up and then pass to the output of the filter giving a delay as described for finite impulse response filters in Sections 4.4.3 and 4.4.4. Instead of the purely real filter characteristic, the filter characteristic shown in Figure 7.9(b) is vector multiplied by the function representing the delay, namely $\exp(-j2\pi f t_d)$, to give the form in Figure 7.9(c). This is similar to the curves in Section 6.3.2, Figure 6.8 for the Fourier transform of a Gaussian distribution with a finite mean.

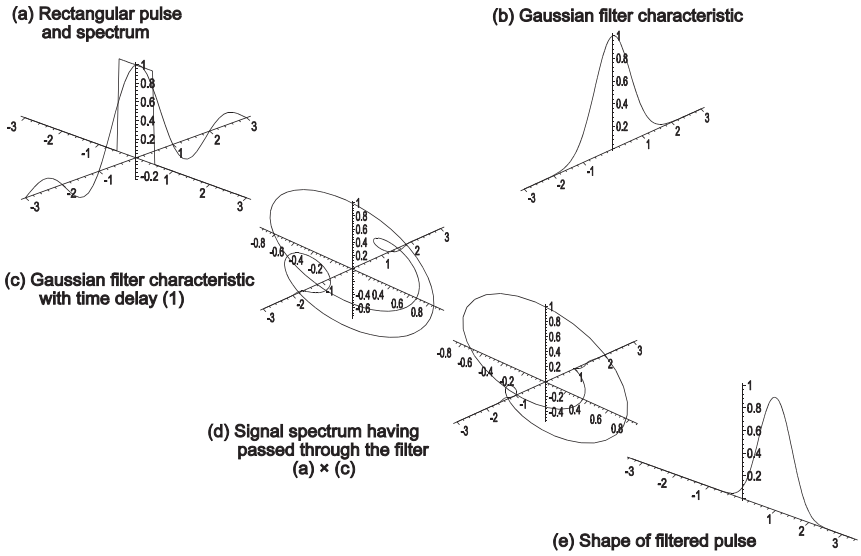

Figure 7.9 The rectangular pulse from Figure 7.7 passing through a Gaussian filter with delay.

When the spectrum in Figure 7.9(a) is multiplied by the filter characteristic in Figure 7.9(c), the spectrum at the output of the filter is shown in Figure 7.9(d). The waveform is obtained from the inverse Fourier transform and is shown in Figure 7.9(e) as a delayed, almost Gaussian, hump.

7.2
Auto- and Cross-correlation Functions

The traditional form of the auto-correlation function for a polyphase voltage is shown in Figure 7.10 [1, Fig 2.11]. For unwieldy waveforms, such as noise, power is computed from the peak of the auto-correlation function, shown in many texts as a triangle.

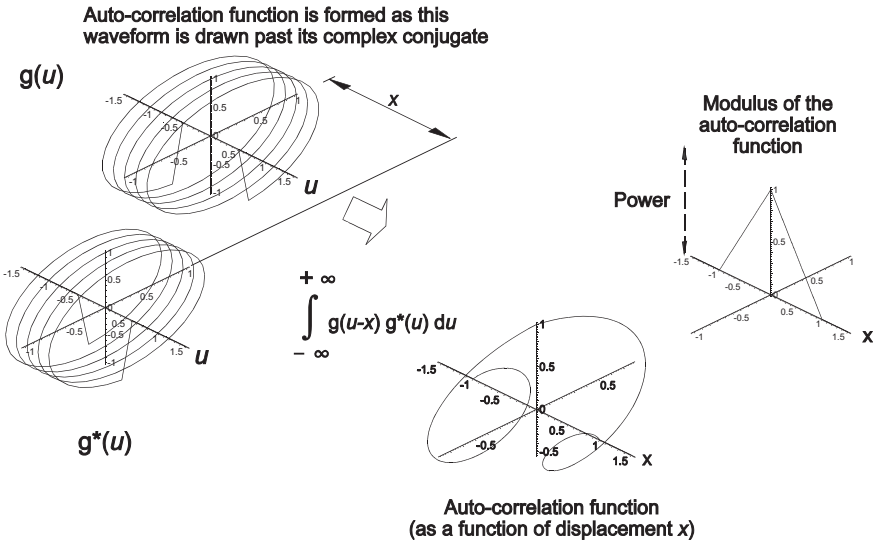

Figure 7.10 The auto-correlation function of a polyphase or spatial spiral voltage. [After: Meikle, H.D., *Modern Radar Systems*, Norwood, Massachusetts: Artech House, 2001].

In the case of noise, Figure 7.11(a) shows a train of noise samples and Figure 7.11(b) the complex conjugate. The product of (a) and (b) at each frequency is shown in vector form in Figure 7.11(c), where the scale has been omitted for clarity, and the absolute values in Figure 7.11(d).

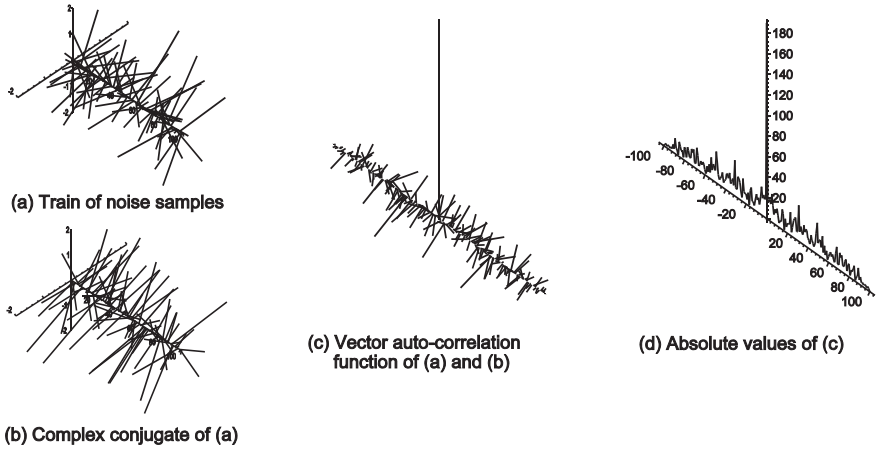

Figure 7.11 The autocorrelation of a train of Gaussian noise pulses.

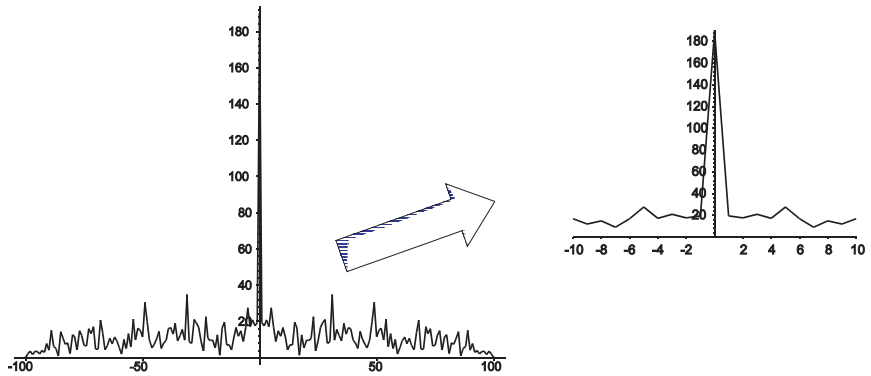

Figure 7.12 The absolute values of the autocorrelation function.

The centre peak is narrow and is shown in detail in Figure 7.12.

With an irregular or stochastic waveform the central peak can be narrow with residues (often called sidelobes) on both sides. The time delay inherent in the filter or correlator avoids the term *before* and after.

A purely real filter characteristic and its complex conjugate are the same. In Section 7.1 there was a purely real signal spectrum with a purely real filter and thus the processes of convolution and correlation are the same. In real life filters can only be designed with time delays, see the lowpass filter in Section 4.4.3 and the use of complex conjugates in the weighting function separate correlation and convolution. In pulse compression radar the rectangular radar pulse is modulated and the echoes signals are multiplied (or weighted) by the complex conjugate of the transmitter pulse modulation signal and the compressed pulse afterward has the form of Figure 7.12. A more complete treatment is given in [1 Section 8.2.1]. Any negative phase sequence components do not correlate but are convolved to add to the sidelobes around the wanted signal.

7.3 Pseudo-random Signals

When a computer modem on an analogue line logs into an Internet provider, the user hears that it starts with a low speed protocol and the speed either increases to the maximum or the maximum that the line distortion and echoes allow. With the switching to 9600 baud noise is heard that is the result if cyphering the data on the line with a standard key. The cyphering avoids abrupt changes from a train of zeroes to a train of ones that can occur in data transmission. The characteristics of the signals are modelled to be as close as possible to noise and may be treated statistically as such.

Correlation with near copies of wanted signals is used in selective voltmeters for sine wave signals.

Pseudo-random waveforms are used in a military situations to hide the nature of the signal either by spreading it in time or in frequency. Both methods reduce the spectral density making it more difficult for a receiver not having a filter that has the characteristic of the complex conjugate of the signal modulation. Systems using this method are called low probability of intercept (LPI) systems.

7.4 Example of the Convolution of Radar Echo Signals and Noise

An important example of the convolution of noise with signals occurs with the calculation of the echo signal-to-noise ratio to give a required probability of detection. The mathematics used has been explained in a number of publications by Marcum [5], Swerling [6], [7, Chapters 9 to 11], and for Swerling cases I and II [8], cases III and IV [8], and frequency diversity [9, 10]. In each case a number of echo signals are added together and a decision is taken as to whether this sum represents the echo signals from an object. In this chapter signal strengths are represented by their powers and *the –f convention is used for Fourier transforms.*

7.4.1 False Alarm Probability with *N* Noise Samples

A radar operator has to have confidence in his equipment: an indication of an echo signal must represent an object that has been seen and not an unfortunate sum of noise spikes. The probability distribution of noise power is a negative exponential distribution (see Section 6.3.4, Figure 6.17, Equation (63) in Chapter 6, and Figure 7.13(a)) and has a characteristic function represented by a single loop, shown in Figure 7.13(b).

The probability distribution function for the noise samples of mean power unity is (see Section 6.3.4)

$$\mathrm{p}(x) = \exp(-x) \tag{17}$$

It has the characteristic function

$$C(\xi) \;=\; \frac{1}{1 + j2\pi\xi} \tag{18}$$

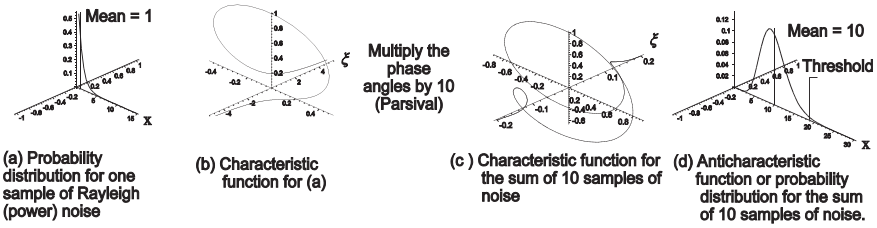

Figure 7.13 The probability distributions of one and ten samples of noise [After: Meikle, H.D., Another way of representing echo signals, their spectra, and their statistics, *Proceedings of the German Radar Symposium GRS 2002*, Bonn, Germany: DGON, 5th to 9th of September 2002, pp. 509–513.]

If, for example, N noise samples are added together the characteristic function of the sum is the characteristic function to the power N, $C(\xi)^N$, as shown in Figure 7.13(c). Note that the range of the ξ axis is one tenth of that in Figure 7.13(b).

$$C(\xi)^N \;=\; \frac{1}{(1 + j2\pi\xi)^N} \tag{19}$$

The anticharacteristic function is a gamma distribution (Section 6.3.4) with $\eta = N$ that has a mode at $N - 1$ and is shown in Figure 7.13(d).

$$p(x) \;=\; \frac{x^{N-1}\exp(-x)}{\Gamma(N)} \tag{20}$$

The area under the curve in Figure 7.13(d) to the right of an abscissa value representing a threshold gives the false alarm probability, 10^{-6} in Figure 7.13(d). If Y_b is the threshold level, then the false alarm probability is

$$p(\text{False alarm}) = \int_{Y_b}^{\infty} \frac{x^{N-1}\exp(-x)}{\Gamma(N)}\, dx \tag{21}$$

The threshold for a false alarm probability of 10^{-6} for the sum of 10 noise pulses in Figure 7.13(d) is 32.71.

7.4.2
Probability of Detection with Signal Plus Noise

Classical radar theory envisages the five possible radar models in Table 7.3. The probability distribution for the Marcum, or the steady signal case, may be obtained directly as in Section 6.3.2 and the Swerling cases [3, 6] by convolution.

Table 7.3 Classical forms of echo signal fluctuation in radar

Model	Cases	Fluctuation (power)	Use
Marcum		None	Steady echoes from spheres, etc.
Swerling	I and II	$\frac{1}{X_m}\exp\left(-\frac{X}{X_m}\right)$	Single frequency Rayleigh distributed echo signals.
Swerling	III and IV	$\frac{4X}{X_m^2}\exp\left(-2\frac{X}{X_m}\right)$	Single frequency chi-squared (gamma) Rayleigh distributed echo signals.

where X is the power variable, the noise power is assumed to be unity, and X_m is the mean signal power or signal to noise ratio, R.

The Marcum, or steady signal case, has been obtained directly from the Rice distribution (see Section 6.3.2) and is repeated here for completeness. The characteristic function for the Rice distribution in the $-f$ notation is from Equation (50) in Chapter 6 [3, Eq. 10.4–12b]

$$C_{\text{Rice}}(\xi) = \frac{j\exp\left(-\frac{2\pi R\xi}{2\pi\xi - j}\right)}{j - 2\pi\xi} \tag{22}$$

where ξ is the variable, here using the $-f$ notation;
R is the signal-to-noise ratio;
j is the square root of minus one.

For N independent samples the characteristic function is $(C_{\text{Rice}}(\xi))^N$ and has the anticharacteristic function from Campbell and Foster's pair 650.0 to give the probability distribution function

$$p(\gamma) = \left(\frac{\gamma}{NR}\right)^{\frac{N-1}{2}} \exp(-\gamma - NR)\ I_{N-1}(\sqrt{4NR\gamma}) \quad \text{Marcum} \tag{23}$$

where γ is the variable;
$I_n(z)$ is a modified Bessel function of the first kind, order n, with imaginary argument [12, 9.6.3 p. 375].

For comparison with the Swerling cases later, a threshold of 32.71 from Figure 7.13(d) is required for a false alarm probability of 10^{-6} with 10 integrated pulses and a signal-to-noise ratio of 3 with 10 pulses gives a probability of detection of 80.5%.

The Swerling cases deal with echoes that fade with the probability distributions in Table 7.3. The odd numbered cases (I and III) may be simulated by taking a random

number from the distribution and using the same value for each of the N echoes, the echo signals are said to be correlated. In contrast, the noise samples are different from pulse to pulse and are uncorrelated. In the even numbered cases, the radar changes frequency from pulse to pulse so that both the echo signal pulses and noise are uncorrelated from pulse to pulse.

In the past mathematicians had to steer their mathematics to lead to solutions where tabulated values were available. The availability of computers and mathematical programs for them, some examples are (the registered names) Maple, Mathematica, MathCad, and so on, gamma distributions may be calculated directly and this allows a simpler, more unified treatment. If the alternate form of the gamma distribution is taken from Equation (61) in Section 6.3.4 with the appropriate substitutions

$$p_\gamma(X,\ N,\ R) \quad = \quad \frac{1}{R\Gamma(N)} \left(\frac{X}{R}\right)^{N-1} \exp\left(-\frac{X}{R}\right) \tag{24}$$

where X is the echo signal power variable;
N is the shape factor;
R is the signal-to-noise ratio.

The shape factor, N, corresponds to the number of independent pulses integrated in the Swerling models are given in Table 7.3. In the example there are 10 pulses with a signal- to-noise ratio of 3.

Table 7.4 The values of N and R in the example for 10 pulses and a signal-to-noise ratio of 3.

Swerling case	Shape factor N	Signal-to-noise ratio R
I	1	30
II	10	1
III	1	30
IV	10	1

The characteristic function of the echo signal is multiplied with the characteristic function of the receiver noise to obtain the characteristic function of signal plus noise. The characteristic functions and their products for the four Swerling models are given in Table 7.5 and illustrated in Figure 7.14.

Table 7.5 The probability distribution functions (p.d.f) and characteristic functions (c.f.) for the Swerling scattering models.

Case		Echo signal	Echo signal + noise	
	p.d.f.	c.f.	c.f.	Probability distribution function (p.d.f)
I	$p(X, 1, NR)$	$\frac{1}{1+j2\pi\xi NR}$	$\frac{1}{(1+j2\pi\xi)^N (1+j2\pi\xi NR)}$	$\frac{1}{N\ R}\left(1+\frac{1}{N\ R}\right)^{N-2} \exp\left(-\frac{y}{1+N\ R}\right) P_\gamma\left(N-1, \frac{y}{1+\frac{1}{N\ R}}\right)$
II	$p(X, N, R)$	$\frac{1}{(1+j2\pi\xi R)^N}$	$\frac{1}{(1+j2\pi\xi)^N} \frac{1}{(1+j2\pi\xi R)^N}$	$\frac{1}{(1+R)^N} \frac{1}{(N-1)!} y^{N-1} \exp\left(-\frac{y}{1+R}\right)$
III	$p(X, 2, NR/2)$	$\frac{1}{(1+j\pi\xi NR)^2}$	$\frac{1}{(1+j\pi\xi NR)^2} \frac{1}{(1+j2\pi\xi)^N}$	$\frac{y^{N-1}\exp(-y)}{\left(1+\frac{NR}{2}\right)(N-1)!} {}_1F_1\left(2,\ N;\ \frac{y}{1+\frac{2}{NR}}\right)$
IV	$p(X, 2N, R/2)$	$\frac{1}{(1+j\pi\xi R)^{2N}}$	$\frac{1}{(1+j2\pi\xi)^N} \frac{1}{(1+j\pi\xi R)^{2N}}$	$\frac{y^{N-1}\exp\left(-\frac{y}{\frac{1+R}{2}}\right)}{(1+R)^{2N}(N-1)!} {}_1F_1\left(-N, N; -\frac{R}{1+R}y\right)$

P_γ is the cumulative gamma distribution function [11, Eq. 6.5.1, p. 260] and the ${}_1F_1$ function is the confluent hypergeometric or Kummer's function [12, Eq. 13.1.2, p. 504].

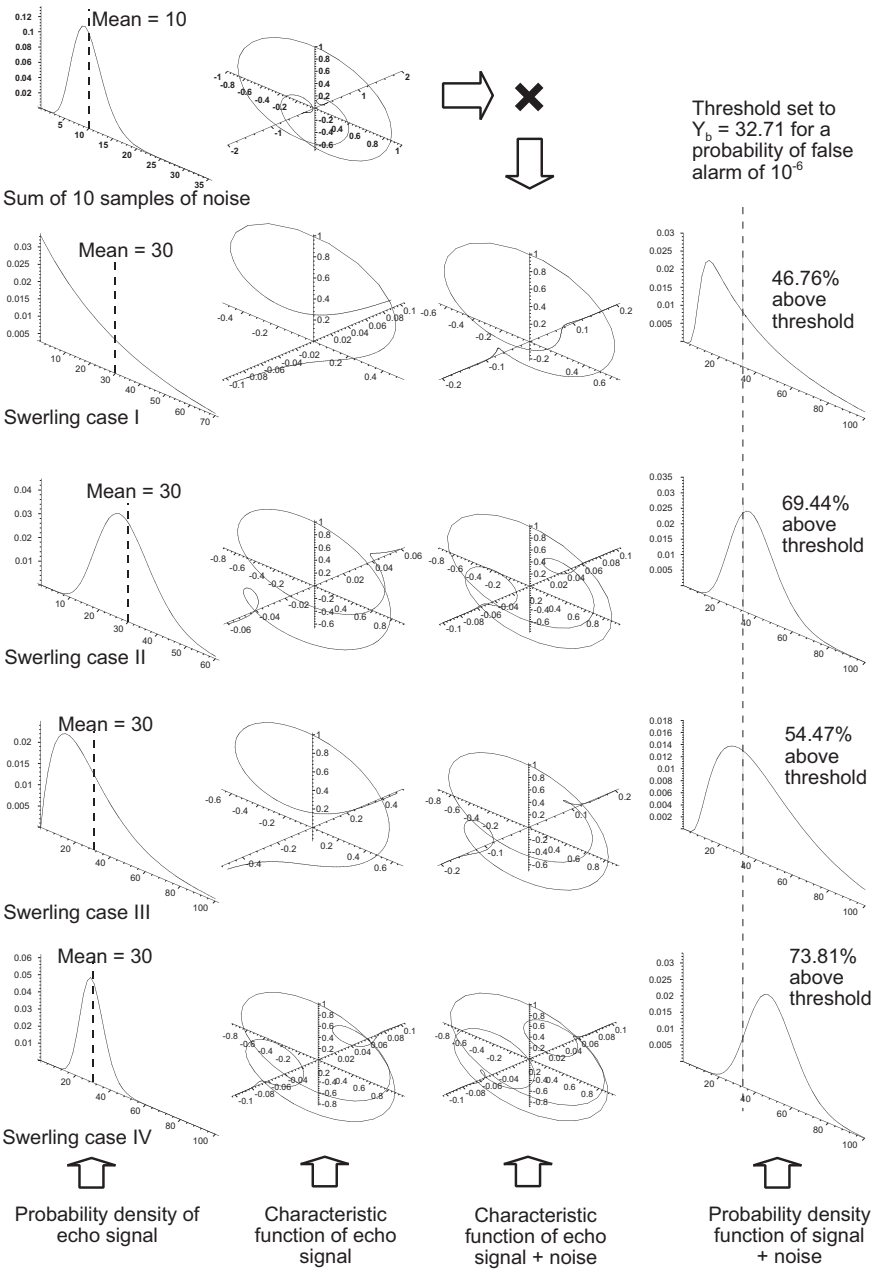

Figure 7.14 The adding of echo signal and noise (convolution) for the four Swerling cases with $N = 10$ and $R = 3$.

Many air traffic control radars use two separate transmitter and receiver combinations with common antenna. It is to be noted that the convolution of two uncorrelated echo signals following the Swerling case I model gives a probability distribution corresponding to Swerling case III and is only the case when the video signals are summed before the threshold. Using the figures from Figure 7.13 the probabilities of detection for 10 pulses with a signal-to-noise ratio of 3 are shown in Table 7.6.

Table 7.6 The probabilities of detection for $N = 10$ and $R = 3$.

Swerling case	Probability of detection	Combination	Combined probability of detection
Swerling case I	46.76%	Each channel	46.76% for each channel
		.AND.	22.81%
		.OR.	77.19%
Swerling case III		Signal sum	73.81%

For triple diversity with Swerling case I fading, the probability distribution of the sum of the echoes on three frequencies is $p_\gamma(X, 3, NR/3)$ and other cases are shown in references [9, 10].

References

1 Meikle, H.D., *Modern Radar Systems*, Artech House, Norwood, Massachusetts, 2001.
2 IEEE, *The New IEEE Standard Dictionary of Electrical and Electronics Terms, IEEE Standard 100*, Institute of Electrical and Electronic Engineers, New York.
3 di Franco, J.V., and W.L. Rubin, *Radar Detection*, Artech House, Dedham, Massachusetts, 1980.
4 Lawson, J.L., and G.E. Uhlenbeck, *Threshold Signals*, MIT Radiation Laboratory Series, Vol. 24, McGraw-Hill, New York, 1950.
5 Marcum, J.I., *A Statistical Theory of Target Detection by Pulsed Radar*, Rand Corporation Research Memorandum RM-754, Santa Monica, California, Reissued 25 April 1952.
6 Swerling P., *Probability of Detection for Fluctuating Targets*, Rand Corporation, RM-1217, March 1954.
7 Bijvoet, J.A., *Standard Methods for Predicting and Specifying Performance of Air Surveillance Radar Systems*, SHAPE Technical Centre, The Hague, report TR-50-U, April 1969.
8 Eendebak J., *Detectability Curves for Swerling Cases III and IV Target Models*, SHAPE Technical Centre, The Hague, Supplement 1 to Report TR-50-U, April 1970.
9 Poelman, A.J., *Performance Evaluation of Frequency Diversity Radars*, SHAPE Technical Centre, The Hague, Supplement 2 to Report TR-50-U, April 1970.
10 Poelman, A.J. and E.J. Benée, *Further Notes on Performance Evaluation of Frequency Diversity Radars*, SHAPE Technical Centre, The Hague, Supplement 3 to Report TR-50-U, May 1973.
11 Campbell, G.A. and R.M. Foster, *Fourier Integrals for Practical Applications*,D. van Nostrand Company, Princeton, New Jersey, 1948. This book replaces the paper The Practical Application of the Fourier Integral, *Bell System Technical Journal*, October 1928, pp. 639–707.
12 Abramowitz, M. and I.A. Stegun, *Handbook of Mathematical Functions*, Dover, New York, 1964.

Appendix A

Glossary

In order to embrace the ideas of spiral functions, a number of new terms are used, some taken from [1], that are included in the list below in *italics*. The main new terms are *rotating* voltage taken from the German *Drehstrom* and *spatial spiral*.

δ – see Delta

Antenna is the component that sends waves from a transmitter into space or receives waves from space. Not all antennae radiate equally in all directions (isotropic) and some radiate in a directional pattern.

Anticharacteristic function The inverse Fourier transform of a characteristic function C(ξ).

$$p(x) = \frac{1}{2\pi} \int_{-\infty}^{+\infty} C(\xi)\, e^{-i\xi x}\, d\xi$$

Apodize The word taper is used here – see Chapter 5.

Baseband The band of frequencies occupied by the signal used to modulate a carrier wave [3].

B.B.C. The British Broadcasting Corporation.

c.d.f. see cumulative distribution function.

Carrier wave An alternating voltage used to "carry" information (modulation) either for radiation as in wireless transmission or for frequency division multiplex transmission [3].

Cartesian detector [1] A form of *vector detector* that gives the x and y components of the modulation, also called the I and Q components.

A New Twist to Fourier Transforms. Hamish D. Meikle

ISBN: 3-527-40441-4

Characteristic function The Fourier transform of a probability distribution function $p(x)$.

$$C(\xi) = \int_{-\infty}^{+\infty} p(x)\, e^{i\xi x}\, dx$$

Continuous Fourier transform is the term in this book used for transforms taken between the limits of plus and minus infinity, namely in the f and ω conventions

$$F(f) = \int_{-\infty}^{+\infty} f(t)\, \exp(-j2\pi ft)\, dt$$

$$C(\xi) = \int_{-\infty}^{+\infty} p(x) \exp(+i\xi x)\, dx$$

Cumulative distribution function is the integral of the probability distribution function.

Delta (δ) function, Dirac [2], notation $\delta(x)$

$$\delta(x) = \text{limit}_{n\to\infty} \frac{1}{2\pi} \frac{\sin\left[\left(n+\frac{1}{2}\right)x\right]}{\sin\left(\frac{x}{2}\right)} \qquad \text{The Dirichlet kernel}$$

$$\text{or} = \text{limit}_{n\to\infty} \frac{\sin nx}{\pi x} = \frac{1}{2\pi} \int_{-\infty}^{+\infty} e^{-jkx}\, dk = \qquad \text{Fourier transform of unity}$$

$\delta(x)$ is a pulse of unit area and width approaching zero at the point x.

Delta (δ) is used for a small increment, example δx

Delta (δ) function, Kronecker [2], notation δ_{ij}

$$\begin{aligned} \delta_{ij} &= 1 \quad \text{when } i = j \\ &= 0 \qquad\quad i \neq j \end{aligned}$$

The Kronecker delta function has a width approaching zero.

Discrete Fourier transform is the term used in this book for the spectra from lists of equally spaced time samples, namely using the f convention

$$F(k) = \frac{1}{N} \sum_{n=0}^{N-1} f[n] \exp\left(-j2\pi \frac{n}{N} k\right)$$

The discrete Fourier transform in this book is sometimes called a *finite Fourier transform*.

Electrical analogue, an analogy with three-phase electrical power, "*rotating voltage etc*" as with the German *Drehstrom*.

Fast Fourier transform is the name given to the Cooley and Tukey [4] and other fast algorithms for discrete Fourier transforms.

Finite Fourier transform is the term in this book used for transforms taken between finite limits, *start* and *end*, namely in the *f* and o conventions

$$\mathrm{F}(f) \;=\; \int_{start}^{end} \mathrm{f}(t)\, \exp(-j2\pi ft)\, \mathrm{d}t$$

$$\mathrm{C}(\xi) \;=\; \int_{start}^{end} \mathrm{p}(x)\, \exp(i\xi x)\, \mathrm{d}x$$

This term is sometimes used for the *discrete Fourier transform*.

Finite impulse response filter is a filter that has no feedback and gives a finite response to a needle pulse at the input.

FIR is the abbreviation for finite impulse response.

Frequency distribution is sometimes called a histogram and has the same form as the probability distribution function. Since the ordinates are counts the area under the curve is not unity.

Gaussian distribution is usually called the *normal distribution* in the literature in English as it is the most common. It is given by

$$\mathrm{p}(x) \;=\; \frac{1}{\sqrt{2\pi}\,\sigma}\, \exp\left(-\left(\frac{x-\mu}{\sigma}\right)^2\right)$$

where μ is the mean and σ is the standard deviation.
The area under the curve is unity.

Gaussian function is used in this book for its simplicity and is given by

$$\exp\left(-\pi(ax)^2\right)$$

The area is $1/a$, the second moment is $1/(2\pi\, a^3)$, variance is $1/(2\pi\, a^2)$, and root mean square width $1/(\sqrt{2\pi}a)$.

Heaviside function has the value zero when $t < 0$ and unity when $t > 0$.

LPI is the abbreviation for *low probability of intercept*.

LSB see least significant bit

m.g.f. see moment generating function.

Median is the 50% point on the ordinate of a cumulative distribution function

Mode is the position of the peak of a probability distribution.

Moment generating function is the function

$$M(t) = \int_{-\infty}^{+\infty} p(x)\ \exp(tx)\ dx \quad \text{continuous distribution}$$

$$= \sum p(x)\ \exp(tx) \quad \text{discrete distribution}$$

Most significant bit The bit representing the greatest increment in a word representing a number, normally the bit on the left.

Moving target indicator (MTI) is a form of signal processing in radar that suppresses echo signals from stationary scatterers such as ground clutter.

MSB, see most significant bit

MTI, see moving target indicator.

Negative phase sequence The sequence of phases opposite to the principal phase rotation [3].

Negative phase sequence component A *rotating* voltage or current representing imbalance in a polyphase circuit [3].

Normal distribution is used in the English literature, *Gaussian distribution* is used in other languages and in this book -see Gaussian distribution.

Offset The origin for rotating voltages or currents

p.d.f. , see probability distribution function.

Percentile The *n*th percentile the point where the curve on a cumulative distribution crosses the *n*% point on the ordinate.

Polar detector [1]. A form of *vector detector* that gives the amplitude, *r*, and phase, ϕ, of the modulation.

Positive phase sequence component The principal or working component in a polyphase circuit [3].

Positive phase sequence The conventional sequence of the rotation of the phases or the sequence in which each phase reaches its maximum [3].

Probability distribution function With a statistical distribution it is the probability that a certain point on the abscissa has that value.

Quartile The first, second, and third quartiles are the points where the cumulative distribution function cuts the 25%, 50% (median), and 75% points on the ordinate.

***Rotating* current** The rotating current vector in a polyphase circuit and is a literal translation of the German word *Drehstrom*.

Rotating voltage This term is used for the voltage vector in a polyphase circuit and is an analogy with the German term *Drehspannung*.

Sideband The spectral components not at the carrier frequency representing the modulation of the carrier wave.

Sidelobe Used mainly for antenna patterns as secondary lobes away from the direction of the main lobe. This term is used figuratively for secondary responses present in Fourier transforms.

Spiral A curve of increasing radius in two dimensions. By analogy to spherical spirals in Figure 2.2(b), curves of varying radius and pitch are called *spatial spirals*.

Spatial spiral A curve similar to a helix that does not have to have a constant radius and pitch.

Standard deviation is the square root of the variance, often denoted by s or σ.

Variance is the second moment about the mean, often denoted by s^2 or σ^2.

***Vector* voltage** A voltage expressed in two dimensions, either Cartesian or polar.

Vector detector [1]. A detector used to recover both the amplitude and phase components of modulation on a carrier wave. Cartesian and polar forms are possible.

Weighting The word taper is used here – see Chapter 5.

Window The word taper is used here – see Chapter 5.

Zero phase sequence component This is the constant direct voltage or current representing the centre point of the circle or ellipse of the positive and negative phase sequence components [3].

References

1 Meikle, H.D., *Modern Radar Systems*, Artech House, Norwood, Massachusetts, 2001.

2 Weisstein, E.W., CRC *Concise Encyclopedia of Mathematics*, Chapman and Hall/CRC, Boca Raton, Florida, 1999.

3 IEEE, *The New IEEE Standard Dictionary of Electrical and Electronics Terms, IEEE Standard 100*, Institute of Electronic Engineers, New York.

4 Cooley, J.W. and J.W. Tukey, An algotithm for the machine calculation of complex Fourier series, American Mathematical Society from the *Mathematics of Computation*, Vol. 19, no. 90, pp. 297–301, 1965.

Appendix B

Maple Graphical Expressions

Technical graphics in three dimensions are notoriously difficult to draw by hand. Luckily a number of mathematics programs are available to do the calculations and produce convincing illustrations. The Maple program has been used extensively to produce the diagrams in [1] and this book and this appendix shows some of the expressions used.

Other mathematics programs also have graphics outputs and there are a number of computer programs that can translate from one language to another.

B.1 Fourier Transforms

The form of the Fourier transform used by Woodward [2] for signal analysis is

$$F(f) = \int_{-\infty}^{+\infty} f(t)\exp(-j2\pi ft)\, dt \qquad (1)$$

where $F(f)$ is the spectrum of the time function, frequency variable f;
$f(t)$ is the time function, time variable t;
j is $\sqrt{-1}$.

The Maple expression for a function expressing (1) is

```
F := (f, remaining parameters)
    -> int( f(t, remaining parameters)*exp(-I*2*Pi*f*t),
t=-infinity..+infinity);
```

Where remaining parameters are any parameters that are needed to be passed into the function F(*f*).

A New Twist to Fourier Transforms. Hamish D. Meikle

ISBN: 3-527-40441-4

The inverse transform is

$$f(t) = \int_{-\infty}^{+\infty} F(f)\exp(+j2\pi ft)\ df \tag{2}$$

giving the Maple expression

```
f := (t, remaining parameters)
   -> int( F(f, remaining parameters)*exp(+I*2*Pi*f*t),
                                        f=-infinity..+infinity);
```

Chapter 6 uses the omega convention with the functions p(x) for probability distributions and C(ξ) for characteristic functions, namely

$$\begin{aligned} C(\xi) &= \int_{-\infty}^{+\infty} p(x)\exp(i\xi x)\ dx \\ p(x) &= \frac{1}{2\pi}\int_{-\infty}^{+\infty} C(\xi)\ \exp(-i\xi x)\ d\xi \end{aligned} \tag{3}$$

where p(x) is the probability distribution function, variable x;
C(ξ) is the characteristic function of the probability distribution, variable ξ;
i is $\sqrt{-1}$.

The Maple expressions for the transform is

```
C := (xi, remaining parameters)
      -> int( p(x, remaining parameters)*exp(I*xi*x),
      x=-infinity..+infinity);
```

and its inverse is

```
p := (x, remaining parameters)
      -> int( C(xi, remaining parameters)*exp(-I*xi*x),
         xi=-infinity..+infinity)/2/Pi;
```

The Fourier transforms that are part of Maple use the omega convention with a negative exponential, namely

$$\begin{aligned} F(\omega) &= \int_{-\infty}^{+\infty} f(t)\ \exp(-i\omega t)\ dt \\ f(t) &= \frac{1}{2\pi}\int_{-\infty}^{+\infty} F(\omega)\ \exp(+i\omega t)\ df \end{aligned} \tag{4}$$

and are called by

```
F := (f, remaining parameters)
-> inttrans[fourier]( f(t, remaining parameters), t, ω);
```

and its inverse is

```
f := (t, remaining parameters)
->inttrans[invfourier](F(ω, remaining parameters), ω, t);
```

B.2 Plotting Expressions

As described in Chapter 3, a new convention [1] is used to display time waveforms, which may be complex, and their spectra orthogonally in three dimensions as shown in Figure B.1. The time and frequency plots must be generated separately.

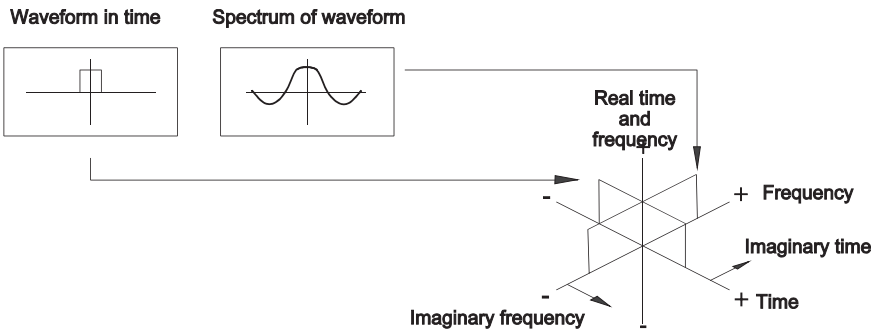

Figure B.1 The common display of time waveforms and their spectra.

B.2.1 Time Plot

The coordinate system is not the default Cartesian system provided by Maple. The Maple plot option `orientation=[-45, 45]` is used to turn the representation to the proper aspect. Thus a time plot is given in Maple by

```
plot_t := plots[spacecurve]([t, Im(Time expression),
Re(Time expression)], t=start..end, orientation=[-45, 45],
colour=black, numpoints = number of points):
```

Often it is necessary to increase the number of points from the default 25 for adaptive plotting to create smooth curves.

The plot is assigned to a variable and the expression ends with a colon so that no list of plotting values is displayed. If necessary `plot_t` may be defined as a function to allow parameters to be passed. An example is shown in Figure B.2.

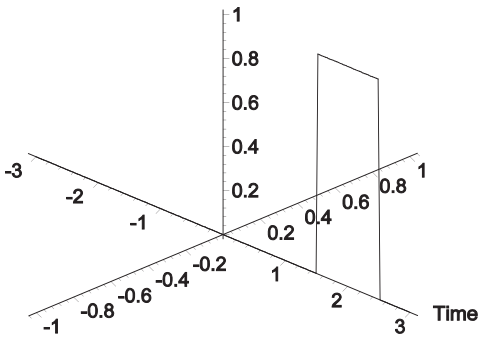

Figure B.2 The time function.

B.2.2

Frequency Plot, Spectrum, or Characteristic Function

In the frequency domain the Maple expression is

```
plot_f := plots[spacecurve]([Im(Frequency expression), f,
Re(Frequency expression)], f=start..end, orientation=[-45, 45],
colour=black, numpoints=number of points):
```

An example of a complex frequency plot on an orthogonal axis is shown in Figure B.3.

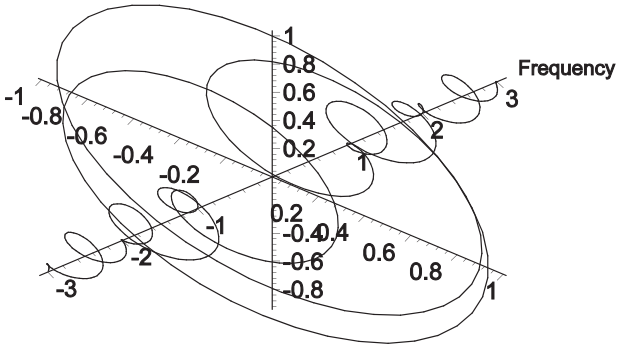

Figure B.3 A frequency plot, spectrum, or characteristic function in statistics..

B.2.3
Combined Plots

The plots in the time and spectral domains may be brought together using the Maple function `plots[display]([plot_t, plot_f, ..])` as in Figure B.4.

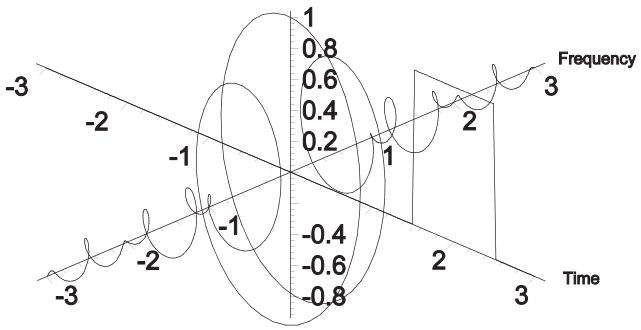

Figure B.4 A combined time and frequency plot.

B.2.4
Exporting Plots

Plots may be copied directly from the screen as bitmaps. For better quality and to be able to add text to the diagrams it is better to export them to file in a vector format, for example Hewlett-Packard Graphics Language (*.PGL) or encapsulated PostScript (*.EPS) format, that can be read by a graphics program. The expressions for this are `plotsetup( hpgl, plotoutput = "drive:\\file.pgl");` for Hewlett-Packard, and `plotsetup( ps , plotoutput = "drive:\\ file .eps");` for PostScript files (do not omit the double \\ or Maple will strike). No options are specified as it is easier to turn, size, and maybe edit the diagrams using a graphics program, for example, often the lines need to be thickened for publication.

Do not forget to return the display function back to the monitor screen with the `plotsetup(inline);` function.

B.2.5
Stereographic Pairs

Plots may be displayed on a monitor screen at slightly different aspects as seen by the left and right eyes by changing the orientation in the `plots[display]` function. Though the space curves may be coloured almost at will, the axes remain black.

When the stereographic pairs are edited using a graphics program, the colours for the left and right eyes may be changed to match the coloured spectacles needed to view them. After this the images may be superimposed for printing or display using the graphics program, as in Figure B.5.

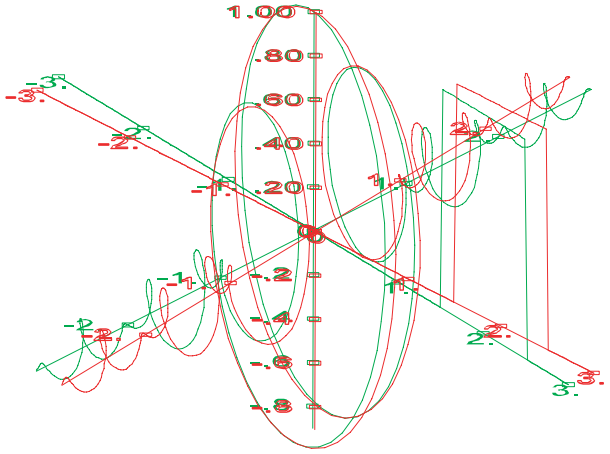

Figure B.5 A red and green stereographic pair with coloured axes.

B.3
Other Types of Plots in Three Dimensions

The use of Maple or other mathematics programs is not limited to complex waveforms and their Fourier transforms and there are other examples in [1]. An example is the Wien bridge shown in Figure B.6.

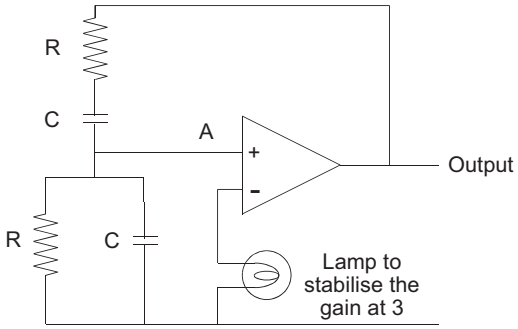

Figure B.6 A Wien bridge oscillator [Source: Meikle, H.D., Modern Radar Systems, Norwood, Massachusetts: Artech House, 2001.

The working point at the point A, referenced to zero by subtracting the network attenuation factor, is given by

$$\text{Working point} = \frac{R}{(j2\pi fCR+1)\left(R+\frac{1}{j2\pi fC}+\frac{R}{j2\pi fCR+1}\right)}-\frac{1}{3} \tag{5}$$

When the phase at point A is the same as that at the output, positive feedback occurs, and the circuit oscillates and the frequency of oscillation as

$$\text{Working frequency} = \frac{1}{2\pi CR} \tag{6}$$

In this example R is 1000 Ω, and C is 1 μF, so that the oscillating frequency, f, is 159.1549 Hz. The phase change varies with frequency continuously and the oscillation point is shown in Figure B.7. Standard Bode diagrams show a phase jump of 180 degrees, or discontinuity, at this point. In Figure B.7 the oscillation point is part of a continuum.

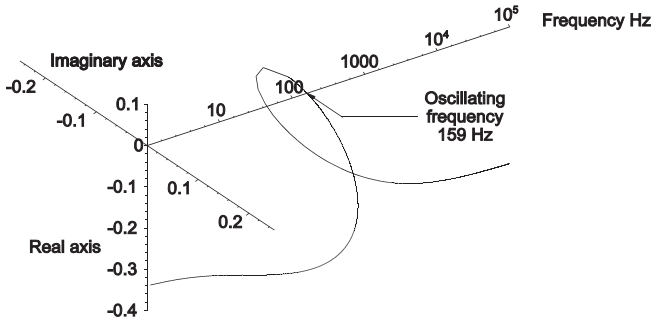

Figure B.7 The complex working point for the Wien bridge oscillator [Source: Meikle, H.D., *Modern Radar Systems*, Norwood, Massachusetts: Artech House, 2001].

References

1 Meikle, H.D., *Modern Radar Systems, Artech House,* Norwood, Massachusetts, 2001.

2 Woodward, P.M., *Probability and Information Theory with Applications to Radar,* 2nd edn, Pergamon Press, Oxford, 1964.

Index

A New Twist to Fourier Transforms. Hamish D. Meikle

ISBN: 3-527-40441-4